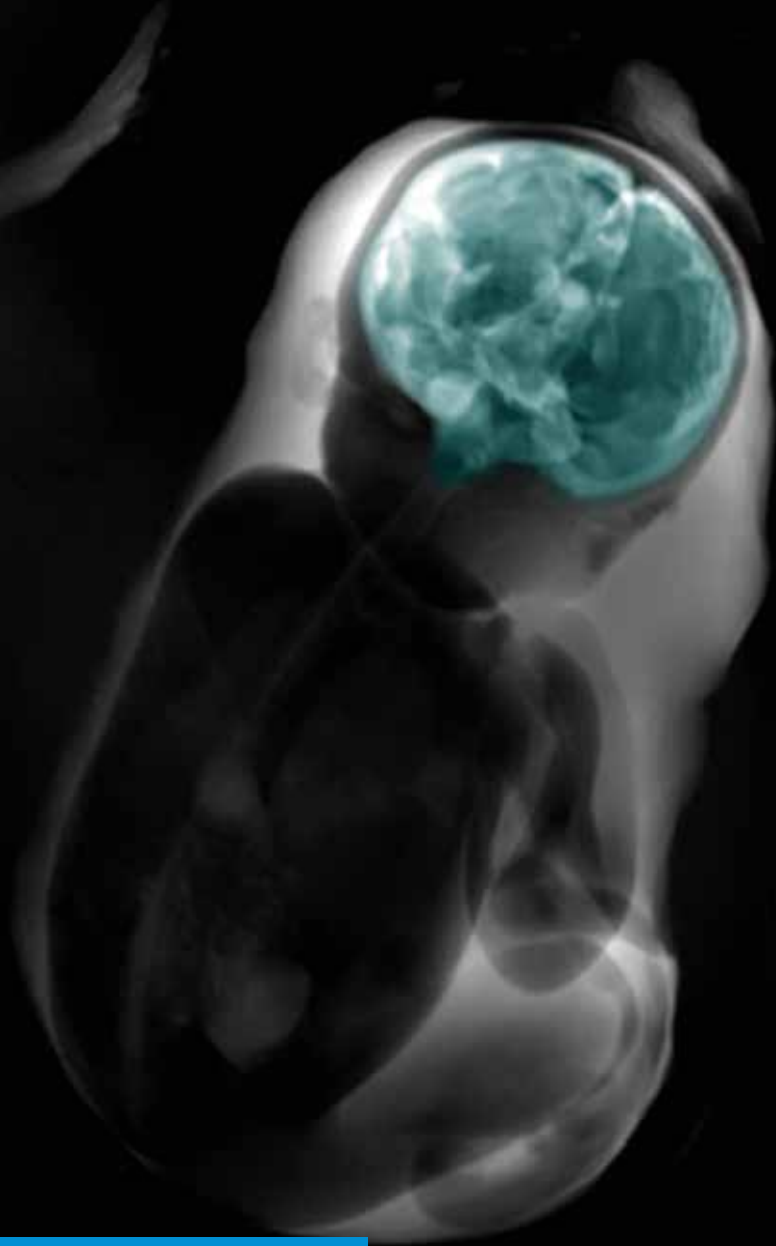# A blueprint of the developing mind

Elise Turk

A blueprint of the developing mind

Elise Turk

A blueprint of the developing mind

Een blauwdruk van het ontwikkelende brein

(met een samenvatting in het Nederlands)

Proefschrift

ter verkrijging van de graad van doctor aan de Universiteit Utrecht op gezag van de rector magnificus, prof.dr. H.R.B.M. Kummeling, ingevolge het besluit van het college voor promoties in het openbaar te verdedigen op donderdag 1 december 2022 des ochtends te 10.15 uur

door
Elise Turk

geboren op 6 januari 1990
te Leiderdorp

**Veel dingen durven we niet te doen omdat ze moeilijk zijn,
maar ze zijn moeilijk omdat we ze niet durven te doen.**

Lucius Annaeus Seneca (circa 4 v.C. – 65 n.C)

Table of Contents

Chapter 1

General introduction

BACKGROUND

The human brain is a complex system. All our actions, thoughts and feelings are a consequence of neuronal processes that are rooted in and fine-tuned by our walnut-like organ. Groups of neurons, the brain's nerve cells, communicate through axonal pathways in an organized way, leading to systematic series of actions directed to specific cognitive, motoric or behavioral outcomes. The brain is mainly formed in utero, it develops over time and everything that we do, eat or experience between conception and death influences the brain's functioning. Establishment of most neuronal components and the largest brain growth take place in the womb, making the fetal period essential for normal development and perturbations to these processes render the brain at risk for neurodevelopmental deficits (Anderson & Thomason, 2013).

Establishment of healthy neural building blocks during the fetal and neonatal period is fundamental to normal growth and development. Within 40 weeks of pregnancy (i.e., gestational weeks) the brain rapidly matures into a complete adult-like organ including all brain structures, 100 billion neurons and the characteristic folded shape of the cortex. Unfortunately, the development of the brain is susceptible for environmental insults, such as extremely preterm birth or maternal inflammation, which may lead into structural and functional malformations of the brain (Dong et al., 2020; Kidokoro et al., 2014) and to psychopathology later in life (Aguilar-Valles et al., 2020; Chen et al., 2020). Brain development is driven by a complex interaction of nature, our DNA, and nurture, the environment. Given the complexity of the accumulation of events and the underlying etiology of developmental disorders, mapping the spatiotemporal progress of neural alterations is not straightforward. In particular not for the fetal brain, due to limited resources of healthy and diseased brains and compatible analyzing techniques. Getting a comprehensive picture of changes in brain function and structure over time and how they are impacted by phenotypic differences and biological processes may contribute to new treatments or interventions.

Our understanding of the development of the human fetal brain, is largely due to advances in animal studies, study of human post mortem tissue (Flechsig, 1920) and ultrasound imaging (Stiles & Jernigan, 2010; Volpe et al., 2006). Acknowledging these sources, we are aware that the human fetal brain already develops shortly after conception and we can globally describe embryonic and fetal brain maturation in utero (Bayer & Altman, 1991; Sidman & Rakic, 1973; Singh, 2017) and neural activity development (Luhmann et al., 2016). Animal models and *in vitro* studies may not show a complete picture of healthy human brain growth and are impracticable to delineate abnormalities *in vivo*. Ultrasound imaging -the technique most commonly used to monitor fetal development- has a resolution that is often too low to detect subtle anatomical malformations and does not provide the opportunity to study the brain's function. Recent progress

of Magnetic Resonance Imaging (MRI) *in utero* and *ex utero*, improved analyzing techniques and new (healthy) study cohorts facilitate new insights into healthy and diseased fetal and neonatal brain morphology and function in more detail. To this date, much remains unknown about the developmental trajectory of fetal and neonatal brain development and thereby opens windows of opportunity for new research.
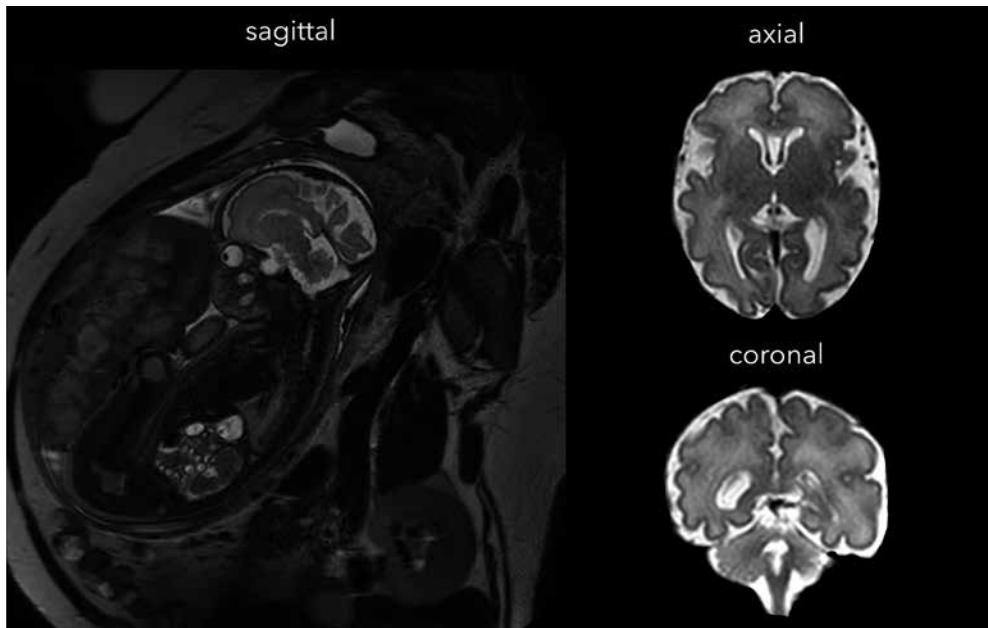
Figure 1. Structural MRI of the fetal brain
Displayed are different orientations of fetal T2-weighted MR Images from the fetus (around 32 weeks of gestation) and mother on the left, and fetal brain on the right. Images are from our YOUth study, University Medical Center Utrecht.

This thesis will focus on the application of advanced fetal and neonatal MRI. I aim to explore both structural maturation as well as functional network development in the second half of pregnancy and newborn period. The availability of normative indices of the brain developing in the healthy fetus may provide critical insights into the timing and progression of impaired brain development in the high-risk fetus and preterm born infants (Clouchoux et al., 2012).

BRAIN DEVELOPMENT IN UTERO

An essential first step in analyzing fetal brain imaging is to understand some basics of prenatal neurodevelopment and brain anatomy. As in other vertebrates, the human brain is largely formed before birth through sequential series of morphogenetic transformations, starting with neurogenesis and proliferation of the precursors of neurons and glia (Stiles & Jernigan, 2010). After cells are formed, this process is followed by migration and differentiation into various neurons and glial cells, and ends with the sprouting of axons and dendrites to form (micro) circuitries between neurons (Stiles & Jernigan, 2010). Myelination of the axonal fiber tracts is the last process and continues long after birth (Jakovcevski et al., 2007). These sequential series of events are uniform throughout the brain but have distinctive timetables for different brain regions. Globally, the brain develops from a caudal to rostral orientation; from the spinal cord, to the midbrain, hindbrain and forebrain.

The major part of the forebrain, the cerebral cortex, is the last structure to develop and mature. Largest changes in brain morphology take place during the second half of pregnancy, when head circumference doubles, the weight of the brain increases threefold and the cortex changes from smooth to a surface full of convolutions, also called sulci and gyri (Chi et al., 1977; Kandel et al., 2000; O'Rahilly & Muller, 2010; Purves et al., 2008). During the middle and late third trimester, the frontal lobe, temporal lobe, parietal lobe and occipital lobe gradually undergo secondary and tertiary foliation (Bayer & Altman, 2003). The layout of the human fetal cerebral cortex is already highly similar to the adult brain by the end of pregnancy (Hill, Dierker, et al., 2010; Hill, Inder, et al., 2010; van den Heuvel et al., 2015).

For centuries, neuroscientists have been especially fascinated by the cerebral cortex due to the large size, the unique blueprint of the cortical mantle and by the many connections to all other parts of the brain. The human cortex is relatively large compared to most animals, but the full-grown relative size of the cortex is highly similar to that of kangaroos, primates and elephants (Finlay, 2019). Unique human behavior, cognition and mental illnesses are often attributed to the cerebral cortex or to neural networks including cortical regions. The landscape of the human cortex is mostly comparable to the chimpanzee brain, but is unique among animals and is probably related to the 'advances' in human intelligence (Fernández et al., 2016). There are several hypotheses regarding the driving force behind gyrification and expansion of the primate cortex (Fernández et al., 2016), such as genetic control (Piao et al., 2004; Rakic, 2004), differences in growth of inner and outer cortical layers (Richman et al., 1975) and the link with white matter connectivity (Van Essen, 1997). Further details on these hypotheses are beyond the scope of this thesis, but I will look further into the association between cortical expansion and genetics. The human brain develops to a precise genetic program,

and though research to which genes control human cortical maturation in utero is still in its infancy, it has the potential to help clarify how the human brain works.

VISUALIZING THE BRAIN'S ANATOMY

In vivo quantification and qualification of fetal and neonatal brains is often obtained using cranial ultrasound imaging. Neurosonography is fast and well suited for clinical use in screening and diagnosing fetal or neonatal abnormalities (Govaert & De Vries, 2010; Monteagudo & Timor-Tritsch, 1997; Ruiz et al., 2006; Toi et al., 2004). Building on this fantastic work, fetal MRI is gaining ground to study normal and abnormal fetal brain development in more detail (Bulas & Egloff, 2013; Pistorius et al., 2008; Plunk & Chapman, 2014a, 2014b).
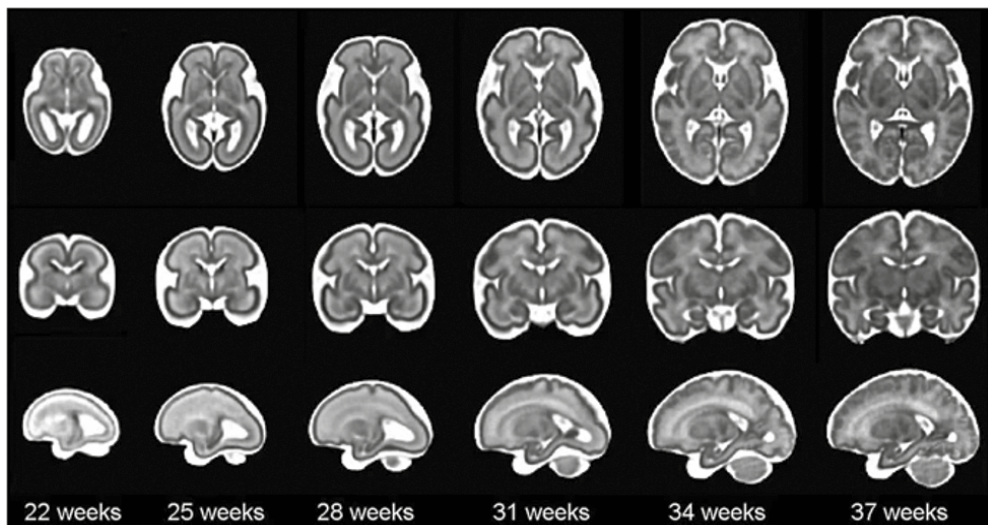
Figure 2. Structural MRI of the developing fetal brain
Displayed are normalized fetal brain images at six time points: 22, 25, 28, 31, 34, and 37 gestational weeks. Each age point includes an axial, coronal, and sagittal view of a T2-weighted MRI. Figure is reproduced from Gholipour et al. (2017), under the terms of the Creative Commons CC BY license.

Fetal MRI
Recent advances in fetal MRI and its post-processing computational methods (Clouchoux et al., 2012; Gholipour et al., 2010; Gholipour et al., 2017; Rousseau et al., 2006) are able to provide new insights into fetal brain maturation and fulfill a role in diagnosing fetal brain abnormalities in utero (Griffiths et al., 2019). The quality and

resolution of 1.5T or 3T MR images is high and therefore allows clinicians to detect brain abnormalities at an early stage, and also brings the opportunity to quantify volumetric and morphological properties of the fetal brain. Additionally, MRI of the fetal brain offers the opportunity to assess brain function and microstructural integrity of specific brain structures.

Performing a quantitative or qualitative analysis of MR images is challenging and often time consuming, due to maternal and fetal motion during the MRI and inhomogeneity due to the maternal tissue surrounding the fetus (Khalili, Turk, et al., 2019). In short, structural fetal imaging usually starts with quality inspection and only images without severe motion artifacts are selected and corrected for intensity non-homogeneity (Howell et al., 2019; Khalili, Lessmann, et al., 2019), followed by motion correction to reduce the effects of interslice motion to facilitate more detailed brain visualization (Gholipour et al., 2011; Rousseau et al., 2006; Rousseau et al., 2010). Accurate segmentation of the brain into tissue classes is the foundation of fetal MRI and can provide a tool for volumetric and morphologic analysis (Clouchoux et al., 2012). In both fetal and preterm neonatal imaging, automatic segmentation often requires time-consuming manual correction (using e.g., the ITK-SNAP software (Yushkevich et al., 2006)) in order to be able to extract essential data such as total brain volume (Andescavage et al., 2017; Ber et al., 2017; Clouchoux et al., 2012; Gholipour et al., 2017; Griffiths et al., 2019 2; Grossman et al., 2006).

Volumetric brain growth
By establishing normal volumes of the various fetal brain regions, we can identify normal margins of brain growth. Pioneering fetal MRI studies examined fetal brain growth during the third trimester of pregnancy, showing an absolute increase in all tissue classes and brain structures (e.g., total brain, cerebrum, cerebellum, brainstem, extra and intra cerebrospinal fluid (CSF) (Andescavage et al., 2017; Clouchoux et al., 2012; Grossman et al., 2006). Further parcellation of the CSF revealed a two-fold increase during the second half of gestation, whereby the absolute volume seemed to decrease after 30 gestational weeks onward in female fetuses only (You et al., 2016). Apart from the lateral ventricle, no gender differences are demonstrated in fetal life (Andescavage et al., 2017).

Some signs of left and right asymmetry are observed comparing fetal hemispheres (Andescavage et al., 2017; Ber et al., 2017). Around term, the cerebellar hemisphere, cortical grey matter (GM) and deep subcortical structures have larger volumes on the left when compared to right (Andescavage et al., 2017; Ber et al., 2017). This is possibly maintained after birth, since the left cerebellar hemisphere is larger than the right in both infants and adults (Bernard & Seidler, 2013; Holland et al., 2014). Furthermore, when investigating the growth rates of various brain structures, most rapid growth is found in

the cerebellum, fetal WM, cortical GM, deep subcortical structures and total CSF, respectively (Andescavage et al., 2017). No additional gender or asymmetry differences were found, although such a comparison is often not incorporated in analyses (Clouchoux et al., 2012; Griffiths et al., 2019; Grossman et al., 2006; Jarvis et al., 2019).

Cortical folding and expansion
During the last trimester of pregnancy, especially cortical white and gray matter undergo impressive morphological transformations. The cortical surface increases enormously and results in complex folding and gyrification of the cortical mantle. Hereby, more neurons can be packed in a smaller space. The fetal folding process covers three stages; primary sulci are developed around 14 weeks of gestational age (GA), secondary sulci around 32 weeks GA and tertiary sulci from 39 weeks GA (Chi et al., 1977). Gyrification rapidly accelerates between 25 and 30 weeks of gestation, with a peak observed in all
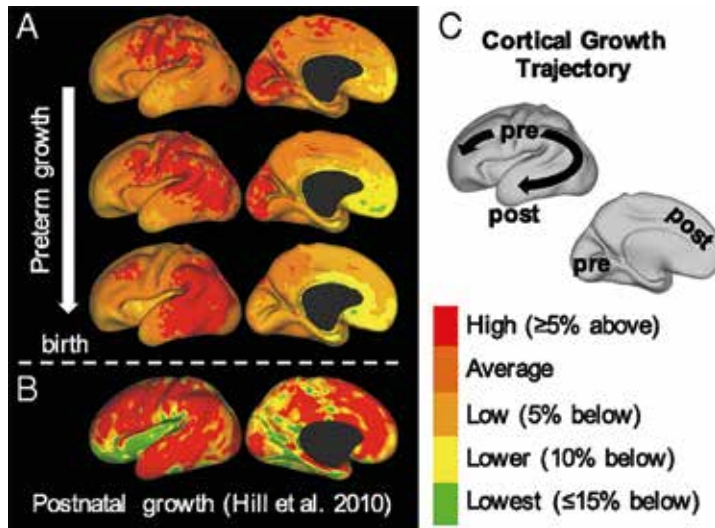
Figure 3. Cortical expansion of the preterm infant brain.
Figure shows the trajectory of cortical growth (A) of preterm infants between postmenstrual week 28 and 38, and (B) from term equivalent age till adult age (Garcia et al., 2018). Panel A displays data from Garcia et al. (2018), showing that highest cortical expansion (in red) migrates from the central sulcus to nearby regions into parietal and then to frontal and temporal regions. Panel B shows data from Hill et al. (2010), reporting on highest expansion rates in parietal, temporal, and frontal lobes, and lowest (green and yellow) in insular and visual cortex. Panel C illustrates the trajectory of the maximum growth. With 'pre' indicating prenatal or preterm and 'post' postnatal development. Figure is reproduced from Garcia et al. (2018), under the license of PNAS for non-commercial purposes.

lobar regions around 30 weeks of gestation (Garel et al., 2001; Hu et al., 2009; Wright et al., 2014). So far, the temporal order of cortical expansion during the third trimester is described best by an MRI study in preterm born infants (Garcia et al., 2018). Around 28 weeks of gestation, expansion rates are highest around the central sulcus and slowly spread with age to parietal, temporal and frontal lobes.

FUNCTIONAL MRI OF THE FETAL BRAIN

Macroscale changes in brain anatomy reflect immense changes at the cellular level. Less is known about the maturation of functional activity across brain areas before full-term birth. Brain activity during fetal gestation is difficult to measure *in vivo*, but with the increasing availability of high-quality functional MRI (fMRI) it has now become feasible to study fetal functional development in unprecedented detail (Jakab et al., 2014; Schöpf et al., 2012; Thomason et al., 2014; Thomason et al., 2013; Thomason et al., 2015; Thomason et al., 2018; Thomason et al., 2019; Wheelock et al., 2019).

Functional connectivity
Functional MR imaging generally refers to the imaging of brain activation, detectable by macroscale changes in cerebral blood flow (ratio of oxyhemoglobin to deoxyhemoglobin) over time. Functional activity of the fetal brain is usually measured during 'rest' without providing external stimuli or tasks. With fMRI, we are able to map circuitry by measuring functional connectivity as the level of co-activation between separated brain regions (van den Heuvel & Hulshoff Pol, 2010).

In the fetal brain, first activity can be observed around week 16 of gestation, when synapses rapidly form and enable neurons to become active (Sidman & Rakic, 1973). Fetal functional connectivity can be detected using fMRI around 20 weeks of gestation (Thomason et al., 2013), making it possible to measure spontaneous activity and to attain information about the neurophysiological correlates of these spontaneous activation patterns (Schöpf et al., 2012).

As with structural fetal MRI, fMRI studies in the fetal brain are challenging due to maternal and fetal motion and the lack of automatic software developments. A number of pioneering studies have successfully investigated fetal functional connectivity and revealed some new insights into fetal functional brain development. In healthy fetuses, cerebellar-cerebral, cortico-cortical, intra-hemispheric and cross-hemispheric connections were found to increase with GA (Thomason et al., 2015), with a linear increase for long range connections (Jakab et al., 2014). Functional synchrony peaks emerge at distinctive timetables for different cortical lobes in a posterior to anterior pattern. The peaks can be found at 24.8 gestational weeks for the occipital lobe, 26 gestational weeks for temporal lobe, 26.4 gestational weeks for the frontal lobe and 27.5 gestational weeks

for the parietal lobe (Jakab et al., 2014), which is in line with the pattern of white matter maturation measured in preterm infants (Childs et al., 1998) and matches the order of myelogenesis in fetal and neonatal specimens (Flechsig, 1920). Similarly, a medial to lateral sequence of functional development was found, suggesting development from short midline connections to more long-range connections throughout the brain (Schöpf et al., 2012; Thomason et al., 2013). The posterior cingulate cortex (PCC) was most strongly related to other brain regions in fetuses (Thomason et al., 2013), as also observed in adults and infants (Gao et al., 2009), possibly indicating an important, and therefore perhaps vulnerable region in development.

Functional Connectome
Healthy brain function, cognition, motor function, memory performance and personality
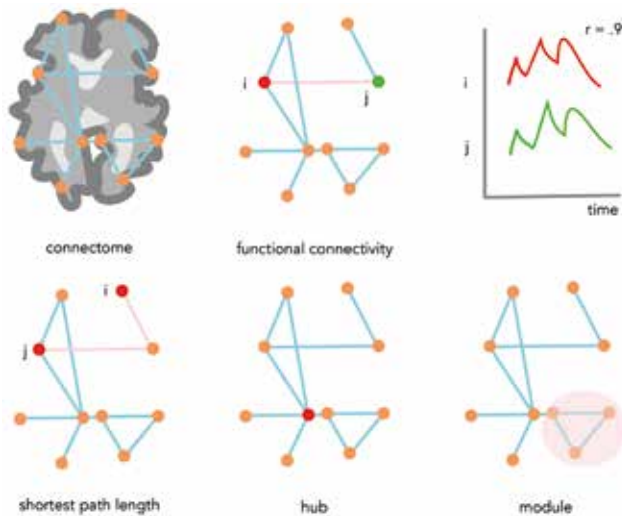
Figure 4. A simplified representation of the neural connectome.
On a macroscale, the connectome contains large brain regions and the axonal connections between them. Different metrics of network organization of the connectome can be analyzed using graph theory. Functional connectivity is displayed next to the connectome. The temporal correlation of the time-series of node i and j represents a functional 'connection' (in light red) with a correlation of 0.9. In the lower left panel, the shortest path length is displayed. Shortest path length can be defined as the average travel distance between node i and j. Additionally, global efficiency of the network is defined as the inverse of the total average shortest path length. In the lower middle panel, a hub node of the network is displayed in red. This node has a high number of connections and is therefore suggested to have an important role in the network. On the lower right panel, a module of strongly interconnected regions (and sparsely connected to other parts of the network) is displayed in the red circle.

traits are not entirely attributable to the properties of certain subsets of brain regions or the specific connections between them. Instead, brain function arises from how the brain is wired and functions as an integrated whole (Bullmore & Sporns, 2009). All connections of the brain can together be described as a connectome, representing a complex network of distinct brain regions (nodes), that communicate through axonal and dendritic wiring (edges) (Sporns, 2013; Sporns et al., 2005). The functional connectome describes the dynamic interactions within a complex network of the brain including all communication paths and subnetworks (i.e., modules) (van den Heuvel & Sporns, 2011), and has a structural basis (Greicius, 2008; van den Heuvel et al., 2009).

The neural connectome displays global overlap between individuals (Bullmore & Sporns, 2009) and is wired for efficient local information processing and global integration of information, facilitated by the network's nodes and edges (Bullmore & Sporns, 2009). Important themes exploring the connectome include the detection of node influence or vulnerability within the network, by identifying hubs or the rich club (Harriger et al., 2012; van den Heuvel & Sporns, 2011). Hubs are central nodes with a high degree of connections, that have high influence on network dynamics and are focal points of communication. The rich club is a backbone of the network that can be identified when hubs have the tendency to highly interconnect, and that supports neural information integration across brain systems (Opsahl & Panzarasa, 2009; van den Heuvel et al., 2012).

Linking micro- to macroscale properties
Region-to-region functional connectivity is established by neuron-to-neuron interactions. In the adult brain, we start to unravel the underlying construct of large-scale functional connectivity patterns. Microscale cytoarchitectonic properties of the brain, such as neuron density and dendritic tree branching (Scholtens et al., 2014; van den Heuvel et al., 2015; Wei, de Lange, et al., 2019), and the excitatory or inhibitory chemoarchitecture (receptors) (van den Heuvel et al., 2016), can be indicative for large-scale structural and functional connectivity patterns. An example of micro and macroscale analysis in the fetal brain can be found by a study of Vasung et al. (2010). This group showed that diffusion tensor imaging reinforces our knowledge on axonal pathway development that we acquired by histology and vice versa (Vasung et al., 2010).

It is believed that large-scale connectome organization depends also on molecular function that can be estimated through gene expression levels (Thompson et al., 2013). The human genome, our DNA, remains the same across the lifespan, still the fetal brain is completely different from the adult brain. DNA is translated differently throughout life and therefore genes fulfill distinct roles in each developmental stage (Miller et al., 2014). The human transcriptome comprises information on the great variety of gene transcriptional profiles, i.e., the variation and amount of RNA molecules in cells that are transcribed throughout the brain. The human transcriptome may therefore bring

new opportunities to study genetic translations in the adult (Hawrylycz et al., 2012) and fetal (Miller et al., 2014) brain in more detail. Indeed, mapping gene expression levels to the connectome, studies show differences on both levels of organization in health and disease (Romme et al., 2017). I therefore believe that multimodal connectomics (or neuroimaging in general) could contribute to a more complete fundamental understanding of brain organization (Wei, Scholtens, et al., 2019), especially during development.

Connectome development

Connectomics is one of the many promising topics in the field of fetal and neonatal MRI, enabling the mapping of structural and functional networks during perinatal brain development. The structural foundation of the connectome develops in utero (Collin et al., 2015), cellularly, but also on a macroscale level by large axonal bundles identifiable using fetal DTI (Bui et al., 2006; Hooker et al., 2020; Kasprian et al., 2008; Khan et al., 2019; Mitter, Jakab, et al., 2015; Mitter, Prayer, et al., 2015; Righini et al., 2003; Schneider et al., 2007; Schneider et al., 2009; Song et al., 2017; Yu et al., 2016; Zanin et al., 2011). From mid gestation to birth, thalamo-cortical and cross-hemispheric commissural fibers extend to the cortex and long-range association fibers expand within each hemisphere
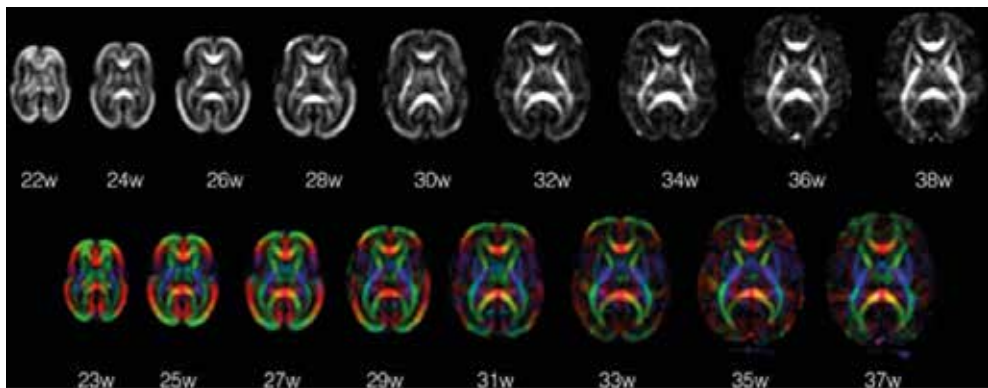
Figure 5. DTI of the fetal brain.

The figure shows DTI scans from healthy fetuses scanned at a gestational age between 21 and 39 weeks (Khan et al., 2019). The upper panel shows gray-scale FA (fractional anisotropy) maps which are based on the amount of diffusion asymmetry within a voxel, with brighter areas are more anisotropic than darker areas. The lower panel shows colored fractional anisotropy maps that are indicative for fiber directions. Red, green and blue represent the x, y and z diffusion directions respectively. Khan et al. show an age-related increase in FA for projection pathways during late second and early third trimesters. Figure is reproduced from Khan et al. (2019) with permission from Elsevier.

(Bui et al., 2006; Kasprian et al., 2008; Khan et al., 2019; Mitter, Jakab, et al., 2015; Mitter et al., 2011; Schneider et al., 2007; Song et al., 2017). The structural building blocks of the early connectome develop over time, presumably forming the foundation for the functional connectome (van den Heuvel et al., 2015). However, research on 'when' and 'how' the functional connectome develops over time is still in its infancy.

Driven by connectional reinforcement and cellular maturation, the human neural connectome develops in utero and is shaped across the lifespan (Collin & van den Heuvel, 2013; Hagmann et al., 2010). The infant brain shows similar -but immature- forms of resting-state fMRI networks, including those important for primary functions (e.g., visual, sensorimotor and auditory), and those for higher-order functions, such as: attention, executive function, memory and self-awareness (Damoiseaux et al., 2006; Yeo et al., 2011). The neonatal connectome has been studied by diffusion tensor imaging (DTI) studies showing that the infrastructure of major white matter pathways is in place after birth (Ball et al., 2014; Brown et al., 2014; Keunen et al., 2018), possibly forming the foundation for adult-like functional networks (Lariviere et al., 2020; van den Heuvel et al., 2015) identified using resting-state fMRI (Fransson et al., 2007; Gao et al., 2009; Smyser et al., 2010). Interestingly, fetal neural network development is highly dynamic, occurs in a relatively short period of time and can since recently be studied through fetal neuroimaging. Immature forms of functional resting state networks have already been found in the motor, visual, thalamic, frontal, temporal and even the default mode network by mid gestation (Jakab et al., 2014; Thomason et al., 2014), with a shift of a portion of inter-modular connections to more intra-modular links (Thomason et al., 2015). Maturational differences between connectomic fingerprints in the fetal period and across childhood presumably underlie changes in and reinforcement of brain functions, though more research is needed to confirm this notion.

Moreover, connectional abnormalities in neural networks, as well as alterations in global and modular network organization, have been observed in many psychiatric and neurodevelopmental disorders (Collin et al., 2016; Craddock et al., 2013). Thus, the functional topography of these systems is highly relevant to cognitive processes and health. An important question is whether these connectomic alterations are congenital in origin, or acquired during development (Di Martino et al., 2014). To address these topics, considerably more needs to be discovered about fetal normative developmental properties of the human connectome (Jakab, 2019).

PRETERM BORN NEONATES

Brain development during the last trimester is more frequently studied using MRI in 'healthy' preterm infants. However, the extent to which the brain can be directly compared between fetuses and preterm infants remains unclear, even in the absence of structural brain injury (Bouyssi-Kobar et al., 2016; Brossard-Racine et al., 2014; Dubois et al., 2008),

since the preterm ex-utero environment has been shown to negatively affect brain development. These differences might be caused by stressful admittance (with clinical complications) to the neonatal intensive care unit (NICU) (Smith et al., 2011), pain exposure (Brummelte et al., 2012; Ranger & Grunau, 2014), early sensory stimuli exposure (Wolke, 1987) and lacking placental intrauterine signals, such as nutrients (e.g., cholesterol) and hormones (e.g., intrauterine growth factor) (Elitt & Rosenberg, 2014).

The preterm brain is particularly vulnerable to early developmental insults that are common in preterm birth, including white matter or cerebellar injury (Ortinau & Neil, 2015; Stoodley & Limperopoulos, 2016; Volpe, 2009b). Available evidence suggests that premature exposure to the extra-uterine environments disrupts the normal developmental course of the brain. Alterations in the structural and functional connectome, decreased white matter volume and cerebellar growth impairment are increasingly detected in survivors of prematurity (Brossard-Racine et al., 2017; de Kieviet et al., 2012). Additionally, longitudinal studies show that preterm born neonates are at greater risk of developing neurodevelopmental deficits and psychiatric disorders than full-term born neonates, even without evidence of macroscopic brain injuries (Ortinau & Neil, 2015; Volpe, 2009a).

Neuroanatomical differences
Literature suggests that preterm infants show divergent volumetric neurodevelopmental growth. For example, the preterm infant brain shows relative (ratio of structure's volume to the total brain volume) decreases in white matter, deep gray matter (basal ganglia and thalami) and intracerebral CSF volumes between 27 and 45 weeks after conception (Makropoulos et al., 2016), while these regions and tissues relatively increase in healthy fetuses with age (Andescavage et al., 2017). Some differences of absolute brain volumes between fetuses and preterm neonates have been pointed out as well. White matter volume at 29 gestation weeks in fetuses (80 cm3) (Andescavage et al., 2017) was bigger compared to preterm infants (50 cm3) (Lefèvre et al., 2015), although similar rates of increase were found. Additionally, absolute larger deep gray matter and cortical gray matter volumes were found in fetuses (Andescavage et al., 2017), when compared to premature infants (Kuklisova-Murgasova et al., 2011). Few cross-sectional studies have directly compared fetal and preterm neonatal brain development using structural MRI. Bouyssi-Kobar et al. (2016) segmented the cerebrum, cerebellum, brainstem, and intracranial cavity in 75 preterm infants and 130 fetuses (GWs: 27-39) (Bouyssi-Kobar et al., 2016). As indicated before (Andescavage et al., 2017; Kuklisova-Murgasova et al., 2011; Lefèvre et al., 2015; Limperopoulos et al., 2005), significantly smaller and slower brain growth in very preterm infants was shown, when compared to fetuses (Bouyssi-Kobar et al., 2016). This study had some intrinsic limitations, since they included participants from two centers with different MRI scanners with different field strengths (1.5T/3T) and probably with differences in clinical care. Additionally, they used cross-sectional cohorts, making it difficult to describe brain growth.

OUTLINE OF THESIS

MR imaging of the fetus and neonate has the potential to assess the earliest point of neural maturation and provide insight into the patterning and sequence of normal and abnormal brain development in the perinatal period. MRI research on fetal brain development is however sparse. There is a growing need for automatic analyzing programs and healthy longitudinal high-quality fetal MR images, which can be representative for normal fetal brain development. By mapping structural volumetric brain development and by establishing normal functional patterns in the fetus we can identify abnormal patterns in preterm neonates who might have a higher risk of functional disabilities such as cognitive impairment later in life (Johnson et al., 2009). The availability of normative indices of cerebral cortex development in the healthy fetus may provide critical insights on the timing and progression of neurodevelopmental impairments in the high-risk fetus and preterm born infants (Clouchoux et al., 2012). Eventually, this may facilitate earlier diagnosis and intervention (Wright et al., 2014). In this thesis, I contribute to the field of advanced fetal brain MRI by studying multiple modalities of the fetal and neonatal brain from 20 weeks of gestation, including structural and functional MRI, the transcriptome and connectome, and the link with cortical chemoarchitecture.

In **chapter 2** I will examine the poorly understood multimodal relationship between fetal cortical expansion and gene expression profiles. By mapping cortical landscape development using fetal MRI and gene expression profiles of fetuses, potential new functional roles of genes can be detected that drive cortical expansion during late prenatal development.

A comprehensive study of the fetal functional connectome and its overlap with the adult connectome is missing from literature. In a unique new study where I got the opportunity to work with fetal MRI pioneer Dr. Thomason, we provide a first in-depth overview of the fetal cortical functional connectome, the results of which I present in **chapter 3**. I further examine fetal brain hubs in **chapter 4** of this thesis using fetal fMRI of healthy pregnant volunteers. Part of the process of functional connectome reconstruction is to understand how functional patterns are established based on the underlying neuro-anatomical construct. I aim to shed light on this concept in **chapter 5**, by studying the relation between chemoarchitecture and induced functional connectivity across cortical areas, as examined by using animal data.

The second part of this thesis contains perinatal MRI data of preterm born infants hospitalized and scanned at the Wilhelmina Children's hospital, University Medical Center Utrecht, and longitudinal scanned healthy fetuses and neonates from the YOUth cohort (youthonderzoek.nl, Onland-Moret et al. 2020). Dr. Manon Benders, dr. Roel de Heus, the study-team and I gathered healthy longitudinal pre- and postnatal MRI scans

to observe early (micro)structural and functional brain development in healthy fetuses and neonates. The additional benefit of healthy fetal MRI is that it can be used as a control group in patient-control studies, such as preterm born neonates or infants with a congenital heart defect. In **chapter 6**, I will give an example of our in-house developed semi-automated method to explore perinatal structural MRI data. To this date, a longitudinal overview of structural volumetric differences of brain regions between healthy fetal and preterm neonatal at the third trimester of pregnancy is missing from literature. Therefore, I explore intra- and extrauterine developmental trajectories by comparing fetal brain growth differences in healthy fetal and neonatal scans in 'YOUth' infants and extremely preterm born neonates in **chapter 7**.

REFERENCES

Aguilar-Valles, A., Rodrigue, B., & Matta-Camacho, E. (2020, 2020-August-21). Maternal Immune Activation and the Development of Dopaminergic Neurotransmission of the Offspring: Relevance for Schizophrenia and Other Psychoses [Mini Review]. Front Psychiatry, 11(852), 852. https://doi. org/10.3389/fpsyt.2020.00852

Anderson, A. L., & Thomason, M. E. (2013, Nov). Functional plasticity before the cradle: a review of neural functional imaging in the human fetus. Neurosci Biobehav Rev, 37(9 Pt B), 2220-2232. https:// doi.org/10.1016/j.neubiorev.2013.03.013

Andescavage, N. N., du Plessis, A., McCarter, R., Serag, A., Evangelou, I., Vezina, G., Robertson, R., & Limperopoulos, C. (2017, Nov 1). Complex Trajectories of Brain Development in the Healthy Human Fetus. Cereb Cortex, 27(11), 5274-5283. https://doi.org/10.1093/cercor/bhw306

Ball, G., Aljabar, P., Zebari, S., Tusor, N., Arichi, T., Merchant, N., Robinson, E. C., Ogundipe, E., Rueckert, D., Edwards, A. D., & Counsell, S. J. (2014, May 20). Rich-club organization of the newborn human brain. Proc Natl Acad Sci U S A, 111(20), 7456-7461. https://doi.org/10.1073/pnas.1324118111

Bayer, S. A., & Altman, J. (1991). Neocortical development (Vol. 1). Raven Press New York.

Bayer, S. A., & Altman, J. (2003). The human brain during the third trimester. CRC Press.

Ber, R., Hoffman, D., Hoffman, C., Polat, A., Derazne, E., Mayer, A., & Katorza, E. (2017, Nov). Volume of Structures in the Fetal Brain Measured with a New Semiautomated Method. AJNR Am J Neuroradiol, 38(11), 2193-2198. https://doi.org/10.3174/ajnr.A5349

Bernard, J. A., & Seidler, R. D. (2013, Oct). Relationships between regional cerebellar volume and sensorimotor and cognitive function in young and older adults. Cerebellum, 12(5), 721-737. https://doi. org/10.1007/s12311-013-0481-z

Bouyssi-Kobar, M., du Plessis, A. J., McCarter, R., Brossard-Racine, M., Murnick, J., Tinkleman, L., Robertson, R. L., & Limperopoulos, C. (2016, Nov). Third Trimester Brain Growth in Preterm Infants Compared With In Utero Healthy Fetuses. Pediatrics, 138(5), e20161640. https://doi.org/10.1542/peds.2016-1640

Brossard-Racine, M., du Plessis, A. J., Vezina, G., Robertson, R., Bulas, D., Evangelou, I. E., Donofrio, M., Freeman, D., & Limperopoulos, C. (2014, Aug). Prevalence and spectrum of in utero structural brain abnormalities in fetuses with complex congenital heart disease. AJNR Am J Neuroradiol, 35(8), 1593-1599. https://doi.org/10.3174/ajnr.A3903

Brossard-Racine, M., Poretti, A., Murnick, J., Bouyssi-Kobar, M., McCarter, R., du Plessis, A. J., & Limperopoulos, C. (2017, Mar). Cerebellar Microstructural Organization is Altered by Complications of Premature Birth: A Case-Control Study. J Pediatr, 182, 28-33 e21. https://doi.org/10.1016/j.jpeds.2016.10.034

Brown, C. J., Miller, S. P., Booth, B. G., Andrews, S., Chau, V., Poskitt, K. J., & Hamarneh, G. (2014, Nov 1). Structural network analysis of brain development in young preterm neonates. NeuroImage, 101, 667-680. https://doi.org/10.1016/j.neuroimage.2014.07.030

Brummelte, S., Grunau, R. E., Chau, V., Poskitt, K. J., Brant, R., Vinall, J., Gover, A., Synnes, A. R., & Miller, S. P. (2012, Mar). Procedural pain and brain development in premature newborns. Ann Neurol, 71(3), 385-396. https://doi.org/10.1002/ana.22267

Bui, T., Daire, J. L., Chalard, F., Zaccaria, I., Alberti, C., Elmaleh, M., Garel, C., Luton, D., Blanc, N., & Sebag, G. (2006, Nov). Microstructural development of human brain assessed in utero by diffusion tensor imaging. Pediatr Radiol, 36(11), 1133-1140. https://doi.org/10.1007/s00247-006-0266-3

Bulas, D., & Egloff, A. (2013, Oct). Benefits and risks of MRI in pregnancy. Semin Perinatol, 37(5), 301-304. https://doi.org/10.1053/j.semperi.2013.06.005

Bullmore, E., & Sporns, O. (2009, Mar). Complex brain networks: graph theoretical analysis of structural and functional systems [10.1038/nrn2575]. Nat Rev Neurosci, 10(3), 186-198. https://doi.org/10.1038/nrn2575

Chen, H. J., Antonson, A. M., Rajasekera, T. A., Patterson, J. M., Bailey, M. T., & Gur, T. L. (2020, Jun 16). Prenatal stress causes intrauterine inflammation and serotonergic dysfunction, and long-term behavioral deficits through microbe- and CCL2-dependent mechanisms. Transl Psychiatry, 10(1), 191. https://doi.org/10.1038/s41398-020-00876-5

Chi, J. G., Dooling, E. C., & Gilles, F. H. (1977, Jan). Gyral development of the human brain. Ann Neurol, 1(1), 86-93. https://doi.org/10.1002/ana.410010109

Childs, A. M., Ramenghi, L. A., Evans, D. J., Ridgeway, J., Saysell, M., Martinez, D., Arthur, R., Tanner, S., & Levene, M. I. (1998, May). MR features of developing periventricular white matter in preterm infants: evidence of glial cell migration. AJNR Am J Neuroradiol, 19(5), 971-976. https://www.ncbi.nlm.nih.gov/pubmed/9613523

Clouchoux, C., Kudelski, D., Gholipour, A., Warfield, S. K., Viseur, S., Bouyssi-Kobar, M., Mari, J. L., Evans, A. C., du Plessis, A. J., & Limperopoulos, C. (2012, Jan). Quantitative in vivo MRI measurement of cortical development in the fetus. Brain Struct Funct, 217(1), 127-139. https://doi.org/10.1007/s00429-011-0325-x

Collin, G., de Nijs, J., Pol, H. H., Cahn, W., & van den Heuvel, M. (2015). Connectome organization is related to longitudinal changes in general functioning, symptoms and IQ in chronic schizophrenia. Schizophrenia Research.

Collin, G., Turk, E., & van den Heuvel, M. P. (2016, May). Connectomics in Schizophrenia: From Early Pioneers to Recent Brain Network Findings. Biol Psychiatry Cogn Neurosci Neuroimaging, 1(3), 199-208. https://doi.org/10.1016/j.bpsc.2016.01.002

Collin, G., & van den Heuvel, M. P. (2013, Dec). The ontogeny of the human connectome: development and dynamic changes of brain connectivity across the life span. Neuroscientist, 19(6), 616-628. https://doi.org/10.1177/1073858413503712

Craddock, R. C., Jbabdi, S., Yan, C. G., Vogelstein, J. T., Castellanos, F. X., Di Martino, A., Kelly, C., Heberlein, K., Colcombe, S., & Milham, M. P. (2013, Jun). Imaging human connectomes at the macroscale. Nat Methods, 10(6), 524-539. https://doi.org/10.1038/nmeth.2482

Damoiseaux, J. S., Rombouts, S. A., Barkhof, F., Scheltens, P., Stam, C. J., Smith, S. M., & Beckmann, C. F. (2006, Sep 12). Consistent resting-state networks across healthy subjects. Proc Natl Acad Sci U S A, 103(37), 13848-13853. https://doi.org/10.1073/pnas.0601417103

de Kieviet, J. F., Zoetebier, L., Van Elburg, R. M., Vermeulen, R. J., & Oosterlaan, J. (2012). Brain development of very preterm and very low-birthweight children in childhood and adolescence: A meta-analysis. Developmental Medicine & Child Neurology, 54(4), 313-323.

Di Martino, A., Fair, D. A., Kelly, C., Satterthwaite, T. D., Castellanos, F. X., Thomason, M. E., Craddock, R. C., Luna, B., Leventhal, B. L., Zuo, X. N., & Milham, M. P. (2014, Sep 17). Unraveling the miswired connectome: a developmental perspective. Neuron, 83(6), 1335-1353. https://doi.org/10.1016/j.neuron.2014.08.050

Dong, J., Lei, J., Elsayed, N. A., Lee, J. Y., Shin, N., Na, Q., Chudnovets, A., Jia, B., Wang, X., & Burd, I. (2020, May). The effect of intrauterine inflammation on mTOR signaling in mouse fetal brain. Dev

Neurobiol, 80(5-6), 149-159. https://doi.org/10.1002/dneu.22755

Dubois, J., Benders, M., Cachia, A., Lazeyras, F., Ha-Vinh Leuchter, R., Sizonenko, S. V., Borradori-Tolsa, C., Mangin, J. F., & Huppi, P. S. (2008, Jun). Mapping the early cortical folding process in the preterm newborn brain. Cereb Cortex, 18(6), 1444-1454. https://doi.org/10.1093/cercor/bhm180

Elitt, C. M., & Rosenberg, P. A. (2014, Sep 12). The challenge of understanding cerebral white matter injury in the premature infant. Neuroscience, 276, 216-238. https://doi.org/10.1016/j.neuroscience.2014.04.038

Fernández, V., Llinares-Benadero, C., & Borrell, V. (2016). Cerebral cortex expansion and folding: what have we learned? The EMBO journal, 35(10), 1021-1044.

Finlay, B. L. (2019, Apr). Human exceptionalism, our ordinary cortex and our research futures. Dev Psychobiol, 61(3), 317-322. https://doi.org/10.1002/dev.21838

Flechsig, P. E. (1920). Anatomie des menschlichen Gehirns und Rückenmarks auf myelogenetischer Grundlage (Vol. 1). G. Thieme.

Fransson, P., Skiold, B., Horsch, S., Nordell, A., Blennow, M., Lagercrantz, H., & Aden, U. (2007, Sep 25). Resting-state networks in the infant brain. Proc Natl Acad Sci U S A, 104(39), 15531-15536. https://doi.org/10.1073/pnas.0704380104

Gao, W., Zhu, H., Giovanello, K. S., Smith, J. K., Shen, D., Gilmore, J. H., & Lin, W. (2009, Apr 21). Evidence on the emergence of the brain's default network from 2-week-old to 2-year-old healthy pediatric subjects. Proc Natl Acad Sci U S A, 106(16), 6790-6795. https://doi.org/10.1073/pnas.0811221106

Garcia, K. E., Robinson, E. C., Alexopoulos, D., Dierker, D. L., Glasser, M. F., Coalson, T. S., Ortinau, C. M., Rueckert, D., Taber, L. A., Van Essen, D. C., Rogers, C. E., Smyser, C. D., & Bayly, P. V. (2018, Mar 20). Dynamic patterns of cortical expansion during folding of the preterm human brain. Proc Natl Acad Sci U S A, 115(12), 3156-3161. https://doi.org/10.1073/pnas.1715451115

Garel, C., Chantrel, E., Brisse, H., Elmaleh, M., Luton, D., Oury, J. F., Sebag, G., & Hassan, M. (2001, Jan). Fetal cerebral cortex: Normal gestational landmarks identified using prenatal MR imaging. American Journal of Neuroradiology, 22(1), 184-189.

Gholipour, A., Estroff, J. A., Barnewolt, C. E., Connolly, S. A., & Warfield, S. K. (2011, May). Fetal brain volumetry through MRI volumetric reconstruction and segmentation. Int J Comput Assist Radiol Surg, 6(3), 329-339. https://doi.org/10.1007/s11548-010-0512-x

Gholipour, A., Estroff, J. A., & Warfield, S. K. (2010, Oct). Robust super-resolution volume reconstruc-

tion from slice acquisitions: application to fetal brain MRI. *IEEE Trans Med Imaging, 29(10), 1739-1758.* https://doi.org/10.1109/TMI.2010.2051680

Gholipour, A., Rollins, C. K., Velasco-Annis, C., Ouaalam, A., Akhondi-Asl, A., Afacan, O., Ortinau, C. M., Clancy, S., Limperopoulos, C., Yang, E., Estroff, J. A., & Warfield, S. K. (2017, Mar 28). A normative spatiotemporal MRI atlas of the fetal brain for automatic segmentation and analysis of early brain growth. *Sci Rep, 7(1), 476.* https://doi.org/10.1038/s41598-017-00525-w

Govaert, P., & De Vries, L. S. (2010). *An atlas of neonatal brain sonography* (Vol. 182). John Wiley & Sons.

Greicius, M. (2008, Aug). Resting-state functional connectivity in neuropsychiatric disorders. *Curr Opin Neurol, 21(4), 424-430.* https://doi.org/10.1097/WCO.0b013e328306f2c5

Griffiths, P. D., Mousa, H. A., Finney, C., Mooney, C., Mandefield, L., Chico, T. J. A., & Jarvis, D. (2019, May). An integrated in utero MR method for assessing structural brain abnormalities and measuring intracranial volumes in fetuses with congenital heart disease: results of a prospective case-control feasibility study. *Neuroradiology, 61(5), 603-611.* https://doi.org/10.1007/s00234-019-02184-2

Grossman, R., Hoffman, C., Mardor, Y., & Biegon, A. (2006, Nov 1). Quantitative MRI measurements of human fetal brain development in utero. *NeuroImage, 33(2), 463-470.* https://doi.org/10.1016/j.neuroimage.2006.07.005

Hagmann, P., Sporns, O., Madan, N., Cammoun, L., Pienaar, R., Wedeen, V. J., Meuli, R., Thiran, J. P., & Grant, P. E. (2010, Nov 2). White matter maturation reshapes structural connectivity in the late developing human brain. *Proc Natl Acad Sci U S A, 107(44), 19067-19072.* https://doi.org/10.1073/pnas.1009073107

Harriger, L., van den Heuvel, M. P., & Sporns, O. (2012). Rich club organization of macaque cerebral cortex and its role in network communication. *PLoS One, 7(9), e46497.* https://doi.org/10.1371/journal.pone.0046497

Hawrylycz, M. J., Lein, E. S., Guillozet-Bongaarts, A. L., Shen, E. H., Ng, L., Miller, J. A., van de Lagemaat, et al. (2012, Sep 20). An anatomically comprehensive atlas of the adult human brain transcriptome. *Nature, 489(7416), 391-399.* https://doi.org/10.1038/nature11405

Hill, J., Dierker, D., Neil, J., Inder, T., Knutsen, A., Harwell, J., Coalson, T., & Van Essen, D. (2010, Feb 10). A surface-based analysis of hemispheric asymmetries and folding of cerebral cortex in term-born human infants. *J Neurosci, 30(6), 2268-2276.* https://doi.org/10.1523/JNEUROSCI.4682-09.2010

Hill, J., Inder, T., Neil, J., Dierker, D., Harwell, J., & Van Essen, D. (2010, Jul 20). Similar patterns of

cortical expansion during human development and evolution. *Proc Natl Acad Sci U S A, 107(29)*, 13135-13140. https://doi.org/10.1073/pnas.1001229107

Holland, D., Chang, L., Ernst, T. M., Curran, M., Buchthal, S. D., Alicata, D., Skranes, J., Johansen, H., Hernandez, A., Yamakawa, R., Kuperman, J. M., & Dale, A. M. (2014, Oct). Structural growth trajectories and rates of change in the first 3 months of infant brain development. *JAMA Neurol, 71(10)*, 1266-1274. https://doi.org/10.1001/jamaneurol.2014.1638

Hooker, J. D., Khan, M. A., Farkas, A. B., Lirette, S. T., Joyner, D. A., Gordy, D. P., Storrs, J. M., Roda, M. S., Bofill, J. A., Smith, A. D., & James, J. R. (2020, Jun). Third-trimester in utero fetal brain diffusion tensor imaging fiber tractography: a prospective longitudinal characterization of normal white matter tract development. *Pediatr Radiol, 50(7)*, 973-983. https://doi.org/10.1007/s00247-020-04639-8

Howell, B. R., Styner, M. A., Gao, W., Yap, P. T., Wang, L., Baluyot, K., Yacoub, E., Chen, G., Potts, T., Salzwedel, A., Li, G., Gilmore, J. H., Piven, J., Smith, J. K., Shen, D., Ugurbil, K., Zhu, H., Lin, W., & Elison, J. T. (2019, Jan 15). The UNC/UMN Baby Connectome Project (BCP): An overview of the study design and protocol development. *NeuroImage, 185*, 891-905. https://doi.org/10.1016/j.neuroimage.2018.03.049

Hu, H. H., Guo, W. Y., Chen, H. Y., Wang, P. S., Hung, C. I., Hsieh, J. C., & Wu, Y. T. (2009, Apr). Morphological regionalization using fetal magnetic resonance images of normal developing brains. *Eur J Neurosci, 29(8)*, 1560-1567. https://doi.org/10.1111/j.1460-9568.2009.06707.x

Jakab, A. (2019, Oct). Developmental Pathoconnectomics and Advanced Fetal MRI. *Top Magn Reson Imaging, 28(5)*, 275-284. https://doi.org/10.1097/RMR.0000000000000220

Jakab, A., Schwartz, E., Kasprian, G., Gruber, G. M., Prayer, D., Schopf, V., & Langs, G. (2014). Fetal functional imaging portrays heterogeneous development of emerging human brain networks. *Front Hum Neurosci, 8*, 852. https://doi.org/10.3389/fnhum.2014.00852

Jakovcevski, I., Mo, Z., & Zecevic, N. (2007, Oct 26). Down-regulation of the axonal polysialic acid-neural cell adhesion molecule expression coincides with the onset of myelination in the human fetal forebrain. *Neuroscience, 149(2)*, 328-337. https://doi.org/10.1016/j.neuroscience.2007.07.044

Jarvis, D. A., Finney, C. R., & Griffiths, P. D. (2019, Jul). Normative volume measurements of the fetal intra-cranial compartments using 3D volume in utero MR imaging. *Eur Radiol, 29(7)*, 3488-3495. https://doi.org/10.1007/s00330-018-5938-5

Johnson, M. B., Kawasawa, Y. I., Mason, C. E., Krsnik, Z., Coppola, G., Bogdanovic, D., Geschwind, D. H., Mane, S. M., State, M. W., & Sestan, N. (2009, May 28). Functional and evolutionary insights into human brain development through global transcriptome analysis. *Neuron, 62(4)*, 494-509. https://

doi.org/10.1016/j.neuron.2009.03.027

Kandel, E. R., Schwartz, J. H., & Jessell, T. M. (2000). Principles of neural science (Vol. 4). McGraw-Hill New York.

Kasprian, G., Brugger, P. C., Weber, M., Krssak, M., Krampl, E., Herold, C., & Prayer, D. (2008, Nov 1). In utero tractography of fetal white matter development. NeuroImage, 43(2), 213-224. https://doi.org/10.1016/j.neuroimage.2008.07.026

Keunen, K., van der Burgh, H. K., de Reus, M. A., Moeskops, P., Schmidt, R., Stolwijk, L. J., de Lange, S. C., Isgum, I., de Vries, L. S., Benders, M. J., & van den Heuvel, M. P. (2018, Dec). Early human brain development: insights into macroscale connectome wiring. Pediatr Res, 84(6), 829-836. https://doi.org/10.1038/s41390-018-0138-1

Khalili, N., Lessmann, N., Turk, E., Claessens, N., Heus, R., Kolk, T., Viergever, M. A., Benders, M., & Isgum, I. (2019, Dec). Automatic brain tissue segmentation in fetal MRI using convolutional neural networks. Magn Reson Imaging, 64, 77-89. https://doi.org/10.1016/j.mri.2019.05.020

Khalili, N., Turk, E., Benders, M., Moeskops, P., Claessens, N. H. P., de Heus, R., Franx, A., Wagenaar, N., Breur, J., Viergever, M. A., & Isgum, I. (2019). Automatic extraction of the intracranial volume in fetal and neonatal MR scans using convolutional neural networks. Neuroimage Clin, 24, 102061. https://doi.org/10.1016/j.nicl.2019.102061

Khan, S., Vasung, L., Marami, B., Rollins, C. K., Afacan, O., Ortinau, C. M., Yang, E., Warfield, S. K., & Gholipour, A. (2019, Jan 15). Fetal brain growth portrayed by a spatiotemporal diffusion tensor MRI atlas computed from in utero images. NeuroImage, 185, 593-608. https://doi.org/10.1016/j.neuroimage.2018.08.030

Kidokoro, H., Anderson, P. J., Doyle, L. W., Woodward, L. J., Neil, J. J., & Inder, T. E. (2014, Aug). Brain injury and altered brain growth in preterm infants: predictors and prognosis. Pediatrics, 134(2), e444-453. https://doi.org/10.1542/peds.2013-2336

Kuklisova-Murgasova, M., Aljabar, P., Srinivasan, L., Counsell, S. J., Doria, V., Serag, A., Gousias, I. S., Boardman, J. P., Rutherford, M. A., Edwards, A. D., Hajnal, J. V., & Rueckert, D. (2011, Feb 14). A dynamic 4D probabilistic atlas of the developing brain. NeuroImage, 54(4), 2750-2763. https://doi.org/10.1016/j.neuroimage.2010.10.019

Lariviere, S., Vos de Wael, R., Hong, S. J., Paquola, C., Tavakol, S., Lowe, A. J., Schrader, D. V., & Bernhardt, B. C. (2020, Jan 10). Multiscale Structure-Function Gradients in the Neonatal Connectome. Cereb Cortex, 30(1), 47-58. https://doi.org/10.1093/cercor/bhz069

Lefèvre, J., Germanaud, D., Dubois, J., Rousseau, F., de Macedo Santos, I., Angleys, H., Mangin, J.-F., Hüppi, P. S., Girard, N., & De Guio, F. (2015). Are Developmental Trajectories of Cortical Folding Comparable Between Cross-sectional Datasets of Fetuses and Preterm Newborns? Cerebral Cortex, bhv123.

Limperopoulos, C., Soul, J. S., Gauvreau, K., Huppi, P. S., Warfield, S. K., Bassan, H., Robertson, R. L., Volpe, J. J., & du Plessis, A. J. (2005, Mar). Late gestation cerebellar growth is rapid and impeded by premature birth. Pediatrics, 115(3), 688-695. https://doi.org/10.1542/peds.2004-1169

Luhmann, H. J., Sinning, A., Yang, J. W., Reyes-Puerta, V., Stuttgen, M. C., Kirischuk, S., & Kilb, W. (2016). Spontaneous Neuronal Activity in Developing Neocortical Networks: From Single Cells to Large-Scale Interactions. Front Neural Circuits, 10, 40. https://doi.org/10.3389/fncir.2016.00040

Makropoulos, A., Aljabar, P., Wright, R., Huning, B., Merchant, N., Arichi, T., Tusor, N., Hajnal, J. V., Edwards, A. D., Counsell, S. J., & Rueckert, D. (2016, Jan 15). Regional growth and atlasing of the developing human brain. NeuroImage, 125, 456-478. https://doi.org/10.1016/j.neuroimage.2015.10.047

Miller, J. A., Ding, S. L., Sunkin, S. M., Smith, K. A., Ng, L., Szafer, A., Ebbert, A., et al. (2014, Apr 10). Transcriptional landscape of the prenatal human brain. Nature, 508(7495), 199-206. https://doi.org/10.1038/nature13185

Mitter, C., Jakab, A., Brugger, P. C., Ricken, G., Gruber, G. M., Bettelheim, D., Scharrer, A., Langs, G., Hainfellner, J. A., Prayer, D., & Kasprian, G. (2015). Validation of In utero Tractography of Human Fetal Commissural and Internal Capsule Fibers with Histological Structure Tensor Analysis. Front Neuroanat, 9, 164. https://doi.org/10.3389/fnana.2015.00164

Mitter, C., Kasprian, G., Brugger, P. C., & Prayer, D. (2011, Feb). Three-dimensional visualization of fetal white-matter pathways in utero. Ultrasound Obstet Gynecol, 37(2), 252-253. https://doi.org/10.1002/uog.8899

Mitter, C., Prayer, D., Brugger, P. C., Weber, M., & Kasprian, G. (2015). In vivo tractography of fetal association fibers. PLoS One, 10(3), e0119536. https://doi.org/10.1371/journal.pone.0119536

Monteagudo, A., & Timor-Tritsch, I. E. (1997, Apr). Development of fetal gyri, sulci and fissures: a transvaginal sonographic study. Ultrasound Obstet Gynecol, 9(4), 222-228. https://doi.org/10.1046/j.1469-0705.1997.09040222.x

O'Rahilly, R., & Muller, F. (2010). Developmental stages in human embryos: revised and new measurements. Cells Tissues Organs, 192(2), 73-84. https://doi.org/10.1159/000289817

Onland-Moret, N. C., Buizer-Voskamp, J. E., Albers, M. E. W. A., Brouwer, R. M., Buimer, E. E. L.,

Hessels, R. S., de Heus, R., Huijding, J., Junge, C. M. M., Mandl, R. C. W., Pas, P., Vink, M., van der Wal, J. J. M., Hulshoff Pol, H. E., & Kemner, C. (2020, 2020/12/01). The YOUth study: Rationale, design, and study procedures. Developmental cognitive neuroscience, 46, 100868. https://doi.org/https://doi.org/10.1016/j.dcn.2020.100868

Opsahl, T., & Panzarasa, P. (2009, May). Clustering in weighted networks. Social networks, 31(2), 155-163. https://doi.org/10.1016/j.socnet.2009.02.002

Ortinau, C., & Neil, J. (2015, Mar). The neuroanatomy of prematurity: normal brain development and the impact of preterm birth. Clin Anat, 28(2), 168-183. https://doi.org/10.1002/ca.22430

Piao, X., Hill, R. S., Bodell, A., Chang, B. S., Basel-Vanagaite, L., Straussberg, R., Dobyns, W. B., Qasrawi, B., Winter, R. M., Innes, A. M., Voit, T., Ross, M. E., Michaud, J. L., Descarie, J. C., Barkovich, A. J., & Walsh, C. A. (2004, Mar 26). G protein-coupled receptor-dependent development of human frontal cortex. Science, 303(5666), 2033-2036. https://doi.org/10.1126/science.1092780

Pistorius, L. R., Hellmann, P. M., Visser, G. H., Malinger, G., & Prayer, D. (2008, Nov). Fetal neuroimaging: ultrasound, MRI, or both? Obstet Gynecol Surv, 63(11), 733-745. https://doi.org/10.1097/OGX.0b013e318186d3ea

Plunk, M. R., & Chapman, T. (2014a, Nov-Dec). The fundamentals of fetal magnetic resonance imaging: Part 2. Curr Probl Diagn Radiol, 43(6), 347-355. https://doi.org/10.1067/j.cpradiol.2014.05.010

Plunk, M. R., & Chapman, T. (2014b, Nov-Dec). The fundamentals of fetal MR imaging: Part 1. Curr Probl Diagn Radiol, 43(6), 331-346. https://doi.org/10.1067/j.cpradiol.2014.05.014

Purves, D., Cabeza, R., Huettel, S. A., LaBar, K. S., Platt, M. L., Woldorff, M. G., & Brannon, E. M. (2008). Cognitive neuroscience. Sunderland: Sinauer Associates, Inc.

Rakic, P. (2004, Mar 26). Neuroscience. Genetic control of cortical convolutions. Science, 303(5666), 1983-1984. https://doi.org/10.1126/science.1096414

Ranger, M., & Grunau, R. E. (2014, Jan). Early repetitive pain in preterm infants in relation to the developing brain. Pain Manag, 4(1), 57-67. https://doi.org/10.2217/pmt.13.61

Richman, D. P., Stewart, R. M., Hutchinson, J. W., & Caviness, V. S., Jr. (1975, Jul 4). Mechanical model of brain convolutional development. Science, 189(4196), 18-21. https://doi.org/10.1126/science.1135626

Righini, A., Bianchini, E., Parazzini, C., Gementi, P., Ramenghi, L., Baldoli, C., Nicolini, U., Mosca, F., & Triulzi, F. (2003, May). Apparent diffusion coefficient determination in normal fetal brain: a prenatal MR imaging study. AJNR Am J Neuroradiol, 24(5), 799-804. https://www.ncbi.nlm.nih.gov/

pubmed/12748074

Romme, I. A., de Reus, M. A., Ophoff, R. A., Kahn, R. S., & van den Heuvel, M. P. (2017, Mar 15). Connectome Disconnectivity and Cortical Gene Expression in Patients With Schizophrenia. Biol Psychiatry, 81(6), 495-502. https://doi.org/10.1016/j.biopsych.2016.07.012

Rousseau, F., Glenn, O. A., Iordanova, B., Rodriguez-Carranza, C., Vigneron, D. B., Barkovich, J. A., & Studholme, C. (2006, Sep). Registration-based approach for reconstruction of high-resolution in utero fetal MR brain images. Acad Radiol, 13(9), 1072-1081. https://doi.org/10.1016/j.acra.2006.05.003

Rousseau, F., Kim, K., Studholme, C., Koob, M., & Dietemann, J.-L. (2010). On super-resolution for fetal brain MRI. International Conference on Medical Image Computing and Computer-Assisted Intervention,

Ruiz, A., Sembely-Taveau, C., Paillet, C., & Sirinelli, D. (2006, Jan). [Sonographic cerebral sulcal pattern in normal fetuses]. J Radiol, 87(1), 49-55. https://doi.org/10.1016/s0221-0363(06)73969-5 (Reperes echographiques de gyration cerebrale foetale normale.)

Schneider, J. F., Confort-Gouny, S., Le Fur, Y., Viout, P., Bennathan, M., Chapon, F., Fogliarini, C., Cozzone, P., & Girard, N. (2007, Sep). Diffusion-weighted imaging in normal fetal brain maturation. Eur Radiol, 17(9), 2422-2429. https://doi.org/10.1007/s00330-007-0634-x

Schneider, M. M., Berman, J. I., Baumer, F. M., Glass, H. C., Jeng, S., Jeremy, R. J., Esch, M., Biran, V., Barkovich, A. J., Studholme, C., Xu, D., & Glenn, O. A. (2009, Oct). Normative apparent diffusion coefficient values in the developing fetal brain. AJNR Am J Neuroradiol, 30(9), 1799-1803. https://doi.org/10.3174/ajnr.A1661

Scholtens, L. H., Schmidt, R., de Reus, M. A., & van den Heuvel, M. P. (2014, Sep 3). Linking macroscale graph analytical organization to microscale neuroarchitectonics in the macaque connectome. J Neurosci, 34(36), 12192-12205. https://doi.org/10.1523/JNEUROSCI.0752-14.2014

Schöpf, V., Kasprian, G., Brugger, P., & Prayer, D. (2012). Watching the fetal brain at 'rest'. International Journal of Developmental Neuroscience, 30(1), 11-17.

Sidman, R. L., & Rakic, P. (1973, Nov 9). Neuronal migration, with special reference to developing human brain: a review. Brain Res, 62(1), 1-35. https://doi.org/10.1016/0006-8993(73)90617-3

Singh, G. (2017). Neuroembryology. In Essentials of Neuroanesthesia (pp. 41-50). Elsevier.

Smith, G. C., Gutovich, J., Smyser, C., Pineda, R., Newnham, C., Tjoeng, T. H., Vavasseur, C., Wallendorf, M., Neil, J., & Inder, T. (2011, Oct). Neonatal intensive care unit stress is associated with brain development in preterm infants. Ann Neurol, 70(4), 541-549. https://doi.org/10.1002/ana.22545

Smyser, C. D., Inder, T. E., Shimony, J. S., Hill, J. E., Degnan, A. J., Snyder, A. Z., & Neil, J. J. (2010, Dec). Longitudinal analysis of neural network development in preterm infants. Cereb Cortex, 20(12), 2852-2862. https://doi.org/10.1093/cercor/bhq035

Song, L., Mishra, V., Ouyang, M., Peng, Q., Slinger, M., Liu, S., & Huang, H. (2017). Human Fetal Brain Connectome: Structural Network Development from Middle Fetal Stage to Birth. Front Neurosci, 11, 561. https://doi.org/10.3389/fnins.2017.00561

Sporns, O. (2013, Oct 15). The human connectome: origins and challenges. NeuroImage, 80, 53-61. https://doi.org/10.1016/j.neuroimage.2013.03.023

Sporns, O., Tononi, G., & Kotter, R. (2005, Sep). The human connectome: A structural description of the human brain. PLoS Comput Biol, 1(4), e42. https://doi.org/10.1371/journal.pcbi.0010042

Stiles, J., & Jernigan, T. L. (2010, Dec). The basics of brain development. Neuropsychol Rev, 20(4), 327-348. https://doi.org/10.1007/s11065-010-9148-4

Stoodley, C. J., & Limperopoulos, C. (2016). Structure–function relationships in the developing cerebellum: evidence from early-life cerebellar injury and neurodevelopmental disorders. Seminars in Fetal and Neonatal Medicine, 21(5), 356-364. https://doi.org/10.1016/j.siny.2016.04.010

Thomason, M. E., Brown, J. A., Dassanayake, M. T., Shastri, R., Marusak, H. A., Hernandez-Andrade, E., Yeo, L., Mody, S., Berman, S., Hassan, S. S., & Romero, R. (2014). Intrinsic functional brain architecture derived from graph theoretical analysis in the human fetus. PLoS One, 9(5), e94423. https://doi.org/10.1371/journal.pone.0094423

Thomason, M. E., Dassanayake, M. T., Shen, S., Katkuri, Y., Alexis, M., Anderson, A. L., Yeo, L., Mody, S., Hernandez-Andrade, E., Hassan, S. S., Studholme, C., Jeong, J. W., & Romero, R. (2013, Feb 20). Cross-hemispheric functional connectivity in the human fetal brain. Sci Transl Med, 5(173), 173ra124. https://doi.org/10.1126/scitranslmed.3004978

Thomason, M. E., Grove, L. E., Lozon, T. A., Jr., Vila, A. M., Ye, Y., Nye, M. J., Manning, J. H., Pappas, A., Hernandez-Andrade, E., Yeo, L., Mody, S., Berman, S., Hassan, S. S., & Romero, R. (2015, Feb). Age-related increases in long-range connectivity in fetal functional neural connectivity networks in utero. Dev Cogn Neurosci, 11, 96-104. https://doi.org/10.1016/j.dcn.2014.09.001

Thomason, M. E., Hect, J., Waller, R., Manning, J. H., Stacks, A. M., Beeghly, M., Boeve, J. L., Wong, K., van den Heuvel, M. I., Hernandez-Andrade, E., Hassan, S. S., & Romero, R. (2018, Aug). Prenatal neural origins of infant motor development: Associations between fetal brain and infant motor development. Dev Psychopathol, 30(3), 763-772. https://doi.org/10.1017/S095457941800072X

Thomason, M. E., Hect, J. L., Rauh, V. A., Trentacosta, C., Wheelock, M. D., Eggebrecht, A. T., Espinoza-Heredia, C., & Burt, S. A. (2019, May 1). Prenatal lead exposure impacts cross-hemispheric and long-range connectivity in the human fetal brain. NeuroImage, 191, 186-192. https://doi.org/10.1016/j.neuroimage.2019.02.017

Thompson, P. M., Ge, T., Glahn, D. C., Jahanshad, N., & Nichols, T. E. (2013, Oct 15). Genetics of the connectome. NeuroImage, 80, 475-488. https://doi.org/10.1016/j.neuroimage.2013.05.013

Toi, A., Lister, W., & Fong, K. (2004). How early are fetal cerebral sulci visible at prenatal ultrasound and what is the normal pattern of early fetal sulcal development? Ultrasound in Obstetrics and Gynecology: The Official Journal of the International Society of Ultrasound in Obstetrics and Gynecology, 24(7), 706-715.

van den Heuvel, M. P., & Hulshoff Pol, H. E. (2010, Aug). Exploring the brain network: a review on resting-state fMRI functional connectivity. Eur Neuropsychopharmacol, 20(8), 519-534. https://doi.org/10.1016/j.euroneuro.2010.03.008

van den Heuvel, M. P., Kahn, R. S., Goni, J., & Sporns, O. (2012, Jul 10). High-cost, high-capacity backbone for global brain communication. Proc Natl Acad Sci U S A, 109(28), 11372-11377. https://doi.org/10.1073/pnas.1203593109

van den Heuvel, M. P., Kersbergen, K. J., de Reus, M. A., Keunen, K., Kahn, R. S., Groenendaal, F., de Vries, L. S., & Benders, M. J. (2015, Sep). The Neonatal Connectome During Preterm Brain Development. Cereb Cortex, 25(9), 3000-3013. https://doi.org/10.1093/cercor/bhu095

van den Heuvel, M. P., Mandl, R. C., Kahn, R. S., & Hulshoff Pol, H. E. (2009, Oct). Functionally linked resting-state networks reflect the underlying structural connectivity architecture of the human brain. Hum Brain Mapp, 30(10), 3127-3141. https://doi.org/10.1002/hbm.20737

van den Heuvel, M. P., Scholtens, L. H., Turk, E., Mantini, D., Vanduffel, W., & Feldman Barrett, L. (2016, Sep). Multimodal analysis of cortical chemoarchitecture and macroscale fMRI resting-state functional connectivity. Hum Brain Mapp, 37(9), 3103-3113. https://doi.org/10.1002/hbm.23229

van den Heuvel, M. P., & Sporns, O. (2011, Nov 2). Rich-club organization of the human connectome. J Neurosci, 31(44), 15775-15786. https://doi.org/10.1523/JNEUROSCI.3539-11.2011

Van Essen, D. C. (1997, Jan 23). A tension-based theory of morphogenesis and compact wiring in the central nervous system. Nature, 385(6614), 313-318. https://doi.org/10.1038/385313a0

Vasung, L., Huang, H., Jovanov-Milosevic, N., Pletikos, M., Mori, S., & Kostovic, I. (2010, Oct). Development of axonal pathways in the human fetal fronto-limbic brain: histochemical characterization and

diffusion tensor imaging. *J Anat, 217(4), 400-417. https://doi.org/10.1111/j.1469-7580.2010.01260.x*

Volpe, J. J. (2009a, Jan). *Brain injury in premature infants: a complex amalgam of destructive and developmental disturbances. Lancet Neurol, 8(1), 110-124. https://doi.org/10.1016/S1474-4422(08)70294-1*

Volpe, J. J. (2009b, Sep). *Cerebellum of the premature infant: rapidly developing, vulnerable, clinically important. J Child Neurol, 24(9), 1085-1104. https://doi.org/10.1177/0883073809338067*

Volpe, P., Paladini, D., Resta, M., Stanziano, A., Salvatore, M., Quarantelli, M., De Robertis, V., Buonadonna, A. L., Caruso, G., & Gentile, M. (2006, May). *Characteristics, associations and outcome of partial agenesis of the corpus callosum in the fetus. Ultrasound Obstet Gynecol, 27(5), 509-516. https://doi.org/10.1002/uog.2774*

Wei, Y., de Lange, S. C., Scholtens, L. H., Watanabe, K., Ardesch, D. J., Jansen, P. R., Savage, J. E., Li, L., Preuss, T. M., Rilling, J. K., Posthuma, D., & van den Heuvel, M. P. (2019, Oct 24). *Genetic mapping and evolutionary analysis of human-expanded cognitive networks. Nat Commun, 10(1), 4839. https://doi.org/10.1038/s41467-019-12764-8*

Wei, Y., Scholtens, L. H., Turk, E., & van den Heuvel, M. P. (2019). *Multiscale examination of cytoarchitectonic similarity and human brain connectivity. Netw Neurosci, 3(1), 124-137. https://doi.org/10.1162/netn_a_00057*

Wheelock, M. D., Hect, J. L., Hernandez-Andrade, E., Hassan, S. S., Romero, R., Eggebrecht, A. T., & Thomason, M. E. (2019, Apr). *Sex differences in functional connectivity during fetal brain development. Dev Cogn Neurosci, 36, 100632. https://doi.org/10.1016/j.dcn.2019.100632*

Wolke, D. (1987). *Environmental and developmental neonatology. Journal of Reproductive and Infant Psychology, 5(1), 17-42.*

Wright, R., Kyriakopoulou, V., Ledig, C., Rutherford, M. A., Hajnal, J. V., Rueckert, D., & Aljabar, P. (2014, May 1). *Automatic quantification of normal cortical folding patterns from fetal brain MRI. NeuroImage, 91, 21-32. https://doi.org/10.1016/j.neuroimage.2014.01.034*

Yeo, B. T., Krienen, F. M., Sepulcre, J., Sabuncu, M. R., Lashkari, D., Hollinshead, M., Roffman, J. L., Smoller, J. W., Zollei, L., Polimeni, J. R., Fischl, B., Liu, H., & Buckner, R. L. (2011, Sep). *The organization of the human cerebral cortex estimated by intrinsic functional connectivity. J Neurophysiol, 106(3), 1125-1165. https://doi.org/10.1152/jn.00338.2011*

You, W., Evangelou, I. E., Zun, Z., Andescavage, N., & Limperopoulos, C. (2016, Apr). *Robust preprocessing for stimulus-based functional MRI of the moving fetus. J Med Imaging (Bellingham), 3(2), 026001. https://doi.org/10.1117/1.JMI.3.2.026001*

Yu, Q., Ouyang, A., Chalak, L., Jeon, T., Chia, J., Mishra, V., Sivarajan, M., Jackson, G., Rollins, N., Liu, S., & Huang, H. (2016, Oct 17). Structural Development of Human Fetal and Preterm Brain Cortical Plate Based on Population-Averaged Templates. Cereb Cortex, 26(11), 4381-4391. https://doi.org/10.1093/cercor/bhv201

Yushkevich, P. A., Piven, J., Hazlett, H. C., Smith, R. G., Ho, S., Gee, J. C., & Gerig, G. (2006, Jul 1). User-guided 3D active contour segmentation of anatomical structures: significantly improved efficiency and reliability. NeuroImage, 31(3), 1116-1128. https://doi.org/10.1016/j.neuroimage.2006.01.015

Zanin, E., Ranjeva, J. P., Confort-Gouny, S., Guye, M., Denis, D., Cozzone, P. J., & Girard, N. (2011, Nov). White matter maturation of normal human fetal brain. An in vivo diffusion tensor tractography study. Brain Behav, 1(2), 95-108. https://doi.org/10.100

Genetic foundation for fetal cortical growth

Elise Turk*, Yongbin Wei*, Lianne Scholtens, Manon Benders, Roel de Heus,
Martijn van den Heuvel
*Shared-first author

ABSTRACT

The cortex undergoes rapid expansion during the third trimester of pregnancy, a process arguably under strong genetic control. Bringing together data on fetal brain growth patterns as measured by MRI and data on cortical spatial gene expression during brain development, we examined the role of spatiotemporal gene transcriptional profiles in this process of cortical growth between 24 and 38 postconceptional weeks (pcw) of pregnancy. We correlate spatial gene expression with cortical growth, and reveal the top 100 correlating genes for three fetal age stages (24-30 pcw, 30-34 pcw, and 34-38 pcw). Gene-set analysis did not show any significant enrichment of the top 100 genes in biological pathways between 24 and 34 pcw, while significant enrichment was found for pathways in "Neurotransmitter receptors and postsynaptic signal transmission", "Transmission across chemical synapses", and "Neuronal system" between 34 and 38 pcw. Moreover, we show that "neural circuitry" genes -genes that are involved in axon growth and synaptogenesis- are particularly associated with the spatial pattern of cortical growth, suggesting that patterns of cortical growth during the last stage of pregnancy are under control of circuitry maturation genes. In conclusion, this study highlights new biological pathways -in axon and synapse development and neurotransmission- that are important for prenatal cortical development near birth.

Keywords: cortical expansion, gene expression, prenatal, fetal MRI, transcriptome

INTRODUCTION

The morphology and organization of the human cerebral cortex largely develops in utero. During the third trimester of pregnancy the cortex grows and changes from a smooth to a convoluted landscape (Bayer & Altman, 2003, 2005), following a clear sequential pattern of distinct phases of growth and folding of cortical areas (Dubois et al., 2008; Garcia et al., 2018). In a relatively short period of time, the global layout of the outer covering of the human fetal cerebri is almost complete and folded in a similar fashion as the adult cortex (Hill, Dierker, et al., 2010; Hill, Inder, et al., 2010). Regional differences in macroscopic transformations of the human cortex reflect spatio-temporal differences in the maturation of micro-elements such as neurons, glial cells, axons and synapses (Nowakowski et al., 2017). However, our understanding of the rules shaping the cortex, involving the formation and maturation of the brain on microlevel, remains sparse.

Prenatal phases of brain development are believed to depend on differential regulation of gene expression across brain regions across time (Kang et al., 2011). The fetal neural transcriptome describes the RNA expression pattern of brain regions and bridges genetic code with local gene function (Miller et al., 2014). Combining transcriptomic data with neuroimaging data allows investigation into the functional role of genes in the devel-

oping brain and how such genes may drive cortical expansion (Kriegstein et al., 2006; Liu et al., 2017). It may explain their role in the development of cognitive function (Wei et al., 2019) and dysfunction (Diez et al., 2020; Romme et al., 2017; Scarr et al., 2018). Studying the fetal transcriptome provides a novel way to gain insight into the etiology of neurodevelopmental disorders (Gulsuner & McClellan, 2014; Willsey et al., 2013), and has the potential to help clarify how the human brain works.

In this study, we combined MRI data of fetal brain expansion with transcriptome data of the fetal brain to examine genetic driving forces behind volumetric maturation of the human fetal cortex. We examined the spatial pattern of cortical growth between 24 and 38 postconceptional weeks of pregnancy as measured by fetal MRI in the context of the spatiotemporal gene transcriptional profile changes of 1) all genes from the BrainSpan dataset and 2) specific sets of interest related to neurodevelopment. Combining the fetal transcriptome with cortical expansion maps of fetuses, we illuminate the genetic features of biological pathways that are associated with fetal cortical growth during the third trimester of pregnancy.

METHODS

Fetal MRI templates
The fetal cortex was reconstructed during four temporal phases of the fetal brain between week 21 and 39 using unique data resources on the fetal brain of the Computational Radiology Laboratory (CRL; http://crl.med.harvard.edu; Gholipour et al., 2017). The CRL fetal brain dataset describes a series of longitudinal brain MRI images constructed using T2-weighted MRI from 81 normal fetuses with an age ranging from 21 to 39 postconceptional weeks (pcw) (Gholipour et al., 2017). The dataset includes 18 brain templates (normalized images) describing 18 developing time points for each postconceptional week. The CRL dataset further contains segmentations of the brain templates at each postconceptional week, with distinct labels for gray matter, white matter, subcortical regions, cerebrospinal fluid, cerebellum and ventricles. Normalized tissue segmentation data at four age stages: 26, 30, 34, and 38 postconceptional week was used to investigate cortical growth during fetal development. Brain templates below 26 postconceptional weeks were excluded as these datasets were not able to be used for complete cortical reconstruction, because automatic cortical volume segmentation did not pass our quality control.

Brain parcellation
We performed fetal cortical reconstructions based on the CRL imaging data as follows. A surrogate T1 image for each developmental stage was created from the T2-weighted images by flipping the image intensity levels. Resulting surrogate T1 images were processed using FreeSurfer's recon-all pipeline (version 5.3.0; http://surfer.nmr.mgh.

harvard.edu/), building a 3D reconstruction of the cortical mantle of the CRL data. 3D cortical reconstructions and brain segmentations produced by FreeSurfer were manually checked for accuracy.
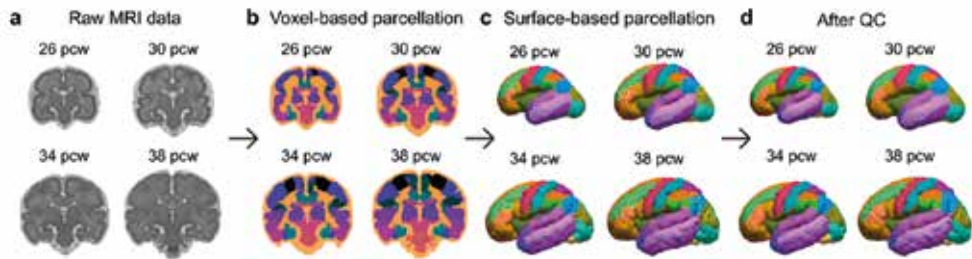
Figure 1. Brain parcellation pipeline at different developmental stages.
Figure illustrates (a) a coronal section of raw MRI data of the CRL fetal brain dataset at 26, 30, 34 and 38 pcw (Gholipour et al., 2017), (b) a coronal section of the voxel based classifications embodied in the CRL fetal brain atlas, (c) freesurfer reconstructions and surface-based parcellation of the reconstructed ribbon of the fetal cortex as derived from the maps in a and b in this study, (d) obtained surface-based parcellation after quality control and manual editing for the four developmental stages. Colors represent different cortical regions of the CRL fetal brain atlas.

Voxel-based brain parcellation embodied in the CRL fetal brain atlas (Gholipour et al., 2017) (describing 90 cortical regions across left and right hemispheres, see for example in **Figure 1a**) were next used to measure regional-level surface area of each of the 90 regions in the four GA stages. Quality control steps included fixing voxels without a label on the pial surface by taking the nearest labels, smoothing the boundaries between cortical parcels, and manually correcting parcellation errors using the tksurfer tool in Freesurfer. CRL voxel-based brain parcellation at each GA was mapped to the middle layer between the white matter surface (i.e., the boundary between labelled gray matter and white matter) and pial surface (i.e., the boundary between labelled gray matter and cerebrospinal fluid) of the FreeSurfer-reconstructed cortical ribbon of the matching developmental stage (**Figure 1b and 1c**). After manual editing of the atlas (**Figure 1d**), surface area of each cortical region in the CRL atlas at each GA was computed.

CORTICAL GROWTH

Absolute cortical growth was computed by comparing cortical surface areas between subsequent stages of development, from 26 to 30 pcw, from 30 to 34 pcw, and from 34 to 38 pcw across all 90 brain regions. Cortical growth (G) was computed as the fold-

change difference between surface areas of two subsequent time points:
$G_{i,j} = S_{i,a} ./ S_{j,a}$ where S is the surface area of region a and i, j the two cortical reconstructions at distinct time points.

GENE EXPRESSION ANALYSIS

Gene expression data

Normalized RNA-sequencing data was obtained from the BrainSpan atlas (https://www.brainspan.org/). BrainSpan includes data of fetal brain gene expression from tissue samples of 26 cortical, subcortical, and cerebellar structures, collected across 20 brain donors with age ranging from 8 pcw to 37 pcw. Normalized RNA-sequencing data were processed using the following steps. Gene expression of tissue samples with the same region label were averaged for multiple samples in a region, followed by log2-transformation with pseudocount one (Watanabe et al., 2017). Expression levels of each gene were transformed to z-scores across brain regions. BrainSpan region labels were then mapped to CRL region labels, resulting in eleven included cortical regions (see Table S1). The opercular, triangular, and orbital parts of the inferior frontal cortex in the CRL atlas were combined into one region, matching to the label of the ventrolateral prefrontal cortex in the BrainSpan atlas. Likewise, the orbital parts of the middle and superior frontal cortex in the CRL atlas were combined into one region, matching to the label of the orbital frontal cortex. To match temporal gene expression patterns to the temporal pattern of the cortical growth analysis, gene expression data of two donors (24 pcw and 37 pcw) of which expression data were available for all eleven cortical regions were selected. Other donors were beyond the age range of the available imaging data (16 donors aged <21 pcw) or missed expression data for more than half of the brain regions (3 donors). Genes with missing expression data in more than two (out of eleven) cortical regions were excluded (9361 genes), resulting in a gene expression data matrix of 16,929 genes, eleven regions, and two individuals. BrainSpan Gene symbols were updated by matching symbols obtained from the HUGO Gene Nomenclature Committee (HGNC) database (http://biomart.genenames.org/). For each gene and each cortical region, delta gene expression (DGE) was computed by subtracting expression values between 37-pcw and 24-pcw.

Gene-enrichment Analysis

Top-correlating genes. Correlation analysis was performed between the pattern of cortical growth and the pattern of the mean gene expression changes (i.e., delta gene expression, further referred to as DGE) between 24 pcw and 37 pcw, for each of the 16,929 genes separately in the BrainSpan dataset. A null distribution of correlation coefficients was yielded based on surrogate brain maps with spatial relationships conserved (1,000 randomizations) to correct for spatial autocorrelation of gene expressions (referred to as null-spatial model) (Burt et al., 2020; Fulcher et al., 2020). A one-sided *p*-value was

computed according to the proportion of the null distribution exceeding the real correlation coefficient. Top 100 genes (lowest *p*-value) were selected for each distinct cortical growth stage (top 200 genes for validation purpose, see Supplementary Information). FUMA gene-set enrichment analysis was performed to test whether these top genes were over-expressed in brain tissue in the GTEx (Genotype-Tissue Expression v8) database (Watanabe et al., 2017).

Further enrichment of top genes in biological pathways was statistically evaluated using hypergeometric tests, testing whether the number of overlapped genes between the top 100 genes and genes from a pathway is beyond what one can expect by chance. Predefined pathways were obtained from MsigDB (Subramanian et al., 2005), including 2,868 canonical pathways derived from the BioCarta, KEGG, Reactome, PID, and WikiPathways database and 10,271 Gene-Ontology (GO) gene-sets annotated to a wide range of biological process, cellular component, and molecular function (http://www.gsea-msigdb.org/gsea/msigdb). The total set of 16,929 genes was taken as a background set against the predefined pathway genes tested. Multiple testing correction was performed per data source using false discovery rate (FDR) correction with *q* < 0.05.

Gene-sets of interest. We next performed gene expression pattern analyses (Gladys et al., 2020; Romme et al., 2017; Wei et al., 2019) for three predefined gene-sets that are known to be related to prenatal neuronal and axonal growth from the MSigDB database (http://www.gsea-msigdb.org/gsea/msigdb):
1) AXON genes. Set I is describing 482 genes involved in axon development and fasciculation defined in the Gene Ontology (GO) database (http://geneontology.org) (referred to as AXON genes). Related molecular and neuronal processes are believed to start at around 8 pcw and last until 12 months after birth (Muller & O'Rahilly, 2011; O'Rahilly & Muller, 2010; Vasung et al., 2010).
2) SYNAPSE genes. Set II is describing 406 genes involved in synapse genesis and organization (referred to as SYNAPSE genes). Related biological processes are believed to start at around 25 pcw and to continue until childhood (Huttenlocher & Dabholkar, 1997).
3) GLIAL genes. Set III is describing 40 genes related to glial cell proliferation (referred to as GLIAL genes). Glial cell proliferation is estimated to begin as early as 10-18 pcw and to end before birth (Lee et al., 2000).

Statistical evaluation over cortical patterns. Spearman's correlation test was used to measure the degree of association between the pattern of cortical growth at three distinct prenatal developmental stages (26-30 pcw, 30-34 pcw, and 34-38 pcw, see above) and the pattern of DGE between 24 pcw and 37 pcw for each gene-set (i.e., AXON, SYNAPSE and GLIAL). We used three null models to examine the spatial specificity and gene specificity of the observed associations and control for the statistical analysis (Wei et al., 2022).

The first null distribution was generated to examine the spatial specificity among cortical regions (Null-spatial model, 1,000 surrogate maps) (Burt et al., 2020). First, we generated 1,000 spatial auto correlations controlled for surrogate cortical growth patterns. Second, we computed the correlation coefficients between the pattern of DGE for each gene and the 1,000 maps. Third, those correlation coefficients together formed the null distribution for the expected value by change. Four, for each gene we estimated the true p-value, by computing the fraction of surrogate maps that were higher than the original correlation coefficients. For example, a p-value of 0.05 was reached when 50 out of 1,000 surrogate maps produced a higher outcome. We examined the gene specificity by generating a second null distribution of correlation coefficients between real cortical growth patterns and DGE patterns of random genes that had the same size and mean co-expression level as the set of interest, selected from the total set of 16,929 genes (null-coexpressed-gene model, 1,000 random gene-sets). We examined the gene specificity concerning genes that are generally enriched in the brain (describing 2,798 genes out of the total 16,929 genes, showing higher expression levels in brain tissue in contrast to other body sites) (Wei et al., 2019). To this end, we generated a fourth null distribution of correlation coefficients between real cortical growth patterns and DGE patterns of genes randomly selected from the set of brain-enriched genes that had the same size as the gene-set of interest (null-brain-gene model, 1,000 random gene-sets). Given the resulting null distributions, effects were assigned a two-sided p-value according to the proportion (P) of random permutations that exceeded the original correlation coefficients of genes ($p = (1 - P) \times 2$ if $P > 0.5$, otherwise $p = P \times 2$).

RESULTS

Fetal cortical growth
Figure 2 shows a side-to-side comparison of the cerebral cortex between 26 and 38 pcw, illustrating a transformation from a smooth to a complexly folded cortical sheet, showing non-uniform growth rates at distinct developmental stages. Between 26 and 30 pcw, the largest cortical growth was observed around the primary motor and sensorimotor cortical regions, including precentral gyrus (left: ×1.9 growth, right: ×1.8 growth), postcentral gyrus (left: ×2.0 growth, right: ×1.9 growth), paracentral lobe (×1.9 growth for both hemispheres), supramarginal gyrus (left: ×2.0 growth), and Heschl gyrus (right: ×1.9 growth; regions with growth > mean + 1.5 standard deviation [SD] across all regions). Conversely, from 30-34 pcw, a more diffuse cortical growth pattern was present, with the left superior occipital lobe (×2.2 growth) and the right Heschl gyrus (×2.4 growth) showing the highest growth. From 34 to 38 pcw (third trimester) the largest growth rates (> mean + 1.5SD) were observed in association regions including the superior frontal gyrus (left: ×1.5 growth, right: ×1.7 growth), middle frontal gyrus (right: ×1.6 growth), posterior cingulate gyrus (×1.5 growth for both hemispheres), inferior temporal gyrus (left: ×1.5 growth) and middle temporal gyrus (right: ×1.5 growth).
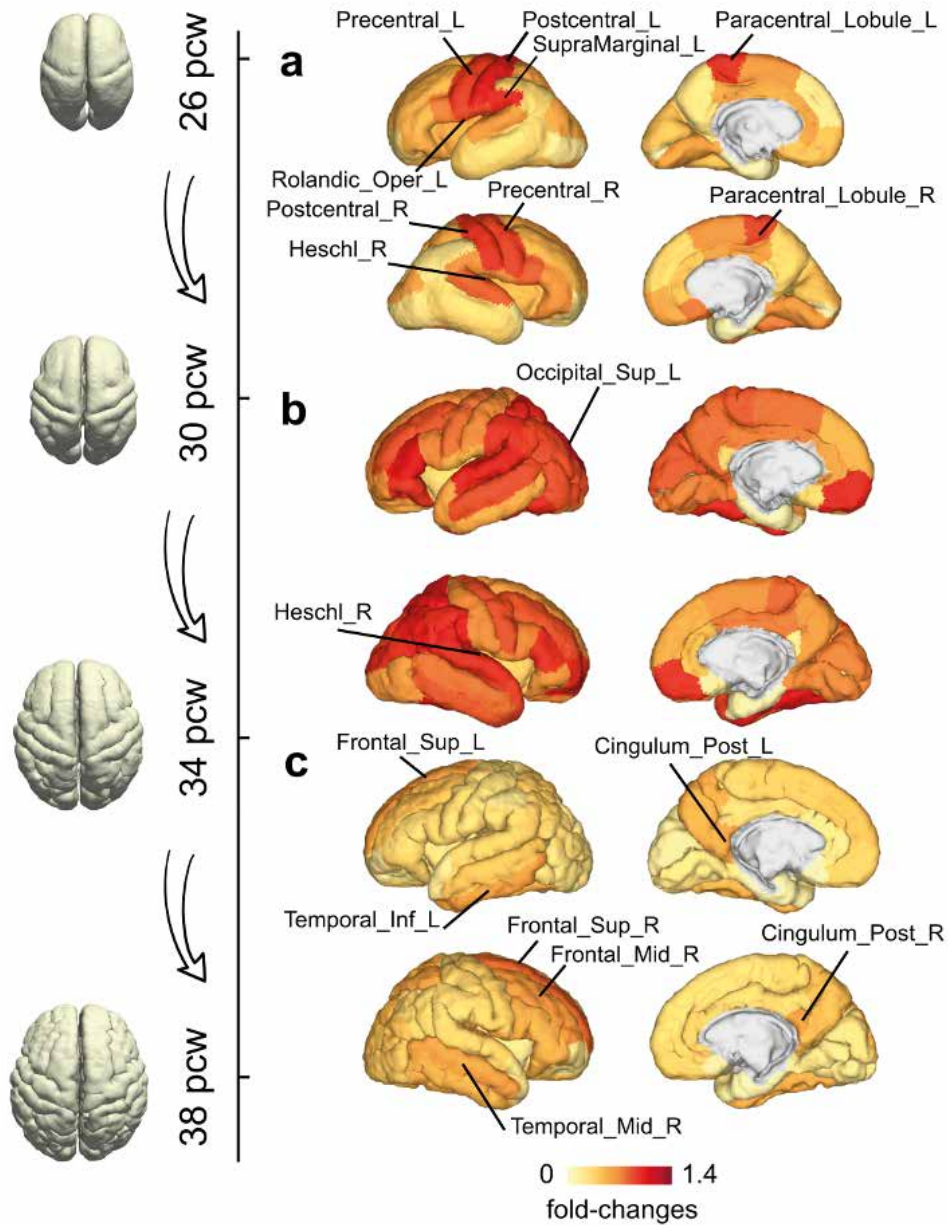
Figure 2. Fetal cortical growth during the third trimester.

Fold changes of pial surface's area are shown for (a) 26 to 30 postconceptional weeks (pcw), (b) 30 to 34 pcw, and (c) 34 to 38 pcw. Relative slowly growing regions are displayed in yellow, medium growing regions in orange and fast-growing regions in red. Region labels are indicated for regions with above average growth (mean + 1.5 standard deviation) across all regions.

Top genes correlated to fetal cortical growth
We continued by investigating the biological properties of the top 100 genes showing the highest levels of spatial overlap with the spatial patterns of fetal cortical growth of the three developmental stages (**Figure 2**, results for top 200 shown in SI).

26-30 pcw. The top 100 genes showing the highest correlation with cortical growth from 26 to 30 pcw (null-spatial model) were found to have significant enrichment for genes differentially expressed in the cerebellum (FUMA hypergeometric test: $q < 0.05$, FDR corrected; GTEx v8). Non-significant, trend effects were also observed for specific brain regions: the pituitary gland, cerebral cortex, and cerebellar hemispheres ($p < 0.05$, not corrected; GTEx v8). FUMA gene-set analysis did not reveal any significant enrichment of the top 100 genes in biological pathways.

30-34 pcw. The top 100 genes correlated with cortical growth from 30 to 34 pcw were found to show significant enrichment for genes differentially expressed in non-brain tissue, such as lung, breast, adipose tissue ($q < 0.05$, FDR corrected; GTEx v8). Gene-set analysis did not show any significant enrichment of the top 100 genes in biological pathways examined in the FUMA platform.

34-38 pcw. The top 100 genes showing the highest correlation with cortical growth from 34 to 38 pcw (null-spatial model) were found to show significant enrichment for genes differentially expressed in brain tissue (GTEx v8), in particular the frontal cortex BA9, anterior cingulate cortex BA24, hypothalamus, hippocampus, basal ganglia, and brain cerebellar hemisphere (FUMA hypergeometric test, $q < 0.05$, FDR corrected; Supplementary **Figure S1**). This suggests that the top 100 genes associated with cortical growth during late-prenatal stages are particularly expressed in brain tissue.
The top 100 genes were further found to be enriched for pathways of "Neurotransmitter receptors and postsynaptic signal transmission", "Transmission across chemical synapses", and "Neuronal system" curated in the Reactome database ($q < 0.05$, FDR corrected; Supplementary Table S3; https://reactome.org/). Top genes were found to be enriched in GO biological processes in relation to "ion transport" and "synaptic signaling" ($q < 0.05$, FDR corrected; Supplementary Table S4; http://geneontology.org/). Of the top 100 genes, 24 genes were found to be down-regulated in the brain of tissue donors of Alzheimer's disease and 8 genes were found to be down-regulated in the aging brain ($q < 0.05$, FDR corrected).
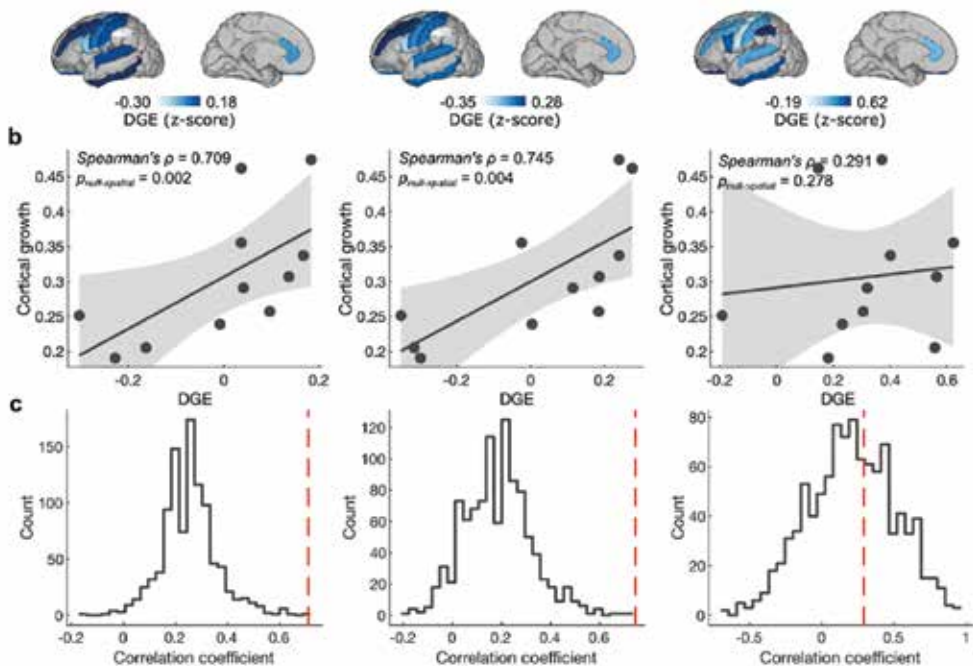
Cortical growth and gene-set of interest
We then further examined the relation between gene-sets of interest and cortical growth at the three different age stages.
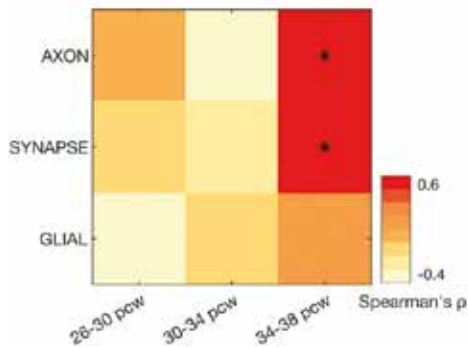
Figure 3. Association between fetal cortical growth and fj gene expression (DGE).
Indicates significant (null-spatial model, Bonferroni corrected).

Figure 4. Association between fetal cortical growth (34-38 pcw) and fj gene expression (DGE).
(a) The pattern of the mean DGE. Gray: no expression data available. (b) The pattern of cortical growth from 34 to 38 pcw correlates best to the pattern of the mean DGE of AXON genes (Spearman's r = 0.709, $p_{null\text{-}spatial}$ = 0.002), and SYNAPSE genes (r = 0.745, $p_{null\text{-}spatial}$ = 0.004). No strong effect was found for GLIAL genes indicating that cortical growth in the third semester may be strongest related to neuronal rather than glial cell processes (r = 0.291, $p_{null\text{-}spatial}$ = 0.278). Gray shades indicate the 95% confidence interval. (c) Null distributions of correlation coefficients derived from the null-coexpressed-gene model, where random genes with similar co-expression level as the gene-set of interest are selected. Red dotted line: correlation coefficients for the gene-set of interest.

26-30 pcw. The regional DGE pattern of the three gene-sets of interest did not show significant correlation with the pattern of cortical growth from 26 to 30 pcw (Spearman's *r* = 0.018, -0.103, -0.406 for AXON, SYNAPSE, GLIAL genes, respectively; *pnull-spatial* > 0.247).

30-34 pcw. Similarly, the regional DGE pattern of the three gene-sets showed a non-significant correlation with the pattern of cortical growth from 30 to 34 pcw (Spearman's *r* = -0.455, -0.285, -0.127 for AXON, SYNAPSE, GLIAL genes, respectively; *pnull-spatial* > 0.191).

34-38 pcw. Regional patterns of DGE of AXON and SYNAPSE genes were found to be significantly associated with the pattern of fetal cortical growth from 34 to 38 pcw (**Figure 3**, Spearman's *r* = 0.709, *pnull-spatial* = 0.002, and *r* = 0.745, *pnull-spatial* = 0.004, separately; Bonferroni corrected over three tests). No effect was found for GLIAL genes (*r* = 0.291, *pnull-spatial* = 0.278). These findings suggest that cortical regions (e.g., middle frontal gyrus and inferior temporal gyrus) with high expression levels of AXON and SYNAPSE genes overlap with areas with the largest growth of the cortical ribbon during fetal brain development in the third trimester. Effects of AXON and SYNAPSE genes well exceeded the null distribution of effect sizes yielded by the same-sized sets of random genes with similar co-expression levels (permutation testing, null-coexpressed-gene model: *p* = 0.002 and 0.001, separately, 1,000 permutations; Bonferroni corrected over three tests; **Figure 4**), indicating the gene specificity of the examined gene-sets (Wei et al., 2022). We next examined the gene specificity of the observed associations concerning brain-enriched genes. We found 191 (out of 482) AXON genes, 195 (out of 406) SYNAPSE genes and 10 out of (40) GLIAL genes to overlap with the set of 2,798 brain-enriched genes. Brain-enriched genes in general were found to show high correlations with the cortical growth pattern between gestational week 34 and 38 compared to non-brain-expressed genes (*rAXON-BRAIN* = 0.763 and *rAXON-non-BRAIN* = 0.418; **r***SYNAPSE-BRAIN* = 0.727 and *rSYNAPSE-non-BRAIN* = 0.563; *rGLIAL-BRAIN* = 0.363 and *rGLIAL-non-BRAIN* = 0.227). Comparing effects resulted by AXON-BRAIN and SYNAPSE-BRAIN genes to null distributions of effects generated by random brain-enriched genes (i.e., null-brain-gene model) however did not show significant results (*p* = 0.248 and 0.440, respectively), suggesting that cortical growth during the third stage might be associated with genes more generally involved in brain processes.

DISCUSSION

Linking fetal MRI to the fetal transcriptome, this study demonstrates the spatiotemporal relationship between cortical growth and gene expression levels of genes that are known to be related to prenatal synapse and axonal growth during the third trimester of pregnancy. Our observed pattern of fetal cortical growth from 26 to 38 postconcep-

tional weeks is in line with previous studies on preterm neonatal brain (Garcia et al., 2018), showing a growth pattern that starts at the primary motor and (somato)sensory cortices and is followed by growth of the occipital cortex, which in turn is followed by maturation of lateral parts of the temporal and frontal lobe. Cortical growth between 34 to 38 postconceptional weeks is in particular found to be under strong genetic control of genes related to axon and synaptic processes, the developmental stage that is known for the acceleration in neural circuit development with rapid axonal outgrowth, dendritic arborization and synaptogenesis (Reissland & Kisilevsky, 2016) and cortical gyrification (de Graaf-Peters & Hadders-Algra, 2006).

The specific growth rates from 34 weeks onwards appear to be particularly driven by genes differentially expressed in brain-tissue. The observed growth-associated genes are specifically involved in neuronal signal transmission processes and thus likely function in the neuronal connectivity microstructures, such as synapses, dendrites, and axons (see Supplementary results, Table S3 and S4). These findings are in line with animal models showing a central role for neuronal complexity and circuitry genes in cortical special-ization during development (see for review, Cadwell et al., 2019). For example, genes involved in neurite outgrowth are a strong factor in the gyrification of the cortical mantle during the second and third trimester of pregnancy in sheep (Quezada et al., 2020). Likewise, genes involved in neuronal complexity and cell-signaling have been shown to guide the development of regional differences of cortical folding in early postnatal ferret brains (de Juan Romero et al., 2015). Our results provide insights into spatiotemporal gene regulatory mechanisms of cellular processes related to the emergence and matura-tion of circuitry development to have a central role in cortical growth near birth.

Perturbations to prenatal growth processes render the brain at risk for neurodevelop-mental deficits. The top genes from our research therefore are potential new candidate genes for understanding the biological mechanisms that may lead into neurodevelop-mental and psychiatric disorders. Our results suggest that genes important for axon and synapse growth support fetal cortical growth. Perturbations in synapse function are linked to many (developmental) neuropsychiatric disorders (see for review, Hu et al., 2014). MTOR for example, is one of our top genes and is linked to developmental epilepsy (Hu et al., 2014). We, however, did not find other significant enrichment of well-known neurodevelopmental disorder genes in our subset of top genes that correspond with fetal cortical expansion. A possible explanation is that the genetic driving force is not driven by the cortical gray matter (alone), but in white matter, subcortical structures or cerebellum instead.

Interestingly, a selection of our top genes from the last developmental stage are down-regulated in the aging brain and in Alzheimer's disease. In parallel, the same regions come forward comparing the developmental cortical expansion patterns between

34 and 38 postconceptional weeks and cortical thinning in the aging and Alzheimer's disease brain. For example, cortical thinning-affected regions in the aging and Alzheimer cortex are found around the superior and middle frontal gyrus, cingulate cortex and inferior and middle temporal gyrus (Fjell et al., 2009; Fjell et al., 2012; Salat et al., 2004). Therefore, it seems that the upregulated genetic and cortical transition profile of an almost completely developed cortex is showing the opposite of the genetic and cortical profiles in aging: i.e., the degradation of that genetic profile and cortical thinning. Further explorations of expression of potential risk genes might be necessary to give more spatial-temporal information on the link between cortical development and aging.

Our results represent a first exploration of the spatial genetic profiles influencing fetal cortical growth in the human brain. Future research implementing additional, novel molecular and/or neuroimaging methodologies would therefore be of high interest. One point that should be taken into account is the relative scarcity of available fetal transcriptome data. Gene expression patterns of two developmental stages (week 24 and week 37) were available and included in our study. This may have resulted in the lack of identification of subtle genetic differences during early and mid-third trimester cortical growth, leaving the specific role of AXON and SYNAPSE genes in early stages of brain development unclear. Another point is that the AXON and SYNAPSE correlations were not found to be particularly specific in terms of other genes enriched in brain tissue, suggesting that these genes are only a subset of brain-related genes that have a role in (and/or can disturb) cortical growth. More insight into the relationship between neural circuitry genes and cortical development could be obtained by supplementing this research with fetal diffusion tensor imaging (DTI), such as the freely available fetal DTI dataset of Khan et al (2019). It would be interesting to examine the link between DTI-based fetal brain connectivity maturation, gene expression levels and cortical growth in the future, with one hypothesis suggesting that cortical growth and gyrification are related to the growth and strengthening of axonal bundles (Van Essen, 1997). A comprehensive analysis of genes-sets (other than genes linked to neural-circuitry) is needed to supplement our knowledge on the influence of microscale processes underlying healthy and perturbed cortical growth. Potential genes-sets for future research could include genes that are associated with neurodevelopmental disorders and evolution. It would be interesting to study whether fetal brain growth matches the cortical pattern of expression of human accelerated genes (HAR-genes). HAR-genes have potentially played an important role in cortical expansion during recent evolution of the human brain (Levchenko et al., 2017), and could thus bring new insights into recent developmental adaptations that facilitated divergent human brain function (Rilling, 2014) and dysfunction (Won et al., 2019).

Combining different opensource databases, this study complements our understanding of the relation between genes and fetal brain development (Bui et al., 2010; Grasby et al., 2020; Kang et al., 2011; Lambert et al., 2011; Quezada et al., 2020), showing that

neural circuitry development genes are important candidates for genetically determined patterns of human cortical formation. Understanding underlying gene regulatory mechanisms that drive and shape cortical expansion during fetal brain development provides new opportunities to study genetic susceptibility to developmental disorders.

REFERENCES

Bayer, S. A., & Altman, J. (2003). The human brain during the third trimester. CRC Press.

Bayer, S. A., & Altman, J. (2005). The human brain during the second trimester. CRC Press.

Bui, Wappler, I., Peters, H., Lindsay, S., Clowry, G. J., & Bayatti, N. (2010). Investigating gradients of gene expression involved in early human cortical development. Journal of anatomy, 217(4), 300-311.

Burt, J. B., Helmer, M., Shinn, M., Anticevic, A., & Murray, J. D. (2020, Oct 15). Generative modeling of brain maps with spatial autocorrelation. NeuroImage, 220, 117038. https://doi.org/10.1016/j.neuroimage.2020.117038

Cadwell, C. R., Bhaduri, A., Mostajo-Radji, M. A., Keefe, M. G., & Nowakowski, T. J. (2019, 2019/09/25/). Development and Arealization of the Cerebral Cortex. Neuron, 103(6), 980-1004. https://doi.org/https://doi.org/10.1016/j.neuron.2019.07.009

de Graaf-Peters, V. B., & Hadders-Algra, M. (2006, 2006/04/01/). Ontogeny of the human central nervous system: What is happening when? Early human development, 82(4), 257-266. https://doi.org/https://doi.org/10.1016/j.earlhumdev.2005.10.013

de Juan Romero, C., Bruder, C., Tomasello, U., Sanz-Anquela, J. M., & Borrell, V. (2015, Jul 14). Discrete domains of gene expression in germinal layers distinguish the development of gyrencephaly. The EMBO journal, 34(14), 1859-1874. https://doi.org/https://doi.org/10.15252/embj.201591176

Diez, I., Larson, A. G., Nakhate, V., Dunn, E. C., Fricchione, G. L., Nicholson, T. R., Sepulcre, J., & Perez, D. L. (2020, Feb 12). Early-life trauma endophenotypes and brain circuit-gene expression relationships in functional neurological (conversion) disorder. Mol Psychiatry, 26(8), 1-12. https://doi.org/10.1038/s41380-020-0665-0

Dubois, J., Benders, M., Cachia, A., Lazeyras, F., Ha-Vinh Leuchter, R., Sizonenko, S. V., Borradori-Tolsa, C., Mangin, J. F., & Huppi, P. S. (2008, Jun). Mapping the early cortical folding process in the preterm newborn brain. Cereb Cortex, 18(6), 1444-1454. https://doi.org/10.1093/cercor/bhm180

Fjell, A. M., Westlye, L. T., Amlien, I., Espeseth, T., Reinvang, I., Raz, N., Agartz, I., Salat, D. H., Greve, D. N., Fischl, B., Dale, A. M., & Walhovd, K. B. (2009, Sep). High Consistency of Regional Cortical

Thinning in Aging across Multiple Samples. Cerebral Cortex, 19(9), 2001-2012. https://doi.org/10.1093/cercor/bhn232

Fjell, A. M., Westlye, L. T., Grydeland, H., Amlien, I., Espeseth, T., Reinvang, I., Raz, N., Dale, A. M., Walhovd, K. B., & Initiative, f. t. A. D. N. (2012, Apr). Accelerating Cortical Thinning: Unique to Dementia or Universal in Aging? Cerebral Cortex, 24(4), 919-934. https://doi.org/10.1093/cercor/bhs379

Fulcher, B. D., Arnatkevičiūtė, A., & Fornito, A. (2020). Overcoming bias in gene-set enrichment analyses of brain-wide transcriptomic data. bioRxiv.

Garcia, K. E., Robinson, E. C., Alexopoulos, D., Dierker, D. L., Glasser, M. F., Coalson, T. S., Ortinau, C. M., Rueckert, D., Taber, L. A., Van Essen, D. C., Rogers, C. E., Smyser, C. D., & Bayly, P. V. (2018, Mar 20). Dynamic patterns of cortical expansion during folding of the preterm human brain. Proc Natl Acad Sci U S A, 115(12), 3156-3161. https://doi.org/10.1073/pnas.1715451115

Gholipour, A., Rollins, C. K., Velasco-Annis, C., Ouaalam, A., Akhondi-Asl, A., Afacan, O., Ortinau, C. M., Clancy, S., Limperopoulos, C., Yang, E., Estroff, J. A., & Warfield, S. K. (2017, Mar 28). A normative spatiotemporal MRI atlas of the fetal brain for automatic segmentation and analysis of early brain growth. Sci Rep, 7(1), 476. https://doi.org/10.1038/s41598-017-00525-w

Gladys, L. H. Y., Fornito, A., & Fulcher, B. D. (2020). Scaling of gene transcriptional gradients with brain size across mouse development. NeuroImage, 117395.

Grasby, K. L., Jahanshad, N., Painter, J. N., Colodro-Conde, L., Bralten, J., Hibar, D. P., Lind, P. et al. & Enhancing NeuroImaging Genetics through Meta-Analysis Consortium -Genetics working, g. (2020, Mar 20). The genetic architecture of the human cerebral cortex. Science, 367(6484). https://doi.org/10.1126/science.aay6690

Gulsuner, S., & McClellan, J. M. (2014). De novo mutations in schizophrenia disrupt genes co-expressed in fetal prefrontal cortex. Neuropsychopharmacology(39), 238-239. https://doi.org/10.1038/npp.2013.219

Hill, J., Dierker, D., Neil, J., Inder, T., Knutsen, A., Harwell, J., Coalson, T., & Van Essen, D. (2010, Feb 10). A surface-based analysis of hemispheric asymmetries and folding of cerebral cortex in term-born human infants. J Neurosci, 30(6), 2268-2276. https://doi.org/10.1523/JNEUROSCI.4682-09.2010

Hill, J., Inder, T., Neil, J., Dierker, D., Harwell, J., & Van Essen, D. (2010, Jul 20). Similar patterns of cortical expansion during human development and evolution. Proc Natl Acad Sci U S A, 107(29), 13135-13140. https://doi.org/10.1073/pnas.1001229107

Hu, W. F., Chahrour, M. H., & Walsh, C. A. (2014). The diverse genetic landscape of neurodevelopmental disorders. Annual review of genomics and human genetics, 15, 195-213. https://doi.org/10.1146/

annurev-genom-090413-025600

Huttenlocher, P. R., & Dabholkar, A. S. (1997, Oct 20). Regional differences in synaptogenesis in human cerebral cortex. J Comp Neurol, 387(2), 167-178. https://doi.org/10.1002/(sici)1096-9861(19971020)387:2<167::aid-cne1>3.0.co;2-z

Kang, H. J., Kawasawa, Y. I., Cheng, F., Zhu, Y., Xu, X., Li, M., Sousa, A. M., Pletikos, M., Meyer, K. A., Sedmak, G., Guennel, T., Shin, Y., Johnson, M. B., Krsnik, Z., Mayer, S., Fertuzinhos, S., Umlauf, S., Lisgo, S. N., Vortmeyer, A., Weinberger, D. R., Mane, S., Hyde, T. M., Huttner, A., Reimers, M., Kleinman, J. E., & Sestan, N. (2011, Oct 26). Spatio-temporal transcriptome of the human brain. Nature, 478(7370), 483-489. https://doi.org/10.1038/nature10523

Khan, S., Vasung, L., Marami, B., Rollins, C. K., Afacan, O., Ortinau, C. M., Yang, E., Warfield, S. K., & Gholipour, A. (2019, Jan 15). Fetal brain growth portrayed by a spatiotemporal diffusion tensor MRI atlas computed from in utero images. NeuroImage, 185, 593-608. https://doi.org/10.1016/j.neuro-image.2018.08.030

Kriegstein, A., Noctor, S., & Martinez-Cerdeno, V. (2006, Nov). Patterns of neural stem and progenitor cell division may underlie evolutionary cortical expansion. Nat Rev Neurosci, 7(11), 883-890. https://doi.org/10.1038/nrn2008

Lambert, N., Lambot, M. A., Bilheu, A., Albert, V., Englert, Y., Libert, F., Noel, J. C., Sotiriou, C., Holloway, A. K., Pollard, K. S., Detours, V., & Vanderhaeghen, P. (2011, Mar 18). Genes expressed in specific areas of the human fetal cerebral cortex display distinct patterns of evolution. PLoS One, 6(3), e17753. https://doi.org/10.1371/journal.pone.0017753

Lee, J. C., Mayer-Proschel, M., & Rao, M. S. (2000, Apr). Gliogenesis in the central nervous system. Glia, 30(2), 105-121. https://doi.org/10.1002/(sici)1098-1136(200004)30:2

Levchenko, A., Kanapin, A., Samsonova, A., & Gainetdinov, R. R. (2017). Human accelerated regions and other human-specific sequence variations in the context of evolution and their relevance for brain development. Genome biology and evolution, 10(1), 166-188.

Liu, J., Liu, W., Yang, L., Wu, Q., Zhang, H., Fang, A., Li, L., Xu, X., Sun, L., Zhang, J., Tang, F., & Wang, X. (2017, Nov 2). The Primate-Specific Gene TMEM14B Marks Outer Radial Glia Cells and Promotes Cortical Expansion and Folding. Cell Stem Cell, 21(5), 635-649 e638. https://doi.org/10.1016/j.stem.2017.08.013

Miller, J. A., Ding, S. L., Sunkin, S. M., Smith, K. A., Ng, L., Szafer, A., Ebbert, A., Riley, Z. L., et al. (2014, Apr 10). Transcriptional landscape of the prenatal human brain. Nature, 508(7495), 199-206. https://doi.org/10.1038/nature13185

Muller, F., & O'Rahilly, R. (2011). The initial appearance of the cranial nerves and related neuronal migration in staged human embryos. Cells Tissues Organs, 193(4), 215-238. https://doi.org/10.1159/000320026

Nowakowski, T. J., Bhaduri, A., Pollen, A. A., Alvarado, B., Mostajo-Radji, M. A., Di Lullo, E., Haeussler, M., Sandoval-Espinosa, C., Liu, S. J., Velmeshev, D., Ounadjela, J. R., Shuga, J., Wang, X., Lim, D. A., West, J. A., Leyrat, A. A., Kent, W. J., & Kriegstein, A. R. (2017, Dec 8). Spatiotemporal gene expression trajectories reveal developmental hierarchies of the human cortex. Science, 358(6368), 1318. https://doi.org/10.1126/science.aap8809

O'Rahilly, R., & Muller, F. (2010). Developmental stages in human embryos: revised and new measurements. Cells Tissues Organs, 192(2), 73-84. https://doi.org/10.1159/000289817

Quezada, S., van de Looij, Y., Hale, N., Rana, S., Sizonenko, S. V., Gilchrist, C., Castillo-Melendez, M., Tolcos, M., & Walker, D. W. (2020, Nov 3). Genetic and microstructural differences in the cortical plate of gyri and sulci during gyrification in fetal sheep. Cereb Cortex, 30(12), 6169-6190. https://doi.org/10.1093/cercor/bhaa171

Reissland, N., & Kisilevsky, B. S. (2016). Fetal development: research on brain and behavior, environmental influences, and emerging technologies. Springer.

Rilling, J. K. (2014, Jan). Comparative primate neuroimaging: insights into human brain evolution. Trends Cogn Sci, 18(1), 46-55. https://doi.org/10.1016/j.tics.2013.09.013

Romme, I. A., de Reus, M. A., Ophoff, R. A., Kahn, R. S., & van den Heuvel, M. P. (2017, Mar 15). Connectome Disconnectivity and Cortical Gene Expression in Patients With Schizophrenia. Biol Psychiatry, 81(6), 495-502. https://doi.org/10.1016/j.biopsych.2016.07.012

Salat, D. H., Buckner, R. L., Snyder, A. Z., Greve, D. N., Desikan, R. S., Busa, E., Morris, J. C., Dale, A. M., & Fischl, B. (2004, Jul). Thinning of the cerebral cortex in aging. Cerebral Cortex, 14(7), 721-730. https://doi.org/10.1093/cercor/bhh032

Scarr, E., Udawela, M., & Dean, B. (2018, Feb 20). Changed frontal pole gene expression suggest altered interplay between neurotransmitter, developmental, and inflammatory pathways in schizophrenia. NPJ Schizophr, 4(1), 4. https://doi.org/10.1038/s41537-018-0044-x

Subramanian, A., Tamayo, P., Mootha, V. K., Mukherjee, S., Ebert, B. L., Gillette, M. A., Paulovich, A., Pomeroy, S. L., Golub, T. R., Lander, E. S., & Mesirov, J. P. (2005, Oct 25). Gene set enrichment analysis: a knowledge-based approach for interpreting genome-wide expression profiles. Proc Natl Acad Sci U S A, 102(43), 15545-15550. https://doi.org/10.1073/pnas.0506580102

Van Essen, D. C. (1997, Jan 23). A tension-based theory of morphogenesis and compact wiring in the central nervous system. *Nature, 385*(6614), 313-318. https://doi.org/10.1038/385313a0

Vasung, L., Huang, H., Jovanov-Milosevic, N., Pletikos, M., Mori, S., & Kostovic, I. (2010, Oct). Development of axonal pathways in the human fetal fronto-limbic brain: histochemical characterization and diffusion tensor imaging. *J Anat, 217*(4), 400-417. https://doi.org/10.1111/j.1469-7580.2010.01260.x

Watanabe, K., Taskesen, E., Van Bochoven, A., & Posthuma, D. (2017, Nov 28). Functional mapping and annotation of genetic associations with FUMA. *Nature communications, 8*(1), 1-11. https://doi.org/10.1038/s41467-017-01261-5

Wei, Y., de Lange, S. C., Pijnenburg, R., Scholtens, L. H., Ardesch, D. J., Watanabe, K., Posthuma, D., & van den Heuvel, M. P. (2022). Statistical testing in transcriptomic-neuroimaging studies: A how-to and evaluation of methods assessing spatial and gene specificity. *Human brain mapping, 43*(3), 885-901. https://doi.org/https://doi.org/10.1002/hbm.25711

Wei, Y., de Lange, S. C., Scholtens, L. H., Watanabe, K., Ardesch, D. J., Jansen, P. R., Savage, J. E., Li, L., Preuss, T. M., Rilling, J. K., Posthuma, D., & van den Heuvel, M. P. (2019, Oct 24). Genetic mapping and evolutionary analysis of human-expanded cognitive networks. *Nat Commun, 10*(1), 4839. https://doi.org/10.1038/s41467-019-12764-8

Willsey, A. J., Sanders, S. J., Li, M., Dong, S., Tebbenkamp, A. T., Muhle, R. A., Reilly, S. K., Lin, et al. (2013, Nov 21). Coexpression networks implicate human midfetal deep cortical projection neurons in the pathogenesis of autism. *Cell, 155*(5), 997-1007. https://doi.org/10.1016/j.cell.2013.10.020

Won, H., Huang, J., Opland, C. K., Hartl, C. L., & Geschwind, D. H. (2019, Jun 3). Human evolved regulatory elements modulate genes involved in cortical expansion and neurodevelopmental disease susceptibility. *Nat Commun, 10*(1), 2396. https://doi.org/10.1038/s41467-019-10248-3

Chapter 3

Functional connectome of the fetal brain

Elise Turk, Marion I. van den Heuvel, Manon J. Benders, Roel de Heus, Arie Franx, Janessa H. Manning, Jasmine L. Hect, Edgar Hernandez-Andrade, Sonia S. Hassan, Roberto Romero, René S. Kahn, Moriah E. Thomason **, Martijn P. van den Heuvel**
** *shared-last author*

ABSTRACT

Large-scale functional connectome formation and re-organization is apparent in the second trimester of pregnancy, making it a crucial and vulnerable time window in connectome development. Here we identified which architectural principles of functional connectome organization are initiated prior to birth, and contrast those with topological characteristics observed in the mature adult brain. A sample of 105 pregnant women participated in human fetal resting-state fMRI studies (fetal gestational age between 20 and 40 weeks). Connectome analysis was used to analyze weighted network characteristics of fetal macroscale brain wiring. We identified efficient network attributes, common functional modules and high overlap between the fetal and adult brain network. Our results indicate that key features of the functional connectome are present in the second and third trimesters of pregnancy. Understanding the organizational principles of fetal connectome organization may bring opportunities to develop markers for early detection of alterations of brain function.

SIGNIFICANCE STATEMENT

The fetal to neonatal period is well known as a critical stage in brain development. Rapid neurodevelopmental processes establish key functional neural circuits of the human brain. Prenatal risk factors may interfere with early trajectories of connectome formation and thereby shape future health outcomes. Recent advances in MRI have made it possible to examine fetal brain functional connectivity. In this study, we evaluate the network topography of normative functional network development during connectome genesis *in utero*. Understanding the developmental trajectory of brain connectivity provides a basis for understanding how the prenatal period shapes future brain function and disease dysfunction.

INTRODUCTION

The brain is organized as a complex network of functionally communicating regions, a network also known as the functional connectome. The macroscale functional connectome is observable using MRI in infancy and studies have reported hallmark features, including the presence of functionally coupled modules, small world organization and putative hubs that facilitate efficient global communication (Ball et al., 2014; Gao et al., 2015; Gao et al., 2009; Lin et al., 2008; Smyser et al., 2010; van den Heuvel et al., 2015). Functional connectome development of older children and adolescents has been characterized by a reconfiguration from a modular into a more global integrated network during adult life (Fair et al., 2009; Power et al., 2010). Examining the specific earlier age-stages of macroscale connectome maturation will provide important new insight into the architecture of human brain structure and function. In this manuscript we will address

important questions about the first phases after connectome genesis by evaluating the human fetal brain prior to birth.

Available evidence suggests that the macroscale connectome begins to take form when the majority of neurons have reached their final destination (Huttenlocher & Dabholkar, 1997; Mrzljak et al., 1991; Sidman & Rakic, 1973). Structural outgrowth is supported by spontaneous firing of neurons that reinforce appropriate connections and trigger essential activity-dependent signaling processes (Thomason, 2018) giving rise to structural and functional cortical connectivity (Kostović & Jovanov-Milošević, 2006; Vasung et al., 2010). This has led to the suggestion that basic principles of the functional connectome are initially established as early as during late second trimester of pregnancy (Collin & van den Heuvel, 2013; Hoff et al., 2013).

The trajectory of functional dynamics of brain development follows multiple stages, all influencing future connectome health. Prenatal processes such as maternal viral infections, extensive stress, food-intake, alcohol and medication use, among others, all have strong influence on later life functional connectivity (FC) of children (de Water et al., 2017; Grewen et al., 2015; Infante et al., 2017; Li et al., 2016; Rudolph et al., 2018; Salzwedel et al., 2016; Salzwedel et al., 2015; van den Bergh et al., 2017). With advances in fetal resting-state neuroimaging it is now possible to measure these functional connectivity (FC) patterns non-invasively *in vivo* (see for review Anderson & Thomason, 2013; van den Heuvel & Thomason, 2016). Mapping and understanding the healthy fetal functional connectome may bring opportunities for early detection of functional alterations of the vulnerable developing brain.

We understand relatively little about the onset of key principles of the functional connectome before birth. Researchers have begun to isolate foundational aspects of prenatal functional brain development, but these studies are strikingly few. Available studies show that fetal FC strength between homologous cortical regions increases with advancing age in a medial to lateral gradient (Thomason et al., 2013). Additionally, long-range functional connections, highly connected primary and association regions and first principals of resting-states networks as observed in (mostly preterm born) neonates have been detected across 20 to 40 weeks of gestational age (Jakab et al., 2014; Schöpf et al., 2012; Schöpf et al., 2014; Thomason et al., 2015; van den Heuvel et al., 2018). However, with the field of fetal FC rapidly growing, much remains to be understood about the onset and development of fundamental connectome properties during the early stages of connectome genesis.

The goal of the present study is to complement the field of fetal fMRI by utilizing a large fetal resting-state fMRI dataset (N= 105) to evaluate the early presence of key characteristics of human connectome organization prior to birth. We aim to shed light on the

blueprint of the connectome by comparing fetal topological characteristics to those observed in the mature adult brain. We apply graph analytical methods to better understand properties of small world organization, modularity, and rich club hub organization of functional brain dynamics during the late second and third trimester of pregnancy.

METHODS

Study population
A total of 139 healthy, non-sedated pregnant women underwent MRI examination in their late second or third trimester of pregnancy. Singleton fetuses were scanned using a 3T MRI system at Wayne State University, Detroit, MI (van den Heuvel et al., 2018). 34 of the 139 cases were excluded prior to analysis due to high movement or due to detectable health complications (e.g., subsequent preterm birth, pre-eclampsia), leaving the inclusion of 105 fetal subjects (39% female, 61% male). Mean age of the fetuses at the time of MRI was 33.5 (S.D. = 3.97) weeks of gestation with a range of 20.6 – 39.6 weeks gestational age. Subjects were born, on average, at 39.3 weeks of gestation (S.D. = 1.22). Ethnic/racial distribution of the subjects was 81% African-American, 10.5% Caucasian, 2.9% Bi-racial, and 5.7% not disclosed. All procedures were carried out as approved by the Institutional Review Board of Wayne State University, Detroit, MI. Written informed consent was obtained from all participants prior to examination.

FETAL RESTING-STATE FMRI

fMRI acquisition
MRI was examined using a Siemens Verio 70-cm open-bore 3T MR system with a 550g abdominal 4-channel Siemens Flex Coil. Echo planar imaging (EPI) BOLD parameters included: TR/TE, 2000/30 ms, 360 axial frames, matrix size 96 x 96 x 25, no slice gap, voxel size 3.4 x 3.4 x 4mm3, 80-degree flip angle, repeated twice. Fetal MRI data, subject demographics, and data variables are available at https://nda.nih.gov/edit_collection. html?id=2434.

Functional data processing
Subsamples of this data have been published before and preprocessing of fetal resting state fMRI followed previously reported methods (Thomason et al., 2013; van den Heuvel et al., 2018). In brief, periods, or epochs, of fetal quiescence were selected using FSL image view (FSL, RRID:SCR_002823), and high motion frames were removed manually. Minimum length of a selected epoch was 20 seconds (10 frames) of low motion (< 2mm translation, < 3 degrees rotation). Cases were required to have a minimum of 4 minutes of low movement resting state fMRI, resulting in the average of 168 frames (SD = 57) across the group. Next, for each dataset, a fetal brain mask was manually drawn around the fetal brain, separately for each low-motion epoch from a single representative image
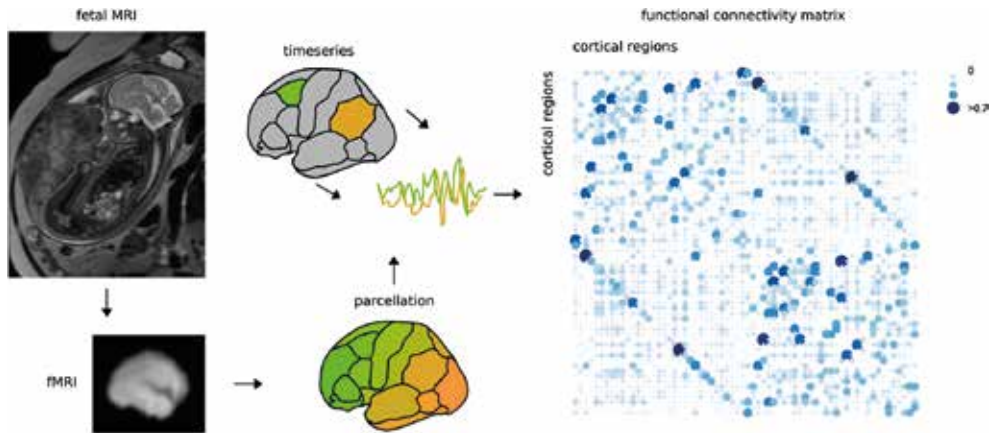
Figure 1. Fetal functional connectome reconstruction.

A total of 105 healthy pregnant women underwent MRI examination of the fetal brain, including T2 and fMRI sequences (upper left T2 image, courtesy of Wilhelmina Children's Hospital, Utrecht, the Netherlands). Preprocessed resting state fMRI images of 105 fetuses were parcellated using a manually annotated Desikan Killiany atlas. Subject-level timeseries from all voxels within a region were averaged and correlated to all other regions of the atlas. This resulted into a FC matrix of 66 cortical nodes, preserving only positive associations (correlation coefficient between 0 and 1) in this visual representation.

within the epoch using BrainSuite (RRID:SCR_006623). This subject-specific brain mask was used to extract the brain from the maternal compartment for the corresponding epoch. Following this, segmented fetal brains were manually reoriented into standard A-P, R-L, and I-S orientation, with the origin set to the middle of the brain. The quality of reorientation was visually assessed by expert raters by manually checking the alignment of the interhemispheric space with the vertical crosshair for transverse and coronal orientations using Statistical Parametric Mapping (SPM8, RRID:SCR_007037) software (Ashburner et al., 2012) implemented in MATLAB. Reoriented, recentered data epochs were then individually realigned and normalized in SPM. Two normalization approaches were tested in order to evaluate potential influence of preprocessing steps on study outcomes. Epochs were normalized to a 32-week infant brain template (Serag et al., 2012), representing the group mean, and to age specific templates see age-specific connectome reconstruction below. Normalization settings were set to standard settings in SPM, regularization settings were set to the average sized template. All normalized images from each segment were then concatenated into one run, realignment was performed on the concatenated time series to address potential epoch misalignment, and, finally spatial smoothing was performed with a 4 mm FWHM Gaussian kernel. Connectivity correlation analysis was performed in CONN software (Connectivity Toolbox v14n, RRID:SCR_009550) implemented in MATLAB. For each subject, the 32-week

brain template was used as an anatomical reference image and ROIs were selected using FreeSurfer's Desikan Killiany atlas (see details below). The following parameters were used in subject level processing: linear detrending, band-pass filtering at 0.008 to 0.09 Hz., and no despiking. Nuisance regression included a CompCor of five principal components extracted from white matter and CSF masks, and also 6 motion parameters produced by SPM during concatenated segment realignment. White matter and CSF probability masks corresponded to the anatomical reference images generated by Serag and colleagues (Serag et al., 2012) used in the preprocessing steps described above.

Functional connectome reconstruction
Brain regions were selected using cortical regions of the FreeSurfer's Desikan Killiany atlas reconstructed (including manual fine-tuning in FreeSurfer, RRID:SCR_001847) onto the fetal brain template (see **Figure 1**). A surrogate T1 image was created from the T2 template image by flipping the image contrast and used as input for the pipeline of Free-surfer. The cortex, subcortex and ribbon labels were visually inspected and manually fine-tuned using tksurfer. Using the new label files, Freesurfer's mris_ca_label and mri_apar-c2aseg were computed, resulting in a fetal parcellation of the cortical mantle of 68 nodes (34 regions in each hemisphere). The reconstructed atlas on the fetal brain and cortical ribbon were visually inspected and evaluated by the research team. Voxels of the left and right isthmus cingulate cortex were excluded from further analysis, because inaccurate segmentation of these areas on the 32-week brain template was observed, resulting in 66 regions taken forward for further analysis. FC between brain regions was computed by means of correlation analysis between the recorded regional BOLD time-series, followed by Z-score transformation. Negative correlations derived from functional resting-state fMRI recordings remain a topic of investigation in the field and were set to zero to reduce contributions of low or potentially spurious cortical interactions. No threshold was used for the modularity analysis to determine resting-state networks (van den Heuvel et al., 2017). A group-averaged fetal connectivity graph was computed across all fetal brains by taking the (non-zero) average of the FC value of all pairs of nodes across all subjects. Connections present in 60% or more of the total group (see Figure 1) were included in the group connectivity matrix.

Age-specific fetal brain atlas connectome reconstruction
A second method of functional data processing was performed. Instead of normalizing individual fMRI data to a commonly used single 32-week infant brain template, we examined the use of multiple age-specific brain templates. For this we utilized an online resource for fetal brain templates and their corresponding atlas and tissue (e.g., developing white matter, CSF) segmentations (CRL Unbiased and Deformable Spatiotemporal Atlas of the Fetal Brain, RRID:SCR_014176, Gholipour et al., 2017). We normalized each fetal fMRI data to a template of the nearest gestational week (which are included in the DSA of 21 to 38 weeks, with increments of 1 week) using standard settings in SPM8.

Visual inspection revealed a total of 90 out of 105 subjects which could be successfully normalized to their age specific brain template and atlas. The 15 subjects that did not properly normalize to their matching template and datasets were excluded from further analysis. Further preprocessing included the same steps implemented with the Desikan Killiany atlas, comprising spatially smoothing, linear detrending and nuisance regression using CompCor analysis including five principal components extracted from the age specific tissue images' white matter and CSF mask, and motion regression. Brain regions for the connectome analysis were selected using cortical regions of the fetal brain atlas (Gholipour et al., 2017) providing a consistent set of 78 regions identified across the fetal brain templates (39 regions in each hemisphere) and functional connectivity between brain regions was computed using correlation analysis. All negative correlations were set to zero to reduce contributions of low or potentially spurious cortical interactions. No threshold was used for the modularity analysis.

Network metrics
Network metrics were computed using the weighted group-averaged FC graph, with metrics computed using both the group-averaged and individual weighted FC graphs of each of the fetal subjects separately. Following prior work, network metrics included calculation of the clustering coefficient, characteristic path length, small world index, rich club index and modularity (Rubinov & Sporns, 2010; van den Heuvel & Sporns, 2011). Permutation testing was used to compare fetal FC patterns against 1,000 random networks preserving the degree distribution (Maslov & Sneppen, 2002). Normalized network metrics were obtained by taking the ratio of the actual graph metrics and graph metrics observed in the random networks. All results were validated for motion artifacts by computing the network metrics on a subsample of the dataset selecting 52 subjects with most fMRI frames (i.e., 50% with lowest movement). Clustering coefficient was computed as the average clustering-coefficient (C_i) over all nodes (i) in the network, with C_i describing the ratio between the number of connections between node i and its neighbor-nodes and the total number of possible connections with neighbors. Characteristic path length was computed by the average minimal travel distance (i.e., shortest paths, L_i) between all nodes in the network. Small-world index was computed as the ratio of normalized global clustering coefficient and normalized characteristic path length, based on the ratio between clustering coefficient (C) and characteristic path length (L) and the clustering and path length of a set of 1,000 random networks (Crandom and Lrandom). A small-world index >1 was used as an indication of a small-world organization of the network.

Rich club organization of a network describes the above random level of connectivity between the high-strength nodes of the network, with the rich club describing a subset of nodes more densely interconnected than expected based on their degree alone (Colizza et al., 2006; Opsahl et al., 2008; van den Heuvel & Sporns, 2011). A functional weighted

rich club coefficient ($\varphi^w(k)$) was computed as the ratio between the total sum of edge weights that connect nodes of strength $>k$ and the total sum of the strength of the whole network (van den Heuvel & Sporns, 2011). $\varphi^w(k)$ was compared with $\varphi^w_{random}(k)$ of a set of 1,000 randomly rewired networks keeping the same degree distribution (Maslov & Sneppen, 2002), with $\varphi^w_{norm}(k)$ the ratio between $\varphi^w(k)$ and $\varphi^w_{random}(k)$. A network is argued to display a rich club organization when $\varphi(k) > \varphi^w_{random}(k)$, or equivalent $\varphi^w_{norm}(k) > 1$ (Colizza et al., 2006; van den Heuvel & Sporns, 2011). A p value was assigned to $\varphi^w(k)$ as the percentage of the null-distribution that exceeded the value of $\varphi^w(k)$. As an alternative definition of centrality, we also examined betweenness centrality, as the fraction of all weighted shortest paths in the network that contain a given node (Ball et al., 2014; Fransson et al., 2010). In this study, the top 15% nodes with the highest strength or largest values for betweenness centrality were included as central nodes (van den Heuvel & Sporns, 2011).

Community structure of the fetal functional brain network was examined by means of decomposing the network into functional resting-state networks, or modules, determined using Louvain's community detection algorithm (Rubinov & Sporns, 2010). Louvain's community detection algorithm was used on the unthresholded fetal graph, allowing the preservation of both negatively and positively correlated brain regions. Modularity (Q) was computed to quantify the degree to which the network can be subdivided in delineated modules.

Adult connectome used for comparison
Preprocessed adult fMRI data (N=42; 26 males) were taken from a previously used dataset (van den Heuvel et al., 2015), including FC matrices and an average participant age of 29 years (S.D. = 8). The adult FC matrices were constructed using the Desikan-Killiany atlas to match the 66 regions of the fetal atlas (i.e., 68 minus bilateral isthmus cingulate cortices), allowing for a direct comparison of network structure between the fetal and adult brain. The adult group-averaged graph was computed using similar procedures as constructing the fetal graph, with additional specifications described in (van den Heuvel et al., 2015).

STATISTICAL EVALUATION

Comparison of the fetal and adult functional connectome
Overlap of the fetal and adult connectome was determined by means of the Mantel test (Mantel, 1967; Scholtens et al., 2014), comparing the level of overlap between the binary group-averaged fetal and adult matrices (threshold = 0). Mantel comparison included the computation of a distance matrix, with cell entry 1 corresponding to overlapping values across the fetal and neonatal matrix and entry 0 to non-corresponding entries between the fetal and adult group matrix, with the level of overlap taken as the density of the distance

matrix, ranging from no overlap (0) to complete overlap (1). Permutation testing with 1,000 random networks involved randomizing the binary fetal and adult matrix while preserving degree sequence. Permutation testing was used to assign a p-value to the level of overlap between the fetal and adult connectome. Weighted overlap was additionally computed as the level of partial correlation between the two weighted group-averaged graphs across the set of connections (excluding zero elements) observed in both the fetal and adult connectome. We controlled for Euclidian distance between brain regions, to confirm that the effect of higher connectivity between spatially close regions was not the driven force of the measured overlap, by means of partial correlation analysis.

Comparison of fetal and adult modular organization
Overlap in adult and fetal modular organization was examined using the Rand index (Rand, 1971), taken a pairwise comparison of the number of node pairs that are classified in the same or different modules across the module assignments of the two compared matrices (Karrer et al., 2008), with a Rand index of 0 indicating no overlap and an index of 1 indicating complete overlap. The modular assignments of the nodes of both the adult and fetus were randomized across 1000 permutations, and the Rand index in the random situations was computed as a null-distribution. The resulting null distribution of random overlap effects was used to assign a p value based on the percentage of observations in the random condition exceeding the original value. Within module connectivity strength was computed for each node (i) as the total number, or degree, of connection, multiplied with their weights, or strength, attached to all nodes in one module.

Evaluation of the robustness of the data
Given the sensitivity of resting state data to motion and complexity of analyzing fMRI in a fetal cohort, multiple control analyses were performed to estimate the variance within and between groups and thereby evaluate the robustness of findings. As a control condition, we examined fetal group network metrics for the subgroup of low-motion participants separately (i.e. 50% of the population with the lowest movement during fMRI acquisition). Additionally, control analyses were performed on the robustness of the fetal group connectome. Fetal subjects were 1,000 times split into two randomly chosen equal-sized groups and new group matrices were computed. Comparing the overlap of different matrices, correlation analyses with and without controlling for the adult connectome were performed on two random fetal group matrices. Third, we addressed potential concerns regarding possible influence of the white matter regressor on the fMRI signal. Performing white matter regression on fMRI is a normal strategy in adult subjects. However, the developing myelination and changing intensity of the white matter in fetal subjects may influence the utility of this regressor at different fetal ages. To address this, all network metrics and the association with the adult connectome were recomputed on fetal matrices computed excluding white matter as a regressor, and results were compared across approaches.

RESULTS

Network metrics

Group-averaged fetal connectome showed a density of 42%, significantly higher clustering (1.20 times higher than one would expect in 1,000 random networks, p < 0.001), longer path length (1.14 times longer than 1,000 random networks, p < 0.001), and a small-world index larger than 1 (1.05 times higher than 1,000 random networks, p < 0.001). Group-averaged fetal connectome reconstructed from the age-matched fetal brain atlas (Gholipour et al., 2017) similarly showed significantly higher clustering (2.62 times higher than one would expect in 1,000 random networks, p < 0.001), longer path length (1.13 times longer than 1,000 random networks, p < 0.001), and a small-world index larger than 1 (1.97 times higher than 1,000 random networks, p < 0.001).
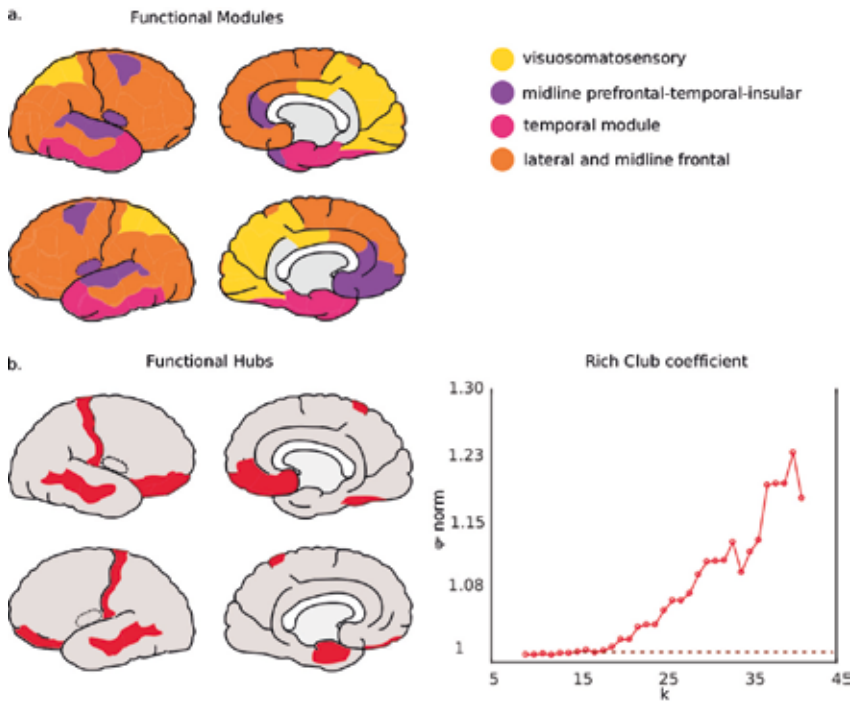
Figure 2. Connectomic features of the fetal group matrix.
Panel (a) shows the modular organization plotted on the fetal cortex, with colors representing composition of four modules observed in fetal brain function. Panel (b) shows the rich club regions in red plotted on the fetal cortex. On the right, the rich club curve (in red) is displayed, with a significant rich club organization for the range of $22 \leq k \leq 38$ ($\varphi^w_{norm}(k) > 1$), strongly suggesting the existence of a densely interconnected network of central hubs in the fetal connectome (van den Heuvel & Sporns, 2011).
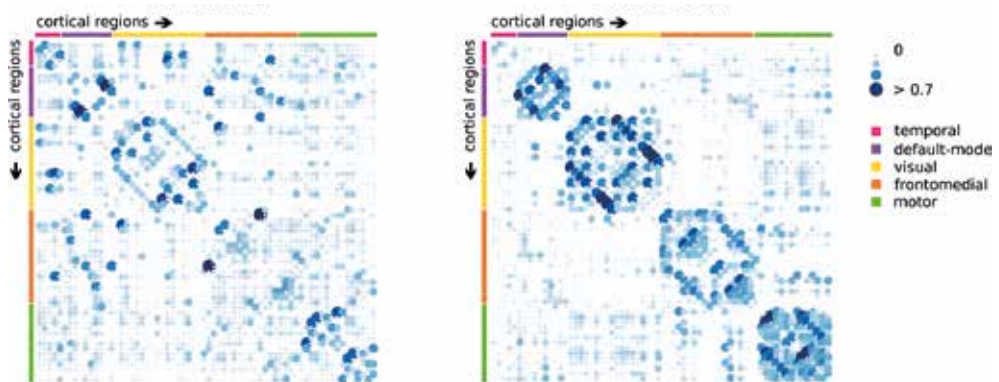
Modular organization

The fetal connectome showed a clear modular organization (Q = 0.28) describing four functional modules. These four functional modules included: 1) an occipital and parietal *visuosomatorsensory* module, with left and right cuneus, lingual, paracentral, pericalcarine, posterior cingulate, precuneus and superior parietal cortical regions, 2) a *midline prefrontal-temporal-insular* module with left and right bankssts (i.e., banks of the superior temporal sulcus), caudal middle frontal, rostral anterior cingulate, superior temporal, transverse temporal, insula, right temporal pole, and left medial orbitofrontal cortical regions, 3) a *temporal* module with left and right entorhinal, fusiform, inferiortemporal, parahippocampal, and left temporal pole cortical regions, 4) an extensive *lateral and midline frontal* module including left and right caudal anterior cingulate, inferior parietal, lateral occipital, lateral orbitofrontal, middle temporal, parsopercularis, parsorbitalis, parstriangularis, postcentral, precentral, rostral middle frontal, superior frontal, supramarginal, frontal pole and right medial orbitofrontal cortical regions (see **Figure** 2a).

The fetal connectome reconstructed from the age-matched fetal brain atlas showed a high modular organization (Q=0.53) revealing two additional functional modules, with this higher number of modules compared to fixed 32-week atlas analysis likely related to the larger number of regions in the age-matched fetal brain atlas. The age-matched fetal brain atlas revealed: 1) a visual module, with left and right superior, middle, inferior occipital cortices, the left and right precuneus, cuneus, calcerine and posterior cingulum. 2) a somatosensory motor module, with left and right superior frontal, superior medial frontal, supplementary motor, paracentral and mid cingulum and left precentral, mid frontal, postcentral, superior and inferior parietal, supramarginal and angular cortices. 4) a temporal and orbitofrontal module with left and right superior, mid, medial and inferior orbitofrontal cortices, left and right olfactory, rectus, parahippocampal, fusiform, mid temporal pole, inferior temporal cortices. 5) a right oriented *mid-frontal-temporal-insular-parietal* module, with right inferior frontal and rolandic operculum, frontal inferior triangularis, anterior cingulum, mid, superior temporal cortices and superior temporal pole, hescl, insular, precentral, frontal, postcentral, superior and inferior parietal, supramaginal and angular cortices. 6) a left oriented *frontal-temporal-insular* module, with left inferior frontal and rolandic operculum, frontal inferior triangularis, anterior cingulum, mid, superior temporal cortices and superior temporal pole, hescl and insular cortices and right anterior cingulum.

Hub organization

The fetal connectome showed a significant rich club organization for the range of 22 ≤ k ≤ 38 ($\varphi^w_{norm}(k) > 1$, p < 0.001, 1000 random networks). The strongest functionally connected nodes of the fetal brain included: bilateral lateral orbitofrontal, postcentral and middle temporal cortical regions, left entorhinal regions as well as the right parsorbitalis, medial orbitofrontal regions and fusiform area. Based on weighted betweenness centrality, the top 15% highest betweenness centrality nodes in the fetal brain included:

bilateral lateral occipital, postcentral, right superior frontal, postcentral, fusiform and left insular, middle temporal, lateral and medial orbitofrontal cortical regions. Rich club index of the Gholipour atlas similarly revealed levels >1 ($p < 0.001$). Based on the functional connectivity strength of the group averaged matrix, the top 15% highest strength nodes included: homologous parts of the precentral, precuneus, postcentral, right insula, and left superior parietal and superior (orbito-) frontal regions. Based on the weighted betweenness centrality, the top 15% densely connected nodes in the fetal cortex included: homologous parts of the superior orbitofrontal cortex, the insula, left mid orbitofrontal cortex, and right regions of the olfactory bulb, angular, mid temporal, rectus, supplementary motor regions, and medial superior frontal cortex. Combining these findings, our results suggest that the strongest functionally connected regions in the fetal brain are predominantly located in the temporal cortical regions and around the midline of the brain including especially frontal, postcentral and insular cortices.

Figure 3. Comparison of group averaged fetal and adult functional connectome modules.
Illustration of the modular organization modules of the fetal (left panel) and adult (right panel)
connectivity matrices. Blue dots represent positive correlations between nodes, the upper 10% of
the highest connections are shown. Both matrices display the adult modular organization, revealing
a temporal, default-mode, visual, frontomedial and motor network.

Overlap between fetal and adult connectome
We continued our analysis by examining the overlap of global and modular organization of the fetal and adult cerebral functional connectome. First, a significant overlap of 61.66% (Mantel test $p < 0.001$) was found between the fetal and adult connectome. The strength of all connections observed in both the fetal and adult cortex showed a significant positive association ($r = 0.389$, $p < 0.001$). The association remained significant when further controlling for Euclidian distance ($r = 0.299$, $p < 0.001$). These data

suggest early presence of an adult-like distribution of FC in the human intrauterine connectome. Secondly, the adult group-averaged matrix revealed five distinct functional modules describing a temporal, default-mode, visual, frontomedial and motor functional network, in contrast to the four modules that were observed in the fetal brain. Side-by-side comparison of the modularity-matrices shows that the fetal connectome has adult-like functional networks components, although they are in an immature state (**Figure 3**). Subsequently, fetal and adult group graphs revealed a high modularity overlap (Rand index: 0.730, $p < 0.001$).

Strong FC overlap between fetal and adult within-module connectivity was found in the visual module ($r = 0.597$, $p < 0.001$), temporal module (0.727, $p < 0.001$), default mode module (0.608, $p < 0.001$), motor module (0.324, $p < 0.001$), while lower overlap was found in the frontomedial module ($r = 0.181$, $p < 0.001$), indicating an early presence of mature networks for four out of five data-derived modules.

ROBUSTNESS ANALYSES

Motion analysis
High clustering, short path length and small-worldness organization were significantly replicated in the subset of 52 low-motion participants (i.e., 50% of the population with lowest movement). Eight out of ten most *functionally* connected areas (highest strength) were replicated. The areas that did not replicate as highly connected areas in the 52 low-motion participants were left postcentral and middle temporal gyrus, which were replaced by left fusiform and left insula. Similarly, eight out of ten most *centrally* connected regions were replicated in the low-motion subgroup. Areas that did not replicate were left middle and medial temporal cortical regions, which were replaced by right insula and left superior frontal cortex. Furthermore, we observed that the modules that were identified were largely replicated when repeating this analysis in the subset of low motion subjects; the only variation observed was expansion of the temporal module to cover a larger extent of the temporal cortex.

Robustness of the fetal group connectome. Splitting the fetal subjects into two random groups, significant associations were found comparing both group matrices (all 1,000 correlations between $r = 0.935$ and $r = 0.975$, $p < 0.001$), and when controlled for the adult matrix, the correlation remained significant ($r = 0.811$ and $r = 0.905$, $p < 0.001$). Correlation analysis between different fetal subgroups revealed strong positive significant within-module connectivity correlations (all $r > 0.9$, $p < 0.001$) for all four modules. *White matter regressor analysis.* Robustness analysis further revealed a significant association ($r = 0.722$, $p < 0.001$) between the mean group matrices of the fetal group computed with and without global white matter correction. A higher density of the group matrix was found (94%, $t = 0$; 58%, $t = 0.1$; 21%, $t = 0.2$; 10%, $t = 0.3$) as a direct

consequence of excluding white matter as a regressor to calculate subject FC matrices. Without global correction of white matter on the fMRI signal, the use of absolute thresholding (i.e., including correlations above a threshold $t > 0.1$) was thus needed to replicate similar network densities, replicating high clustering, short path length and small-worldness organization in the fetal group matrix reconstructed from fetal FC analysis without white matter regression. The overlap of the strongest functionally connected nodes ranged between 20 ($t = 0.3$), 30 ($t = 0.1$) and 40% ($t = 0.2$) and central nodes ranged between 50 ($t = 0.1$), 50 ($t = 0.3$) and 70% ($t = 0.2$), varying threshold t. Four functional modules were again observed, with the original fetal group graphs, with and without white matter regression, showing a high level of modularity overlap (Rand index: 0.675, $p < 0.001$). Significant associations were revealed comparing the alternative fetal and adult matrices using different thresholds ($t = 0.1$, $r = 0.504$, $p < 0.001$; $t = 0.2$, $r = 0.476$, $p < 0.001$ and $t = 0.3$, $r = 0.402$, $p < 0.001$), remaining significant when controlled for Euclidian Distance (respectively, $r = 0.365$, $p < 0.001$; $r = 0.429$, $p < 0.001$ and $r = 0.465$, $p < 0.001$).

DISCUSSION

The present study confirms the presence of a functional brain connectomic blueprint in the second and third trimester of pregnancy *in utero*. The results of this large fetal functional resting-state MRI cohort show the early presence of fundamental properties of the neural connectome, including a functional small-world, modular and rich club architecture. Our findings suggest the presence of both primary motor and sensory networks as well as the first signs of higher order networks that are pruned for later-life cognition. We observe a high overlap between adult and fetal functional organization of the cortex, indicating that mature functional dynamics have their origin prior to birth. Extending previous observations of (premature) neonatal resting-state networks (De Asis-Cruz et al., 2015; Doria et al., 2010; Fransson et al., 2010; Fransson et al., 2009; Gao et al., 2015; Gao et al., 2009; He & Parikh, 2016; Schöpf et al., 2012; Smyser et al., 2010; Thomason et al., 2013) our results complement the notion of the early presence of a blueprint of the formation of resting-state networks in the healthy second to third trimester fetal brain, now shown for the fetal developing brain. The connectome emerges and is detectable with fetal fMRI in the second trimester of pregnancy, when FC patterns show first signs of organization into a complex network of communicating brain regions.

MRI studies have shown a small world type of network organization with functional and structural rich-club hubs, increasing global efficiency, as well as structural and functional architectural coupling in the developing (preterm) neonatal brain (Cao et al., 2016; De Asis-Cruz et al., 2015; Fransson et al., 2010; Scheinost et al., 2016; van den Heuvel et al., 2015). Major white matter pathways associated with the development of the structural rich club in preterm neonates are established before the third trimester of pregnancy (Ball et al., 2014; van den Heuvel et al., 2015). Our findings show that the most densely

functionally connected areas (which one could refer to as 'functional hubs') in the fetal cortex are predominantly confined to temporal and midline cortical regions of the insular and frontal lobes, as well as the primary somatosensory regions. Functional MRI and EEG studies analyzing functional hub organization of the neonatal brain show similar findings, with medial temporal, fusiform and primary somatosensory regions commonly identified as densely connected hub areas in the early developing brain (Arichi et al., 2017; De Asis-Cruz et al., 2015; Fransson et al., 2010; Gao et al., 2009; van den Heuvel et al., 2018), as well as inferior frontal (Fransson et al., 2010) and orbitofrontal regions (e.g., as part of the rolandic operculum in (De Asis-Cruz et al., 2015), and insular cortices (Arichi et al., 2017; De Asis-Cruz et al., 2015; Gao et al., 2011). Combining fetal and preterm neonatal findings, we hypothesize that fetal hubs fulfill an important role in coordinating activity, predominantly linked to brain functions that are associated with primary functions.

Our results show high overlap of fetal and adult resting-state networks that are pruned to coordinate motor, visual, auditory and some cognitive functions, while the frontomedial network that is especially associated with higher cognitive functions, shows a less strong association. These findings are in line with previous fMRI findings in preterm neonates showing that prototypes of resting-state networks are developed before or around term birth (Doria et al., 2010; Gao et al., 2009; Schöpf et al., 2012; Smyser et al., 2010; Thomason et al., 2013; Thomason et al., 2015; van den Heuvel et al., 2015). In contrast, the frontoparietal network is still fragmented around birth and during the first year of life (Fransson et al., 2009; Gao et al., 2015; He & Parikh, 2016). Disruptions of the developing somatomotor and frontoparietal functional networks around term equivalent age has been recently linked to motor impairments in the first four to eight months of life (Linke et al., 2018). Combining these findings, we observe that local development of the functional architecture of the brain before birth is dynamic and develops in a sequential primary to higher cognitive fashion (Doria et al., 2010; Gao et al., 2009; Schöpf et al., 2012; Smyser et al., 2010; Thomason et al., 2013; Thomason et al., 2015; van den Heuvel et al., 2015).

The participant group and the nature of the imaging technique include several limitations. The following points should thus be taken into consideration when interpreting our presented findings. First, we included fetuses that were examined at a wide range of ages, which enabled cross-sectional developmental assessment, but also resulted in averaging across a large age range when making group level comparisons. Similar to former studies, we limited this effect through spatial normalization and realignment of fMRI volumes to a standard average 32-week gestation template brain (Serag et al., 2012), but larger statistical variation in the fetal group is to be expected. We therefore validated our results by including a second normalization method using age specific brain templates (Gholipour et al., 2017). Second, another major consideration is that

imaging the fetal brain *in vivo* is influenced by maternal respiration, high movement, and the changing position of the fetus (Ferrazzi et al., 2014). Although post-processing techniques within this study include several steps to reduce motion artifacts such as regression out of motion parameters and manual scrubbing, noisy artifacts may remain in the study data. Noisy artifacts can lead to a reduction of long-range connectivity between distant regions, and as well to an increase in connectivity between proximal brain regions (Power et al., 2012; Van Dijk et al., 2012). Despite the challenging analysis, our findings suggest that motion and other artifacts are not the main driving factors of our presented results. Furthermore, changing white matter intensities with time due to myelination maturation may influence the fMRI signal. Including white matter regression brings the opportunity to take out signals from within the brain that capture both signals arising from the white matter and potential spurious contributions of noise. Our results show that comparable results are found in- and excluding the white matter signal as a regressor in the FC analysis, but dissimilarities can be pointed out as well due to the difference in global correction. Furthermore, the high overlap between resting-state functional connectivity distributions of the fetal and healthy adult brain indicates high enough accuracy in measurement of prenatal functional connectivity. Third, in the discussion, we compare our fetal fMRI findings with reports on preterm neonatal brain organization. The brain of preterm infants without overt brain injury provides insight into the same time period, and properties of global functional dynamics measured *in utero* appear to largely overlap with those observed in preterm infants (Ferrazzi et al., 2014). It should be noted that the preterm neonatal brain is not a perfect surrogate for typical processes of brain circuitry development, since premature birth, absence of neuroprotective elements, NICU environment and medical interventions can be harmful for the developing brain (Brummelte et al., 2012; Groppo et al., 2014; Karmel et al., 2010; Pritchard et al., 2014; Smyser et al., 2012). Additionally, early exposure to the extra-uterine environment may accelerate brain function due to introduction of sensory stimuli (Klebermass et al., 2006). Fetal fMRI-based network analysis is therefore crucial in understanding healthy connectome development. Results presented here show that the fetal period is important for the development of specialized functional domains in an economic and integrative network before birth, suggesting that the prenatal period is important to point out vulnerable windows for developing later life brain function deficits. It does not show a complete model yet, but our findings do provide new insights into foundational aspects of fetal brain development.

Our findings suggest that fetal MRI provides the possibility to map the blueprint of functional connectome organization during the earliest phases of brain development. The rapid nature of neurodevelopmental processes during pregnancy may render the human brain at elevated risk for connectome alterations. Fetal MRI currently serves as a clinical tool for the early detection of brain abnormalities such as corpus agenesis and other cerebral anomalies (Volpe et al., 2006) or delayed brain maturation in fetuses with

severe congenital heart disease (Claessens et al., 2019). Considering that organizational properties of brain networks associated with later life motoric and cognitive functioning are already apparent in the fetal brain across 20 to 40 weeks of gestation, it may in the future be possible to complement clinical tools to detect early signs, or origins, of psychopathology using fetal fMRI. It would be interesting to search deeper into possible risk factors, such as maternal stress, alcohol and drugs intake, prematurity, fetal growth restriction, premature birth or cardiac dysfunction, that could influence healthy fetal brain circuitry, with lasting implication for individual trajectories of human development. Further, it will be important to link early functional dynamics to structural patterns. Few studies have examined functional or structural differences between healthy fetal and preterm neonatal development (Bouyssi-Kobar et al., 2016; Thomason et al., 2017) and they have shown that both altered functional connectivity and cortical folding differences can already discernable in this period.

REFERENCES

Anderson, A. L., & Thomason, M. E. (2013). Functional plasticity before the cradle: a review of neural functional imaging in the human fetus. Neuroscience & Biobehavioral Reviews, 37(9), 2220-2232.

Arichi, T., Whitehead, K., Barone, G., Pressler, R., Padormo, F., Edwards, A. D., & Fabrizi, L. (2017). Localization of spontaneous bursting neuronal activity in the preterm human brain with simultaneous EEG-fMRI. Elife, 6, e27814. https://www.ncbi.nlm.nih.gov/pmc/articles/PMC5595428/pdf/elife-27814.pdf

Ashburner, J., Barnes, G., Chen, C., Daunizeau, J., Flandin, G., Friston, K., Gitelman, D., Kiebel, S., Kilner, J., & Litvak, V. (2012). SPM8 manual. Functional Imaging Laboratory, Institute of Neurology.

Ball, G., Aljabar, P., Zebari, S., Tusor, N., Arichi, T., Merchant, N., Robinson, E. C., Ogundipe, E., Rueckert, D., & Edwards, A. D. (2014). Rich-club organization of the newborn human brain. Proceedings of the National Academy of Sciences, 111(20), 7456-7461.

Bouyssi-Kobar, M., du Plessis, A. J., McCarter, R., Brossard-Racine, M., Murnick, J., Tinkleman, L., Robertson, R. L., & Limperopoulos, C. (2016). Third Trimester Brain Growth in Preterm Infants Compared With In Utero Healthy Fetuses. Pediatrics, e20161640.

Brummelte, S., Grunau, R. E., Chau, V., Poskitt, K. J., Brant, R., Vinall, J., Gover, A., Synnes, A. R., & Miller, S. P. (2012). Procedural pain and brain development in premature newborns. Annals of neurology, 71(3), 385-396. https://onlinelibrary.wiley.com/doi/pdf/10.1002/ana.22267

Cao, M., He, Y., Dai, Z., Liao, X., Jeon, T., Ouyang, M., Chalak, L., Bi, Y., Rollins, N., & Dong, Q. (2016). Early development of functional network segregation revealed by connectomic analysis of

the preterm human brain. Cerebral Cortex, 27(3), 1949-1963.

Claessens, N., Khalili, N., Isgum, I., ter Heide, H., Steenhuis, T., Turk, E., Jansen, N., de Vries, L., Breur, J., & de Heus, R. (2019). Brain and CSF Volumes in Fetuses and Neonates with Antenatal Diagnosis of Critical Congenital Heart Disease: A Longitudinal MRI Study. American Journal of Neuroradiology.

Colizza, V., Flammini, A., Serrano, M. A., & Vespignani, A. (2006). Detecting rich-club ordering in complex networks. Nature physics, 2(2), 110-115.

Collin, G., & van den Heuvel, M. P. (2013). The Ontogeny of the Human Connectome Development and Dynamic Changes of Brain Connectivity Across the Life Span. The Neuroscientist, 19(6), 616-628.

De Asis-Cruz, J., Bouyssi-Kobar, M., Evangelou, I., Vezina, G., & Limperopoulos, C. (2015). Functional properties of resting state networks in healthy full-term newborns. Scientific reports, 5.

de Water, E., Proal, E., Wang, V., Medina, S. M., Schnaas, L., Téllez-Rojo, M. M., Wright, R. O., Tang, C. Y., & Horton, M. K. (2017). Prenatal Manganese Exposure and Intrinsic Functional Connectivity of Emotional Brain Areas in Children. NeuroToxicology.

Doria, V., Beckmann, C. F., Arichi, T., Merchant, N., Groppo, M., Turkheimer, F. E., Counsell, S. J., Murgasova, M., Aljabar, P., & Nunes, R. G. (2010). Emergence of resting state networks in the preterm human brain. Proceedings of the National Academy of Sciences, 107(46), 20015-20020.

Fair, D. A., Cohen, A. L., Power, J. D., Dosenbach, N. U., Church, J. A., Miezin, F. M., Schlaggar, B. L., & Petersen, S. E. (2009). Functional brain networks develop from a "local to distributed" organization. PLoS computational biology, 5(5), e1000381. https://www.ncbi.nlm.nih.gov/pmc/articles/PMC2671306/pdf/pcbi.1000381

Ferrazzi, G., Kuklisova Murgasova, M., Arichi, T., Malamateniou, C., Fox, M. J., Makropoulos, A., Allsop, J., Rutherford, M., Malik, S., Aljabar, P., & Hajnal, J. V. (2014, Nov 1). Resting State fMRI in the moving fetus: a robust framework for motion, bias field and spin history correction. NeuroImage, 101, 555-568. https://doi.org/10.1016/j.neuroimage.2014.06.074

Fransson, P., Åden, U., Blennow, M., & Lagercrantz, H. (2010). The functional architecture of the infant brain as revealed by resting-state fMRI. Cerebral Cortex, 21(1), 145-154.

Fransson, P., Skiöld, B., Engström, M., Hallberg, B., Mosskin, M., Åden, U., Lagercrantz, H., & Blennow, M. (2009). Spontaneous brain activity in the newborn brain during natural sleep—an fMRI study in infants born at full term. Pediatric research, 66(3), 301-305.

Gao, W., Alcauter, S., Smith, J. K., Gilmore, J. H., & Lin, W. (2015). Development of human brain

cortical network architecture during infancy. *Brain Structure and Function, 220(2), 1173-1186.*

Gao, W., Gilmore, J. H., Giovanello, K. S., Smith, J. K., Shen, D., Zhu, H., & Lin, W. (2011). *Temporal and spatial evolution of brain network topology during the first two years of life. PloS one, 6(9), e25278.* https://www.ncbi.nlm.nih.gov/pmc/articles/PMC3179501/pdf/pone.0025278

Gao, W., Zhu, H., Giovanello, K. S., Smith, J. K., Shen, D., Gilmore, J. H., & Lin, W. (2009). *Evidence on the emergence of the brain's default network from 2-week-old to 2-year-old healthy pediatric subjects. Proceedings of the National Academy of Sciences, 106(16), 6790-6795.*

Gholipour, A., Rollins, C. K., Velasco-Annis, C., Ouaalam, A., Akhondi-Asl, A., Afacan, O., Ortinau, C. M., Clancy, S., Limperopoulos, C., & Yang, E. (2017). *A normative spatiotemporal MRI atlas of the fetal brain for automatic segmentation and analysis of early brain growth. Scientific reports, 7(1), 476.* https://www.ncbi.nlm.nih.gov/pmc/articles/PMC5428658/pdf/41598_2017_Article_525

Grewen, K., Salzwedel, A. P., & Gao, W. (2015). *Functional connectivity disruption in neonates with prenatal marijuana exposure. Frontiers in human neuroscience, 9, 601.* https://www.ncbi.nlm.nih.gov/pmc/articles/PMC4631947/pdf/fnhum-09-00601

Groppo, M., Ricci, D., Bassi, L., Merchant, N., Doria, V., Arichi, T., Allsop, J. M., Ramenghi, L., Fox, M. J., & Cowan, F. M. (2014). *Development of the optic radiations and visual function after premature birth. Cortex, 56, 30-37.*

He, L., & Parikh, N. A. (2016). *Brain functional network connectivity development in very preterm infants: The first six months. Early human development, 98, 29-35.*

Hoff, G. A.-J., Van den Heuvel, M., Benders, M. J., Kersbergen, K. J., & De Vries, L. S. (2013). *On development of functional brain connectivity in the young brain. Frontiers in human neuroscience, 7.*

Huttenlocher, P. R., & Dabholkar, A. S. (1997). *Regional differences in synaptogenesis in human cerebral cortex. Journal of Comparative Neurology, 387(2), 167-178.*

Infante, M. A., Moore, E. M., Bischoff-Grethe, A., Tapert, S. F., Mattson, S. N., & Riley, E. P. (2017). *Altered functional connectivity during spatial working memory in children with heavy prenatal alcohol exposure. Alcohol, 64, 11-21.*

Jakab, A., Schwartz, E., Kasprian, G., Gruber, G. M., Prayer, D., Schöpf, V., & Langs, G. (2014). *Fetal functional imaging portrays heterogeneous development of emerging human brain networks. Frontiers in human neuroscience, 8.*

Karmel, B. Z., Gardner, J. M., Meade, L. S., Cohen, I. L., London, E., Flory, M. J., Lennon, E. M.,

Miroshnichenko, I., Rabinowitz, S., & Parab, S. (2010). Early medical and behavioral characteristics of NICU infants later classified with ASD. Pediatrics, peds. 2009-2680.

Karrer, B., Levina, E., & Newman, M. E. (2008). Robustness of community structure in networks. Physical review E, 77(4), 046119.

Klebermass, K., Kuhle, S., Olischar, M., Rücklinger, E., Pollak, A., & Weninger, M. (2006). Intra-and extrauterine maturation of amplitude-integrated electroencephalographic activity in preterm infants younger than 30 weeks of gestation. Neonatology, 89(2), 120-125.

Kostović, I., & Jovanov-Milošević, N. (2006). The development of cerebral connections during the first 20–45 weeks' gestation. Seminars in Fetal and Neonatal Medicine, 11(6), 415-422. https://doi.org/https://doi.org/10.1016/j.siny.2006.07.001

Li, X., Andres, A., Shankar, K., Pivik, R., Glasier, C., Ramakrishnaiah, R., Zhang, Y., Badger, T., & Ou, X. (2016). Differences in brain functional connectivity at resting state in neonates born to healthy obese or normal-weight mothers. International Journal of Obesity, 40(12), 1931-1934.

Lin, W., Zhu, Q., Gao, W., Chen, Y., Toh, C.-H., Styner, M., Gerig, G., Smith, J., Biswal, B., & Gilmore, J. (2008). Functional connectivity MR imaging reveals cortical functional connectivity in the developing brain. American Journal of Neuroradiology, 29(10), 1883-1889.

Linke, A. C., Wild, C., Zubiaurre-Elorza, L., Herzmann, C., Duffy, H., Han, V. K., Lee, D. S., & Cusack, R. (2018). Disruption to functional networks in neonates with perinatal brain injury predicts motor skills at 8 months. NeuroImage: Clinical, 18, 399-406.

Mantel, N. (1967). The detection of disease clustering and a generalized regression approach. Cancer research, 27(2 Part 1), 209-220.

Maslov, S., & Sneppen, K. (2002). Specificity and stability in topology of protein networks. Science, 296(5569), 910-913.

Mrzljak, L., Uylings, H. B., Van Eden, G. G., & Judáš, M. (1991). Neuronal development in human prefrontal cortex in prenatal and postnatal stages. Progress in brain research, 85, 185-222.

Opsahl, T., Colizza, V., Panzarasa, P., & Ramasco, J. J. (2008). Prominence and control: the weighted rich-club effect. Physical Review Letters, 101(16), 168702.

Power, J. D., Barnes, K. A., Snyder, A. Z., Schlaggar, B. L., & Petersen, S. E. (2012). Spurious but systematic correlations in functional connectivity MRI networks arise from subject motion. NeuroImage, 59(3), 2142-2154.

Power, J. D., Fair, D. A., Schlaggar, B. L., & Petersen, S. E. (2010). *The development of human functional brain networks.* Neuron, 67(5), 735-748.

Pritchard, V. E., Bora, S., Austin, N. C., Levin, K. J., & Woodward, L. J. (2014). *Identifying very preterm children at educational risk using a school readiness framework.* Pediatrics, 134(3), e825-e832.

Rand, W. M. (1971). *Objective criteria for the evaluation of clustering methods.* Journal of the American Statistical association, 66(336), 846-850.

Rubinov, M., & Sporns, O. (2010). *Complex network measures of brain connectivity: uses and interpretations.* NeuroImage, 52(3), 1059-1069.

Rudolph, M. D., Graham, A. M., Feczko, E., Miranda-Dominguez, O., Rasmussen, J. M., Nardos, R., Entringer, S., Wadhwa, P. D., Buss, C., & Fair, D. A. (2018). *Maternal IL-6 during pregnancy can be estimated from newborn brain connectivity and predicts future working memory in offspring.* Nature neuroscience, 21(5), 765.

Salzwedel, A. P., Grewen, K. M., Goldman, B. D., & Gao, W. (2016). *Thalamocortical functional connectivity and behavioral disruptions in neonates with prenatal cocaine exposure.* Neurotoxicology and teratology, 56, 16-25.

Salzwedel, A. P., Grewen, K. M., Vachet, C., Gerig, G., Lin, W., & Gao, W. (2015). *Prenatal drug exposure affects neonatal brain functional connectivity.* Journal of Neuroscience, 35(14), 5860-5869.

Scheinost, D., Kwon, S. H., Shen, X., Lacadie, C., Schneider, K. C., Dai, F., Ment, L. R., & Constable, R. T. (2016). *Preterm birth alters neonatal, functional rich club organization.* Brain Structure and Function, 221(6), 3211-3222.

Scholtens, L. H., Schmidt, R., de Reus, M. A., & van den Heuvel, M. P. (2014). *Linking macroscale graph analytical organization to microscale neuroarchitectonics in the macaque connectome.* Journal of Neuroscience, 34(36), 12192-12205.

Schöpf, V., Kasprian, G., Brugger, P., & Prayer, D. (2012). *Watching the fetal brain at 'rest'.* International Journal of Developmental Neuroscience, 30(1), 11-17.

Schöpf, V., Schlegl, T., Jakab, A., Kasprian, G., Woitek, R., Prayer, D., & Langs, G. (2014). *The relationship between eye movement and vision develops before birth.* Frontiers in human neuroscience, 8.

Serag, A., Aljabar, P., Ball, G., Counsell, S. J., Boardman, J. P., Rutherford, M. A., Edwards, A. D., Hajnal, J. V., & Rueckert, D. (2012). *Construction of a consistent high-definition spatio-temporal atlas of the developing brain using adaptive kernel regression.* NeuroImage, 59(3), 2255-2265.

Sidman, R. L., & Rakic, P. (1973). Neuronal migration, with special reference to developing human brain: a review. Brain research, 62(1), 1-35.

Smyser, C. D., Inder, T. E., Shimony, J. S., Hill, J. E., Degnan, A. J., Snyder, A. Z., & Neil, J. J. (2010). Longitudinal analysis of neural network development in preterm infants. Cereb Cortex, 20(12), 2852-2862.

Smyser, C. D., Kidokoro, H., & Inder, T. E. (2012). Magnetic resonance imaging of the brain at term equivalent age in extremely premature neonates: to scan or not to scan? Journal of paediatrics and child health, 48(9), 794-800.

Thomason, M. E. (2018). Structured Spontaneity: Building Circuits in the Human Prenatal Brain. Trends Neurosci, 41(1), 1-3.

Thomason, M. E., Dassanayake, M. T., Shen, S., Katkuri, Y., Alexis, M., Anderson, A. L., Yeo, L., Mody, S., Hernandez-Andrade, E., & Hassan, S. S. (2013). Cross-hemispheric functional connectivity in the human fetal brain. Science translational medicine, 5(173), 173ra124-173ra124.

Thomason, M. E., Grove, L. E., Lozon, T. A., Vila, A. M., Ye, Y., Nye, M. J., Manning, J. H., Pappas, A., Hernandez-Andrade, E., & Yeo, L. (2015). Age-related increases in long-range connectivity in fetal functional neural connectivity networks in utero. Developmental cognitive neuroscience, 11, 96-104.

Thomason, M. E., Scheinost, D., Manning, J. H., Grove, L. E., Hect, J., Marshall, N., Hernandez-Andrade, E., Berman, S., Pappas, A., & Yeo, L. (2017). Weak functional connectivity in the human fetal brain prior to preterm birth. Scientific reports, 7, 39286. https://www.ncbi.nlm.nih.gov/pmc/articles/PMC5221666/pdf/srep39286.pdf

van den Bergh, B. R. H., van den Heuvel, M. I., Lahti, M., Braeken, M., de Rooij, S. R., Entringer, S., Hoyer, D.,

Roseboom, T., Räikkönen, K., King, S., & Schwab, M. (2017, 2017/07/28/). Prenatal developmental origins of behavior and mental health: The influence of maternal stress in pregnancy. Neuroscience & Biobehavioral Reviews. https://doi.org/https://doi.org/10.1016/j.neubiorev.2017.07.003

van den Heuvel, M. I., & Thomason, M. E. (2016, Dec). Functional Connectivity of the Human Brain in Utero. Trends Cogn Sci, 20(12), 931-939. https://doi.org/10.1016/j.tics.2016.10.001

van den Heuvel, M. I., Turk, E., Manning, J. H., Hect, J., Hernandez-Andrade, E., Hassan, S. S., Romero, R., van den Heuvel, M. P., & Thomason, M. E. (2018). Hubs in the Human Fetal Brain Network. Developmental cognitive neuroscience.

van den Heuvel, M. P., de Lange, S. C., Zalesky, A., Seguin, C., Yeo, B. T., & Schmidt, R. (2017). Proportional thresholding in resting-state fMRI functional connectivity networks and consequences for patient-control connectome studies: Issues and recommendations. Neuroimage, 152, 437-449.

van den Heuvel, M. P., Kersbergen, K. J., de Reus, M. A., Keunen, K., Kahn, R. S., Groenendaal, F., de Vries, L. S., & Benders, M. J. (2015). The neonatal connectome during preterm brain development. Cerebral Cortex, 25(9), 3000-3013.

van den Heuvel, M. P., & Sporns, O. (2011, 2011-11-02 00:00:00). Rich-Club Organization of the Human Connectome. The Journal of Neuroscience, 31, 15775-15786.

Van Dijk, K. R., Sabuncu, M. R., & Buckner, R. L. (2012). The influence of head motion on intrinsic functional connectivity MRI. NeuroImage, 59(1), 431-438.

Vasung, L., Huang, H., Jovanov-Milošević, N., Pletikos, M., Mori, S., & Kostović, I. (2010). Development of axonal pathways in the human fetal fronto- limbic brain: histochemical characterization and diffusion tensor imaging. Journal of Anatomy, 217(4), 400-417.

Volpe, P., Paladini, D., Resta, M., Stanziano, A., Salvatore, M., Quarantelli, M., De Robertis, V., Buonadonna, A., Caruso, G., & Gentile, M. (2006). Characteristics, associations and outcome of partial agenesis of the corpus callosum in the fetus. Ultrasound in Obstetrics and Gynecology: The Official Journal of the International Society of Ultrasound in Obstetrics and Gynecology, 27(5), 509-516.

Chapter 4

Hubs in the human fetal brain network

Marion I. van den Heuvel, Elise Turk, Janessa H. Manning, Jasmine Hect,
Edgar Hernandez-Andrade, Sonia S. Hassan, Roberto Romero,
Martijn P. van den Heuvel, Moriah E. Thomason

ABSTRACT

Advances in neuroimaging and network analyses have led to discovery of highly connected regions, or hubs, in the connectional architecture of the human brain. Whether these hubs emerge in utero, has yet to be examined. The current study addresses this question and aims to determine the location of neural hubs in human fetuses. Fetal resting-state fMRI data (N=105) was used to construct connectivity matrices for 197 discrete brain regions. We discovered that within the connectional functional organization of the human fetal brain key hubs are emerging. Consistent with prior reports in infants, visual and motor regions were identified as emerging hub areas, specifically in cerebellar areas. We also found evidence for network hubs in association cortex, including areas remarkably close to the adult fusiform facial and Wernicke areas. Functional significance of hub structure was confirmed by computationally deleting hub versus random nodes and observing that global efficiency decreased significantly more when hubs were removed (p < .001). Taken together, we conclude that both primary and association brain regions demonstrate centrality in network organization before birth. While fetal hubs may be important for facilitating network communication, they may also form potential points of vulnerability in fetal brain development.

Keywords: Prenatal, Functional connectivity, Hubs, Brain networks, Development, Fetus

INTRODUCTION

Advances in neuroimaging and network analyses have revealed the existence of sets of highly connected regions, often called "hubs", that are critically important for enabling efficient neuronal signaling and communication (van den Heuvel and Sporns, 2013; Sporns et al., 2007). In the adult human brain network, functional hubs are consistently found in the ventral and dorsal precuneus, posterior and anterior cingulate gyrus, ventromedial frontal cortex, and interior parietal brain regions (Zuo et al., 2012; Tomasi and Volkow, 2011), brain areas with considerable overlap with sub regions of the default mode network (DMN) (Greicius et al., 2003). Accumulating evidence suggests that, because of their high functional connectedness in the brain, hubs support information integration that forms the foundation for numerous aspects of complex cognitive function. Another consideration is that this high level of centrality in the brain may make hubs highly susceptible to insults and/or disconnection (Crossley et al., 2014; Aerts et al., 2016; Bullmore and Sporns, 2012). In line with this, abnormal hub organization has been implicated in several neurological and psychiatric brain disorders (Bullmore and Sporns, 2012; Bassett and Bullmore, 2009). Given the central role of hubs in brain organization, knowledge about properties of hubs at the beginning of human life is particularly valuable and may offer insight into the origins of developmental and psychiatric disorders.

Developmental studies in the first year of life have shown that functional hubs are

already observable in infancy and are, while not fully mature, transitioning to an adult configuration (De Asis-Cruz et al., 2015; Fransson et al., 2011; Gao et al., 2009, 2011; van den Heuvel et al., 2015). While initial studies reported that functional hubs were largely confined to primary sensory and motor brain regions in the infant brain (Fransson et al., 2011; Gao et al., 2011), a more recent study found functional hubs in other areas of the infant brain, such as subcortical-limbic-paralimbic areas, and reported that functional hub organization may constitute a more mature configuration than previously thought (De Asis-Cruz et al., 2015). Further support for nascent hub structure comes from examination of the default mode network in infancy. An immature and incomplete DMN is present in 2-week-olds and the posterior cingulate cortex (PCC) seems to anchor this configuration as the main functional "hub" within this network (Gao et al., 2009). Together, these studies show that a hub configuration, although immature, already exist in the infant brain. The question remains, however, whether functional hub configuration of the brain emerges before birth, as networks already begin to form in utero (Thomason et al., 2014, 2013, 2015; Schöpf et al., 2012).

Insight into hub emergence before birth may be of great importance, since the fetal period is a critical time in brain development (Rice and Barone, 2000; Keunen et al., 2017) in which seemingly small disturbances, insults or exposures can produce lifelong changes in neurological and mental functioning. Consistent with this notion, the origins of neurodevelopmental disorders are increasingly attributed to alterations occurring during the prenatal period (Di Martino et al., 2014; Paneth et al., 2005; Rosenbaum et al., 2007) despite onsets in symptomatology between the 3rd and 20th years of life (Paus et al., 2008). Studies involving premature infants have started to examine hub development as a proxy for prenatal brain development, scanning neonates with MRI prior to post conception week 42. These studies have revealed the existence of hubs and demonstrate that hubs are highly connected, an observation suggesting a functional rich-club organization is present in the brain network in very early life (van den Heuvel et al., 2015; Ball et al., 2014). Although these studies provide valuable insights into hub development in the antenatal period, several factors inevitably linked to preterm birth, including premature exposure to the extra uterine world and deprivation from a variety of hormones (i.e., IGF-1, estrogens, progesterone and thyroid hormones) that are normally provided during (late) pregnancy (Berger and Soder, 2015; Elitt and Rosenberg, 2014), make generalizing the results from these studies to normal fetal hub development challenging.

Until now, information about fetal functional hub development in vivo has been utterly absent as information about human fetal brain function has been inaccessible. Recently, new advances in MRI have overcome this limitation. It is now possible to examine coordinated action in the human brain before birth (for a recent review, see van den Heuvel and Thomason, 2016). Pioneering cross-sectional studies on fetal resting-state functional connectivity (RSFC) have begun to map development of the brain function

before birth and have shown that intra-hemispheric, cross-hemispheric, and long-range connectivity become stronger with advancing fetal age (Thomason et al., 2014, 2013, 2015). Additionally, fetal fMRI studies have postulated the importance of PCC connectivity for the fetal brain network (Thomason et al., 2014, 2015). Nevertheless, functional hub development during the prenatal period remains unstudied. The current study addresses the question whether functional hubs are operational before birth and aims to isolate and describe those neural hubs in a large sample of human fetuses using network analyses. In network analyses, the brain is viewed as a network or "graph" consisting of nodes (brain regions; ROIs) that are connected by edges (connectivity strength between nodes). Hubs will be identified based on graph theoretical measures of nodal importance (van den Heuvel and Sporns, 2013; Sporns et al., 2007; Rubinov and Sporns, 2010). Based on previous reports on hubs in infants (De Asis-Cruz et al., 2015; Fransson et al., 2011), we expect to find functional hubs mostly in primary sensory and motor brain areas in the fetal brain. After isolation of the putative hubs, we will examine whether the identified hubs are critical for efficient functioning of the fetal brain network by testing how the fetal brain network responds to computational attack targeted on hubs as opposed to attack on random non-hub nodes.

MATERIALS AND METHODS

Participants
Healthy pregnant women were recruited in Metro Detroit, USA to participate in a fetal magnetic resonance imaging (MRI) brain study in the second and third trimester. Inclusion criteria for scanning were: maternal age>18 years, English as first language, singleton pregnancies, and typical fetal brain development (as assessed by ultrasound and anatomical MRI examination prior to functional MRI scanning). From the 138 fetuses available for this study with preprocessed fMRI data, we excluded those that were later born moderately or extremely premature and/or had low birth weight (< 35 weeks of GA, <2400 g; N=9), were born to a mother that was older than 40 years of age (N=1), and/ or were diagnosed as high-risk pregnancies (i.e., PPROM, IUGR, preeclampsia; N=15). Additionally, we excluded those fetuses of which fMRI data did not meet quality criteria after removing high movement volumes (< 100 low-motion volumes; N=7) and/ or motion (1.7mm max excursion, 0.6mm mean; rotational:>2.5°; N=1).
These quality criteria resulted in a final sample of 105 fetuses (64 male; 41 female). Included fetuses had a mean gestational age of 33.49 (range=20.6–39.6 weeks of gestation; s.d. = 3.97) weeks at scanning and were born, on average, at 39.25 (s.d. = 1.22) weeks of gestation. Gestational age was determined by a study physician (E.H.-A.) by ultrasound examination within 1 week of MRI testing. More detailed characteristics of our sample are provided in **Table 1**.

Table 1. Characteristics of mother and fetus (N=105)

Outcome	Value
Maternal age, years	24.84 ± 4.46
Race/ethnicity, %	
Caucasian	10.5
African–American	81
Bi-racial	2.9
Not disclosed	5.7
Child sex, %	
Female	39
Male	61
Gestational age at scan, weeks	33.49 ± 3.97
Gestational age at birth, weeks	39.25 ± 1.22
Birth weight, grams	3304.05 ± 438.6

Values presented as mean ± SD where appropriate

Functional data acquisition and preprocessing

Between 12 and 24 min of fetal brain resting-state fMRI data were collected using a 3-T Siemens Verio 70-cm large bore system and 4- Channel Siemens Flex Abdominal Coil. Images were collected with the following parameters: echo planar imaging (EPI) BOLD, TR/TE 2000/ 30 ms, 360 frames, axial 4mm slice thickness (voxel size: 3.4×3.4×4 mm). This fMRI sequence was repeated a second time within the same scan session to maximize available resting-state fMRI data. Computed SAR values=0.22 (SD=0.07). For the final sample included in analyses, frame count, after excluding high motion frames, was range=100–332, mean=168 (SD=57). Time frames corresponding to periods of head motion<1mm frame-to-frame displacement and<1.5° rotation in the fetus were identified using FSL image viewer (FSL, 2018). Brainsuite (Shattuck and Leahy, 2002) was used to manually draw 3D masks for a reference frame from each period of fetal movement quiescence. Masks were binarized and applied only to frames corresponding to their select segment, and only those data were retained for further analyses. 56% of data collected were retained after motion censoring. Subsequent within-segment preprocessing steps included reorientation, realignment and normalization to an average 32-week gestational age fetal anatomical template (Serag et al., 2012) using SPM8 (Statistical Parametric Mapping 8 from the Wellcome Trust Centre for Neuroim-

aging, 2009). To correct for variation in normalization across segments, within-participant normalized images were then concatenated into one time-series, realigned, and smoothed using a 4mm Gaussian kernel across.

Regions of interest
A spatially constrained group level clustering approach (Craddock et al., 2012) was used to parcellate the preterm template brain at 32 weeks of gestation (Serag et al., 2012) into spatially contiguous, similarly sized ROIs. Briefly, this method produces functionally homogenous clusters at the individual level by assessing voxel-level timeseries similarity in a given data set, using Pearson correlations, then iteratively merging voxels whose within-cluster similarity is maximal and between-cluster similarity is minimal. Next, it identifies the most representative clusters of voxels using a normalized cut algorithm (van den Heuvel et al., 2008) and performs group level clustering. This method produces ROIs that are optimally functionally homogenous and consistent across individuals. Seventy-six concatenated fetal fMRI data sets, processed in the same manner as stated above and occur in the sample analyzed here, were submitted to this procedure. 200 ROIs distributed across the cortex, subcortical structures, and the cerebellum were generated, three of the which were anomalous and excluded from analysis, resulting in a fetal ROI Pycluster atlas of N=197 regions, available for download at www.brainnexus.com.

Connectivity matrices and computation of hub measures
The CONN-fMRI Toolbox (Whitfield-Gabrieli and Nieto Castanon, 2012) was used to compute functional connectivity (FC) matrices. The anatomical component correction (aCompCor) method of estimating and removing noise (Behzadi et al., 2007; Chai et al., 2012) was applied. Principal components of signals from white matter and cerebral spinal fluid, as well as translational and rotational movement parameters (with another six parameters representing their first order temporal derivatives), were removed with covariate regression analysis. Pearson's correlation coefficients were then estimated from time series data for each pair of nodes. Fisher's transformation was used to convert coefficients to z-scores to produce FC correlation matrices for each participant.

From these matrices, measures of network centrality, degree and betweenness centrality (BC), were computed for every region by means of graph theoretical analysis, using the brain connectivity toolbox for Matlab (Rubinov and Sporns, 2010). The degree of a node is the number of connections that node has with other nodes, while the BC of a node is the number of times that node is included in the shortest path of each node to every other node (van den Heuvel and Sporns, 2013; Rubinov and Sporns, 2010). We used a threshold of T=0.25 (medium-high zscores) for the computation of our network metrics, to minimize the effect of spurious correlations. To mitigate potential influence of the threshold set for participant functional graphs (T=0.25) (van den Heuvel et al., 2017),

we adjusted the threshold to T=0 (i.e., no thresholding, negative correlations removed), T=0.35, and T=0.45, recomputed resulting graph metrics, and compared our results with the T=0.25 results (cf. van den Heuvel et al., 2015). A graphical representation of our preprocessing steps is presented in **Figure 1**.
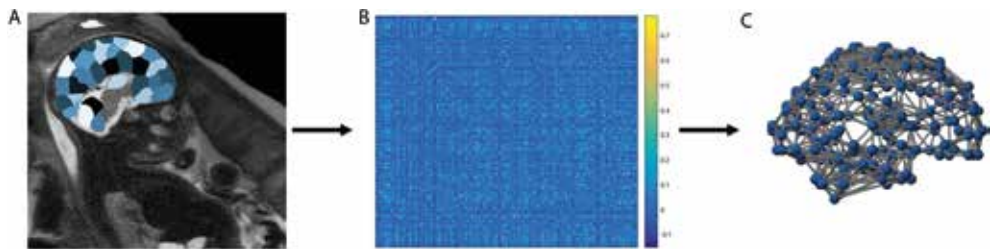
Figure 1. Graphical representation of preprocessing steps.
After acquiring fetal resting-state functional MRI data in N=105 fetuses, a data-driven functional parcellation strategy was used to divide a 32-week template fetal brain into 197 similarly sized regions of interest (ROIs; panel A). Functional connectivity strength between every pair of ROIs was then computed to construct connectivity matrices for every fetus (panel B). In a final step, graph theoretical metrics, degree and betweenness centrality, were computed from connectivity matrices to identify functional hubs in the fetal network (panel C).

Analytic approach
In line with the work of Fransson et al. (2011), the 10 regions with highest weighted degree and betweenness centrality were identified. Subsequently, putative hubs were classified by hemisphere, by lobe, and by coordinates corresponding to the center of mass for the 32-week GA fetal template brain (Serag et al., 2012). Next, we examined hub network development by using a median split of our data to create two gestational age groups. The top 10 nodes in both groups were identified for both gestational age groups separately and compared. Finally, we examined the effect of computational attack to measure the relative importance of hub nodes in facilitation of efficiency in the overall fetal network as compared to random non-hub nodes. For this simulated attack, we first computed the global efficiency of the network by computing the inverse of the average number of steps needed to travel from every node in the network to every other node in the network, with longer paths being less efficient. We then simulated an attack to random nodes by randomly selecting 12 nodes and deleting all connections of those nodes with others from the group matrix and subsequently re-computing the global efficiency. The same was performed for the 12 nodes that were identified as hubs. To generate an empirical cumulative distribution function amenable to statistical testing, we repeated the random deletion procedure 1000 times, as has been done in prior works

(Hwang et al., 2013; van den Heuvel and Sporns, 2011). We then compared the resulting global efficiency after deleting hub nodes with the group average global efficiency after deleting random nodes with a one-sampled t-test. To create a measure of change, we computed the percentage change between the non-attacked and attacked global efficiency for both the randomly and targeted (hub) attack.

RESULTS

Isolation of fetal brain hubs
We computed two measures of nodal importance: weighted degree (i.e., strength) and betweenness centrality (BC). The weighted degree of a node, or strength, is the sum of all connection weights of the nodes that are connected with that node, while the BC of a node is the sum of the connection weights of all shortest paths of each node to every other node that "run through" that node (Rubinov and Sporns, 2010). Consistent with Fransson et al. (2011), we report the 10 strongest degree and BC nodes as hubs. We found that resultant degree and BC hubs have strong overlap, with 8 nodes falling in the top 10 for both degree and BC.
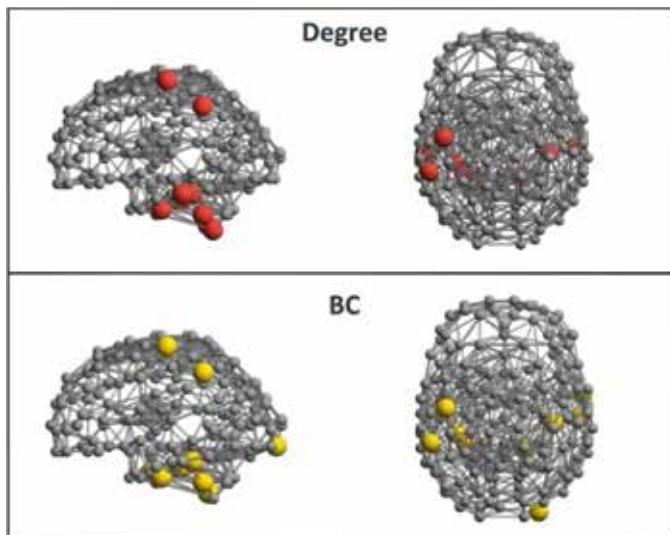
Figure 2. Location of putative hubs in the fetal brain.
Graphs were constructed with connections showing at threshold T=0.25, separately for weighted degree (upper panel; larger red spheres) and betweenness centrality hubs (lower panel; larger yellow spheres). Grey spheres represented other non-hub nodes in the network. Hubs were observed in areas of the cerebellum, inferior temporal gyrus, precentral gyrus, angular gyrus, medial temporal lobe, and the primary visual cortex.

In line with our hypothesis, several hubs were located in primary sensory and motor brain areas, specifically the left and right cerebellum, left precentral gyrus, and right primary visual cortex. In addition, hubs were identified in association cortex, including left and right inferior temporal gyrus, angular gyrus, and medial temporal lobe. depicts the spatial distribution of top identified hubs as defined by degree and BC. Notably, hubs identified in the left and right inferior temporal lobe are close to the area that will later develop into the fusiform facial area. Further, the area identified as hub in the left angular gyrus seems to overlap with what will develop as Wernicke's area. We also found that hub development follows a pattern of myelination, as 25% of peak hubs reside in the cerebellum, one of the earliest brain regions to myelinate (Deoni et al., 2011). Additionally, all isolated cortical hubs are located in areas marked as earliest to myelinate by Glasser and Van Essen (Glasser and Van Essen, 2011). It is also noteworthy that several hubs were localized in homologous contralateral brain areas, including bilateral cere-

Table 2. Identified hubs in the fetal brain network

| Hub #	Region	Left/Right	Coordinates		
			x	y	z
Overlapping Hubs					
1	Inferior Temporal Gyrus	Left	-24	0	-26
2	Inferior Temporal Gyrus	Right	30	-6	-22
3	Cerebellum	Right	8	-18	-32
4	Precentral Gyrus	Left	-24	-2	24
5	Cerebellum	Left	-16	-16	-28
6	Medial Temporal Lobe	Left	-20	-12	-20
7	Agular Gyrus	Left	-30	-16	14
8	Medial Temporal Lobe	Right	20	-8	-22
Degree Hubs					
9	Cerebellum	Left	-10	-20	-34
10	Inferior Temporal Gyrus	Left	-32	-8	-20
BC Hubs					
11	Primary Visual Cortex (V1)	Right	14	-44	-14
12	Inferior Temporal Gyrus	Right	32	4 -	24

bellum and medial temporal lobes. Overall, more hubs were observed in the left rather than right hemisphere (7 versus 5 hubs), suggesting some asymmetry of hub organization in our findings. Spatial coordinates for characterized hubs are provided in **Table 2**.

Influence of thresholding on derived fetal graphs

Since network metrics computed with graph theoretical analyses can vary with different thresholds (Drakesmith et al., 2015), our next step was to test the influence of different thresholds (T) on our results. We computed weighted degree and BC with three different thresholds, T=0, T=0.35, and T=0.45, and re-isolated the top 10 degree and BC hubs (cf. van den Heuvel et al., 2015). The different thresholds yielded very similar results, indicating the robustness of our findings to thresholding. Additionally, binary metrics (i.e., not weighted) resulted in similar results than the weighted measures.

Age differences in hub development

To examine potential effects of fetal age on hub localization, we performed a secondary analysis, splitting the sample at median age, 35 weeks gestational age, and recomputing degree and BC within older and younger fetal subgroups. The process resulted in N=49 < 35 weeks, and N=59 > 35 weeks with very similar hub locations. The most consistent pattern was observed for the cerebellum; all three cerebellar hubs observed in the full
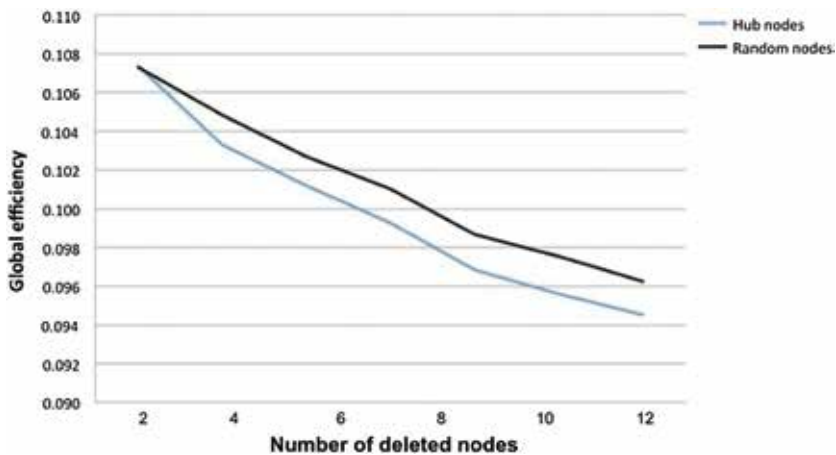
Figure 3. Computational attack of hub nodes versus random nodes.

The plot presents changes in global neural efficiency of the fetal brain in response to computational attack of hub nodes (blue) and random nodes (black). The plot shows that global efficiency decreases faster when hub nodes are computationally deleted from the network then when to random nodes are deleted. Attacking the 12 putative hubs decreased global efficiency more than attacking random nodes (p < .0001).

group were also observed when splitting the data. Some hubs were only observed at earlier or later gestational age only: The left Medial Temporal Lobe and right Inferior Temporal Gyrus were identified as hub in the later gestational age group only, whereas the Precentral Gyrus and Angular Gyrus were only observed as hubs in earlier gestational age group. Similar effects were obtained for degree and BC hubs.

Importance of hubs for network efficiency in the fetal brain
To address the functional relevance of derived hub versus non-hub nodes, the consequences of node elimination on overall network efficiency was assessed. When simulating random attack by deleting random nodes from the network the global efficiency degraded with a 12.7% change. In contrast, when simulating targeted attack by deleting the hub nodes only, neural global efficiency degraded with a 14.5% change. The change resulting from targeted attack is significantly higher (t=46.910, p < .001) as compared to change resulting from random attack, indicating that, as expected, the hubs are more important for global network efficiency than the randomly selected nodes. Change in global neural efficiency when removing hub nodes and random nodes one by one is reported in**.** Global efficiency decreases more when hub nodes are computationally removed from the network then when to random nodes are removed. These results suggest that hubs may already have a key role in facilitating efficiency in the network before birth.

DISCUSSION

This is the first study to examine functional hubs in the human brain prior to birth in utero. We discovered that within the connectional functional organization of the human fetal brain there are hubs and that they are already important for neural efficiency in the fetal brain. Both primary (visual cortex, precentral gyrus) and association brain regions (inferior temporal gyrus, medial temporal lobe) demonstrated centrality in network organization before birth. Interestingly, 25% of hubs were localized in the cerebellum and all other hubs were located in areas marked to myelinate first according to Glasser and Van Essen (Glasser and Van Essen, 2011), which suggests that hub emergence in the fetal brain may follow early myelination patterns. Additionally, several interesting observations were made: 1) hubs were found in areas close to adult fusiform facial area and Wernicke's area, 2) several hubs were located in homologous areas, and 3) more hubs were located in the left than the right hemisphere. Taken together, these results suggest that hubs emerge before birth and that they may serve as important building blocks for early brain development, making them points of vulnerability in the developing network.

Fetal hubs are located in both primary and association cortices
The location of the identified fetal hubs largely overlaps with hubs located in preterm and term neonates in previous studies (De Asis-Cruz et al., 2015; Fransson et al., 2011;

van den Heuvel et al., 2015; Gao et al., 2011; Ball et al., 2014). Consistent with prior reports in infants (Fransson et al., 2011; Gao et al., 2011), we have identified visual and motor regions as functional connectivity hubs. Studies examining structural hubs in the neonatal network also found a large portion of hubs in sensorimotor areas (van den Heuvel et al., 2015; Ball et al., 2014). Interestingly, we also found evidence for network hubs in inferior temporal and medial frontal regions, indicating that functional hubs are also present in association cortex. This latter finding is in line with more recent reports on early hub development in term newborns (De Asis-Cruz et al., 2015). Similar hubs, located in temporal and frontal areas, have been derived from assessment of structural architecture of the preterm and neonatal cortex using diffusion tensor imaging (DTI) (van den Heuvel et al., 2015; Ball et al., 2014). Furthermore, our observation of hubs in the fusiform gyrus was also observed in two other studies examining hubs in health term newborns (De Asis-Cruz et al., 2015) and preterm infants (van den Heuvel et al., 2015). One brain area that was consistently reported in previous postnatal studies, both structural (Ball et al., 2014) and functional (De Asis-Cruz et al., 2015; Fransson et al., 2011; Gao et al., 2011), was not found in the current study: the insula. Gao et al. (2011) even observed the insula as major hub in all three age groups investigated (newborn, 1-year-olds, and 2-year-olds). The lack of hubs identified in the insula in the fetal period could point to a developmental trajectory of centrality in this area, with higher centrality emerging around birth and continuing into the first few years of life. Another notable difference in hub locations observed in our study compared to previous reports is the finding of hubs in the cerebellar area. This is most likely the result of the fact that previous studies have not considered the cerebellum into their analyses. Our results emphasize the importance for future studies to include cerebellar regions into hub analyses.

Taken together, our results show considerable overlap with previous reported hubs in term and preterm neonates and indicate that both primary and association brain regions demonstrate centrality in network organization beginning in fetal life. The fetal brain network may not be wired to solely support tasks that are of a perception–action nature, as has previously been thought, but instead, prepare the brain for higher order cognitive functioning that develops later in life. In this view, fetal network hubs may be important building blocks for later life cognition and emotion development.

Hubs follow developmental pathways of brain development
The identified fetal hubs seem to follow the characteristics of early brain development. For instance, several hubs were located at homologous areas, such as in the cerebellar and medial temporal regions. This finding is in line with reports of cross-hemispheric connectivity increases with advancing age in the fetal brain (Thomason et al., 2013). Additionally, we observed more hubs in the left hemisphere than in the right. This latter finding fits with prior studies reporting left-hemisphere asymmetry (Dehaene-Lambertz

et al., 2002) and more rapid myelination of the left hemisphere in early infancy (Deoni et al., 2011). This, together with the finding of a putative hub in the proto-Wernicke's area, seems to suggest emerging asymmetry of the fetal brain focused around the language system. Furthermore, we found hubs in the left and right inferior temporal gyrus that are close to the fusiform facial area in adults, suggesting the intriguing possibility that the developing brain may prepare for recognizing faces before birth. However, more research is necessary to confirm this theory.

Additionally, the observation of multiple hubs in the cerebellum could be related to the finding that myelination starts in this region (Deoni et al., 2011; Yakolev and Lecours, 1967; Gilles and Dooling, 1983; Barkovich et al., 1988). Mature myelin is already detected from 37 to 40 weeks of gestation in the cerebellum (Dubois et al., 2014). Hubs were also identified in the primary visual area and motor area, which are both areas that are reported to myelinate early in development (Deoni et al., 2011; Glasser and Van Essen, 2011; Dubois et al., 2014). One could speculate that the high centrality of hub regions creates high regional functional signaling, which, in turn, may stimulate myelin forma-tion. This possible explanation for the simultaneous emergence of hubs and myelination in the same area is supported by the recent demonstration that neuronal activity regu-lates changes in myelin-forming cells within an active circuit in the mouse brain (Gibson et al., 2014). Moreover, animal models have shown that spontaneous bursts of synchro-nized neuronal activity, or spindle bursts, play an instructive role in key developmental processes that set early cortical circuits (Hanganu-Opatz, 2010). Interestingly, a recent study in preterm human infants found that spontaneous bursting neuronal activity was mostly found in the insula and temporal cortices (Arichi et al., 2017), two areas that have been identified as hubs in the developing brain (see discussion in Thomason, 2018). Our observation of several fetal hubs in the temporal cortex could fit with the notion that hubs arise in brain areas with spontaneous bursting activity, or vice versa. Again, the insula may only become a hub in later prenatal and early postnatal stages. The relation-ship between myelination, spontaneous bursting neuronal activity, and hub topology over development should be investigated more closely in future studies.

Cerebellar hubs: importance of cerebellum in the fetal period
The cerebellum may be of particular importance for the fetal brain network, as cerebellar growth is known to be exceptionally rapid over the third trimester of pregnancy and unparalleled by any other brain structure during this period (Limperopoulos et al., 2005). Accumulating research has emphasized the importance of this region in the early devel-oping brain (Volpe, 2009). Moreover, alterations in cerebellar structure and function are frequently implicated in major developmental neuropsychological disorders, such as ADHD and autism (Seidman et al., 2005; Castellanos et al., 2002; Wang et al., 2014; Stoodley, 2014), and are assumed to develop prenatally. Recent work has also revealed that the fetal cerebellum may be particularly sensitive to premature birth (Limperopoulos

et al., 2005; Pierson and Al Sufiani, 2016) and prenatal exposure to maternal psychological stress (Ulupinar and Yucel, 2005;). The results of the current study demonstrate that there are cerebellar hubs in the fetal brain network, both in the left and right hemisphere, and that the cerebellum is consistent hub in both earlier (< 35 weeks) and later gestation (> 35 weeks), emphasizing the importance of this structure for developing neural architecture. The fact that we consistently identified the cerebellum as hub in earlier gestation, as well as late gestation, shows that this brain region may already become important early in gestation. However, we cannot infer any conclusions from our data about the cerebellum as hub in the first half of pregnancy, as our data starts at 20.6 weeks of gestation. Interestingly, cerebellar hubs have also been identified in late childhood and adolescence (Hwang et al., 2013), suggesting a prolonged role of the cerebellum in brain networks over development. Given prior assertions that the centrality of hubs increases their susceptibility to insults (Crossley et al., 2014; Aerts et al., 2016; Bullmore and Sporns, 2012), and given prior reports of the importance of the cerebellum for early development, our results provide new data suggesting the cerebellum may be a particularly vulnerable brain region in early life.

Hubs as early markers of neurological and psychiatric brain disorders
Our data suggest that the identified hubs may already have a key role in facilitating efficiency in the brain network before birth. Global efficiency of the fetal network decreased more when computationally removing hub nodes than when removing random nodes. This finding is in line with Hwang et al. (2013), who reported that lesioning functional hubs significantly reduced efficiency compared with lesioning random nodes across all age groups studied (10–12, 13–17, and 18–20 years of age). Additionally, Gao et al. (2011) reported that maturation of network topology and hubs make the infant brain at age 2 years more resilient to both random errors and targeted attack than the newborn brain. Building on this latter, hubs may be particular vulnerable in the prenatal and early postnatal period and abnormal functioning of hubs during this period may serve as useful early markers of neurological and psychiatric brain disorders. There is accumulating evidence available for altered hub topology in psychiatric disorders, such as autism and schizophrenia (Crossley et al., 2014; Bassett et al., 2008; Itahashi et al., 2014; van den Heuvel et al., 2013). More research is necessary to fill the gap in our knowledge about hub development in both typically and abnormally developing fetuses.

Limitations
Several challenges are inherent in using resting-state fMRI to study the fetal brain (reviewed by van den Heuvel and Thomason, 2016). An important issue in fetal imaging that is relevant to the current study is the lack of fetal atlases. As a result, there are limits on the specificity of nomenclature used for regions isolated as hubs in the current study. Taking this limitation into account, we have restricted our report to very broad areas (left/right, medial/lateral, lobe), and report localization of hubs in fusiform facial and

Wernicke's areas as putative, in the fetal brain. Another critical issue is movement of the fetus during scanning. Motion in the fetus and mother contribute to changes in image signal intensity that is difficult to separate from signals of interest (van den Heuvel and Thomason, 2016; Ferrazzi et al., 2014). To mitigate movement related errors, we have developed a 3-step method: 1) we select frames of quiescence, 2) we quantify total movement for each subject and eliminate frames or cases as needed based on strict quality and motion criteria (translational:>1.7mm max excursion, 0.6mm mean; rotational:>2.5°), and 3) we eliminate any cases with frame number less than 100 frames. A limitation of this approach is that, by discarding high motion frames, we may have biased our results to reflect a particular behavioral (i.e., quiet sleep) or neurological state. Another limitation that warrants mentioning is that our approach of cropping and concatenating data may have caused edge artifacts that can affect autocorrelation correction, potentially creating an artificial pattern of correlations. Finally, the relatively wide age range of our sample (~8 weeks) could be considered as a limitation as well. This limitation is partly tackled by normalizing and realigning all data to a 32 weeks of gestation template. Although realignment to one template likely has a positive effect on the stability of our group level connectivity patterns, the wide age range could still be considered a limitation given the very rapid development in utero. Future studies should include more restricted age range or compare several age groups to test for developmental effects of hub development. A final concern is the fact that more male than female fetuses were scanned in this study. Since research has shown sex differences in brain connectivity maturation over development in childhood/adolescence (De Bellis et al., 2001; Satterthwaite et al., 2015) and even in infancy (Gao et al., 2015), this has potential to influence our results.

CONCLUSION

In sum, we report that within the connectional functional organization of the human fetal brain there are hubs, or regions that are central to the connectional architecture of neural circuitry. Putative hubs were identified in visual and motor areas, as expected, but also in association cortices. Interestingly, several of the derived connectivity hubs were localized in cerebellar regions, supporting the novel theory that hubs emerge in areas that are early to myelinate. It could be speculated that, because of their high centrally in the network, hub regions produce high levels of neural activity, which, in turn, stimulates myelin development in these regions. Furthermore, results from computationally attacking hubs compared to random nodes demonstrated that hubs are important for global efficiency of the fetal brain, emphasizing their importance in the fetal network. These results indicate that the fetal brain network may not be wired to solely support tasks that are of a perception–action nature, as previously been thought, but instead, prepare the brain for higher order cognitive functioning that develops later in life. This work raises the intriguing question as to whether the areas we have identified as hubs

in the fetal brain also constitute areas of selective vulnerability, and whether functional connectivity profiles of these regions may in the future illuminate ontological bases of neurodevelopmental disorders or serve as biomarkers for later life neurodevelopmental health.

REFERENCES

Aerts H, Fias W, Caeyenberghs K, Marinazzo D (2016) Brain networks under attack: robustness properties and the impact of lesions. Brain 139:3063-3083.

Anonymous (2009) Statistical Parametric Mapping 8 from the Wellcom Trust Center for Neuroimaging.

Ball G, Aljabar P, Zebari S, Tusor N, Arichi T, Merchant N, Robinson EC, Ogundipe E, Rueckert D, Edwards AD, Counsell SJ (2014) Rich-club organization of the newborn human brain. Proc Natl Acad Sci U S A 111:7456-7461.

Bassett DS, Bullmore ET (2009) Human Brain Networks in Health and Disease. Current opinion in neurology 22:340-347.

Bassett DS, Bullmore E, Verchinski BA, Mattay VS, Weinberger DR, Meyer-Lindenberg A (2008) Hierarchical Organization of Human Cortical Networks in Health and Schizophrenia. The Journal of Neuroscience 28:9239.

Behzadi Y, Restom K, Liau J, Liu TT (2007) A component based noise correction method (CompCor) for BOLD and perfusion based fMRI. Neuroimage 37:90-101.

Berger R, Soder S (2015) Neuroprotection in preterm infants. BioMed Research International 2015:257139.

Bullmore E, Sporns O (2012) The economy of brain network organization. Nature reviews Neuroscience 13:336-349.

Castellanos F, Lee PP, Sharp W, et al. (2002) Developmental trajectories of brain volume abnormalities in children and adolescents with attention-deficit/hyperactivity disorder. JAMA 288:1740-1748.

Chai XJ, Castanon AN, Ongur D, Whitfield-Gabrieli S (2012) Anticorrelations in resting state networks without global signal regression. Neuroimage 59:1420-1428.

Collin G, Sporns O, Mandl RCW, van den Heuvel MP (2014) Structural and Functional Aspects Relating to Cost and Benefit of Rich Club Organization in the Human Cerebral Cortex. Cerebral Cortex 24:2258-2267.

Craddock RC, James GA, Holtzheimer PE, 3rd, Hu XP, Mayberg HS (2012) A whole brain fMRI atlas generated via spatially constrained spectral clustering. Hum Brain Mapp 33:1914-1928.

Crossley NA, Mechelli A, Scott J, Carletti F, Fox PT, McGuire P, Bullmore ET (2014) The hubs of the human connectome are generally implicated in the anatomy of brain disorders. Brain 137:2382-2395.

De Asis-Cruz J, Bouyssi-Kobar M, Evangelou I, Vezina G, Limperopoulos C (2015) Functional properties of resting state networks in healthy full-term newborns. Scientific Reports 5:17755.

De Bellis MD, Keshavan MS, Beers SR, Hall J, Frustaci K, Masalehdan A, Noll J, Boring AM (2001) Sex Differences in Brain Maturation during Childhood and Adolescence. Cerebral Cortex 11:552-557.

Dehaene-Lambertz G, Dehaene S, Hertz-Pannier L (2002) Functional Neuroimaging of Speech Perception in Infants. Science 298:2013.

Deoni SCL, Mercure E, Blasi A, Gasston D, Thomson A, Johnson M, Williams SCR, Murphy DGM (2011) Mapping Infant Brain Myelination with Magnetic Resonance Imaging. The Journal of Neuroscience 31:784.

Di Martino A, Fair DA, Kelly C, Satterthwaite TD, Castellanos FX, Thomason ME, Craddock RC, Luna B, Leventhal BL, Zuo X-N, Milham MP (2014) Unraveling the Miswired Connectome: A Developmental Perspective. Neuron 83:1335-1353.

Drakesmith M, Caeyenberghs K, Dutt A, Lewis G, David AS, Jones DK (2015) Overcoming the effects of false positives and threshold bias in graph theoretical analyses of neuroimaging data. NeuroImage 118:313-333.

Dubois J, Dehaene-Lambertz G, Kulikova S, Poupon C, Hüppi PS, Hertz-Pannier L (2014) The early development of brain white matter: A review of imaging studies in fetuses, newborns and infants. Neuroscience 276:48-71.

Elitt CM, Rosenberg PA (2014) The challenge of understanding cerebral white matter injury in the premature infant. Neuroscience 276:216-238.

Ferrazzi G, Kuklisova Murgasova M, Arichi T, Malamateniou C, Fox MJ, Makropoulos A, Allsop J, Rutherford M, Malik S, Aljabar P, Hajnal JV (2014) Resting State fMRI in the moving fetus: A robust framework for motion, bias field and spin history correction. NeuroImage 101:555-568.

Fransson P, Åden U, Blennow M, Lagercrantz H (2011) The Functional Architecture of the Infant Brain as Revealed by Resting-State fMRI. Cerebral Cortex 21:145-154. FSL FMRIB Software Library. http://wwwfmriboxacuk/fsl/.

Gao W, Alcauter S, Smith JK, Gilmore JH, Lin W (2015) Development of human brain cortical network architecture during infancy. Brain Structure and Function 220:1173-1186.

Gao W, Zhu H, Giovanello KS, Smith JK, Shen D, Gilmore JH, Lin W (2009) Evidence on the emergence of the brain's default network from 2-week-old to 2-year-old healthy pediatric subjects. Proceedings of the National Academy of Sciences 106:6790-6795.

Gao W, Gilmore JH, Giovanello KS, Smith JK, Shen D, Zhu H, Lin W (2011) Temporal and Spatial Evolution of Brain Network Topology during the First Two Years of Life. PLOS ONE 6:e25278.

Gibson EM, Purger D, Mount CW, Goldstein AK, Lin GL, Wood LS, Inema I, Miller SE, Bieri G, Zuchero JB, Barres BA, Woo PJ, Vogel H, Monje M (2014) Neuronal Activity Promotes Oligodendrogenesis and Adaptive Myelination in the Mammalian Brain. Science 344.

Glasser MF, Van Essen DC (2011) Mapping Human Cortical Areas In Vivo Based on Myelin Content as Revealed by T1- and T2-Weighted MRI. The Journal of Neuroscience 31:11597.

Greicius MD, Krasnow B, Reiss AL, Menon V (2003) Functional connectivity in the resting brain: A network analysis of the default mode hypothesis. Proceedings of the National Academy of Sciences 100:253-258.

Hwang K, Hallquist MN, Luna B (2013) The Development of Hub Architecture in the Human Functional Brain Network. Cerebral Cortex 23:2380-2393.

Itahashi T, Yamada T, Watanabe H, Nakamura M, Jimbo D, Shioda S, Toriizuka K, Kato N, Hashimoto R (2014) Altered Network Topologies and Hub Organization in Adults with Autism: A Resting-State fMRI Study. PLOS ONE 9:e94115.

Keunen K, Counsell SJ, Benders MJNL (2017) The emergence of functional architecture during early brain development. NeuroImage.

Limperopoulos C, Soul JS, Gauvreau K, Huppi PS, Warfield SK, Bassan H, Robertson RL, Volpe JJ, du Plessis AJ (2005) Late Gestation Cerebellar Growth Is Rapid and Impeded by Premature Birth. Pediatrics 115:688.

Paneth N, Korzeniewski S, Hong T (2005) The Role of the Intrauterine and Perinatal Environment in Cerebral Palsy. NeoReviews 6:e133.

Paus T, Keshavan M, Giedd JN (2008) Why do many psychiatric disorders emerge during adolescence? Nat Rev Neurosci 9:947-957.

Pierson CR, Al Sufiani F (2016) Preterm birth and cerebellar neuropathology. Seminars in Fetal and Neonatal Medicine 21:305-311.

Rice D, Barone S (2000) Critical periods of vulnerability for the developing nervous system: evidence from humans and animal models. Environmental Health Perspectives 108:511-533.

Rosenbaum P, Paneth N, Leviton A, Goldstein M, Bax M, Damiano D, Dan B, Jacobsson B (2007) The definition and classification of cerebral palsy. Developmental Medicine & Child Neurology 109:8-14.

Rubinov M, Sporns O (2010) Complex network measures of brain connectivity: uses and interpretations. Neuroimage 52:1059-1069.

Satterthwaite TD, Wolf DH, Roalf DR, Ruparel K, Erus G, Vandekar S, Gennatas ED, Elliott MA, Smith A, Hakonarson H, Verma R, Davatzikos C, Gur RE, Gur RC (2015) Linked Sex Differences in Cognition and Functional Connectivity in Youth. Cerebral Cortex 25:2383-2394.

Schöpf V, Kasprian G, Brugger PC, Prayer D (2012) Watching the fetal brain at 'rest'. International Journal of Developmental Neuroscience 30:11-17.

Seidman LJ, Valera EM, Makris N (2005) Structural Brain Imaging of Attention-Deficit/Hyperactivity Disorder. Biological Psychiatry 57:1263-1272.

Serag A, Aljabar P, Ball G, Counsell SJ, Boardman JP, Rutherford MA, Edwards AD, Hajnal JV, Rueckert D (2012) Construction of a consistent high-definition spatio-temporal atlas of the developing brain using adaptive kernel regression. Neuroimage 59:2255-2265.

Shattuck DW, Leahy RM (2002) BrainSuite: an automated cortical surface identification tool. Med Image Anal 6:129-142.

Sporns O, Honey CJ, Kötter R (2007) Identification and Classification of Hubs in Brain Networks. PLOS ONE 2:e1049.

Stoodley CJ (2014) Distinct regions of the cerebellum show gray matter decreases in autism, ADHD, and developmental dyslexia. Frontiers in Systems Neuroscience 8:92.

Thomason ME, van den Heuvel MI, Waller R, Turk E, van den Heuvel MP, Manning JH, Hect J, Hernandez-Andrade E, Hassan SS, Romero R (under review) Maternal intrauterine stress programming of human fetal neural network efficiency.

Thomason ME, Brown JA, Dassanayake MT, Shastri R, Marusak HA, Hernandez-Andrade E, Yeo L, Mody S, Berman S, Hassan SS, Romero R (2014) Intrinsic Functional Brain Architecture Derived from

Graph Theoretical Analysis in the Human Fetus. Plos One 9:10.

Thomason ME, Dassanayake MT, Shen S, Katkuri Y, Alexis M, Anderson AL, Yeo L, Mody S, Hernandez-Andrade E, Hassan SS, Studholme C, Jeong JW, Romero R (2013) Cross-hemispheric functional connectivity in the human fetal brain. Science Translational Medicine 5.

Thomason ME, Grove LE, Lozon Jr TA, Vila AM, Ye Y, Nye MJ, Manning JH, Pappas A, Hernandez-Andrade E, Yeo L, Mody S, Berman S, Hassan SS, Romero R (2015) Age-related increases in long-range connectivity in fetal functional neural connectivity networks in utero. Developmental Cognitive Neuroscience 11:96-104.

Tomasi D, Volkow ND (2011) Association between Functional Connectivity Hubs and Brain Networks. Cerebral Cortex 21:2003-2013.

Ulupinar E, Yucel F (2005) Prenatal stress reduces interneuronal connectivity in the rat cerebellar granular layer. Neurotoxicology and Teratology 27:475-484.

van den Heuvel M, Mandl R, Hulshoff Pol H (2008) Normalized cut group clustering of resting-state FMRI data. PLoS One 3:e2001.

van den Heuvel M, de Lange S, Zalesky A, Seguin C, Yeo T, Schmidt R (2017) Proportional thresholding in resting-state fMRI functional connectivity networks and consequences for patient-control connectome studies: Issues and recommendations. Neuroimage.

van den Heuvel MI, Thomason ME (2016) Functional Connectivity of the Human Brain in Utero. Trends in cognitive sciences 20:931-939.

van den Heuvel MP, Sporns O (2011) Rich-Club Organization of the Human Connectome. The Journal of Neuroscience 31:15775.

van den Heuvel MP, Sporns O (2013) Network hubs in the human brain. Trends in cognitive sciences 17:683-696.

van den Heuvel MP, Sporns O, Collin G, et al. (2013) Abnormal rich club organization and functional brain dynamics in schizophrenia. JAMA Psychiatry 70:783-792.

van den Heuvel MP, Kersbergen KJ, de Reus MA, Keunen K, Kahn RS, Groenendaal F, de Vries LS, Benders MJNL (2015) The Neonatal Connectome During Preterm Brain Development. Cerebral Cortex 25:3000-3013.

Volpe JJ (2009) Cerebellum of the Premature Infant: Rapidly Developing, Vulnerable, Clinically

Important. Journal of child neurology 24:1085-1104.

Wang Samuel SH, Kloth Alexander D, Badura A (2014) The Cerebellum, Sensitive Periods, and Autism. Neuron 83:518-532.

Whitfield-Gabrieli S, Nieto Castanon A (2012) Conn: A functional connectivity toolbox for correlated and anticorrelated brain networks. Brain Connectivity.

Zuo X-N, Ehmke R, Mennes M, Imperati D, Castellanos FX, Sporns O, Milham MP (2012) Network Centrality in the Human Functional Connectome. Cereb Cortex 22:1862-1875.

[1]

Chapter 5

Cortical chemoarchitecture shapes macroscale effective functional connectivity patterns in macaque cerebral cortex

Elise Turk*, Lianne H. Scholtens*, Martijn P. van den Heuvel
authors contributed equally

ABSTRACT

The mammalian cortex is a complex system of—at the microscale level—interconnected neurons and—at the macroscale level—interconnected areas, forming the infrastructure for local and global neural processing and information integration. While the effects of regional chemoarchitecture on local cortical activity are well known, the effect of local neurotransmitter receptor organization on the emergence of large-scale region-to-region functional interactions remains poorly understood. Here, we examined reports of effective functional connectivity—as measured by the action of strychnine administration acting on the chemical balance of cortical areas—in relation to underlying regional variation in microscale neurotransmitter receptor density levels in the macaque cortex. Linking cortical variation in microscale receptor density levels to collated information on macroscale functional connectivity of the macaque cortex, we show macroscale patterns of effective corticocortical functional interactions— and in particular, the strength of connectivity of efferent macroscale pathways—to be related to the ratio of excitatory and inhibitory neurotransmitter receptor densities of cortical areas. Our findings provide evidence for the microscale chemoarchitecture of cortical areas to have a direct stimulating influence on the emergence of macroscale functional connectivity patterns in the mammalian brain.

Key words: functional connectivity; brain networks; graph theory; strychnine; neurotransmitter receptors

INTRODUCTION

Brain function emerges from neural interactions between individually connected neurons, as well as between globally interconnected areas (Passingham et al., 2002; Sporns et al., 2005; van den Heuvel & Sporns, 2013). At the microscale level of brain organization functional organization entails signal transduction between neurons (Cossell et al., 2015; Ullo et al., 2014; Yuste, 2011). At the macroscale, functional connectivity of macroscale neuronal circuits describes interactions between large-scale cortical areas (Rubinov & Sporns, 2010; van den Heuvel et al., 2012) shaped by the underlying anatomical wiring infrastructure of the brain (Adachi et al., 2012; Honey et al., 2010; van den Heuvel & Sporns, 2013). Much is known about how signaling on the neuronal level depends on the local cyto-, myelo- and chemoarchitecture of cortical areas (Amunts & von Cramon, 2006; Zilles et al., 2002; Zilles et al., 1995). Functional activity of cortical areas on the microscale is shaped by local interactions between large numbers of neurons and their cortico-cortical interconnections with other brain regions (Kandel et al., 2000). A large proportion of these interactions is communicated through chemical transmission (Kandel et al., 2000). Whether a connected target area will fire depends on the summation of many factors, such as the neuronal types present in that region (Ullo

et al., 2014), as well on their excitatory and inhibitory synaptic input (Kandel et al., 2000) and their excitatory and inhibitory balance (Duncan et al., 2014; Kapogiannis et al., 2013). However, how underlying microscale structural and chemical architecture of cortical regions shapes the emergence of macroscale brain-wide functional connectivity patterns is less well understood (Honey et al., 2010; Kötter, 2007; Passingham et al., 2002).

In this study we set about to provide insight into this matter by examining a potential interplay between the chemoarchitecture of cortical areas and the formation of macroscale effective functional connectivity patterns in the macaque brain. Data on density of six common regional neurotransmitter receptors was collated from the pioneering autoradiography work of Kötter and Zilles and colleagues, reporting on regional neurotransmitter receptor densities of the macaque cortical surface (Kotter et al., 2001). Induced functional connectivity of macaque cortical areas was derived from a collation of strychninization studies made by Stephan and colleagues (Stephan et al., 2000). Strychnine studies provide detailed information on a rather unique type of directed functional connectivity resulting from strychnine-induced regional cortical disinhibition. Targeted administration of strychnine on a cortical region leads to a temporary excitatory reaction at the local source region and subsequently an increase in neural activity in remote cortical areas by means of glutamate mediated excitatory long-range projecting axons of the source region (a detailed description of strychnine functional connectivity is given in the method section). Combining chemoarchitectural receptor densities operating at the nanoscale of brain organization with measurements of macroscale strychnine-derived functional connectivity we show effective functional connectivity patterns of cortical areas to be modulated by regional variation in excitatory and inhibitory receptor density.

MATERIALS AND METHODS

Macroscale strychnine-induced functional connectivity
Data on effective functional connectivity of the macaque cortex was derived from the strychnine-based functional connectivity dataset as collated by Stephan and coworkers in their seminal paper on strychnine induced effective functional connectivity of the macaque cortex (Stephan et al., 2000). Since the neuronographic studies from which the strychnine functional connectivity data was collated did not usually state in which hemisphere activity was recorded, Stephan et al. pooled connections across hemispheres, leaving a single mono-hemispheric connectivity matrix. Originally, the in vivo technique of strychninization has been designed to reveal functional relations between cortical areas and bodily movements by stimulation of motor regions of the macaque cerebral cortex (De Barenne, 1924). Later, local strychnine application was used to determine the boundaries between cortical areas based on their functional projections (De Barenne & McCulloch, 1938). Functional interaction between cortical source and target areas was observed as alterations in electrocorticography activity of target areas following

strychninization of source regions. Connectivity patterns similar to those observed after electrical stimulation of that same source region were demonstrated labeling strychninization as an effective methodology for mapping cortico-cortical projections (De Barenne & McCulloch, 1938). It is now known that strychnine acts as an antagonist for the neuronal glycine receptor (GlyR) and as a partial antagonist for the γ-aminobutyric acid type A receptor (GABAA) (Curtis et al., 1971; Davidoff et al., 1969) partially blocking the function of inhibitory postsynaptic potentials. The resulting disinhibition of strychninized areas increases the chance of pyramidal neurons -in particular layer 2 and 3 pyramidal neurons, neurons of which their projections are important for cortico-cortical signal transduction (Salling & Harrison, 2014)- to spike and to propagate action potentials along their long-range axons projecting to distinct cortical areas. At the macroscale level of brain organization, the net effect of strychnine administration is thus a strong stimulating action on target areas.

In their article, Stephan and colleagues (2000) collated functional connectivity data across 19 strychnine studies (see
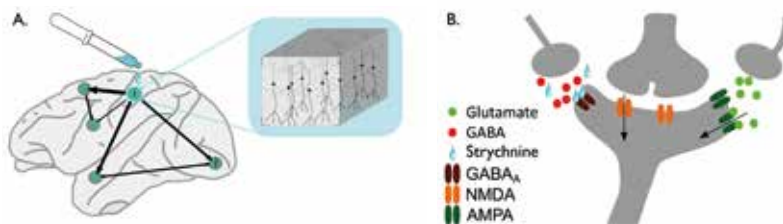
Figure 1. Schematic representation of workings of strychnine induced functional connevity.
Figure shows a schematic presentation of the biological mechanism of the workings of strychninization (see also the main text). (A) During a strychnine experiment, strychnine (blue) is administered to a source region i. The schematic drawing (blue box) illustrates the strychnine to have an effect on the cortical column and to particularly act on layer 3 pyramidal cells. (B) At the nanoscale receptor level, local administration of strychnine (depicted by the blue drops) results in the blocking of inhibitory glycine receptors and partially blocking of the GABA_A receptors (dark red), therewith strongly reducing GABA-mediated influx (red dots) into the source neuron. The lack of GABAergic modulation increases the excitability of the source neuron and results in a strong sensitivity of the neuron to incoming glutamatergic-mediated excitatory activity (green dots) via –for example– AMPA receptors (dark green) and second messenger dependent excitatory neurotransmission (orange receptor). At the microscale cellular level this has the net effect of an overall increase in the excitability of the source neuron. Taken across the entire stimulated area (thus involving a large number of neurons) the source region's macroscale net excitatory impulse on its short and long-range connected cortical regions increases. This outgoing functional influence of source region i to these other regions j of the cortex is measured by means of electroencephalography recordings of an increase in cortical activity at the target regions j of the cortex.

(Stephan et al., 2000) for a complete list) for each cortical source region of the Walk-er-vonBonin&Bailey atlas (WBB47). The WBB47 atlas is a combination of cortical areas of the von Bonin and Bailey atlas (Von Bonin & Bailey, 1947) and frontal areas of the Walker atlas (Walker, 1940) and was first used by Stephan and coworkers (Stephan et al., 2000) and later by others for the analysis of anatomical cortico-cortical connectivity (e.g. (Scholtens et al., 2014)). The WBB47 describes the whole (unihemispheric) surface of the macaque cortex in 39 non-overlapping areas (including 5 frontal, 10 prefrontal, 7 parietal, 9 temporal, 3 occipital, 2 insular and 3 cingulate regions) (Stephan et al., 2000). **Figure 2B** shows a schematic illustration of the 39 WBB47 regions on the macaque cortical surface. Using the WBB47 atlas, Stephan and coworkers collated reports across literature on cortico-cortical strychnine functional connectivity (i.e., net excitatory effect) of the 39 WBB47 cortical regions with all other cortical regions in a 39x39 functional connectivity matrix. Information on the presence or absence and information on the strength of present connections was reported as '0' (connection explicitly mentioned to be absent), '1' (connection present, strength: weak), '2' (connection present, strength: moderate), '3' (connection present, strength: strong), 'X' (connection present, strength: unreported) or '-' when no information on a cortico-cortical connection could be found was stored in the connectivity matrix. Of the connections for which a specific strength was reported (64% of all 221 connections), the majority (52.7%) was reported to be weak ($s = 1$), 20.6% of connections was of moderate strength ($s = 2$) and 26.7% was strong ($s = 3$). For our analysis, connections of which clear presence but no information on strength was reported in literature (i.e., the 'X' connections) were taken as connections with the strength most prevalent in our dataset ($s = 1$); connection pairs of which no information could be collated across literature (i.e., the '-' connections) were taken as an empty entry (i.e., absence of connection, $s = 0$) in the connectivity matrix following the procedures by Stephan and colleagues. [For additional analyses excluding all connections of unknown strength see supplementary methods and **Table S1 and Figure S1**]. In all, the examined connectivity matrix described 39 areas (nodes) of the WBB47 atlas, with 175 weak connections (edges), 20 medium strength connections, and 26 strong connections.

Region-wise strychnine functional connectivity strength
Basic graph analysis was used as a theoretical framework to explore topological structure of the strychnine-induced functional network. For each cortical area the regional *out-strength* defined as the sum across all outgoing projections of a region and *in-strength* defined as the sum across all ingoing connections of a region were computed.

Regional neurotransmitter receptor levels
Receptor levels. Information on the chemoarchitecture of macaque cortical regions was taken from the study of Kötter and colleagues (Kotter et al., 2001). The Kötter study reports on densities of (in total) 9 excitatory and inhibitory neurotransmitter receptors
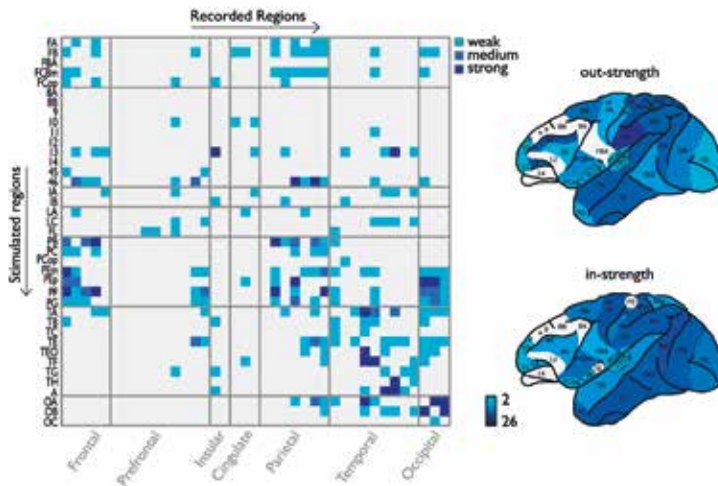
Figure 2. Regional strychnine functional connectivity matrix.
Panel A shows the strychnine-induced functional connectivity matrix of the 39 WBB47 areas of the macaque cortex as reported by Stephan and coworkers (Stephan et al., 2000). Connection strength of pathways is given from weak (represented as 1, light blue) to moderate (2, medium blue) and strong (3, dark blue). Panel B shows regional levels of functional in-strength and out-strength mapped onto a lateral view of the macaque cortex, with regional in-strength and out-strength computed as column and row summation of strength values of the matrix. Regional strength values ranged from 2 (weakest connected region depicted in light blue) to 26 (strongest functionally connected cortical region, shown in dark blue).

(in fmol/mg protein) of 29 smaller sub-areas of the visual, motor and somatosensory system of the macaque cortex, densities obtained by means of *in vitro* autoradiography using receptor-specific radiolabeled receptor binding ligands (collated density levels are displayed in **Figure 3**). Data reported on receptors involved in excitatory neurotransmission included (receptor 1) glutamatergic AMPA receptor (α-amino-3-hydroxy-5-methyl-4-isoxazolepropionic acid receptor), (2) glutamatergic kainate receptor, (3) serotonin 5-HT2A receptor (5-hydroxytryptamine receptor type 2A) and (4) acetylcholine receptor M1 (muscarinic receptor type 1). Data reported on receptors involved in inhibitory neurotransmission included (5) the GABAA receptor (type A of the γ-aminobutyric acid receptor) and (6) the acetylcholine receptor M2 (muscarinic receptor type 2). Receptors 7 to 9 (respectively, NMDA, α1 and α2h) were measured in motor areas only (just 4 regions in the used WBB47 atlas, see below) and therefore not included in our study, resulting in the examination of 6 receptor levels.

Mapping of receptor data to strychnine functional connectivity. To enable cross-modal
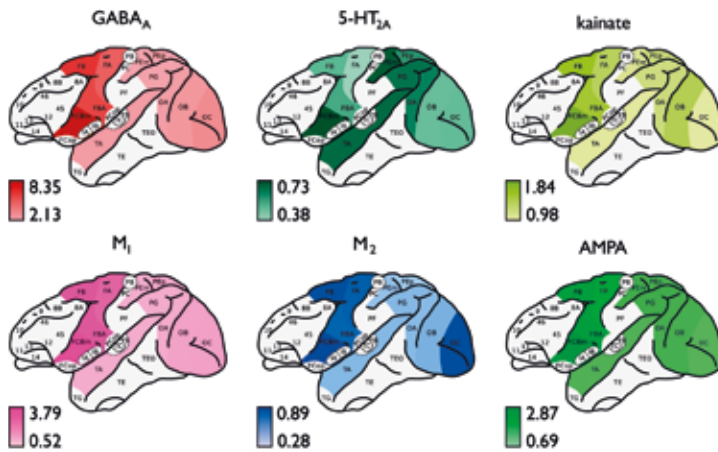
Figure 3. Cortical layout of mapped regional density levels.

Figure shows the regional densities of the 6 examined receptors for the included macaque WBB47 cortical regions (see Table 2). Figure shows the density distributions of inhibitory receptors $GABA_A$ (red) and M_2 (pink), and density distributions of excitatory receptors AMPA (light green), $5-HT_{2A}$ (dark green), M_1 (blue) and, kainate (yellow). Binding density levels are depicted in fmol/mg·10^3 protein ranging from minimum values (light colors) to maximum values (dark colors). Data as collated from the study of Kötter and coworkers (Kotter et al., 2001) (see main text).

analysis between the receptor data and macroscale strychnine functional connectivity data derived for the WBB47 cortical areas the 29 smaller areas reported by Kötter and coworkers were manually mapped to the regions of the WBB47 parcellation atlas. The WBB47 atlas and mapping was used in previous studies of our group on macroscale anatomical connectivity of the macaque cortex, and provide a detailed description of the performed mapping (**Table S2**) (Scholtens et al., 2014; van den Heuvel, de Reus, et al., 2015). Mapping of receptor density data to the WBB47 atlas resulted in receptor data for a total of 11 WBB47 cortical regions (FA, FB, FBA, FCBm, PEp, PEm, PG, TA, OA, OB and OC) (Scholtens et al., 2014). The resulting receptor density levels for the 6 examined receptors of the 11 cortical regions are shown in **Figure 3**.

Excitatory-Inhibitory ratio. For each region a net excitatory character was examined by means of computation of the Excitatory-Inhibitory *ExIn* ratio, calculated as the mean excitatory receptor density (mean over AMPA, 5-HT2A, kainate and M1) divided by the mean inhibitory receptor density (mean over M2 and GABAA). As such, a larger ExIn ratio indicated less inhibitory neurotransmission as mediated by receptor densities (Kapogiannis et al., 2013). To eliminate potential influences of differences in absolute

Table 1. Pearson correlations (R) between neurotransmitter receptor level densities and total out-/in-strength of strychnine-induced functional connectivity of cortical areas

	Out-strength		In-strength	
	R	p	R	p
AMPA	-0.1328	0.7146	-0.1741	0.6086
5-HT$_{2A}$	0.6194	0.0561	-0.0283	0.9342
Kainate	-0.0817	0.8224	-0.0873	0.7985
M$_1$	-0.3278	0.3551	-0.2044	0.5466
M$_2$	-0.7577	0.0111*	-0.1292	0.7049
GABA$_A$	-0.3372	0.3408	-0.1861	0.5838
ExIn ratio	0.8259	0.0032*	0.1256	0.7129

*Receptor levels are based on autoradiography measurements reported by Kötter et al. (2001). Correlations were calculated between excitatory receptor levels (AMPA, 5HT2A, kainate, and M1), inhibitory receptors (GABAA and M2), and the in- and out-strength of strychnine functional connectivity of cortical areas. *Effects reaching a partial Bonferroni corrected α of 0.0125.*

Table 2. Mapping of Kötter (2001) subregions to the WBB47 atlas

WBB47 region	Kötter (2001) subregions								
FA	F1								
FB	F2v	F2d	F3	F6	F7				
FBA	F4v	F4d							
FCBm	F5								
PEm	VIP								
PEp	PO	MIP	PEP						
PG	LIP	PG	MST						
TA	FST								
OA	V3v	V3d	V3A	V4v	V4d	V6A	V4t	MT	MTp
OB	V2v	V2d							
OC	V1								

The first column lists all cortical regions of the WBB47 parcellation that were included in the analysis. Remaining columns show the included subregions from the Kötter (2001) study (for which receptor density information was available) per WBB47 region.

receptor densities, we calculated an alternative ExIn ratio using normalized receptor densities. Values for each receptor were rescaled by dividing each density by the largest value for that specific receptor, excluding any effect of differences in absolute receptor density.

Statistical analysis

Pearson's correlation was used to test a potential interplay between regional receptor densities and functional connectivity, cross-correlating the 6 receptor density levels plus the ExIn ratio with nodal functional out- and in-strength. Area FBA lacked any recordings of efferent strychnine functional connectivity and with such (functional) disconnection believed to be related to a shortage of measurements rather than a true effect of regions being completely unconnected to the rest of the brain, FBA was excluded from further analysis. This resulted in a dataset on chemoarchitecture-connectomics comparison for 10 cortical regions. Across these 10 regions, a total of 7 x 2 = 14 statistical tests were performed (6 receptors plus ExIn ratio; in- and out-strength), yielding the need for correction for multiple testing. With a strongly dependent nature of the receptor density data (showing an average correlation of r = 0.6296 between the 6 receptor levels) a principal component analysis was performed to assess the true number of independent tests performed (Gao et al., 2008). PCA resulted in the identification of 2 components in the receptor data explaining >99% of the total variance, yielding a partial Bonferroni-corrected α of 0.05/(2 x 2) = 0.0125 correcting for the number of independent tests of 2 receptor components x 2 functional connectivity metrics (i.e. out- and in-strength). Effects reaching this partial Bonferroni corrected alpha of 0.0125 were taken as significant (Gao et al., 2008; Li & Ji, 2005; Scholtens et al., 2014). Further taking into account the notion of the data not being normally distributed findings were verified with non-parametric Spearman's Rank correlations. Similar results were observed (see supplemental results), but we believe that due to the low power of the data (n=10) Spearman's tests might have overestimated relationships (see Supplementary Materials, **Table S2**), thus we favored Pearson's correlation analysis.

RESULTS

Table 1 lists all correlations between receptor levels and regional functional out- and in-strength (see also supplemental materials **Figures S2 and S3** for overview of all interactions). Correlating the 6 receptor densities with regional out-strength revealed a significant negative effect of inhibitory M2 receptors and strychnine-induced functional out-strength (r=-0.7577, p=0.0111, reaching partial Bonferroni correction) (see **Figure S4**). No effects between regional variation of GABAA, AMPA, kainate, 5-HT2A or M1 neurotransmitter receptor densities and regional functional out-strength were observed (see Table 1 and supplemental materials **Figure S2** for overview of all correlations). Moreover, in particular receptor ExIn ratio and functional out-strength showed a strong

positive correlation (r=0.8259, p=0.0032, see **Figure 4**), indicating an overall more excitatory and less inhibitory chemoarchitecture of cortical regions to be related to more and stronger outgoing macroscale effective functional projections. Using the normalized ExIn ratio yielded similar results (r=0.8439, p=0.0021). As hypothesized based on the workings of strychninization, no correlation was found between macroscale functional in-strength connectivity patterns and cortical variation in excitatory/inhibitory receptor level densities.
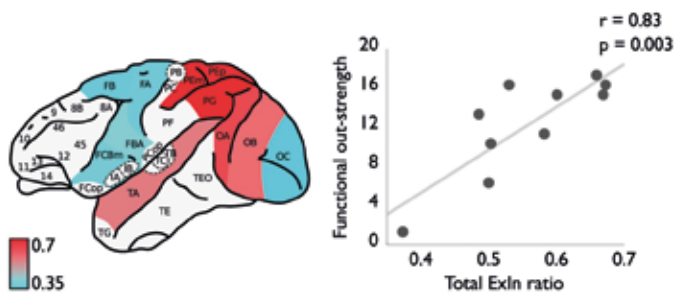
Figure 4. Interplay between receptor ExIn ratio and macroscale functional out-strength connectivity.
Panel A shows cortical ExIn ratios (high ratio values in red, low values in blue). Red regions depict cortical areas with a (relatively) excitatory chemoarchitecture, blue regions depict regions with a (relatively) inhibitory character. Panel B depicts the observed positive association between local chemoarchitecture ExIn ratio (x-axis) and the level of macroscale strychnine functional out-strength of cortical areas (y-axis) (r=0.83, p=0.0032). Figure illustrates the main finding of our study of the local excitatory chemoarchitecture of cortical areas to be of positive influence on outgoing global interregional functional influence of cortical areas.

DISCUSSION

Our findings show evidence of a direct interplay between the excitatory chemoarchitecture of cortical areas and their effective functional connectivity pattern on the macroscale of brain organization. Supported by the receptor-driven neurobiological underpinnings of strychninization (Curtis et al., 1971) our study shows the out-strength of cortical connectivity of cortical areas to be related to the excitatory and inhibitory nature of cortical areas, and in particular their balance herein. A micro-macro interplay between regional variation in receptor densities and macroscale functional cortical connectivity contributes to the hypothesis of the emergence of global brain patterns to be dependent on microscale neuronal properties (Scholtens et al., 2014; Zilles et al., 1995). Considering the original intentions of Dusser de Barenne to reveal the functional organization

of regions of the visual, sensory, motor and frontal cortex it is not surprising that the strychnine functional modules as shown in the study of Stephan are in line with common functional (Stephan et al., 2000) and anatomical (Scholtens et al., 2014) subdivisions of the macaque cortex. Interestingly, direct relations between receptor levels and structural connectivity have not been reported by initial studies (Kotter et al., 2001; Scholtens et al., 2014). Even stronger, these studies have mentioned the absence of a direct interplay between anatomical connectivity and cortical chemoarchitecture, arguing that macro-scale structural organization may be more related to cytoarchitectural properties. Pandya and colleagues showed in the macaque and human cortex that distinct cytoarchitectonic subregions have unique patterns of cortico-cortical connectivity (Pandya & Sanides, 1973; Petrides & Pandya, 1999, 2002). Furthermore, Beul and colleagues recently showed a relation between cytoarchitectonic type and structural connectivity (Beul et al., 2015), and we showed highly connected cortical areas to have higher neuronal complexity (Scholtens et al., 2014; van den Heuvel, Scholtens, Barrett, et al., 2015; van den Heuvel, Scholtens, de Reus, et al., 2015). Taken together, cytoarchitectonic characteristics have been suggested to be potentially more directly related to anatomical projections and less to the smaller and more functionally operating scale of chemoarchitecture. In contrast, chemoarchitectural modulation –and in particular rich variation in cortical 'receptor fingerprints'– has been hypothesized to rather relate to the *functional* organization of cortical regions (Zilles et al., 2002; Zilles et al., 2004) with receptors and their corre-sponding neurotransmitters modulating neuronal signal transduction by means of integration and summation of excitatory and inhibitory input (Salling & Harrison, 2014). Our current observations are in favor of such an important role of the chemoarchitecture of cortical areas in the emergence of large-scale functional connectivity patterns across regions, showing evidence of the extent of effective functional connectivity of cortical regions to depend on their underlying chemical excitatory and inhibitory nature.

Whether the observed across-region relationship between microscale chemoarchitecture and macroscale functional connectivity also holds within an individual region across time (e.g. on the relatively short timescale of task performance or on the much longer timescale of brain development) would be an interesting topic for future research. Over time, neurotransmitter receptors traffic between intracellular compartments and the neuronal membrane, thereby changing the distribution of active excitatory and inhibi-tory receptors (Choquet & Triller, 2013; Kneussel et al., 2014). The receptor distributions included in our study are static snapshots of the macaque cortex at a certain time point and therefore do not enable examination of the influence of subtle changes in excit-atory and inhibitory balance on the strength of functional connectivity within a region across time. Complementary research measuring changes in functional dynamics and receptor binding densities at different time points can contribute to a more complete understanding of the relationship between a region's chemoarchitecture and functional connectivity.

Our findings of cortical chemoarchitecture to play a modulating role in large-scale functional processes are in line with earlier observations on positive interactions between functional connectivity as derived from resting-state fMRI recordings and Magnetic Resonance Spectroscopy (MRS) estimations of the chemical balance of cortical regions. As recently reviewed by Duncan and colleagues (Duncan et al., 2014) human MRI studies have reported on inverse interactions between individual variation in functional MRI measured cortical activity and GABA levels (e.g. (Donahue et al., 2010)), and positive relationships between functional connectivity and glutamate levels (e.g. (Schmaal et al., 2012)). Furthermore, Kapogiannis and colleagues reported on higher levels of precuneus functional cortical activity and connectivity to be linked to local availability of glutamate and GABA transmitters,,with in particular the ratio of excitatory glutamate and inhibitory GABA neurotransmission to show the strongest relationship with resting-state fMRI functional connectivity patterns (Kapogiannis et al., 2013). This further underscores the importance of the excitatory/inhibitory chemical character of cortical regions in influencing global whole-brain functional connectivity patterns (Duncan et al., 2014).

Induced functional connectivity patterns by strychninization are a consequence of a net excitatory reaction to a cortical target area by suppressing the receptor function of inhibitory glycine receptors and (partially) GABAA strychnine-sensitive receptors in the source regions (De Barenne & McCulloch, 1938; Salling & Harrison, 2014). In this context, it is worth to note that as a result of the strychnine administration the retained inhibitory role of M2 receptors has been reported to become (relatively) more important in the local chemical balance of the source region, due to the temporary elimination of glycine and GABAergic receptor activity at the site of administration (Brown, 2010). This is consistent with our findings showing strychnine-induced functional connectivity out-strength to have an inverse relationship with regional M2 receptor density (shown in **Figure S4** and **Table 1**). Moreover, while strychninization may modulate inhibitory receptor action in the source region, the inhibitory mechanisms of the target regions are thought to be left unaffected, with the overall incoming (i.e. afferent) level of influence of other regions on the target region believed to remain relatively unchanged (Stephan et al., 2000). Whether or not the target region will eventually become activated depends –among other things– on the neuron type on which the majority of the efferents from the source region project, as well as on neuronal interactions within the target regions. As a result, strychninization is thought to have only a minimal influence on incoming signals of cortical areas, which is indeed consistent with our observations showing no strong relationships between receptor levels and cortical in-strength.

As noted by Stephan and Kötter and coworkers (Stephan et al., 2000), functional connectivity patterns derived from strychninization are known to be highly stable within and between specimens, as well as to be highly comparable to electroencephalography patterns acquired from direct electrical stimulation (De Barenne & McCulloch, 1938).

Comparable modern-day examinations might include the study of effects of transcranial direct-current stimulation (tDCS) and transcranial magnetic stimulation (TMS) on functional brain connectivity, techniques that both modulate cortical activity and therewith connectivity, albeit –clearly– in a much less invasive way than cortical strychninization (Pascual-Leone et al., 2000). TMS in the motor cortex has indeed been suggested to result in a temporary local decrease in GABAergic neurotransmission together with enhanced cortical excitability and to modulate global resting-state functional connectivity patterns of the motor system (Stagg et al., 2011; Stagg et al., 2009).

Considerations about the receptor densities have to be kept in mind when interpreting our presented findings on functional organization. First, it is important to note that neurotransmitter receptors are likely to act on multiple cellular mechanisms and may thus involve a long chain of both excitatory and inhibitory events, making the overall interpretation of their resulting modulatory effect on neuronal excitability considerably more complex. Ionotropic kainate receptors mediate postsynaptic glutamatergic neurotransmission having an overall excitatory effect on the postsynaptic neuron (Kandel et al., 2000). Kainate receptors have, however, also been reported to play an indirect modulating role in the release of presynaptic GABA (see (Contractor et al., 2011) for an overview on the workings of kainate receptors). Second, in addition to classifying receptors based on their inhibitory and excitatory role, receptors are also often categorized according to their ionotropic or metabotropic nature. Ionotropic receptors such as AMPA, GABAA, and kainate (ion channels) are known for their fast and direct influence on the membrane potential, while slower acting metabotropic G-protein coupled receptors such as M1, M2 and 5-HT2A have been shown to have a more modulatory role on the membrane potential (see for an overview (Hammond, 2008)). We incorporated both types of receptors in our study, arguing that in the timespan of measured strychnine-inducted cortical activity (ranging from 2 to 15 minutes, see (De Barenne & McCulloch, 1938)) both types of receptors will have had an influence on neuronal activity. Third, autoradiography studies have noted the distribution of neurotransmitter receptors to vary widely across cortical layers (Geyer et al., 1998). Layer specific information about connectivity modulating could thus have been lost when taking the average receptor density over cortical layers. High densities of kainate receptors have been reported in cortical layer 4 (described as an important layer for driving processes (Shipp, 2005) from subcortical and thalamic projections (Jones, 1998)), suggesting that kainate receptors may be particularly involved in reception of input from subcortical rather than cortico-cortical projections (Douglas & Martin, 2004). In contrast, the highest densities of AMPA receptors have been noted in layer 2/3 cortical motor areas (Geyer et al., 1998), described as important target and source layers for cortico-cortical projections (Douglas & Martin, 2004)). Fourth, data on glutamatergic NMDA receptor levels was only available for a small number of WBB47 areas and we therefore excluded recordings of this type of receptor from our analysis. However, NMDA is one of the most prevalent

excitatory receptor in the central nervous system, with receptor densities in the macaque visual, motor and sensory cortex recorded to range from 19% to 46% of all excitatory synapses (Huntley et al., 1994). Examination of NMDA receptors in relation to macro-scale functional connectivity patterns may thus include an interesting and important topic for future studies.

We report on a small but potentially important next step in understanding a micro-macro interplay of mammalian brain organization. Our findings may be of interest to studies examining changes in functional connectivity in neurological and psychiatric disorders, as such conditions are often reported to involve alterations in both receptor and neurotransmitter levels (see for example a review about serotonin receptors (Naughton et al., 2000)) as well as large-scale changes in interareal functional connectivity (see for example (Greicius, 2008) for review). Considering the interplay between macroscale cortical patterns and (dys-)function of the chemoarchitecture of neural elements at the microscale may form a potential fruitful way to get insight into the biological underpinnings of large-scale disruptions of functional connectivity in brain disorders.

REFERENCES

Adachi, Y., Osada, T., Sporns, O., Watanabe, T., Matsui, T., Miyamoto, K., & Miyashita, Y. (2012). Functional connectivity between anatomically unconnected areas is shaped by collective network-level effects in the macaque cortex. Cerebral Cortex, 22(7), 1586-1592.

Amunts, K., & von Cramon, D. Y. (2006). The anatomical segregation of the frontal cortex: what does it mean for function? Cortex, 42(4), 525-528.

Beul, S. F., Grant, S., & Hilgetag, C. C. (2015, Nov). A predictive model of the cat cortical connectome based on cytoarchitecture and distance. Brain Struct Funct, 220(6), 3167-3184. https://doi.org/10.1007/s00429-014-0849-y

Brown, D. A. (2010, Jul). Muscarinic acetylcholine receptors (mAChRs) in the nervous system: some functions and mechanisms. J Mol Neurosci, 41(3), 340-346. https://doi.org/10.1007/s12031-010-9377-2

Choquet, D., & Triller, A. (2013, Oct 30). The dynamic synapse. Neuron, 80(3), 691-703. https://doi.org/10.1016/j.neuron.2013.10.013

Contractor, A., Mulle, C., & Swanson, G. T. (2011, Mar). Kainate receptors coming of age: milestones of two decades of research. Trends Neurosci, 34(3), 154-163. https://doi.org/10.1016/j.tins.2010.12.002

Cossell, L., Iacaruso, M. F., Muir, D. R., Houlton, R., Sader, E. N., Ko, H., Hofer, S. B., & Mrsic-Flogel, T. D. (2015, Feb 19). Functional organization of excitatory synaptic strength in primary visual cortex.

Nature, 518(7539), 399-403. https://doi.org/10.1038/nature14182

Curtis, D., Duggan, A., & Johnston, G. (1971). The specificity of strychnine as a glycine antagonist in the mammalian spinal cord. Experimental brain research, 12(5), 547-565.

Davidoff, R. A., Aprison, M. H., & Werman, R. (1969, Mar). The effects of strychnine on the inhibition of interneurons by glycine and gamma-aminobutyric acid. Int J Neuropharmacol, 8(2), 191-194. https://doi.org/10.1016/0028-3908(69)90013-6

De Barenne, J. D. (1924). Experimental researches on sensory localization in the cerebral cortex of the monkey (Macacus). Proceedings of the Royal Society of London. Series B, Containing Papers of a Biological Character, 272-291.

De Barenne, J. D., & McCulloch, W. S. (1938). Functional organization in the sensory cortex of the monkey (Macaca mulatta). Journal of neurophysiology, 1(1), 69-85.

Donahue, M. J., Near, J., Blicher, J. U., & Jezzard, P. (2010, Nov 1). Baseline GABA concentration and fMRI response. NeuroImage, 53(2), 392-398. https://doi.org/10.1016/j.neuroimage.2010.07.017

Douglas, R. J., & Martin, K. A. (2004). Neuronal circuits of the neocortex. Annu Rev Neurosci, 27, 419-451. https://doi.org/10.1146/annurev.neuro.27.070203.144152

Duncan, N. W., Wiebking, C., & Northoff, G. (2014, Nov). Associations of regional GABA and glutamate with intrinsic and extrinsic neural activity in humans-a review of multimodal imaging studies. Neurosci Biobehav Rev, 47(0), 36-52. https://doi.org/10.1016/j.neubiorev.2014.07.016

Gao, X., Starmer, J., & Martin, E. R. (2008, May). A multiple testing correction method for genetic association studies using correlated single nucleotide polymorphisms. Genet Epidemiol, 32(4), 361-369. https://doi.org/10.1002/gepi.20310

Geyer, S., Matelli, M., Luppino, G., Schleicher, A., Jansen, Y., Palomero-Gallagher, N., & Zilles, K. (1998, Jul 27). Receptor autoradiographic mapping of the mesial motor and premotor cortex of the macaque monkey. J Comp Neurol, 397(2), 231-250. https://doi.org/10.1002/(sici)1096-9861(19980727)397:2<231::aid-cne6>3.0.co;2-1

Greicius, M. (2008, Aug). Resting-state functional connectivity in neuropsychiatric disorders. Curr Opin Neurol, 21(4), 424-430. https://doi.org/10.1097/WCO.0b013e328306f2c5

Hammond, C. (2008). Cellular and molecular neurophysiology. Academic Press.

Honey, C. J., Thivierge, J. P., & Sporns, O. (2010, Sep). Can structure predict function in the human

brain? *NeuroImage, 52(3),* 766-776. https://doi.org/10.1016/j.neuroimage.2010.01.071

Huntley, G. W., Vickers, J. C., & Morrison, J. H. (1994, Dec). Cellular and synaptic localization of NMDA and non-NMDA receptor subunits in neocortex: organizational features related to cortical circuitry, function and disease. *Trends Neurosci, 17(12),* 536-543. https://doi.org/10.1016/0166-2236(94)90158-9

Jones, E. G. (1998, Jul). Viewpoint: the core and matrix of thalamic organization. *Neuroscience, 85(2),* 331-345. https://doi.org/10.1016/s0306-4522(97)00581-2

Kandel, E. R., Schwartz, J. H., & Jessell, T. M. (2000). *Principles of neural science (Vol. 4).* McGraw-Hill New York.

Kapogiannis, D., Reiter, D. A., Willette, A. A., & Mattson, M. P. (2013, Jan 1). Posteromedial cortex glutamate and GABA predict intrinsic functional connectivity of the default mode network. *NeuroImage, 64(0),* 112-119. https://doi.org/10.1016/j.neuroimage.2012.09.029

Kneussel, M., Triller, A., & Choquet, D. (2014, Jun 19). SnapShot: receptor dynamics at plastic synapses. *Cell, 157(7),* 1738-1738 e1731. https://doi.org/10.1016/j.cell.2014.06.002

Kötter, R. (2007). Anatomical concepts of brain connectivity. In *Handbook of brain connectivity* (pp. 149-167). Springer.

Kotter, R., Stephan, K. E., Palomero-Gallagher, N., Geyer, S., Schleicher, A., & Zilles, K. (2001, Oct). Multimodal characterisation of cortical areas by multivariate analyses of receptor binding and connectivity data. *Anat Embryol (Berl), 204(4),* 333-350. https://doi.org/10.1007/s004290100199

Li, J., & Ji, L. (2005, Sep). Adjusting multiple testing in multilocus analyses using the eigenvalues of a correlation matrix. *Heredity (Edinb), 95(3),* 221-227. https://doi.org/10.1038/sj.hdy.6800717

Naughton, M., Mulrooney, J. B., & Leonard, B. E. (2000, Aug). A review of the role of serotonin receptors in psychiatric disorders. *Hum Psychopharmacol, 15(6),* 397-415. https://doi.org/10.1002/1099-1077(200008)15:6<397::AID-HUP212>3.0.CO;2-L

Pandya, D. N., & Sanides, F. (1973, Mar 20). Architectonic parcellation of the temporal operculum in rhesus monkey and its projection pattern. *Z Anat Entwicklungsgesch, 139(2),* 127-161. https://doi.org/10.1007/BF00523634

Pascual-Leone, A., Walsh, V., & Rothwell, J. (2000, Apr). Transcranial magnetic stimulation in cognitive neuroscience--virtual lesion, chronometry, and functional connectivity. *Curr Opin Neurobiol, 10(2),* 232-237. https://doi.org/10.1016/s0959-4388(00)00081-7

Passingham, R. E., Stephan, K. E., & Kotter, R. (2002, Aug). The anatomical basis of functional localization in the cortex. Nat Rev Neurosci, 3(8), 606-616. https://doi.org/10.1038/nrn893

Petrides, M., & Pandya, D. N. (1999, Mar). Dorsolateral prefrontal cortex: comparative cytoarchitectonic analysis in the human and the macaque brain and corticocortical connection patterns. Eur J Neurosci, 11(3), 1011-1036. https://doi.org/10.1046/j.1460-9568.1999.00518.x

Petrides, M., & Pandya, D. N. (2002, Jul). Comparative cytoarchitectonic analysis of the human and the macaque ventrolateral prefrontal cortex and corticocortical connection patterns in the monkey. Eur J Neurosci, 16(2), 291-310. https://doi.org/10.1046/j.1460-9568.2001.02090.x

Rubinov, M., & Sporns, O. (2010, 9//). Complex network measures of brain connectivity: Uses and interpretations. NeuroImage, 52(3), 1059-1069. https://doi.org/http://dx.doi.org/10.1016/j.neuroimage.2009.10.003

Salling, M. C., & Harrison, N. L. (2014). Strychnine-sensitive glycine receptors on pyramidal neurons in layers II/III of the mouse prefrontal cortex are tonically activated. Journal of Neurophysiology, 112(5), 1169-1178.

Schmaal, L., Goudriaan, A. E., Meer, J., Brink, W., & Veltman, D. J. (2012). The association between cingulate cortex glutamate concentration and delay discounting is mediated by resting state functional connectivity. Brain and behavior, 2(5), 553-562.

Scholtens, L. H., Schmidt, R., de Reus, M. A., & van den Heuvel, M. P. (2014). Linking macroscale graph analytical organization to microscale neuroarchitectonics in the macaque connectome. The Journal of Neuroscience, 34(36), 12192-12205.

Shipp, S. (2005). The importance of being agranular: a comparative account of visual and motor cortex. Philosophical Transactions of the Royal Society B: Biological Sciences, 360(1456), 797-814.

Sporns, O., Tononi, G., & Kötter, R. (2005). The Human Connectome: A Structural Description of the Human Brain. PLoS Comput Biol, 1(4), e42. https://doi.org/10.1371/journal.pcbi.0010042

Stagg, Charlotte J., Bachtiar, V., & Johansen-Berg, H. (2011, 3/22/). The Role of GABA in Human Motor Learning. Current Biology, 21(6), 480-484. https://doi.org/http://dx.doi.org/10.1016/j.cub.2011.01.069

Stagg, C. J., Best, J. G., Stephenson, M. C., O'Shea, J., Wylezinska, M., Kincses, Z. T., Morris, P. G., Matthews, P. M., & Johansen-Berg, H. (2009, April 22, 2009). Polarity-Sensitive Modulation of Cortical Neurotransmitters by Transcranial Stimulation. The Journal of Neuroscience, 29(16), 5202-5206. https://doi.org/10.1523/jneurosci.4432-08.2009

Stephan, K. E., Hilgetag, C. C., Burns, G. A., O'Neill, M. A., Young, M. P., & Kotter, R. (2000). Computational analysis of functional connectivity between areas of primate cerebral cortex. Philosophical Transactions of the Royal Society B: Biological Sciences, 355(1393), 111-126.

Ullo, S., Nieus, T. R., Sona, D., Maccione, A., Berdondini, L., & Murino, V. (2014). Functional connectivity estimation over large networks at cellular resolution based on electrophysiological recordings and structural prior. Front Neuroanat, 8, 137. https://doi.org/10.3389/fnana.2014.00137

van den Heuvel, M. P., de Reus, M. A., Feldman Barrett, L., Scholtens, L. H., Coopmans, F. M., Schmidt, R., Preuss, T. M., Rilling, J. K., & Li, L. (2015). Comparison of diffusion tractography and tract-tracing measures of connectivity strength in rhesus macaque connectome. Human brain mapping.

van den Heuvel, M. P., Kahn, R. S., Goñi, J., & Sporns, O. (2012, July 10, 2012). High-cost, high-capacity backbone for global brain communication. Proceedings of the National Academy of Sciences, 109(28), 11372-11377. https://doi.org/10.1073/pnas.1203593109

van den Heuvel, M. P., Scholtens, L. H., Barrett, L. F., Hilgetag, C. C., & de Reus, M. A. (2015). Bridging cytoarchitectonics and connectomics in human cerebral cortex. The Journal of Neuroscience, 35(41), 13943-13948.

van den Heuvel, M. P., Scholtens, L. H., de Reus, M. A., & Kahn, R. S. (2015). Associated microscale spine density and macroscale connectivity disruptions in schizophrenia. Biological psychiatry.

van den Heuvel, M. P., & Sporns, O. (2013, Sep 4). An anatomical substrate for integration among functional networks in human cortex. J Neurosci, 33(36), 14489-14500. https://doi.org/10.1523/JNEUROSCI.2128-13.2013

Von Bonin, G., & Bailey, P. (1947). The neocortex of Macaca mulatta.(Illinois Monogr. med. Sci., 5, No. 4.).

Walker, A. E. (1940). A cytoarchitectural study of the prefrontal area of the macaque monkey. Journal of Comparative Neurology, 73(1), 59-86.

Yuste, R. (2011, Sep 8). Dendritic spines and distributed circuits. Neuron, 71(5), 772-781. https://doi.org/10.1016/j.neuron.2011.07.024

Zilles, K., Palomero-Gallagher, N., Grefkes, C., Scheperjans, F., Boy, C., Amunts, K., & Schleicher, A. (2002, 12//). Architectonics of the human cerebral cortex and transmitter receptor fingerprints: reconciling functional neuroanatomy and neurochemistry. European Neuropsychopharmacology, 12(6), 587-599. https://doi.org/http://dx.doi.org/10.1016/S0924-977X(02)00108-6

Zilles, K., Palomero-Gallagher, N., & Schleicher, A. (2004). Transmitter receptors and functional anatomy of the cerebral cortex. Journal of Anatomy, 205(6), 417-432.

Zilles, K., Schlaug, G., Matelli, M., Luppino, G., Schleicher, A., Qü, M., Dabringhaus, A., Seitz, R., & Roland, P. E. (1995). Mapping of human and macaque sensorimotor areas by integrating architectonic, transmitter receptor, MRI and PET data. Journal of Anatomy, 187(Pt 3), 515-537. http://www.ncbi.nlm.nih.gov/pmc/articles/PMC1167457/

SUPPLEMENTARY METHODS
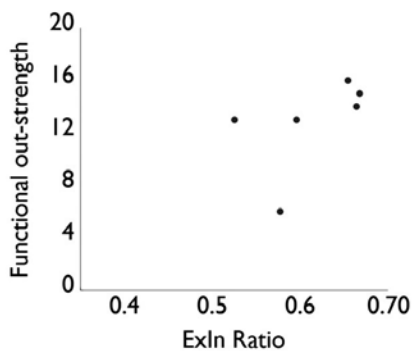
Figure S1. Interplay between receptor ExIn chemoarchitecture and macroscale functional out-strength connectivity.

The graph shows a non-significant association between local chemoarchitecture ExIn ratio (x-axis) and the level of macroscale strychnine functional out-strength of cortical areas (y-axis, note that the out-strength is calculated without all unknown connections, n=6). Figure illustrates the re-examined main finding of our study of the local excitatory chemoarchitecture of cortical areas to be of positive influence on outgoing global interregional functional influence of cortical areas when all unknown connections strength were removed (i.e., depicted as an 'X' in the connectivity matrix).

Alternative Statistical analyses

For each cortical area the out- and in-strength of functional connectivity strength were re-examined, by excluding all connections of unknown strength from the matrix (i.e., all connections with X). Pearson's correlation was used to test the relation between regional receptor densities and functional connectivity (see **Table S1** and **Figure S1** for results), cross-correlating the 6 receptor density levels and the ExIn ratio with the nodal functional out- and in-strength values of the residual regions (n=6).

SUPPLEMENTARY RESULTS

Alternative Statistical results

To validate our main findings, we removed all (124) pathways with an unknown connection strength (i.e., depicted as an 'X' in the connectivity matrix). Fourteen relations were represented between all excitatory receptor levels, inhibitory receptors, ExIn ratio and the (out or in-) strength of the functional connections (**Table S1**). Similar correlation coefficients were found using the complete dataset (as reported in main text), although we believe that due to the low power of the data (n=6) lower p-values are found when all unknown connection strengths are removed (**Figure S1**).

Spearman Rank correlation coefficients (R) between neurotransmitter receptor level densities and out-strength or in-strength of the strychnine-induced functional regions are represented in **Table S2, Figure S2** and **Figure S3**. Receptor levels are collated from the study of Kötter and colleagues (Kötter, 2001). Relations were calculated between all
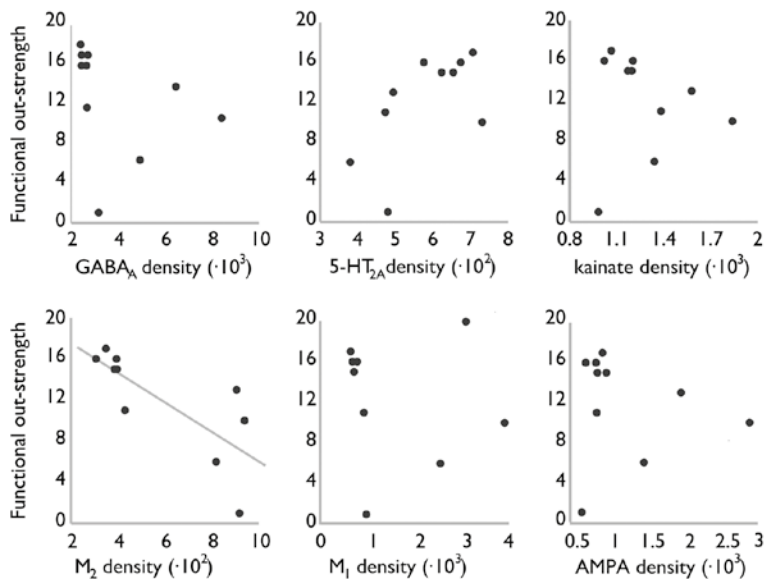
Supplemental Figure S2. Overview of associations between receptor densities and out-strength.
Figure shows the scatterplots of the 6 receptor densities (on x-axis, in fmol/mg·10^3 protein) and strychnine-induced functional out-strength (y-axis). Plots of inhibitory $GABA_A$ and M_2 receptors are shown on the left, and plots of excitatory 5-HT$_{2A}$, M_1, kainate and AMPA receptors are presented in the middle and right. Figure illustrates an exclusive correlation between M_2 receptor densities and functional out-strength (R = -0.76, p = 0.0111, see Figure S4).
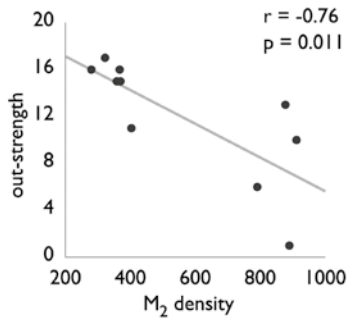
Table S1. Correlations of regional receptor levels and functional outward connection strength.

	Out-strength		In-strength	
	R	p	R	p
AMPA	0.2073	0.6935	-0.1899	0.5760
5-HT$_{2A}$	0.8286	0.0416	-0.2038	0.5479
Kainate	-0.7710	0.0727	-0.1602	0.6381
M$_1$	-0.8621	0.0272	-0.1557	0.6475
M$_2$	-0.7554	0.0824	0.1171	0.7318
GABA$_A$	-0.9094	0.0119	-0.1292	0.7050
ExIn ratio	0.5254	0.2844	-0.2297	0.4969
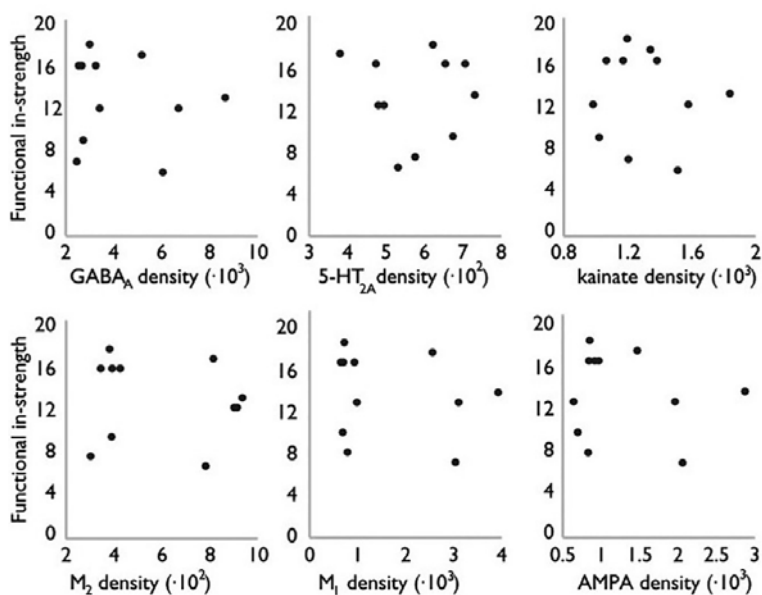
Supplemental Figure S3. Overview of associations between receptor densities and in-strength.
Figure shows the scatterplots of the 6 receptor densities (on x-axis, in fmol/mg·10³ protein) and strychnine-induced functional in-strength (y-axis). Plots of inhibitory GABA$_A$ and M$_2$ receptors are shown on the left, and plots of excitatory 5-HT$_{2A}$, M$_1$, kainate and AMPA receptors are presented in the middle and on the right. As expected, (see main text for description), correlations revealed no significant relationships.

Supplemental Figure S4. Association of M$_2$ receptor density and macroscale functional out-strength connectivity.

Figure shows a negative correlation (r=-0.76, p=0.0111), between regional M$_2$ density (on x-axis) and the level of strychnine-induced functional out strength (on y-axis), illustrating the influence of inhibitory M$_2$ receptors on the strength of cortico-cortical activity.

Table S2. Spearman Rank Correlations of regional receptor levels and functional connection strength.

	Out-strength		In-strength	
	R	p	R	p
AMPA	-0.1707	0.6372	0.0736	0.8298
5-HT$_{2A}$	0.5549	0.0959	-0.069	0.8403
Kainate	-0.2927	0.4118	-0.0782	0.8193
M$_1$	-0.7988	0.0056*	-0.2253	0.5054
M$_2$	-0.8659	0.0012*	-0.0598	0.8614
GABA$_A$	-0.7744	0.0085*	-0.2529	0.4531
ExIn ratio	0.7561	0.0114*	0.0966	0.7776

Chapter 6

Automatic extraction of the intracranial volume in fetal and neonatal MR scans using convolutional neural networks

N. Khalili, E. Turk, M.J.N.L. Benders, P. Moeskops, N.H.P. Claessens, R. de Heus, A. Franx, N. Wagenaar, J.M.P.J. Breur, M.A. Viergever, I. Îsgum

ABSTRACT

MR images of infants and fetuses allow noninvasive analysis of the brain. Quantitative analysis of brain development requires automatic brain tissue segmentation that is typically preceded by segmentation of the intracranial volume (ICV). Fast changes in the size and morphology of the developing brain, motion artifacts, and large variation in the field of view make ICV segmentation a challenging task. We propose an automatic method for segmentation of the ICV in fetal and neonatal MRI scans. The method was developed and tested with a di verse set of scans regarding image acquisition parameters (i.e., field strength, image acquisition plane, image resolution), infant age (23-45 weeks post menstrual age), and pathology (posthaemorrhagic ventricular dilatation, stroke, asphyxia, and Down syndrome). The results demonstrate that the method achieves accurate segmentation with a Dice coefficient (DC) ranging from 0.98-0.99 in neonatal and fetal scans regardless of image acquisition parameters or patient characteristics. Hence, the algorithm provides a generic tool for segmentation of the ICV that may be used as a preprocessing step for brain tissue segmentation in fetal and neonatal brain MR scans.

Keywords: Brain extraction, neonatal MRI, fetal MRI, skull stripping, brain segmentation, deep learning, intracranial volume segmentation

INTRODUCTION

Magnetic resonance imaging (MRI) is a clinically used non-invasive tool for monitoring brain development in fetuses and neonates. The analysis usually comprises of quantification of brain tissue volumes and cortical morphology to extract meaningful information for diagnosis or prognosis (Claessens et al., 2016; Drost et al., 2018; Dubois et al., 2007; Inder et al., 1999; Kersbergen et al., 2016; Moeskops et al., 2015, 2017). Automatic quantification of these indices requires segmentation of brain tissue classes. To allow dedicated analysis within the brain, automatic methods typically perform extraction of the intracranial volume (ICV) prior to further analysis (Išgum et al., 2015; Moeskops et al., 2016).

A number of methods for segmentation of ICV in adult MR scans have been applied to analysis of T1- and T2-weighted neonatal MR images (Eskildsen et al., 2012; Iglesias et al., 2011; Ségonne et al., 2004; Smith, 2002). Brain Extraction Tool (BET) Smith (2002) is a publicly available tool used as a preprocessing step by many automatic brain segmentation methods (Išgum et al., 2015). BET iteratively deforms a sphere to fit it on the brain surface using a geometric algorithm. Robust Brain Extraction tool (ROBEX) is another commonly used and publicly available tool for segmentation of the ICV in adult MR images (Iglesias et al., 2011). ROBEX first employs a Random Forest classifier to detect the brain boundary and thereafter uses a point distribution model that ensures a plau-

sible result. Furthermore, Brain Extraction based on non-local Segmentation Technique (BEaST) is a publicly available tool for ICV segmentation (Eskildsen et al., 2012). BEaST is a patch-based segmentation method exploiting the similarity between the patches in the region of interest and predefined patches in a library.

Because of the lack of publicly available tools developed for ICV segmentation of neonatal brain MRI, these methods designed to analyze brain MR scans of adults are frequently used to segment the ICV in neonatal scans. Consequently, they generally do not produce highly accurate results when applied to neonatal brain MR scans (Yamaguchi et al., 2010). Moreover, these methods typically fail when applied to fetal MR scans. Hence, several methods specifically designed to extract the ICV in MR scans of neonates have been proposed. Serag et al. (2016); Yamaguchi et al. (2010) proposed a method for segmentation of the ICV in brain MRI of neonates and children aged between 36 weeks post menstrual age (PMA) and 4 years. The method uses fuzzy logic and it is applicable to images without severe pathology acquired sagittally. In the first step the intensity distributions of white matter (WM), gray matter (GM), cerebrospinal fluid (CSF), fat, and other tissues visible in the scan are estimated using Bayesian classification and a Gaussian mixture model. Segmentation of brain tissue classes is thereafter performed by means of a fuzzy active surface model using distributions of WM, GM and CSF from the previous step. The qualitative evaluation of this method demonstrated improved performance over BET. Later, Mahapatra (2012) proposed a shape model with graph cuts for segmentation of the ICV in neonatal MRI. The shape model is generated by averaging manually labeled images which is afterwards used with graph cut for segmentation. This method was applied to term-born infants imaged at about three weeks of age. Serag et al. (2016) proposed an atlas-based segmentation of the ICV. To eliminate the need for representative training data i.e., data coming from the same distribution, atlases that are uniformly distributed were selected. The algorithm was applied to T1-weighted and T2-weighted MR scans without visible pathology of preterm infants scanned at term equivalent age. The method showed high segmentation accuracy and it outperformed publicly available tools such as BET and ROBEX.

Similar to methods dedicated to segmentation of the ICV in neonatal MR scans, a number of studies proposed segmentation of the ICV in fetal MRI. Anquez et al. (2009) proposed a method that first localizes the eyes and exploits this information to segment the ICV using a graph cut approach guided by shape, contrast, and biometrical priors. The method was applied to scans with unknown fetal orientation and the results demonstrated high segmentation accuracy. In recent years, convolutional neural networks (CNNs) have become the most popular method for automatic image segmentation in medical images (Litjens et al., 2017). Several studies investigated different CNN architectures for brain tissue segmentation (Akkus et al., 2017; Chen et al., 2018; Dolz et al., 2018; Makropoulos et al., 2018; Tu and Bai, 2010) and brain extraction (Dey and

Hong, 2018; Dolz et al., 2017; Kleesiek et al., 2016) in adult MRI. Wachinger et al. (2018) proposed a network that combines brain extraction and brain tissue segmentation.

A few studies used CNNs to segment ICV from fetal or neonatal MRI. Rajchl et al. (2017) proposed a weakly supervised deep learning approach for ICV segmentation in fetal MRI that combines a convolutional neural network and iterative graph optimization. The network was trained with bounding boxes around the brain as weak labels. The method was applied to fetal MR scans and achieved high segmentation accuracy. In another study, Rajchl et al. (2016) investigated the use of crowd sourcing platform for ICV segmentation of fetal MRI using convolutional neural network. Salehi et al. (2017) proposed an iterative deep learning segmentation method that uses U-net-like convolutional neural network (Auto-net). In this approach, the fetal brain is segmented from a localized bounding box which was defined manually using ITKSNAP (Yushkevich et al., 2006). In a subsequent study, Salehi et al. (2018) evaluated Auto-net on fetal MRI without any preprocessing steps such as defining a bounding box. The method was trained on a very large number of manually annotated fetal MRI and demonstrated accurate segmentation results in fetal scans. Recently, Khalili et al. (2017) proposed multi-scale convolutional neural network for ICV segmentation of fetal MRI.

Unlike methods performing ICV segmentation directly, several methods perform brain localization as a step prior to fetal ICV segmentation (Ison et al., 2012; Keraudren et al., 2013, 2014; Taimouri et al., 2015). Recently, Tourbier et al. (2017) proposed a pipeline that sequentially performs ICV localization, ICV segmentation and superresolution reconstruction in fetal MR scans. In this method a template matching approach, with age as prior knowledge, is used to segment the ICV in fetal MRI. A limitation of template-based techniques is that they are typically computationally more expensive than machine learning algorithms. In addition, they have a high chance of failure if representative age-matched templates are not available. Moreover, to segment brain tissue classes, methods employing brain localization require subsequent segmentation of the ICV.

All aforementioned methods were evaluated either on neonatal or fetal MR scans, without visible pathology. To the best of our knowledge, thus far no study proposed a generic method that performs segmentation of the ICV in neonatal and fetal MRI. In this study, we propose a method for automatic segmentation of the ICV in neonatal and fetal T2-weighted MR scans that is robust to imaging parameters (field strength, image acquisition plane, image resolution), and pathology and patient characteristics (posthaemorrhagic ventricular dilatation (PHVD), stroke, asphyxia, Down syndrome). The method employs a convolutional neural network with a U-net architecture (Ronneberger et al., 2015). The network was trained with a combination of fetal and preterm born neonatal scans acquired in axial, coronal and sagittal orientation. The age of patients at the time of scanning in the training set ranged from 23 to 35 weeks PMA. The method was eval-

uated using images of fetuses and infants between 23 weeks PMA and 3 months of age at the time of scanning, ranging from absence of visible pathology to presence of severe pathology such as stroke or PHVD. This work builds upon our preliminary study that described segmentation of the ICV in fetal MRI using a multi-scale convolutional neural network (Khalili et al., 2017).

MATERIALS

In this study diverse sets of fetal and neonatal T2-weighted MR scans were used. Fetal scans were acquired in axial, sagittal and coronal image planes and did not contain visible pathology. Neonatal images include scans of preterm and term-born infants. The scans were acquired in axial or coronal image planes, and include images without and with pathology. Examples of fetal and neonatal images included in the study are illustrated in **Figure 1**. As shown in the figure, fetal MRIs have a larger field of view that visualizes the entire fetus as well as parts of the maternal body. Moreover, we include scans which were acquired with different scanner-vendors (Philips, Siemens) and field strength (1,5T and 3T). The neuroimaging data were obtained as part of the clinical protocol, written informed consent for use of the clinically acquired data and approval of the experiments and methodology was waived by the institutional review board of the University Medical Center Utrecht, The Netherlands.
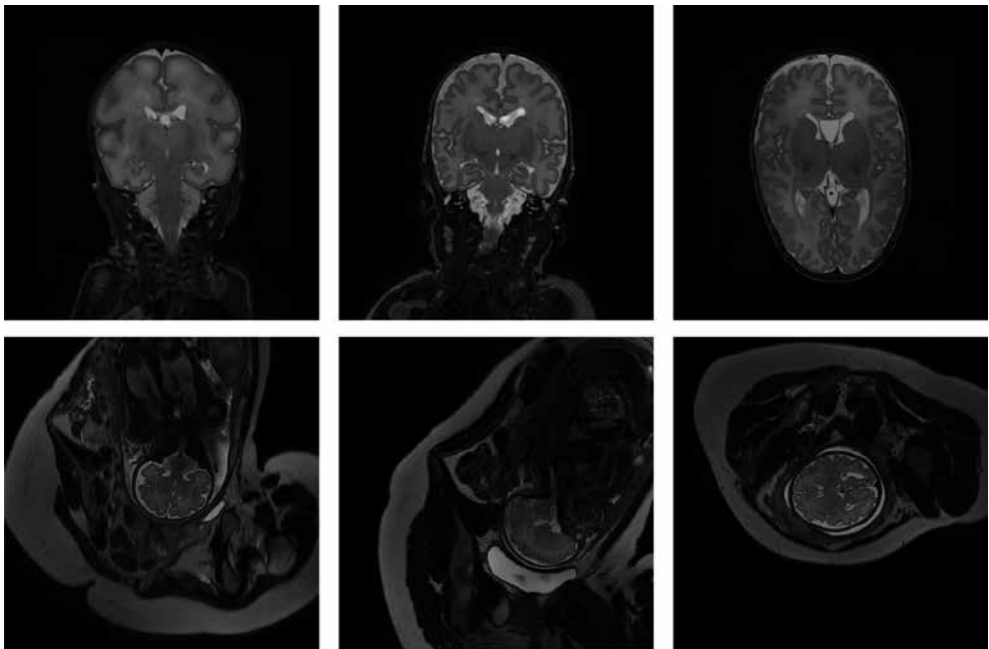
Fetal MRI
Two sets of fetal MR scans were used. The first set (Set 1) includes T2-weighted MR scans of fetuses (age: 23–35 weeks PMA). Images were acquired on a Philips Achieva 3T scanner at the University Medical Center (UMC) Utrecht, Utrecht, the Netherlands using a turbo fast spinecho sequence. The dataset contains 45 scans in total: 17 scans acquired in axial direction, 15 scans in coronal direction and 13 scans in sagittal direction. The images were acquired with voxel sizes of 1.25 X 1.25 X 2.5 mm3 and reconstructed to 0.7 X 0.7 X 1.25 mm3 with reconstruction matrix of 512 X 512 X 80. The scans were reconstructed by the scanner's algorithm and no further reconstruction (e.g., super-resolution processing) of the acquired images was performed. Furthermore, the proposed approach was applied to the 2D MRI slices without any prepossessing steps such as intensity inhomogeneity or motion correction.

The second set (Set 2) contains publicly available T2-weighted MR scans of 17 fetuses (age range: 29 ± 5 weeks PMA) which present a subset of scans described by Salehi et al. (2018). Scans were acquired on a 3T Siemens Skyra scanner at Boston Childeren's Hospital, Boston, US in axial, sagittal and coronal direction. The scans were acquired with voxel sizes of 1 X 1 X 2 mm3 with a reconstruction matrix of 256 X 256; the number of slices varied from 48 to 54.

The third set (Set 3) includes fetal T2-weighted MR scans acquired on Philips Achieva 1.5T scanner at the UMC Utrecht, Utrecht, the Netherlands. The dataset contains 18 scans: 6 scans were acquired in axial direction, 6 in coronal and 6 in sagittal direction. The scans were reconstructed to a voxel size of 1.18 X 1.18 X 1.25 mm3 and reconstruction matrix of 288 X 288 X 80.

Neonatal MRI
All neonatal scans were acquired on a Philips Achieva 3T scanner at the University Medical Center Utrecht, Utrecht, the Netherlands. We divided the data according to age of the infants at the time of acquisition, image acquisition plane, and presence and type of visible pathology. As shown in **Figure 1**, there are variations in the neonatal scans, especially between 30- and 40-weeks PMA, when the brains exhibit important structural development, including cortical folding, and changes in shape and volume.

Figure 1. Examples of preterm neonatal and fetal MR scans included in the study.
Top: coronal MRI acquired at 30 weeks PMA (left), coronal MRI acquired at 40 weeks PMA (middle), axial MRI acquired at 40 weeks PMA (right). Bottom: fetal MRI acquired in coronal (left), sagittal (middle) and axial (right) directions.

Preterm born infants without visible pathology
This set consists of three different subsets. The first one - 30-weeks coronal MRI - comprises 20 scans of preterm born infants imaged at 30 weeks PMA. The second set - 40-weeks coronal MRI - contains 17 scans of preterm born infants imaged at term equivalent age. The third set - 40-weeks axial MRI - contains 15 scans of preterm born infants imaged at term equivalent age. This set includes all 22 scans from the NeoBrainS12 challenge. Detailed data description is provided in a former study (Išgum et al., 2015).

Cross-sectional cohort
A set of 10 T2-weighted MRI scans were taken from a study investigating neonatal brain development that were made shortly after birth (29–43 weeks PMA) Keunen (2017). The scans were selected to include images of 10 neonates covering the complete available infant age range. Hence, this set includes preterm and full-term born infants.

Infants with congenital heart disease (CHD)
The set consists of 10 T2-weighted MRI scans of 10 patients with critical congenital heart disease (CHD). These infants were scanned before and after univentricular or biventricular cardiac repair using cardiopulmonary bypass within the first 30 days of life (Claessens et al., 2018). We selected 5 scans made before and 5 scans after surgery, of different patients. The images visualized WM lesions indicating mild to moderate brain injuries. However, the brain morphology was not significantly altered.

Infants with PHVD
A set of 10 T2-weigted MRI scans of 10 infants with germinal matrixintraventricular hemorrhage (GMH-IVH) and subsequent PHVD requiring intervention were selected randomly from a clinical study on PHVD infants (Brouwer et al., 2016). The infants included in this study received a ventricular shunt that is next to the substantial ventricular dilatation visible in MR images. An example of this is illustrated in Figure 2. Note that the ventricles are substantially enlarged typically resulting in a deformed brain shape. Moreover, these patients often have a temporary ventricular shunt which is visible in a number of scan slices.

Infants with stroke
This set consists of 10 T2-weighted MRI scans of 10 infants with arterial ischemic stroke (Benders et al., 2014). These neonates were treated with 1000 IU/kg rhEPO immediately after diagnosis. A secondary MRI was performed when the patients were 3 months of age. We included 5 primary and 5 secondary scans showing WM degradation. Primary and secondary scans were not showing the same patients. **Figure 2** illustrates an example of a secondary scan when the stroke-affected area is filled with CSF.

Infants with asphyxia

This set consists of 9 T2-weighted MRI scans of 9 patients with perinatal asphyxia (Alderliesten et al., 2017). These scans present diffuse hypoxic-ischemic injury demonstrated as hypointensities in the images that can be present throughout the brain tissue.

Infants with down syndrome (DS)

This set consist of 10 T2-weighted MRI scans imaging 10 infants with Down syndrome. In these patients, the brain volume is smaller because of delayed brain growth and gyrification compared with healthy infants (Coyle et al., 1986). **Figure 2** illustrates a typical example of a Down syndrome infant demonstrating abnormal shape of the head, the brain and delayed gyrifcation.
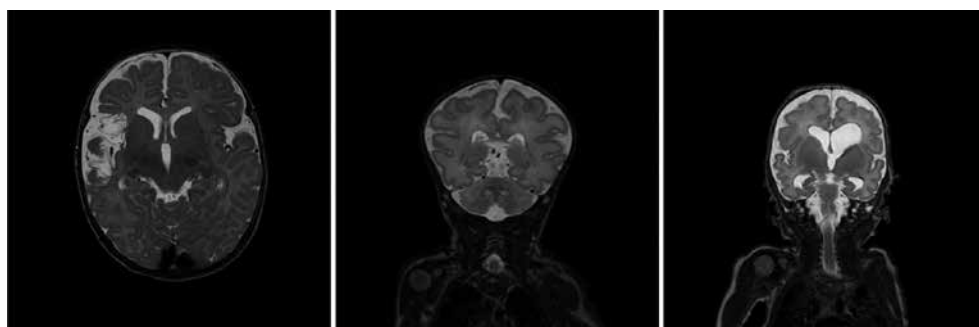
Figure 2. Examples of neonatal neural anomalies included in this study.
Figure shows T2-weighted MR scans of preterm born neonates with ischemic stroke (left), Down syndrome (middle), and PHVD (right).

Infant scans with artifacts

This set consist of 10 T2-weighted MRI scans acquired in coronal orientation from preterm born infants imaged at term equivalent age (40 weeks of post menstrual age). 5 scans contain intensity inhomogeneity artifacts and 5 scans show motion artifacts. Details on image acquisition parameters for all sets are listed in **Table 1**.

Reference standard

To establish the reference standard, manual segmentation of the ICV was performed by a trained medical student. Manual annotation was accomplished using in-house developed software by painting ICV voxels in each image slice. ICV included brain, cerebellum and extracranial cerebrospinal fluid. Skull and skin were excluded from the segmentation. We followed the definition of the eight tissue types provided by the NeoBrainS12 challenge for ending point of the brain stem (Išgum et al., 2015). Note that the reference

Table 1. Parameters of neonatal MRI scans.

	Nr	Age	Orientation	Matrix	Voxel size	Training / test
30-weeks coronal	20	30.7 ± 1.0	Cor	384 × 384 × 50	0.34 × 0.34 × 2.0	3 / 17
40-weeks coronal	15	41.2 ± 0.9	Cor	512 × 512 × 110	0.35 × 0.35 × 1.2	3 / 12
40-weeks axial	17	41.3 ± 0.8	Ax	512 × 512 × 50	0.35 × 0.35 × 2.0	3 / 14
Cross-sectional cohort	10	36.9 ± 5.0	Cor	512 × 512 × 110	0.35 × 0.35 × 1.2	0 / 10
Infants with CHD	10	41.0 ± 1.7	Cor	512 × 512 × 110	0.35 × 0.35 × 1.2	0 / 10
Infants with PHVD	10	41.0 ± 0.7	Cor	512 × 512 × 110	0.35 × 0.35 × 1.2	0 / 10
Infants with stroke	10	44.1 ± 6.2	Ax	512 × 512 × 50	0.35 × 0.35 × 2.0	0 / 10
Infants with asphyxia	9	39.2 ± 1.7	Ax	512 × 512 × 50	0.35 × 0.35 × 2.0	0 / 10
Infants with DS	10	37.9 ± 5.9	Cor and Ax	512 × 512 × 110	0.35 × 0.35 × 1.2	0 / 10
Scans with artifacts	10	41.12 ± 0.7	Cor	512 × 512 × 110	0.35 × 0.35 × 1.2	0/10

For each set the table lists total number of scans (Nr) in a set, average and standard deviation of the infant age at the time of scanning expressed in weeks of PMA (Age), image acquisition (Orientation) as axial (Ax) or coronal (Cor), reconstruction matrix (Matrix), reconstructed voxel sizes expressed in mm and the number of scans used in training and test set (Training/Test).

standard for Set 3 of fetal MRI and infants scans with artifacts was not available, hence the segmentation performance on these two sets was evaluated visually.
To estimate inter-observer variability, three slices of 7 scans were segmented by different observers. Two scans from 30 weeks coronal MRI, three scans from 40 weeks coronal MRI and two scans from 40 weeks axial MRI were selected. Furthermore, the slice representing the middle of the brain and subsequently, the first and last slice on which each tissue was visible were identified.

METHOD

Our aim is to train a single network that is able to perform segmentation of the ICV in a diverse set of scans where the diversity comprises differences in field of view, age of the scanned subjects, orientation of image acquisition, image resolution and presence of pathology. Our method employs a fully convolutional network (FCN) with U-net like architecture (Ronneberger et al., 2015) since such networks have demonstrated accurate segmentation performance in a number of different segmentation tasks (Litjens et al., 2017). We have used a smaller version of U-net to avoid over-fitting. The network has a contracting path and an expanding path. The contracting path consists of repeated 3
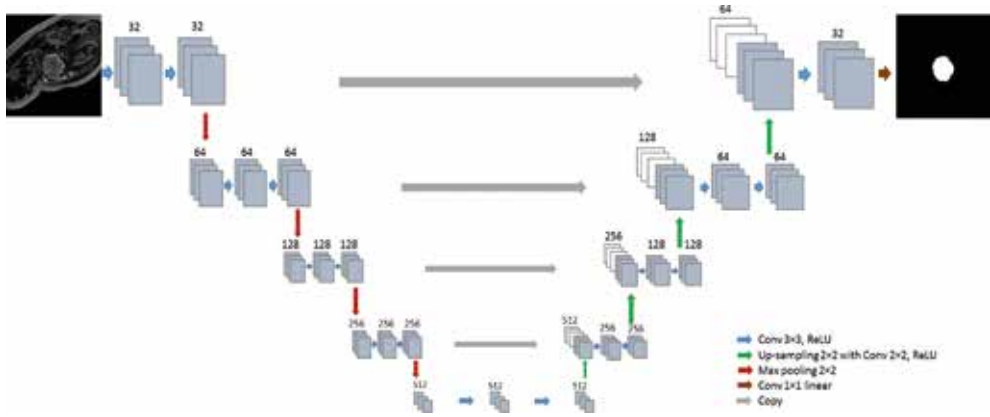
Figure 3. Network architecture: The network consists of a contracting path and an expanding path.
The contracting path consists of repeated convolution layers followed by max pooling, and the expansion path consists of convolution layers followed by up-sampling.

X 3 zero padded convolutions where each convolution is followed by a rectified linear unit (ReLU). 2 X 2 max pooling layers with stride 2 downsample the feature maps. The number of the feature maps doubles after every two convolutional layers. In the expanding path, up-sampling with stride 2 is followed by a 2 X 2 transposed convolution which halves the number of feature channels. The resulting feature maps were concatenated with the corresponding feature map of the contracting path and convolved by two 3 X 3 convolutional layers followed by ReLU. At the final layer, a 1 X 1 convolution map each component of feature vector to the desired number of classes. A softmax function is applied in the last layer to classify ICV and background. As a loss function, cross-entropy between the output layer and the manual segmentation reference is used. For optimization, Nesterov Adam optimizer is applied (Dozat, 2016; Kingma and Adam, 2015). In order to increase the mean learning rate, batch normalization (Ioffe and Szegedy, 2015) is used after each convolutional layer (Convolution, Batch Normalization, ReLU) Ioffe and Szegedy (2015). The learning rate of Adam optimization is set to 0.0001. The hyper-parameters were tuned using cross-validation on the training set. The training was stopped after 300 epochs when the loss function became stable. The network is trained with 2D slices and batch size is 30 for each iteration. The image intensity was normalized to the range [0, 1023] before feeding them to the network. Data augmentation was applied during the training by random flipping and rotation of 2D slices. The rotations ranged between 0 to 360 degrees to mimic fetal brain angle variations. As all image intensities were normalized between [0, 1023], we did not vary image intensities nor the contrast as an augmentation. We have implemented the network in Keras, an open-source neural-network library written in Python (Chollet et al., 2015).

Given that the network performs voxel classification, ICV segmentation may result in small isolated clusters of voxels outside the ICV. To prevent this, 3D connected components smaller than 3 cm3 are discarded. Similarly, possibly remaining holes in the binary mask automatically are filled.

Evaluation

The automatic ICV segmentations were evaluated in 3D by means of the Dice coefficient, the mean surface distance and the Hausdorff distance (Taha and Hanbury, 2015) between the manual and automatic segmentations per image per set.

Table 2.

	Neonatal and Fetal			Fetal			Representative		
	DC	MSD	HD	DC	MSD	HD	DC	MSD	HD
Set 1	0.976	0.34	**10.58**	**0.980**	**0.32**	16.89	0.978	0.36	15.45

	Neonatal and Fetal			Neonatal			Representative		
	DC	MSD	HD	DC	MSD	HD	DC	MSD	HD
30-weeks coronal	**0.993**	**0.11**	**6.19**	0.988	0.18	7.87	0.992	0.12	
40-weeks coronal	0.993	0.18	**7.98**	**0.994**	**0.14**	8.32	0.993	0.16	9.64
40-weeks axial	**0.988**	**0.22**	**7.60**	0.988	0.24	7.67	0.987	0.44	25.89
Cross-sectional cohort	0.987	0.35	11.13	0.990	**0.19**	**8.88**	**0.991**	0.22	13.94
Infants with CHD	0.987	0.53	17.19	**0.990**	**0.19**	**8.57**	0.985	0.64	
Infants with PHVD	0.987	**0.29**	**14.67**	**0.988**	0.31	15.89	0.986	0.35	17.34
Infants with stroke	0.987	**0.30**	14.68	**0.988**	0.46	**11.09**	0.984	0.58	19.05
Infants with asphyxia	**0.980**	**0.34**	**10.58**	0.970	0.62	15.54	0.963	0.80	16.41
Infants with DS	0.982	0.46	**12.52**	**0.983**	**0.38**	14.36	0.983	0.58	25.87

Performance of the automatic segmentation expressed by the average Dice coefficient (DC), mean surface distance (MSD) in mm, and Hausdorff distance (HD) in mm. Columns show experiments where the network was trained with: 1) a combination of fetal and neonatal MRI (Fetal and Neonatal) 2) fetal MRI when the test images were from fetuses (Fetal) or neonatal MRI when test images were from neonates (Neonatal) 3) Only a representative set of images. For each test set best results among the three experiments are indicated in bold.

EXPERIMENTS AND RESULTS

Training with joint neonatal and fetal scans

We performed segmentation in fetal and neonatal MRI scans using a single trained network. The training set consisted of 21 fetal and 9 neonatal scans. Fetal scans in the training contained 7 scans acquired in axial, 7 scans acquired in coronal and 7 scans acquired in sagittal imaging orientations (21 scans) of 7 patients from Set 1. Neonatal scans were from preterm born infants without visible pathology. Neonatal scans included in the training consisted of 3 coronal scans acquired at 30 weeks PMA, 3 coronal scans acquired at 40 weeks PMA, and 3 axial scans acquired at 40 weeks PMA. Note that the training and test set were separated per subject. During the training, only
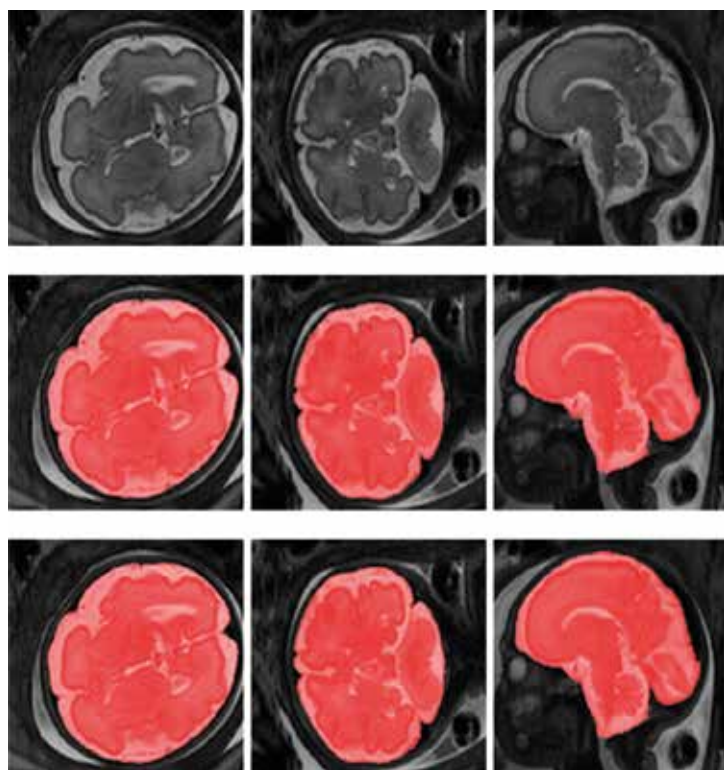
Figure 4. ICV segmentation of fetal T2.

Figure shows examples of ICV segmentation in slices from fetal scans acquired in axial (left), coronal (middle) and sagittal (right) image planes. The images are selected from the test set. A slice from T2-weighted image (top); segmentation achieved by the proposed method trained with a combination of neonatal and fetal MRI (middle); manual segmentation (bottom).

in joint training scenario, each batch was balanced between fetal scans, 30 weeks coronal neonatal, 40 weeks axial neonatal and 40 weeks coronal neonatal scans.

The method was tested with the remaining 24 fetal scans from Set 1 that were acquired in axial, coronal and sagittal orientation, and neonatal scans of the remaining 110 patients. The obtained quantitative results ar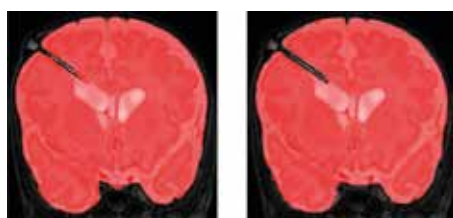e listed in **Table 2** (first three columns). **Figure 4** illustrates examples of the obtained ICV segmentations in images acquired in

Figure 7. Segmentation of MRI with shunt.
Example of ICV segmentation in one test neonate with PHVD on the left compared with manual segmentation on the right. The infants received a temporary ventricular shunt that is visible in some slices. The images were selected from the test set.

Figure 5. Examples of ICV segmentation in a fetal scan acquired in sagittal plane.
A slice from T2-weighted fetal MRI scan (top row), segmentation obtained with joint training (middle row) and manual segmentation (bottom row). The first column illustrates the segmentation in the in-plane view. Second and third columns illustrated out-of-plane views. The slices were selected from the test set.

Figure 8. Segmentation of different cerebellar volumes.
A slice from a scan of infant with PHVD (left) where the joint training undersegmented cerebellum (middle) compared with reference annotation (right). The cerebellar volume, shape and image intensity are typically different in infants with PHVD from infants without visible pathology. The images were selected from the test set.
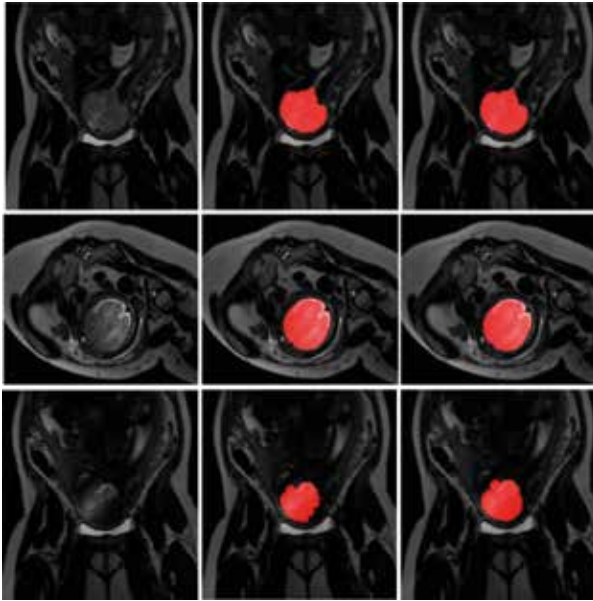
Figure 6. Examples of ICV segmentation in slices from fetal scans that visualized intensity inhomogeneity.

A slice from T2-weighted image (left); segmentation achieved by the proposed method trained with a combination of neonatal and fetal MRI (middle) and manual segmentation (right). The images were selected from the test set.

axial, coronal and sagittal image planes. **Figure 5** illustrates ICV segmentation results in one scan acquired in sagittal imaging plane. The segmentation results are shown in the acquisition plane as well as in planes perpendicular to the acquisition plane. Furthermore, **Figure 6** illustrates examples of the ICV segmentations in slices with intensity inhomogeneity. Moreover, **Figure 7** shows an example of ICV segmentation in a neonate with PHVD. The automatic segmentation excluded the inserted shunt from the brain mask even though PHVD scans were not included in the training data. **Figure 8** illustrates another example of ICV segmentation in a neonate with PHVD where the cerebellum was undersegmented. It may be observed that in this case cerebellum has voxels of lower intensity than images without visible pathology.

Training with neonatal or fetal scans
Manual annotation in a large set of scans is time-consuming and expensive. Hence, to estimate whether the method performs better on forms better on neonatal images when trained with neonatal images only, additional experiments were performed. For this, two separate networks were trained. The first network was trained using only fetal images.

This set included scans of 7 fetuses with images acquired in axial, coronal and sagittal directions. The second network was trained using only neonatal images. This training set included images of infants scanned at 30- and 40- weeks PMA acquired in axial and coronal directions. In both experiments, the training images were the same training images that were used in the experiment described in Section 4 A when the fetal and neonatal training images were used together in the training. No other changes in the network architecture or training procedure were applied. The obtained results are listed in **Table 2** (middle three columns).

Training with representative scans
To evaluate whether it might be advantageous to train the network using representative data only, three instances of the original network were trained. One instance was trained and tested with scans of neonates acquired at 30 weeks PMA coronal, another instance was trained and tested with scans of neonates acquired at 40 weeks PMA coronal, and last instance was trained and tested with scan of neonates acquired at 40 weeks PMA axial. Training images represent subsets of scans used in the experiment where all training data was mixed. The obtained results are listed in **Table 2** (last three columns).

Table 6.

	First Observer			Second Observer		
	DC	MSD	HD	DC	MSD	HD
30-weeks coronal	0.993	0.656	11.52	0.983	1.660	16.92
40-weeks coronal	0.992	0.891	9.231	0.994	0.474	6.332

Evaluating joint training segmentation performance with manual segmentation obtained by two different observers. The results are expressed in terms of Dice coefficient (DC), Hausdorff distance (HD) and mean surface distance (MSD). The HD and MSD are expressed in mm. Note that the evaluation was performed in 3 slices in 7 scans, totalling to 21 slices. The segmentations are compared with the segmentations of the first observer in the same slices.

Second observer evaluation
To evaluate inter-observer variability, we obtained second observer manual annotations for small subset of neonatal data. The evaluation was performed on 3 slices of 7 scans, i.e., 21 slices in total and the results were compared to corresponding slices annotated by the first observer. The results are listed in **Table 6.**

Table 5.

	Joint training			BET		
	DC	MSD	HD	DC	MSD	HD
30-weeks coronal	0.99	0.11	6.19	0.91	2.05	24.92
40-weeks coronal	0.99	0.18	7.98	0.94	1.92	27.91
40-weeks axial	0.99	0.22	7.60	0.94	1.39	34.63
Cross-sectional cohort	0.99	0.35	11.13	0.93	1.83	26.76
Infants with CHD	0.99	0.53	17.19	0.95	2.36	36.46
Infants with PHVD	0.99	0.29	14.67	0.94	1.72	24.16
Infants with stroke	0.99	0.30	14.68	0.95	1.33	30.80
Infants with asphyxia	0.98	0.34	10.58	0.95	1.33	32.88
Infants with DS	0.98	0.46	12.52	0.95	1.43	14.69

Performance of the joint training using fetal and neonatal scans for ICV segmentation compared with BET. The results are expressed using the average Dice coefficient (DC), mean surface distance (MSD) in mm, and Hausdorff distance (HD) in mm.
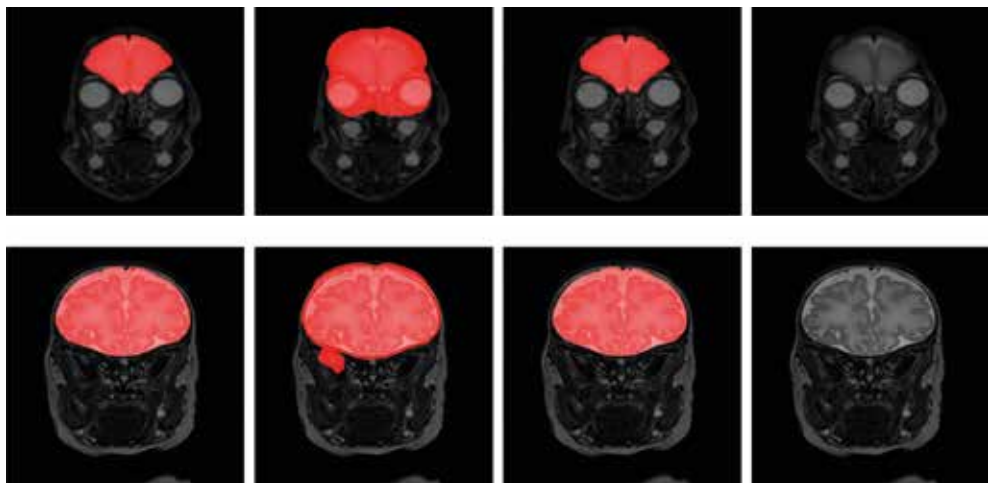
Figure 10. Different segmentation methods.
Examples of ICV segmentation in neonates acquired at 30 weeks PMA (top row) and 40 weeks PMA (bottom row). Results of the joint training (first column), the result obtained with BET (second column), manual annotation (third column) and the original T2-weighted MRI (last column). The images were selected from the test set.

Comparison with state-of-the art methods

The performance of the proposed method was compared with publicly available ICV segmentation tools. Given that BET is frequently used to segment the ICV in premature neonatal images (Moeskops et al., 2016), we have applied it to segment images in our test set. The fractional intensity threshold (-f) is empirically set to 0.3. The obtained results are presented in **Table 5.** They demonstrate that BET achieved better performance in neonatal MRI acquired at 40 weeks PMA than in neonatal MRI acquired at 30 weeks PMA. **Figure 10** shows segmentations obtained with BET and joint training in a slice from a scan acquired at 30 weeks PMA and one acquired at 40 weeks PMA.

Both slices illustrate oversegmentation of the ICV along the whole boundary, which is a frequent error of the BET tool visible in our test set. Quantitative results listed in **Table 5** show that joint training consistently achieved higher DC and lower HD and MSD than BET.

To investigate robustness of our method to variation in scanner characteristics and patient population, the joint training model was evaluated using publicly available fetal MRI scans from another hospital (Set 2). The results were compared with a publicly available Autonet (Salehi et al., 2018) model trained on a much larger set of representative fetal scans from the same hospital. Even though, U-net or any fully convolutional neural network can take any arbitrary image size but the segmentation performance will likely drop if the images in the training and test set do not have the same resolution. Given that scans in Set 2 have different voxel sizes than our fetal images (Set 1) used
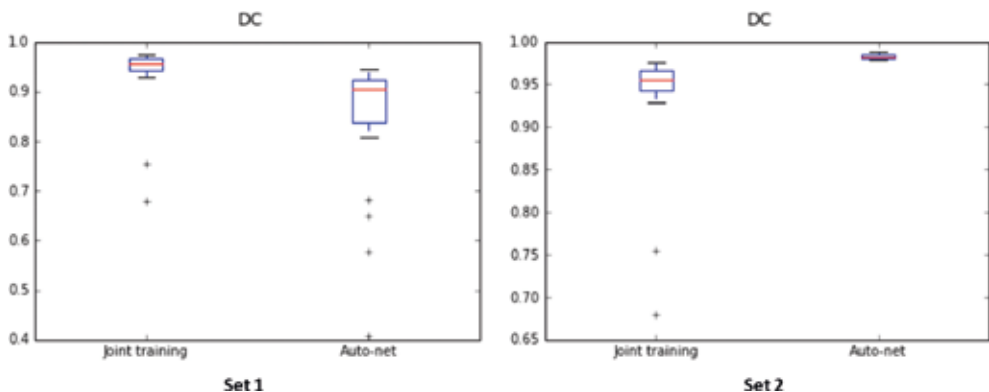
Figure 9. Dice coefficients.

Figure displays dice coefficients achieved by the proposed method using joint training with 21 fetal and 9 neonatal MRI scans, and by the publicly provided Auto-net trained with 260 fetal MRI scans. Both methods were tested on Set 1 (left) and Set 2 (right).

Table 3.

|	DC	MSD	HD
Joint training	0.94 ± 0.02	1.7 ± 0.72	34.5 ± 16.11
Auto-net	0.98 ± 0.01	0.2 ± 0.04	10.1 ± 5.45

Performance of the proposed method using joint training with 21 fetal and 9 neonatal MRI scans, and performance of the publicly provided Auto-net trained with 260 fetal MRI scans. Both methods were tested on publicly available fetal scans from Set 2. The results are expressed by the average Dice coefficient (DC), mean surface distance (MSD) in mm, and Hausdorff distance (HD) in mm.

Table 4.

	DC	MSD	HD
Joint training	0.98 ± 0.02	0.3 ± 0.36	10.6 ± 5.73

Performance of the proposed method using joint training with 21 fetal and 9 neonatal MRI scans and performance of the publicly available Auto-net trained with 260 MRI scans. Both methods were tested with fetal images from Set 1. The results are expressed by average Dice coefficient (DC), Mean surface distance (MSD) in mm, and Hausdorff distance (HD) in mm.

in the training, prior to analysis scans from Set 2 were resampled to the resolution of our training images. Furthermore, the images were normalized between [0, 1023]. All obtained results are listed in **Table 3** and shown in **Figure 9**. Note that this model was only trained on fetal MRI and training data did not include any neonatal MRI data. Therefore, the evaluation was performed on fetal MRI only.

In addition, Auto-net was evaluated on fetal images from our hospital (Set 1). Quantitative results are listed in **Table 4.** As in the previous experiment scans from Set 1 were resampled to the same resolution of the images used to train Auto-net (Set 2). Furthermore, the scans were normalized between [0, 1023]. **Figure 9** illustrates the segmentation performance in a box plot. Note that even though the scans were resampled to the same resolution in both experiments, the images had different field of view.

Evaluation on scans acquired with 1.5 Tesla scanner
To demonstrate the performance of the proposed method on images acquired with a scanner exploiting a different field strength, the joint training model was evaluated
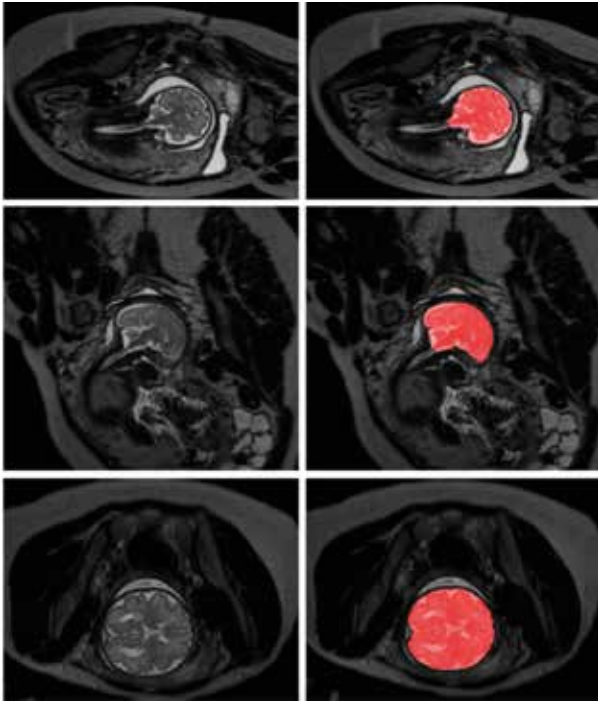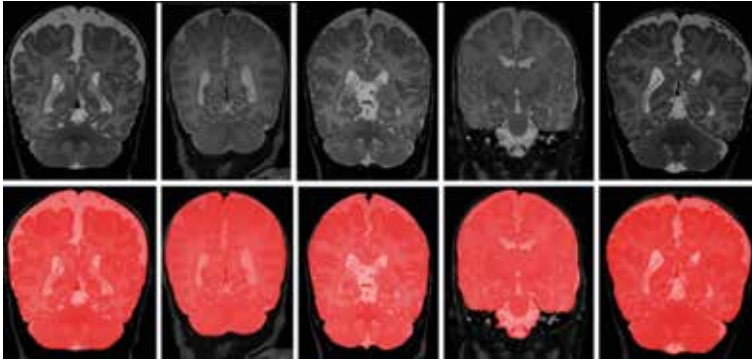
Examples of ICV segmentation in slices from fetal scans acquired with 1.5 Tesla scanner in coronal (top), sagittal (middle) and axial (bottom) image planes. A slice from T2-weighted image (left) and segmentation achieved by the proposed method trained with a combination of neonatal and fetal MRIs (right).

on fetal MRI scans (Set 3) acquired with 1.5 Tesla scanner. We illustrate segmentation results in the three scans without reference standard in **Figure 11.** Visual inspection of the results in these scans reveals that the joint training model produced accurate ICV segmentations in scans with different field strength, although the model was not trained with such scans.

Evaluation on scans with artifacts

To demonstrate the performance of proposed method on scans with intensity inhomogeneity and motion artifacts, the joint training model was evaluated on 5 neonatal scans with intensity inhomogeneity and 5 neonatal scans with motion artifacts. We illustrate segmentation results in the five scans with intensity inhomogeneity in **Figure 12** and five scans with motion artifacts in **Figure 13.** Visual inspection of the results in these scans reveals that the joint training model produced accurate ICV segmentation in scans with motion artifacts and intensity inhomogeneity.

Figure 12.

Examples of ICV segmentation in 5 neonatal MR scans with intensity inhomogeneity artifacts. A slice from T2-weighted fetal MRI scan (first row); segmentation obtained with joint training (second row).
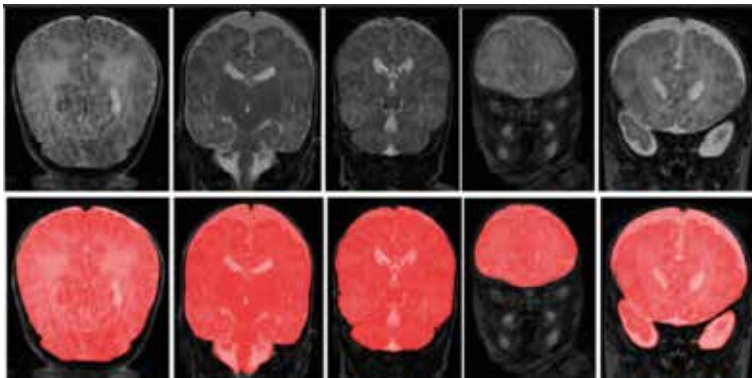
Figure 13.

Examples of ICV segmentation in 5 neonatal MR scans with motion artifacts. A slice from T2-weighted fetal MRI scan (first row); segmentation obtained with joint training (second row).

Second observer evaluation

Manual annotation in a large set of scans is time-consuming and expensive. Hence, to estimate inter-observer variability, second observer performed manual annotations in a small subset of neonatal data. The evaluation was performed on 3 slices of 7 scans, totally in 21 slices. These segmentations were compared with the segmentations of the first observer in the same slices. The results are listed in **Table 6.**

DISCUSSION

An automatic method for segmentation of the ICV in fetal and neonatal brain MR scans was presented. The proposed method employs a fully convolutional network with U-net architecture. It was trained by using a combination of neonatal and fetal MRI and the results demonstrate accurate segmentation of ICV in fetal and neonatal MR scans regardless the orientation of the image acquisition, the age of infants at the time of scanning or the presence of pathology. Unlike previous ICV segmentation methods developed for fetal or neonatal MRI (Anquez et al., 2009; Keraudren et al., 2013; Taimouri et al., 2015), the proposed method does not require brain localization or prior information about the patient age or expected anatomy.

In this study, 2D analysis was applied. Even though 3D analysis regularly allows better exploitation of the available information compared to 2D analysis, 2D analysis was advantageous as it minimized the risk of overfitting and allowed analysis of scans with large slice thickness that led to substantial changes in the anatomy (Havaei et al., 2017; Moeskops et al., 2016; Wolterink et al., 2016). Moreover, 2D analysis was less influenced by missing and corrupted slices resulting from continuous fetal motion.

Generating manual segmentation is a cumbersome and extremely time-consuming task. The results illustrate that with a small number of available manual segmentation used for training, the network achieves a competitive and robust results in a large test set. Using semi-automatic segmentation comprised of automatic pre-segmentation and subsequent manual correction to generate reference standard for training purposes could make the process faster. Availability of a large training set could offer possibility to investigate the impact of the size of the training set on the method performance as well as research towards the requirements regarding characteristics of the training set for employment in the MRIs presenting pathology or artifacts. This may be interesting direction for future research.

Although the network was trained with images containing no visible pathology, the evaluation was performed on a large and diverse set of scans, which includes scans with pathology. The segmentation results in neonatal scans with or without lesions are comparable. Note that large lesions in the brain strongly affecting tissue appearance (infants with stroke), morphological changes (infants with Down syndrome and PHVD), and presence of implants (shunts) that were mostly excluded (PHVD) (see **Figure 7**).

We evaluated the proposed method on scans with artifacts such as intensity inhomogeneity and motion artifacts. The visual inspection demonstrates that even though scans with artifacts were not in the training, the proposed approach is able to segment ICV. Furthermore, we investigated whether it is feasible to train a single instance of the

network applicable to both fetal and neonatal scans, or whether better performance can be achieved by training a separate network using only fetal or only neonatal scans. The results show that in both cases DC ranges from 0.98 to 0.99. Moreover, we compared performance using joint training with fetal and neonatal scans against training using representative scans only. The results demonstrate that in both cases accurate segmentation was achieved when evaluating the overlap between automatic and reference segmentations (0.98 to 0.99 Dice coefficient). The results also demonstrate that training with diverse images using fetal and neonatal scans reduced false positive voxels far from the intracranial volume surface leading to lower Hausdorff distances and mean surface distances in all sets. Training with both fetal and neonatal scans indicated the most noticeable improvement in infants with asphyxia. Despite the differences in image acquisition, image orientation, and brain morphology, fetal and neonatal scans share common features that improve the ability of the network to generalize, making it more robust and compensating for the lack of representative data.

To investigate robustness of the proposed method to variations in scanner characteristics and patient population, the method was evaluated using publicly available fetal MRI scans from another hospital (Set 2). The results were compared with a publicly available Auto-net (Salehi et al., 2018) model trained on a much larger set of representative fetal scans from the same hospital. The results show that our model did not outperform the dedicated data-specific approach. Nevertheless, it achieved DC, MSD and HD of 0.94, 1.7 and 34.5 respectively. Similarly, we evaluated Auto-net on fetal scans from our hospital (Set 1). The results demonstrate that the proposed method trained on representative fetal scans from our hospital outperformed Auto-net trained on different data. The two experiments indicate that reasonable performance can be achieved using different scans but also underline the importance of training with representative data. In future research, investigating interpretability of model using saliency map (Simonyan et al., 2013) can demonstrate a better understanding of limitations in network performance. In addition, the proposed method was compared with the publicly available and widely used BET for the segmentation of neonatal MRIs. Although BET is known to achieve accurate segmentation of ICV in adults, our results demonstrate that it is less suited for neonatal brain. Our dedicated method clearly outperformed BET.

CONCLUSION

To conclude, this study presented a method for automatic ICV segmentation in neonatal and fetal MRI. Despite the variability among the evaluated scans, the method obtained accurate segmentation results in both fetal and neonatal MR scans. Hence, the algorithm provides a generic tool for segmentation of the ICV that may be used as a preprocessing step for brain tissue segmentation in fetal and neonatal brain MR scans.

REFERENCES

Akkus, Z., Galimzianova, A., Hoogi, A., Rubin, D.L., Erickson, B.J., 2017. Deep learning for brain MRI segmentation: state of the art and future directions. J. Digit. Imaging 30 (4), 449–459.

Alderliesten, T., de Vries, L.S., Staats, L., van Haastert, I.C., Weeke, L., Benders, M.J., Koopman-Esseboom, C., Groenendaal, F., 2017. MRI and spectroscopy in (near) term neonates with perinatal asphyxia and therapeutic hypothermia. Arch. Dis. Child. Fetal Neonatal Edition 102 (2), F147–F152.

Anquez, J., Angelini, E.D., Bloch, I., 2009. Automatic segmentation of head structures on fetal MRI. The IEEE International Symposium on Biomedical Imaging (ISBI). IEEE, pp. 109–112.

Benders, M.J., van der Aa, N.E., Roks, M., van Straaten, H.L., Isgum, I., Viergever, M.A., Groenendaal, F., de Vries, L.S., van Bel, F., 2014. Feasibility and safety of erythropoietin for neuroprotection after perinatal arterial ischemic stroke. J. Pediatr. 164 (3), 481–486.

Brouwer, M.J., De Vries, L.S., Kersbergen, K.J., Van Der Aa, N.E., Brouwer, A.J., Viergever, M.A., Išgum, I., Han, K.S., Groenendaal. F., Benders, M.J., 2016. Effects of posthemorrhagic ventricular dilatation in the preterm infant on brain volumes and white matter diffusion variables at term-equivalent age. J. Pediatr. 168, 41–49.

Chen, H., Dou, Q., Yu, L., Qin, J., Heng, P.-A., 2018. Voxresnet: deep voxelwise residual networks for brain segmentation from 3D MR images. Neuroimage 170, 446–455.

Chollet, F., et al., 2015. Keras. https://keras.io.

Claessens, N.H., Algra, S.O., Jansen, N.J., Groenendaal, F., de Wit, E., Wilbrink, A.A., Haas, F., Schouten, A.N., Nievelstein, R.A., Benders, M.J., et al., 2018. Clinical and neuroimaging characteristics of cerebral sinovenous thrombosis in neonates undergoing cardiac surgery. J. Thorac. Cardiovasc. Surg. 1150–1158.

Claessens, N.H., Moeskops, P., Buchmann, A., Latal, B., Knirsch, W., Scheer, I., Išgum, I., De Vries, L.S., Benders, M.J., Von Rhein, M., 2016. Delayed cortical gray matter development in neonates with severe congenital heart disease. Pediatr. Res. 80 (5), 668–674.

Coyle, J.T., Oster-Granite, M., Gearhart, J.D., 1986. The neurobiologie consequences of down syndrome. Brain Res. Bull. 16 (6), 773–787.

Dey, R., Hong, Y., 2018. Compnet: complementary segmentation network for brain MRI extraction. arXiv preprint arXiv:1804.00521.

Dolz, J., Desrosiers, C., Ayed, I.B., 2018. 3D fully convolutional networks for subcortical segmentation in mri: a large-scale study. Neuroimage 170, 456–470.

Dolz, J., Desrosiers, C., Wang, L., Yuan, J., Shen, D., Ayed, I. B., 2017. Deep CNN ensembles and suggestive annotations for infant brain MRI segmentation. arXiv preprint arXiv:1712.05319.

Dozat, T., 2016. Incorporating nesterov momentum into Adam. 4th International Conference on Learning Representations, Workshop.

Drost, F.J., Keunen, K., Moeskops, P., Claessens, N.H., van Kalken, F., Išgum, I., Voskuil- Kerkhof, E.S., Groenendaal, F., de Vries, L.S., Benders, M.J., et al., 2018. Severe retinopathy of prematurity is associated with reduced cerebellar and brainstem volumes at term and neurodevelopmental deficits at two years. Pediatr. Res. 818–824.

Dubois, J., Benders, M., Cachia, A., Lazeyras, F., Ha-Vinh Leuchter, R., Sizonenko, S., Borradori-Tolsa, C., Mangin, J., Hüppi, P.S., 2007. Mapping the early cortical folding process in the preterm newborn brain. Cereb. Cortex 18 (6), 1444–1454.

Eskildsen, S.F., Coup., P., Fonov, V., Manj.n, J.V., Leung, K.K., Guizard, N., Wassef, S.N., .stergaard, L.R., Collins, D.L., The Alzheimer's Disease Neuroimaging Initiative, 2012. Beast: brain extraction based on nonlocal segmentation technique. Neuroimage 59 (3), 2362–2373.

Havaei, M., Davy, A., Warde-Farley, D., Biard, A., Courville, A., Bengio, Y., Pal, C., Jodoin, P.-M., Larochelle, H., 2017. Brain tumor segmentation with deep neural networks. Med. Image Anal. 35, 18–31.

Iglesias, J.E., Liu, C.-Y., Thompson, P.M., Tu, Z., 2011. Robust brain extraction across datasets and comparison with publicly available methods. IEEE Trans. Med. Imaging 30 (9), 1617–1634.

Inder, T.E., Huppi, P.S., Warfield, S., Kikinis, R., Zientara, G.P., Barnes, P.D., Jolesz, F., Volpe, J.J., 1999. Periventricular white matter injury in the premature infant is followed by reduced cerebral cortical gray matter volume at term. Ann. Neurol. 46 (5), 755–760.

Ioffe, S., Szegedy, C., 2015. Batch normalization: accelerating deep network training by reducing internal covariate shift. The 32nd International Conference on Machine Learning (ICML-15). pp. 448–456.

Išgum, I., Benders, M.J., Avants, B., Cardoso, M.J., Counsell, S.J., Gomez, E.F., Gui, L., Hüppi, P.S., Kersbergen, K.J., Makropoulos, A., et al., 2015. Evaluation of automatic neonatal brain segmentation algorithms: the NeoBrainS12 challenge. Med. Image Anal. 20 (1), 135–151.

Ison, M., Donner, R., Dittrich, E., Kasprian, G., Prayer, D., Langs, G., 2012. Fully automated brain

extraction and orientation in raw fetal MRI. Workshop on Paediatric and Perinatal Imaging, MICCAI. pp. 17–24.

Keraudren, K., Kuklisova-Murgasova, M., Kyriakopoulou, V., Malamateniou, C., Rutherford, M.A., Kainz, B., Hajnal, J.V., Rueckert, D., 2014. Automated fetal brain segmentation from 2D MRI slices for motion correction. Neuroimage 101, 633–643.

Keraudren, K., Kyriakopoulou, V., Rutherford, M., Hajnal, J.V., Rueckert, D., 2013. Localisation of the brain in fetal MRI using bundled sift features. MICCAI, LNCS. Springer, pp. 582–589.

Kersbergen, K.J., Leroy, F., Išgum, I., Groenendaal, F., de Vries, L.S., Claessens, N.H., van Haastert, I.C., Moeskops, P., Fischer, C., Mangin, J.-F., et al., 2016. Relation between clinical risk factors, early cortical changes, and neurodevelopmental outcome in preterm infants. Neuroimage 142, 301–310.

Keunen, K., 2017. The Neonatal Brain: Early Connectome Development and Childhood Cognition. Utrecht University Ph.D. thesis.

Khalili, N., Moeskops, P., Claessens, N., Scherpenzeel, S., Turk, E., de Heus, R., Benders, M., Viergever, M., Pluim, J., Išgum, I., 2017. Automatic segmentation of the intracranial volume in fetal MR images. Fetal, Infant and Ophthalmic Medical Image Analysis. pp. 42–51.

Kingma, D., Adam, J.B., 2015. A method for stochastic optimisation. International Conference on Learning Representations.

Kleesiek, J., Urban, G., Hubert, A., Schwarz, D., Maier-Hein, K., Bendszus, M., Biller, A., 2016. Deep MRI brain extraction: a 3D convolutional neural network for skull stripping. Neuroimage 129, 460–469.

Litjens, G., Kooi, T., Bejnordi, B.E., Setio, A.A.A., Ciompi, F., Ghafoorian, M., van der Laak, J.A., van Ginneken, B., S.nchez, C.I., 2017. A survey on deep learning in medical image analysis. Med. Image Anal. 42, 60–88.

Mahapatra, D., 2012. Skull stripping of neonatal brain MRI: using prior shape information with graph cuts. J. Digit. Imaging 25 (6), 802–814.

Makropoulos, A., Counsell, S.J., Rueckert, D., 2018. A review on automatic fetal and neonatal brain MRI segmentation. Neuroimage 170, 231–248.

Moeskops, P., Benders, M.J., Kersbergen, K.J., Groenendaal, F., de Vries, L.S., Viergever, M.A., Išgum, I., 2015. Development of cortical morphology evaluated with longitudinal MR brain images of preterm infants. PLoS One 10 (7), e0131552.

Moeskops, P., Išgum, I., Keunen, K., Claessens, N.H., Haastert, I.C., Groenendaal, F., Vries, L.S., Viergever, M.A., Benders, M.J., 2017. Prediction of cognitive and motor outcome of preterm infants based on automatic quantitative descriptors from neonatal brain images. Sci. Rep. 7 (1), 2163.

Moeskops, P., Viergever, M.A., Mendrik, A.M., de Vries, L.S., Benders, M.J., Išgum, I., 2016. Automatic segmentation of MR brain images with a convolutional neural network. IEEE Trans. Med. Imaging 35 (5), 1252–1261.

Rajchl, M., Lee, M.C., Oktay, O., Kamnitsas, K., Passerat-Palmbach, J., Bai, W., Damodaram, M., Rutherford, M.A., Hajnal, J.V., Kainz, B., et al., 2017. Deepcut: object segmentation from bounding box annotations using convolutional neural networks. IEEE Trans. Med. Imaging 36 (2), 674–683.

Rajchl, M., Lee, M. C., Schrans, F., Davidson, A., Passerat-Palmbach, J., Tarroni, G., Alansary, A., Oktay, O., Kainz, B., Rueckert, D., 2016. Learning under distributed weak supervision. arXiv preprint arXiv:1606.01100.

Ronneberger, O., Fischer, P., Brox, T., 2015. U-net: Convolutional networks for biomedical image segmentation. MICCAI, LNCS. Springer, pp. 234–241.

Salehi, S.S.M., Erdogmus, D., Gholipour, A., 2017. Auto-context convolutional neural network (auto-net) for brain extraction in magnetic resonance imaging. IEEE Trans. Med. Imaging 36 (11), 2319–2330.

Salehi, S.S.M., Hashemi, S.R., Velasco-Annis, C., Ouaalam, A., Estroff, J.A., Erdogmus, D., Warfield, S.K., Gholipour, A., 2018. Real-time automatic fetal brain extraction in fetal MRI by deep learning. Biomedical Imaging (ISBI 2018), 2018 IEEE 15th International Symposium on. IEEE, pp. 720–724.

Ségonne, F., Dale, A.M., Busa, E., Glessner, M., Salat, D., Hahn, H.K., Fischl, B., 2004. A hybrid approach to the skull stripping problem in MRI. Neuroimage 22 (3), 1060–1075.

Serag, A., Blesa, M., Moore, E.J., Pataky, R., Sparrow, S.A., Wilkinson, A., Macnaught, G., Semple, S.I., Boardman, J.P., 2016. Accurate learning with few atlases (alfa): an algorithm for MRI neonatal brain extraction and comparison with 11 publicly available methods. Sci. Rep. 6, 23470.

Simonyan, K., Vedaldi, A., Zisserman, A., 2013. Deep inside convolutional networks: visualising image classification models and saliency maps. arXiv preprint arXiv:1312. 6034. Smith, S.M., 2002. Fast robust automated brain extraction. Hum. Brain Mapp. 17 (3), 143–155.

Taha, A.A., Hanbury, A., 2015. Metrics for evaluating 3D medical image segmentation: analysis, selection, and tool. BMC Med. Imaging 15 (1), 29.

Taimouri, V., Gholipour, A., Velasco-Annis, C., Estroff, J.A., Warfield, S.K., 2015. A template-to-slice block matching approach for automatic localization of brain in fetal MRI, Taimouri, V., Gholipour, A., Velasco-Annis, C., Estroff, J. A., & Warfield, S. K. (2015, April). A template-to-slice block matching approach for automatic localization of brain in fetal MRI. In 2015 IEEE 12th International Symposium on Biomedical Imaging (ISBI), 144–147.

Tourbier, S., Velasco-Annis, C., Taimouri, V., Hagmann, P., Meuli, R., Warfield, S.K., Cuadra, M.B., Gholipour, A., 2017. Automated template-based brain localization and extraction for fetal brain MRI reconstruction. Neuroimage 155, 460–472.

Tu, Z., Bai, X., 2010. Auto-context and its application to high-level vision tasks and 3d brain image segmentation. IEEE Trans. Pattern Anal. Mach. Intell. 32 (10), 1744–1757.

Wachinger, C., Reuter, M., Klein, T., 2018. Deepnat: deep convolutional neural network for segmenting neuroanatomy. Neuroimage 170, 434–445.

Wolterink, J.M., Leiner, T., de Vos, B.D., van Hamersvelt, R.W., Viergever, M.A., Išgum, I., 2016. Automatic coronary artery calcium scoring in cardiac ct angiography using paired convolutional neural networks. Med. Image Anal. 34, 123–136.

Yamaguchi, K., Fujimoto, Y., Kobashi, S., Wakata, Y., Ishikura, R., Kuramoto, K., Imawaki, S., Hirota, S., Hata, Y., 2010. Automated fuzzy logic based skull stripping in neonatal and infantile MR images. Fuzzy Systems (FUZZ), 2010 IEEE International Conference. pp. 1–7.

Yushkevich, P.A., Piven, J., Hazlett, H.C., Smith, R.G., Ho, S., Gee, J.C., Gerig, G., 2006. User-guided 3D active contour segmentation of anatomical structures: significantly improved efficiency and reliability. Neuroimage 31 (3), 1116–1128.

Third trimester brain growth in extremely preterm born neonates compared to intrauterine growth in a pilot study

E. Turk, E. Overbeek, R. de Heus, N. Khalili, A. Franx, Martijn van den Heuvel, Nathalie Claessens, F. Lammertink, M. Nijman; I. Isgum, M.J.N.L. Benders

ABSTRACT

Preterm born infants are at greater risk of developing neurodevelopmental deficits and psychiatric disorders than full-term born infants. Even without macroscopic brain injury, infants that are born preterm have decreased total brain volumes, white matter volumes and gray matter volumes measured later in life. The effect of extremely preterm birth on brain development during the time that is equivalent to the third trimester remains poorly understood. Therefore, the current study aimed to compare global and regional brain volumes and growth trajectories from extremely preterm born infants compared to typically developing infants during the third trimester in utero and first month of life as a control. Healthy developing infants and preterm infants were scanned twice: around the beginning of the third trimester and again, around term equivalent age. Results showed a delay in growth for almost all (regional) brain volumes in extremely preterm born neonates around 32 weeks of gestation. Around term equivalent age, ventricles were larger, cortical gray matter was reduced, and myelination of white matter was accelerated in extremely preterm born infants. Differences were absent for the intracranial volume, total brain volume, unmyelinated white matter, deep grey matter, brainstem and cerebellum around term equivalent age. These results suggest that the delay in growth shortly after preterm birth seem compensated by acceleration of (regional) brain growth during the third trimester for most regions. However, ventricles remain larger and cortical gray matter remains decreased. Moreover, it shows that myelination of white matter occurs earlier or faster after extreme preterm birth. Understanding the developmental trajectory of healthy and preterm born infants provide insights in the influences of neonatal intensive care on brain growth.

INTRODUCTION

The last trimester of pregnancy is marked by essential steps in fetal brain development (Bayer & Altman, 2003). Migration of neurons and maturation of cortical connections cause an immense expansion of the cerebral cortical surface area, white matter tissue and cerebellum (Andescavage et al., 2016; Garcia et al., 2018). The complexity and quantity of changes during this period make the brain particularly susceptible to early developmental insults that are common in preterm born infants (Ortinau & Neil, 2015; Stoodley & Limperopoulos, 2016; Volpe, 2009a, 2009b).

While full-term born infants spent this vulnerable period in utero, extremely preterm born infants (born before 28 weeks of gestation) are prematurely exposed to the extra uterine environment, many perinatal risk factors and postpartum complications including respiratory and circulatory problems and infections that may impact the rest of their lives (Humberg et al., 2020; Lewandowski et al., 2020). Despite the incredible advancement of neonatal intensive care, preterm born neonates are at greater risk

of developing neurodevelopmental deficits and psychiatric disorders later in life than full-term born neonates (Ortinau & Neil, 2015; Volpe, 2009a). The common believe is that these developmental insults may deleteriously have an impact on microscale (van Tilborg et al., 2018) and macroscale neonatal brain growth trajectories around term equivalent age (Kelly et al., 2016; Monson et al., 2016) and during childhood (de Kieviet et al., 2012; Lax et al., 2013; Ment et al., 2009; Nosarti et al., 2014; Taylor et al., 2011; Young et al., 2020). Even in the absence of macroscopic brain damage, decreases in brain volumes in preterm born children are predictors for general cognitive function impairments later in life (Cheong et al., 2013; Hadaya & Nosarti, 2020; Kelly et al., 2016; Keunen et al., 2016; Nosarti et al., 2008; Taylor et al., 2011; Thompson et al., 2013). Although the preterm brain has been studied intensively, preterm neonatal brain growth trajectories during the time that is equivalent to the third trimester of pregnancy have been studied less extensively and healthy controls are often absent in the analysis.

Improvements in fetal and neonatal neuroimaging over the past decade have provided new possibilities within the field. Two pioneering MRI studies of Bouyssi-Kobar et al. (Bouyssi-Kobar et al., 2018; Bouyssi-Kobar et al., 2016) already showed a delay in cerebellar and global volumetric brain growth in extremely preterm neonates compared to healthy infants during the third trimester of pregnancy. The goal of this preliminary study was to extent our knowledge on volumetric brain growth in preterm infants by utilizing serial structural MRI of preterm infants and healthy controls to examine total and tissue-specific brain growth between 29 and 45 weeks post menstrual age (PMA). Specifically, we aimed to (1) describe volumetric tissue-specific differences between healthy and preterm born infants around 30 and 40 weeks PMA, and (2) estimate early (between 29 and 34 weeks PMA) and late (between 39 and 45 weeks PMA) brain growth trajectories cross-individuals of healthy and preterm born infants. As we are still collecting more data of healthy fetuses and neonates, the last aim (3) to study differences in individual growth trajectories of preterm and term born infants along 29 to 45 weeks PMA, will be added later when analyses will be more trustworthy due to the larger size of the sample.

METHODS

Subjects
Structural MRI scans were collected from two longitudinal cohort studies of extremely preterm born infants (born <28 weeks of gestation) and healthy controls scanned twice around 30 and 40 weeks postmenstrual age.

Preterm born cohort. MRI data of 133 extremely preterm born neonates (mean PMA of 26.4 weeks ± 7 days at birth), were collected retrospectively (between May 2008 and January 2017) from standard clinical observations performed at the University Medical Center Utrecht. Extremely preterm born neonates were scanned twice: around 30 weeks (

Table 1. Characteristics of included subjects at the two moments of scanning

Characteristics	Scan 1		Scan 2	
	Preterm (n = 109)	Control (n = 25)	Preterm (n = 103)	Control (n = 12)
Female, n (%)	52 (47)	18 (72)	51 (50)	9 (75)
PMA at MRI, wk				
Mean ± SD	30.8 ± 0.8	32.4 ± 1.1	41.1 ± 0.6	42.6 ± 1.6
Range	29.4 - 34.3	30.2 - 34	38.9- 43.1	39.6 − 44.9
PMA at Birth, wk				
Mean ± SD	26.6 ± 1.0	-	26.6 ± 1.0	40.0 ± 1.0
Range	24.3 − 27.9	-	24.3 − 27.9	38.3 − 42.1
Periventricular White Matter Loss[A]				
Non existent	74	25	67	25
Mild abnormality	35	0	36	0
Intraventricular hemorrhage[A]				
Non existent	72	25	70	25
Type 1	19	0	16	0
Type 2	18	0	17	0
White Matter Injury[B]				
Non existent	30	25	30	25
Mild abnormality	79	0	73	0

[A] Scored by specialized neonatologists at scan 1. [B] Scored by specialized neonatologists at scan 2. PMA = postmenstrual age

30.6 weeks ± 6 days PMA at scan) and again around 40 weeks (41.2 weeks ± 7 days PMA at scan) of postmenstrual age. Inclusion required a normal to mild Woodward score for white matter injury and periventricular white matter loss (Keunen et al., 2012). In case of existence of intraventricular hemorrhages only neonates with mild hemorrhages (type 1 and 2) were included (Kidokoro et al., 2014). Brain abnormalities were visually evaluated and scored by neonatologists. After exclusion of low-quality images, data of 109 preterm born infants was included for the first scan and 103 for the second. An overview of characteristics of subjects can be found in **Table 1**. Written parental consent was waved and the study was approved by the local Institutional Review Board.

Healthy control group. The current study is the first within the Netherlands to collect fetal and neonatal MRI data of a healthy cohort. Twenty-nine healthy pregnant women were recruited for participation in the current study (2018-2019) and are participating in the YOUth study (for an overview of the rationale and open data repository see, Onland-

Moret et al., 2020). Written informed consent was obtained for both scans: first for the fetal MRI of the pregnant mothers and from her partner, and secondly for the baby MRI from both parents. All mothers were approached after a routine 20 weeks anatomy ultrasound scan and were considered at low risks for structural anomalies. At the moment of the first scan the fetuses had a gestational age between 30 and 34 weeks (32.3 weeks ± 8.0 days PMA at scan). Twelve neonates were scanned again within a month after birth (40 weeks ± 7 days PMA at birth, 42.4 weeks ± 11 days PMA at scan). After exclusion of low-quality images, data of 25 out of 29 fetuses were included for the first, and twelve neonates were included for the second scan. Only twelve infants were scanned twice; reasons for withdrawal of the study were: no parental consent for a second scan, no natural sleep of the neonate before the start of the MRI, health issues of the mother after giving birth, closure due to COVID-19 and other logistic problems. For a descriptive table about subjects, see **Table 1**. The study was approved by the local Institutional Review Board (YOUth 16424).

Fetal MRI acquisition
Both cohorts were scanned at a 3T Philips scanner at the University Medical Center Utrecht. MRI acquisition included coronal, sagittal and axial T2 turbo fast spin-echo sequences. Pregnant women and fetuses were not sedated before or during scanning. Mothers were comfortably positioned slightly or completely tilted to their left side to prevent compression of the vena cava inferior, unless another lying position was preferred by the mother. To determine the position of the fetus, as a first step a survey scan was made to decide how the x, y, and z-axis of the brain were oriented. The scan protocol had a maximum duration of 35 minutes to prevent unnecessary discomfort for the mother.

Neonatal MRI acquisition
Extremely preterm born neonates were sedated with chloral hydrate to minimize movement during the scan. Typically developing neonates were not sedated. Instead, typically developing neonates were scanned during natural sleep after feeding. When sleep was interrupted during the time of scanning, the scan was discontinued until the neonate fell asleep again. All neonates were provided with three layers of hearing protection. First, neonatal noise attenuators were applied over the ears of the infant (Mini muffs: Natus UK, Hampden House, Monument Business park, Warpsgrove Lane, Chalgrove Oxford, OX44 7RW). Second, earmuffs (EM's for kids, Brisbane, Australia) were placed over the noise attenuators. Third, a foam cushion placed over the head coil as another protection layer. A neonatologist or physician assistant was present at all times to monitor the infants' comfort, heart rate, respiratory rate and blood saturation.

Tissue segmentation and volumetric quantification
Coronal T2 images of which more than 10% of the slices contained serious artifacts
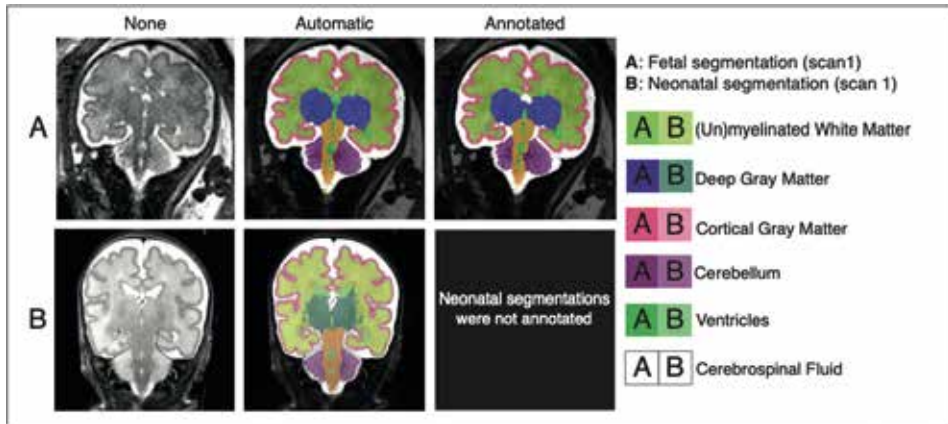
Figure 1. Fetal and neonatal brain segmentations.
Figure displays the visualization of our segmentation steps (raw image, automatic segmentation, and manually annotated segmentation) in the fetal brain, panel A, and neonatal brain, panel B. The colors represent different tissue classes, see legend.

were excluded from the data-analysis. If the quality of the coronal image was not sufficient, the axial or sagittal image was evaluated, and, if of good quality, included instead. All (preterm) neonatal data were automatically segmented into tissue classes using in house developed and validated sequential forward floating selection (SFFS) algorithms. This automatic segmentation technique does not show differences from manual segmentation methods (Moeskops et al., 2015)

Automatically segmented T2 images of the typically developing fetuses were visually checked and manually annotated using Image Explorer segmentation painter, an in-house developed software program (Khalili, Lessmann, et al., 2019; Khalili, Turk, et al., 2019). An example of our fetal and neonatal brain segmentations can be found in **Figure 1**. Brain classes included: cerebellum, deep gray matter, ventricles, myelinated white matter, unmyelinated white matter, brainstem, deep gray matter (basal ganglia and thalamus), cortical gray matter and cerebrospinal fluid (Moeskops et al., 2015). Myelinated white matter was only segmented in the images of the second scans, since the onset of white matter myelination is around the start of the third trimester and therefore hard to detect on MRI.

To calculate the absolute volume of each structure, the number of labeled voxels per structure was extracted from the segmented images. The number of voxels was then multiplied by the voxel dimension resulting into absolute volumes in mm3 and converted to ml (1 mm3 = 0.001 mL). Volume of the intracranial cavity was calculated as the sum of

Table 2. Results of the multiple regression analysis for the parameters of interest and the effects of a covariate.

Variable	Scan	Preterm mean ± SD (ml)	Typical mean ± SD (ml)	Covariate F/p	Group F/p	Interaction F/p
Intracranial Volume	1	201.0 ± 25.8	303.6 ± 48.7	271.0/<0.001*	105.7/<0.001*	3.7/<0.001*
	2	481.1 ± 52.6	493.3 ± 46.2	6.8/0.010*	0.4/0.538	0.1/0.738
Total Brain Volume	1	143.0 ± 18.5	203.2 ± 36.4	242.4/<0.001*	58.5/<0.001*	14.1/<0.001*
	2	342.6 ± 32.9	372.4 ± 40.3	16.8/<0.001*	1.2/0.282	1.6/0.206
Cerebrospinal Fluid	1	51.4 ± 9.4	94.4 ± 18.4	180.1/<0.001*	151.7/<0.001*	3.3/0.073
	2	125.8 ± 23.8	113.3 ± 12.9	0.03/0.873	4.7/0.032*	1.0/0.322
Ventricles	1	6.7 ± 2.1	6.0 ± 1.8	0.5/0.470	5.5/0.020*	1.0/0.331
	2	12.6 ± 3.5	7.5 ± 1.8	1.6/0.208	24.9/<0.001*	0.2/0.656
Cortical Gray Matter	1	29.5 ± 4.8	56.8 ± 10.3	587.8/<0.001*	275.6/<0.001*	13.6/<0.001*
	2	114.8 ± 12.8	135.0 ± 18.8	47.5/<0.001*	4.7/0.031*	0.8/0.383
Unmyelinated White Matter	1	94.1 ± 12.9	116.8 ± 21.3	109.2/<0.001*	7.7/0.006*	9.0/0.003*
	2	172.8 ± 17.6	179.7 ± 17.6	1.6/0.205	0.6/0.458	1.0/0.311
Myelinated White Matter	2	3.6 ± 0.4	3.5 ± 0.8	27.8/<0.001*	13.8/<0.001*	3.1/0.083
Cerebellum	1	6.1 ± 1.2	10.7 ± 2.2	206.5/<0.001*	108.8/<0.001*	18.7/<0.001*
	2	23.8 ± 3.3	25.6 ± 5.6	21.6/<0.001*	0.5/0.067	5.0/0.028*
Deep Gray Matter	1	11.1 ± 1.5	15.1 ± 3.2	95.0/<0.001*	33.3/<0.001*	11.2/0.001*
	2	21.7 ± 2.0	22.4 ± 3.9	8.7/0.004*	0.3/0.584	4.3/0.041*
Brainstem	1	2.1 ± 0.5	3.8 ± 0.9	118.9/<0.001*	95.6/<0.001*	17.2/<0.001*
	2	5.9 ± 0.5	6.3 ± 0.6	16.6/<0.001*	0.6/0.454	0.1/0.784

the cerebellum, deep gray matter, ventricles, (un)myelinated white matter, brainstem, cortical gray matter and cerebrospinal fluid. The total brain volume was calculated as the volume of the intracranial cavity minus the volume of the cerebrospinal fluid and ventricles. Relative tissue volumes were calculated as a percentage of the intracranial volume.

Statistical analysis
A multiple regression analysis was performed to test for the interaction of group factor (preterm and healthy infants) and the effect of age (as a covariate) on the dependent variables (brain volumes including cerebellum, deep gray matter, ventricles, myelinated white matter, unmyelinated white matter, brainstem, cortical gray matter and cerebrospinal fluid). Multiple regression analyses revealed a significant effect of postmen-
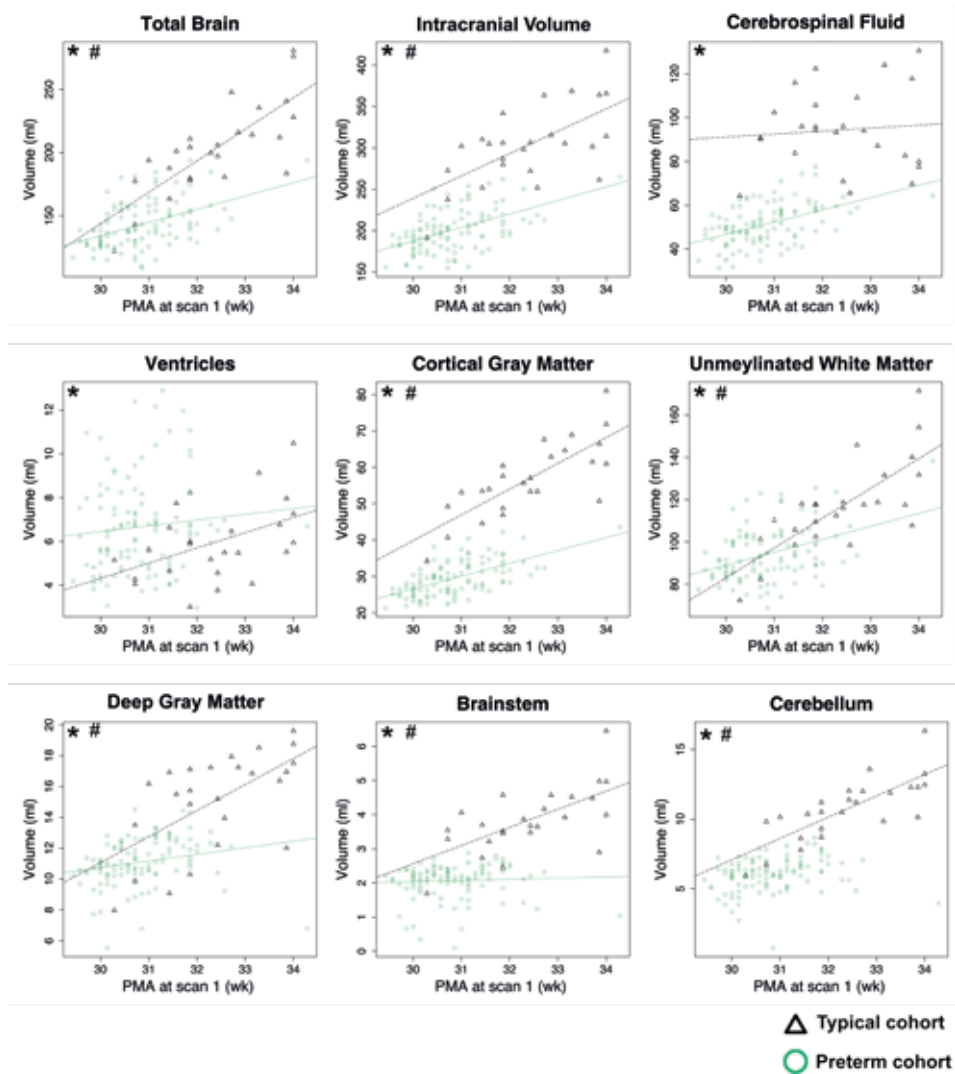
Figure 2. Brain volumes estimated from first MRI scan
*Figure displays volumes of neural tissue classes of fetuses (typical cohort) and preterm born infants (preterm cohort) plotted against age in postconceptional weeks. *Significant difference in intercepts. #Significant difference in slope.*

strual age at the moment of the scan for most (regional) brain volumes. Therefore, age was included as a covariate in the multiple regression analysis, which will be further described as ANCOVA. Only ventricle volumes were not significantly affected by age at the moment of both scans. Also, at the moment of the second scan, age did not have a significant effect on cerebrospinal fluid and unmyelinated white matter volumes. All following results take the effect of age on volume size into account.

As a control analysis, multiple regression analysis was performed for relative volumes (computed by taking each volume as a percentage of the total intracranial volume) of all structures (see supplementary). Relative brain volumes were used as a control rather than outcome variable, because the volume of the cerebrospinal fluid has a large effect on this measure. The cerebrospinal fluid is relatively large in fetuses compared to neonates, because perinatal factors cause a decrease in cerebrospinal fluid. This makes volumes as a percentage of the intracranial cavity an inaccurate measure for demonstrating differences between preterm neonates and typically developing fetuses. However, it does provide insights into proportional brain growth. Therefore, the analysis of relative brain volumes is added as a control analysis in the supplementary index. Post-menstrual age was expressed in weeks from the first day of the last menstrual periods before pregnancy. All statistical tests were performed using R software (version 1.2.1335, http://www.r-project.org/). A p-value of <0.05 was considered statistically significant.

RESULTS

Volumetric tissue-specific differences around 30 weeks PMA
At the first MRI scan, absolute volumetric group differences (corrected for age) were observed for all brain tissues. Intracranial, total brain, cerebrospinal fluid, cortical gray matter, unmyelinated white matter, cerebellum, deep gray matter and brainstem volumes showed to be smaller in preterm born infants. While ventricle volumes were larger in preterm infants. All group differences reached significance levels in the ANCOVA, see Table 2 for an overview for all volumes (in ml), F and p values. Differences remained significant, comparing relative volumes of both groups (see supplemental **Table S1**, and **Figure S1**).

Volumetric tissue-specific differences around 40 weeks PMA
At the second MRI scan, absolute volumetric group differences (corrected for age) were observed for cerebrospinal fluid, ventricles, cortical gray matter and myelinated white matter (**Figure 3**). Larger cerebrospinal fluid, ventricles and myelinated white matter volumes were larger in preterm born neonates, while cortical gray matter volumes were larger in typically developing infants (significant group differences, see **Figure 3** and Table 2 for an overview for all volumes (in ml), F and p values). Intracranial, total brain, unmyelinated white matter, cerebellum, deep gray matter and brainstem volumes were
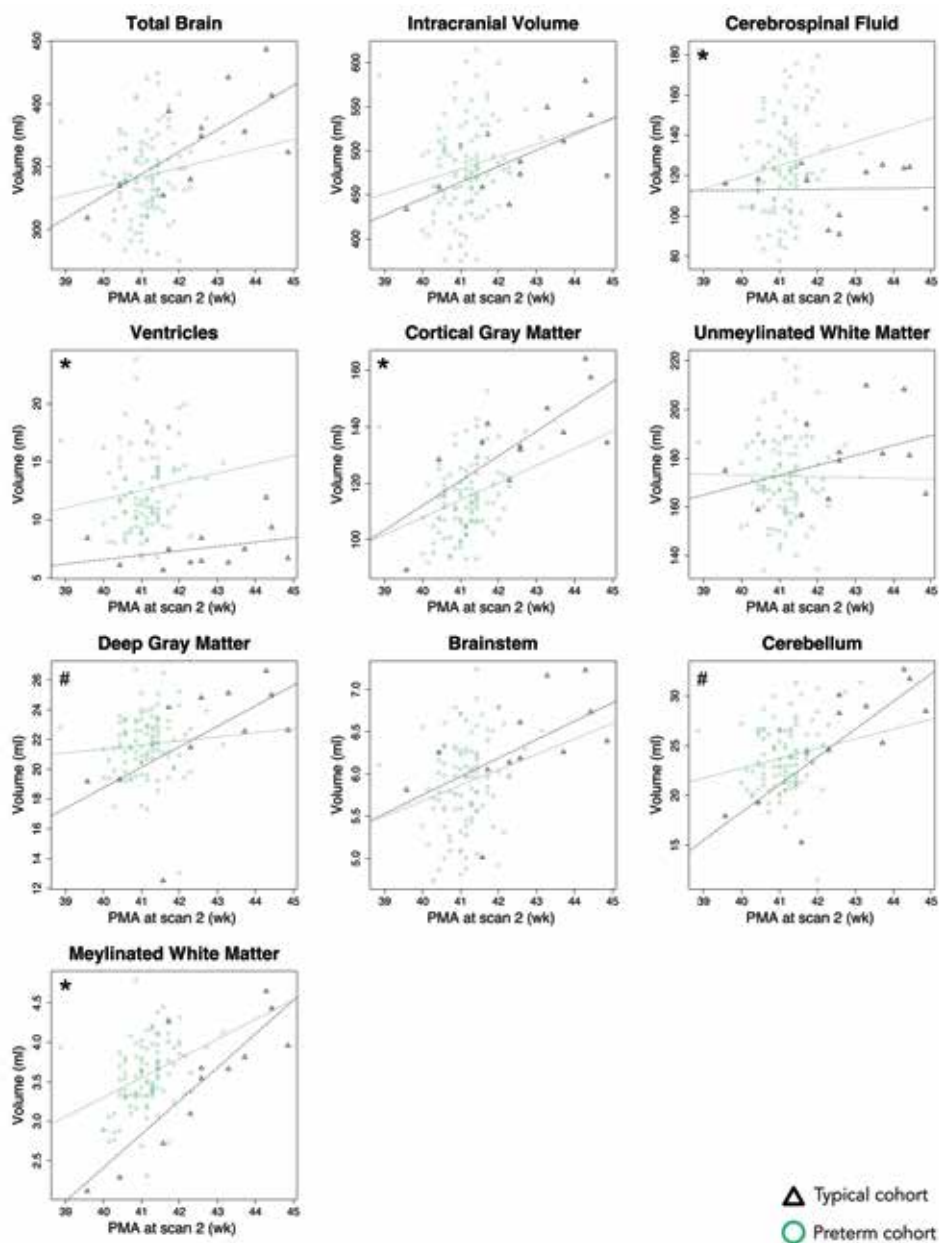
Figure 3. Brain volumes estimated from second MRI scan

Figure displays volumes of neural tissue classes of fetuses (typical cohort) and preterm born infants (preterm cohort) plotted against age in postconceptional weeks. *Significant difference in intercepts. #Significant difference in slope.

larger in typically developing infants, but differences did not reach significance levels. Comparable results were found comparing relative volumes in the two groups significant differences were found for intracranial, total brain, cerebrospinal fluid, cortical gray matter, unmyelinated white matter volumes, and not for cerebellum, deep gray matter and brainstem volumes (see supplemental table S1, **Figure S2**).

Differences in brain growth trajectories around 30 weeks PMA
Results from the ANCOVA showed significant differences in absolute volumetric growth of intracranial, total brain, cortical gray matter, unmyelinated white matter, cerebellum, deep gray matter and brainstem. No significant differences in growth rates were found for the cerebrospinal fluid and ventricles. Early developmental growth rates were estimated (cross-individuals) from interactions between group differences (preterm born neonates and healthy fetuses) and age around 30 weeks PMA (ranging between 29 and 34 weeks), see **Figure 2** and Table 2 for an overview.

Differences in brain growth trajectories around 40 weeks PMA
Results from the ANCOVA showed significant differences in absolute volumetric growth of cerebellum, deep gray matter and brainstem. No significant differences in growth rates were found for the intracranial, total brain, cortical gray matter, unmyelinated white matter, cerebrospinal fluid and ventricles. Early developmental growth rates were estimated (cross-individuals) from interactions between group differences (preterm born neonates and healthy fetuses) and age around 30 weeks PMA (ranging between 29 and 34 weeks), see **Figure 3** and **Table 2** for an overview.

DISCUSSION

Longitudinally examining a small cohort of healthy perinates in contrast to preterm born infants, this study demonstrates decreased size and growth of almost all (regional) brain volumes in extremely preterm born infants around 30 weeks of gestation. On the contrary, volume size differences were absent for most volumes (intracranial volume, total brain volume, unmyelinated white matter, deep grey matter, brainstem and cerebellum) around term equivalent age. Regional and global brain growth is delayed in neonates short after extremely preterm birth, but seem to catch up by an acceleration of brain growth during the third trimester, resulting in limited differences in regional and global brain volumes at the end of the third trimester for most structures. Whereas volumes of the cortical gray matter remained decreased, volumes of the ventricles remained increased, and myelination of cortical white matter was accelerated in preterm born infants compared to typically developing infants around the end of the third trimester. These preliminary results show that, brain growth of extremely preterm born neonates results in altered regional brain sizes and accelerated regional brain growth already at the third trimester of pregnancy. In line with former fetal DTI and T2-weighted imaging research (Bouyssi-Kobar et al.,

2018; Bouyssi-Kobar et al., 2016; Brossard-Racine et al., 2017), our results show smaller regional brain tissues (intracranial, total brain, and cerebellum volumes) in extremely preterm born infants around 30 weeks PMA. Additional to these studies, we show increased deep gray matter, brainstem, white and gray matter volumes in the healthy fetuses. While differences of most tissue classes seem to be limited around term equivalent age, clear differences between cortical gray matter are presented here in our longitudinal cohort and in other cross-sectional cohorts (Bouyssi-Kobar et al., 2016; Clouchoux et al., 2012). Our results demonstrate smaller cortical gray matter volumes in preterm born infants in the whole neonatal period (30-45 PMA), suggesting a progressive decline in gray matter tissue growth in the first weeks of life. Interestingly, cortical folding has been shown to be accelerated in preterm born infants during the third trimester (Lefèvre et al., 2015). It is important to investigate if the combination of delayed cortical growth and accelerated cortical folding has an impact on neurodevelopment. MRI studies comparing preterm and term born cohort at different ages, show that this difference in volume growth is still detectable during childhood and adolescence (de Kieviet et al., 2012; Inder et al., 2005; Peterson et al., 2003). Delayed cortical gray matter development in preterm born infants are linked to neurodevelopmental disabilities later in life, such as impaired language development (Kersbergen, Leroy, et al., 2016; Kersbergen, Makropoulos, et al., 2016; Munakata et al., 2013; Peterson et al., 2003). Our results show that altered growth of cortical gray matter is already detectable early after preterm birth, in a cohort without visible brain damage and abnormalities, indicating that altered gray matter growth is induced by early environmental and genetic factors.

The extra uterine environment, preterm birth and NICU related risk factors may harm brain tissue on the microscale and may result in smaller brain tissues or enlarged brain fluids detectable on MRI, even without absence of visible brain damage (Volpe, 2009a, 2009b). In addition to smaller brain tissues, our results indeed show that ventricles were enlarged in preterm born infants compared to typically developing infants around the beginning, and even more so, around the end of the third trimester. This is in line with earlier studies that found enlarged ventricles and CSF volumes in preterm born children around birth, childhood and adolescents (Inder et al., 2005; Nosarti et al., 2002; Taylor et al., 2011). Enlarged ventricle and CSF are taking up unnecessary space at the expense of other brain tissue and thereby indirectly negatively influence neurodevelopment (de Kieviet et al., 2012). For example, multiple studies show that ventricle expansion correlates with thinning of the corpus callosum (Iwata et al., 2016; Nosarti et al., 2004; Rademaker et al., 2004), which together are strong indicators of later life motor and cognitive impairments in preterm born infants (Iwata et al., 2016; Northam et al., 2011; Nosarti et al., 2004; Rademaker et al., 2004). Although the current study found increased ventricle volumes around the end of the third trimester -besides the decrease in cortical gray matter- no decrease in absolute white matter or total brain volumes were found. It has to be noted that, the alternative comparison of relative brain volumes (see

supplemental results) showed significant decreases in relative white matter volume and relative total brain volumes in preterm infants. It is possible that the space that is taken up by the ventricles is relatively subtle for the other tissue classes that were measured in the current study. As former research already showed in preterm infants at term equivalent age, distinguishing between clinical risk factors, such as reason of prematurity (e.g., spontaneous or intrauterine growth restriction), might explain even more variation in brain volume differences (Parikh et al., 2013; Thompson et al., 2013; Thompson et al., 2006). In combination with a sample size of only twelve typically developing infants, this could have left absolute total brain or white matter differences undetected. Additionally, CSF was increased in healthy fetuses around 30 weeks PMA, while it was decreased around 45 weeks PMA. The transition of birth (from intrauterine to extrauterine environment) is possibly accountable for the large volumetric difference of the CSF, but more research is needed to explain this. In future studies, larger sample sizes and further subdivision of brain regions could perhaps demonstrate the cause-effect of ventricle and CSF expansion on (sub) regional brain volumes.

Our results show that myelination of white matter was enhanced in preterm born infants compared to typically developing infants around the end of the third trimester. This result suggests that the myelination process takes place earlier or faster in preterm born infants, supporting the theory of accelerated brain development in preterm born infants during the third trimester. A possible explanation for the early reinforcement of white matter tracts in extremely preterm born infants is the early exposure to ex utero sensory input. For example, in contrast to fetuses, preterm born infants are exposed to many visual stimuli, forcing the visual system to develop early and enhance early neural activity (Madan et al., 2005). Combined EEG and MRI research in preterm infants indeed show that increased fractional anisotropy was associated with more brain activity (Tataranno et al., 2018). The acceleration of white matter myelination demonstrates the remarkable capacity of the preterm brain to adapt to the environment. However, there is a possibility that the brain is taking developmental steps, such as myelination and cortical folding before the brain has had the time to finetune. This raises the question if acceleration of myelination and early enhanced neural activity following premature birth are beneficial for later life cognition, and if they are indicative for resilience or vulnerability of the developing brain (Lammertink et al., 2021).

It is important to note that alterations of one region may result in alterations of other regions that remained undetected in the current study, or manifesting in later life (Hack & Taylor, 2000; Nosarti et al., 2008). We excluded extremely preterm infants that showed more than mild brain damage on the first or second scan. Therefore, white matter injury, periventricular white matter loss or intraventricular hemorrhages did not influence the results. However, other factors may have had an effect on brain development in preterm born neonates. Diversity in the reason of prematurity, health issues, drugs, stress and

sleep could explain larger heterogeneity of the extremely preterm cohort data compared to the typically developing cohort. For example, many of the included subjects were delivered extremely preterm per caesarean section for various reasons. It is important to note that the current study focused on brain development in extremely preterm born neonates (born before 28 weeks of gestation), it is therefore unclear to what extent the results are applicable in very preterm or late-preterm born infants. Our study contained some limitations that might have had an influence on the results. First, the sample size of the typically developing cohort was small, especially for the second scan. Second, within the typically developing cohort there was little variation in parental educational levels, ethnicity, and socio-economic backgrounds. Also, female participants were over represented in the healthy cohort. Therefore, the sample might not be representative for the true population of interest. A third limitation was the difference in scanning protocol and processing for the fetal and neonatal cohort. Since fetuses are scanned in utero, the quality of the images is different from neonatal T2 images due to movement artefacts and interference of maternal body tissue around the fetus. This could have led to an overestimation of volume differences between typically developing fetuses and preterm born neonates.

Concluding remarks
To our knowledge, our study is the first to demonstrate differences in third trimester brain development between typically developing fetuses and extremely preterm born neonates without major brain damage. By using high-quality 3.0-T MR images and improved in-house segmentation methods we extend earlier findings by adequately demonstrating third trimester brain growth in typical developing fetuses and neonates and preterm born neonates. Our research group continues to include more typically developing fetuses and neonates in the YOUth cohort, creating even greater possibilities for future studies comparing healthy and clinical cohorts (e.g., congenital heart disease or intrauterine growth restriction). Overall, the current research is providing the first steps towards discovering the cause, timing and consequences of altered brain development after extremely preterm birth.

REFERENCES

Andescavage, N. N., DuPlessis, A., McCarter, R., Vezina, G., Robertson, R., & Limperopoulos, C. (2016). *Cerebrospinal Fluid and Parenchymal Brain Development and Growth in the Healthy Fetus. Dev Neurosci, 38(6), 420-429. https://doi.org/10.1159/000456711*

Bayer, S. A., & Altman, J. (2003). *The human brain during the third trimester. CRC Press.*

Bouyssi-Kobar, M., Brossard-Racine, M., Jacobs, M., Murnick, J., Chang, T., & Limperopoulos, C. (2018). *Regional microstructural organization of the cerebral cortex is affected by preterm birth. Neuroimage Clin, 18, 871-880. https://doi.org/10.1016/j.nicl.2018.03.020*

Bouyssi-Kobar, M., du Plessis, A. J., McCarter, R., Brossard-Racine, M., Murnick, J., Tinkleman, L., Robertson, R. L., & Limperopoulos, C. (2016, Nov). *Third Trimester Brain Growth in Preterm Infants Compared With In Utero Healthy Fetuses. Pediatrics, 138(5), e20161640. https://doi.org/10.1542/peds.2016-1640*

Brossard-Racine, M., Poretti, A., Murnick, J., Bouyssi-Kobar, M., McCarter, R., du Plessis, A. J., & Limperopoulos, C. (2017, Mar). *Cerebellar Microstructural Organization is Altered by Complications of Premature Birth: A Case-Control Study. J Pediatr, 182, 28-33 e21. https://doi.org/10.1016/j.jpeds.2016.10.034*

Cheong, J. L., Anderson, P. J., Roberts, G., Burnett, A. C., Lee, K. J., Thompson, D. K., Molloy, C., Wilson-Ching, M., Connelly, A., Seal, M. L., Wood, S. J., & Doyle, L. W. (2013). *Contribution of brain size to IQ and educational underperformance in extremely preterm adolescents. PLoS One, 8(10), e77475. https://doi.org/10.1371/journal.pone.0077475*

Clouchoux, C., Kudelski, D., Gholipour, A., Warfield, S. K., Viseur, S., Bouyssi-Kobar, M., Mari, J. L., Evans, A. C., du Plessis, A. J., & Limperopoulos, C. (2012, Jan). *Quantitative in vivo MRI measurement of cortical development in the fetus. Brain Struct Funct, 217(1), 127-139. https://doi.org/10.1007/s00429-011-0325-x*

de Kieviet, J. F., Zoetebier, L., Van Elburg, R. M., Vermeulen, R. J., & Oosterlaan, J. (2012). *Brain development of very preterm and very low-birthweight children in childhood and adolescence: A meta-analysis. Developmental Medicine & Child Neurology, 54(4), 313-323.*

Garcia, K. E., Robinson, E. C., Alexopoulos, D., Dierker, D. L., Glasser, M. F., Coalson, T. S., Ortinau, C. M., Rueckert, D., Taber, L. A., Van Essen, D. C., Rogers, C. E., Smyser, C. D., & Bayly, P. V. (2018, Mar 20). *Dynamic patterns of cortical expansion during folding of the preterm human brain. Proc Natl Acad Sci U S A, 115(12), 3156-3161. https://doi.org/10.1073/pnas.1715451115*

Hack, M., & Taylor, H. G. (2000, Oct 18). *Perinatal brain injury in preterm infants and later neurobehavioral function. Jama, 284(15), 1973-1974. https://doi.org/10.1001/jama.284.15.1973*

Hadaya, L., & Nosarti, C. (2020). The neurobiological correlates of cognitive outcomes in adolescence and adulthood following very preterm birth. Seminars in Fetal and Neonatal Medicine,

Humberg, A., Fortmann, I., Siller, B., Kopp, M. V., Herting, E., Göpel, W., & Härtel, C. (2020). Preterm birth and sustained inflammation: consequences for the neonate. Seminars in Immunopathology,

Inder, T. E., Warfield, S. K., Wang, H., Hüppi, P. S., & Volpe, J. J. (2005, Feb). Abnormal Cerebral Structure Is Present at Term in Premature Infants. Pediatrics, 115(2), 286. https://doi.org/10.1542/peds.2004-0326

Iwata, S., Katayama, R., Kinoshita, M., Saikusa, M., Araki, Y., Takashima, S., Abe, T., & Iwata, O. (2016, Sep 23). Region-specific growth restriction of brain following preterm birth. Sci Rep, 6, 33995. https://doi.org/10.1038/srep33995

Kelly, C. E., Cheong, J. L., Gabra Fam, L., Leemans, A., Seal, M. L., Doyle, L. W., Anderson, P. J., Spittle, A. J., & Thompson, D. K. (2016, Mar). Moderate and late preterm infants exhibit widespread brain white matter microstructure alterations at term-equivalent age relative to term-born controls. Brain Imaging Behav, 10(1), 41-49. https://doi.org/10.1007/s11682-015-9361-0

Kersbergen, K. J., Leroy, F., Isgum, I., Groenendaal, F., de Vries, L. S., Claessens, N. H. P., van Haastert, I. C., Moeskops, P., Fischer, C., Mangin, J. F., Viergever, M. A., Dubois, J., & Benders, M. (2016, Nov 15). Relation between clinical risk factors, early cortical changes, and neurodevelopmental outcome in preterm infants. NeuroImage, 142, 301-310. https://doi.org/10.1016/j.neuroimage.2016.07.010

Kersbergen, K. J., Makropoulos, A., Aljabar, P., Groenendaal, F., de Vries, L. S., Counsell, S. J., & Benders, M. J. (2016, Nov). Longitudinal Regional Brain Development and Clinical Risk Factors in Extremely Preterm Infants. J Pediatr, 178, 93-100 e106. https://doi.org/10.1016/j.jpeds.2016.08.024

Keunen, K., Isgum, I., van Kooij, B. J., Anbeek, P., van Haastert, I. C., Koopman-Esseboom, C., Fieret-van Stam, P. C., Nievelstein, R. A., Viergever, M. A., de Vries, L. S., Groenendaal, F., & Benders, M. J. (2016, May). Brain Volumes at Term-Equivalent Age in Preterm Infants: Imaging Biomarkers for Neurodevelopmental Outcome through Early School Age. J Pediatr, 172, 88-95. https://doi.org/10.1016/j.jpeds.2015.12.023

Keunen, K., Kersbergen, K. J., Groenendaal, F., Isgum, I., de Vries, L. S., & Benders, M. J. (2012, Apr). Brain tissue volumes in preterm infants: prematurity, perinatal risk factors and neurodevelopmental outcome: a systematic review. J Matern Fetal Neonatal Med, 25 Suppl 1(sup1), 89-100. https://doi.org/10.3109/14767058.2012.664343

Khalili, N., Lessmann, N., Turk, E., Claessens, N., Heus, R., Kolk, T., Viergever, M. A., Benders, M., & Isgum, I. (2019, Dec). Automatic brain tissue segmentation in fetal MRI using convolutional neural networks. Magn Reson Imaging, 64, 77-89. https://doi.org/10.1016/j.mri.2019.05.020

Khalili, N., Turk, E., Benders, M., Moeskops, P., Claessens, N. H. P., de Heus, R., Franx, A., Wagenaar, N., Breur, J., Viergever, M. A., & Isgum, I. (2019). Automatic extraction of the intracranial volume

in fetal and neonatal MR scans using convolutional neural networks. Neuroimage Clin, 24, 102061. https://doi.org/10.1016/j.nicl.2019.102061

Kidokoro, H., Anderson, P. J., Doyle, L. W., Woodward, L. J., Neil, J. J., & Inder, T. E. (2014, Aug). Brain injury and altered brain growth in preterm infants: predictors and prognosis. Pediatrics, 134(2), e444-453. https://doi.org/10.1542/peds.2013-2336

Lammertink, F., Vinkers, C. H., Tataranno, M. L., & Benders, M. J. N. L. (2021, 2021-January-08). Premature Birth and Developmental Programming: Mechanisms of Resilience and Vulnerability [Review]. Frontiers in Psychiatry, 11(1515), 531571. https://doi.org/10.3389/fpsyt.2020.531571

Lax, I. D., Duerden, E. G., Lin, S. Y., Mallar Chakravarty, M., Donner, E. J., Lerch, J. P., & Taylor, M. J. (2013, Mar). Neuroanatomical consequences of very preterm birth in middle childhood. Brain Struct Funct, 218(2), 575-585. https://doi.org/10.1007/s00429-012-0417-2

Lefèvre, J., Germanaud, D., Dubois, J., Rousseau, F., de Macedo Santos, I., Angleys, H., Mangin, J.-F., Hüppi, P. S., Girard, N., & De Guio, F. (2015). Are Developmental Trajectories of Cortical Folding Comparable Between Cross-sectional Datasets of Fetuses and Preterm Newborns? Cerebral Cortex, bhv123.

Lewandowski, A. J., Levy, P. T., Bates, M. L., McNamara, P. J., Nuyt, A. M., & Goss, K. N. (2020, Oct). Impact of the Vulnerable Preterm Heart and Circulation on Adult Cardiovascular Disease Risk. Hypertension, 76(4), 1028-1037. https://doi.org/10.1161/HYPERTENSIONAHA.120.15574

Madan, A., Jan, J. E., & Good, W. V. (2005, Apr). Visual development in preterm infants. Dev Med Child Neurol, 47(4), 276-280. https://doi.org/10.1017/s0012162205000514

Ment, L. R., Kesler, S., Vohr, B., Katz, K. H., Baumgartner, H., Schneider, K. C., Delancy, S., Silbereis, J., Duncan, C. C., Constable, R. T., Makuch, R. W., & Reiss, A. L. (2009, Feb). Longitudinal brain volume changes in preterm and term control subjects during late childhood and adolescence. Pediatrics, 123(2), 503-511. https://doi.org/10.1542/peds.2008-0025

Moeskops, P., Benders, M. J., Chit, S. M., Kersbergen, K. J., Groenendaal, F., de Vries, L. S., Viergever, M. A., & Isgum, I. (2015, Sep). Automatic segmentation of MR brain images of preterm infants using supervised classification. NeuroImage, 118, 628-641. https://doi.org/10.1016/j.neuroimage.2015.06.007

Monson, B. B., Anderson, P. J., Matthews, L. G., Neil, J. J., Kapur, K., Cheong, J. L., Doyle, L. W., Thompson, D. K., & Inder, T. E. (2016, Aug 1). Examination of the Pattern of Growth of Cerebral Tissue Volumes From Hospital Discharge to Early Childhood in Very Preterm Infants. JAMA Pediatr, 170(8), 772-779. https://doi.org/10.1001/jamapediatrics.2016.0781

Munakata, S., Okada, T., Okahashi, A., Yoshikawa, K., Usukura, Y., Makimoto, M., Hosono, S., Takahashi, S., Mugishima, H., & Okuhata, Y. (2013, Jan). Gray matter volumetric MRI differences late-preterm and term infants. Brain Dev, 35(1), 10-16. https://doi.org/10.1016/j.braindev.2011.12.011

Northam, G. B., Liegeois, F., Chong, W. K., Wyatt, J. S., & Baldeweg, T. (2011, Apr). Total brain white matter is a major determinant of IQ in adolescents born preterm. Ann Neurol, 69(4), 702-711. https://doi.org/10.1002/ana.22263

Nosarti, C., Al-Asady, M. H., Frangou, S., Stewart, A. L., Rifkin, L., & Murray, R. M. (2002, Jul). Adolescents who were born very preterm have decreased brain volumes. Brain, 125(Pt 7), 1616-1623. https://doi.org/10.1093/brain/awf157

Nosarti, C., Giouroukou, E., Healy, E., Rifkin, L., Walshe, M., Reichenberg, A., Chitnis, X., Williams, S. C., & Murray, R. M. (2008, Jan). Grey and white matter distribution in very preterm adolescents mediates neurodevelopmental outcome. Brain, 131(Pt 1), 205-217. https://doi.org/10.1093/brain/awm282

Nosarti, C., Nam, K. W., Walshe, M., Murray, R. M., Cuddy, M., Rifkin, L., & Allin, M. P. (2014). Preterm birth and structural brain alterations in early adulthood. Neuroimage Clin, 6, 180-191. https://doi.org/10.1016/j.nicl.2014.08.005

Nosarti, C., Rushe, T. M., Woodruff, P. W., Stewart, A. L., Rifkin, L., & Murray, R. M. (2004, Sep). Corpus callosum size and very preterm birth: relationship to neuropsychological outcome. Brain, 127 (Pt 9), 2080-2089. https://doi.org/10.1093/brain/awh230

Onland-Moret, N. C., Buizer-Voskamp, J. E., Albers, M. E. W. A., Brouwer, R. M., Buimer, E. E. L., Hessels, R. S., de Heus, R., Huijding, J., Junge, C. M. M., Mandl, R. C. W., Pas, P., Vink, M., van der Wal, J. J. M., Hulshoff Pol, H. E., & Kemner, C. (2020, 2020/12/01/). The YOUth study: Rationale, design, and study procedures. Developmental cognitive neuroscience, 46, 100868. https://doi.org/https://doi.org/10.1016/j.dcn.2020.100868

Ortinau, C., & Neil, J. (2015, Mar). The neuroanatomy of prematurity: normal brain development and the impact of preterm birth. Clin Anat, 28(2), 168-183. https://doi.org/10.1002/ca.22430

Parikh, N. A., Lasky, R. E., Kennedy, K. A., McDavid, G., & Tyson, J. E. (2013). Perinatal Factors and Regional Brain Volume Abnormalities at Term in a Cohort of Extremely Low Birth Weight Infants. PLoS One, 8(5), e62804. https://doi.org/10.1371/journal.pone.0062804

Peterson, B. S., Anderson, A. W., Ehrenkranz, R., Staib, L. H., Tageldin, M., Colson, E., Gore, J. C., Duncan, C. C., Makuch, R., & Ment, L. R. (2003, May). Regional Brain Volumes and Their Later Neurodevelopmental Correlates in Term and Preterm Infants. Pediatrics, 111(5), 939. https://doi.org/10.1542/peds.111.5.939

Rademaker, K., Lam, J., Van Haastert, I., Uiterwaal, C., Lieftink, A., Groenendaal, F., Grobbee, D., & De Vries, L. (2004). Larger corpus callosum size with better motor performance in prematurely born children. Seminars in Perinatology,

Stoodley, C. J., & Limperopoulos, C. (2016). Structure–function relationships in the developing cerebellum: evidence from early-life cerebellar injury and neurodevelopmental disorders. Seminars in Fetal

and Neonatal Medicine, 21(5), 356-364. https://doi.org/10.1016/j.siny.2016.04.010

Tataranno, M. L., Claessens, N. H., Moeskops, P., Toet, M. C., Kersbergen, K. J., Buonocore, G., Išgum, I., Leemans, A., Counsell, S., & Groenendaal, F. (2018, Apr). Changes in brain morphology and microstructure in relation to early brain activity in extremely preterm infants. Pediatric research, 83(4), 834-842. https://doi.org/10.1038/pr.2017.314

Taylor, H. G., Filipek, P. A., Juranek, J., Bangert, B., Minich, N., & Hack, M. (2011). Brain volumes in adolescents with very low birth weight: effects on brain structure and associations with neuropsychological outcomes. Dev Neuropsychol, 36(1), 96-117. https://doi.org/10.1080/87565641.2011.540544

Thompson, D. K., Adamson, C., Roberts, G., Faggian, N., Wood, S. J., Warfield, S. K., Doyle, L. W., Anderson, P. J., Egan, G. F., & Inder, T. E. (2013, Apr 15). Hippocampal shape variations at term equivalent age in very preterm infants compared with term controls: perinatal predictors and functional significance at age 7. NeuroImage, 70, 278-287. https://doi.org/10.1016/j.neuroimage.2012.12.053

Thompson, D. K., Warfield, S. K., Carlin, J. B., Pavlovic, M., Wang, H. X., Bear, M., Kean, M. J., Doyle, L. W., Egan, G. F., & Inder, T. E. (2006, Mar). Perinatal risk factors altering regional brain structure in the preterm infant. Brain, 130(3), 667-677. https://doi.org/10.1093/brain/awl277

van Tilborg, E., de Theije, C. G. M., van Hal, M., Wagenaar, N., de Vries, L. S., Benders, M. J., Rowitch, D. H., & Nijboer, C. H. (2018, Feb). Origin and dynamics of oligodendrocytes in the developing brain: Implications for perinatal white matter injury. Glia, 66(2), 221-238. https://doi.org/10.1002/glia.23256

Volpe, J. J. (2009a, Jan). Brain injury in premature infants: a complex amalgam of destructive and developmental disturbances. Lancet Neurol, 8(1), 110-124. https://doi.org/10.1016/S1474-4422(08)70294-1

Volpe, J. J. (2009b, Sep). Cerebellum of the premature infant: rapidly developing, vulnerable, clinically important. J Child Neurol, 24(9), 1085-1104. https://doi.org/10.1177/0883073809338067

Young, J. M., Vandewouw, M. M., Whyte, H. E. A., Leijser, L. M., & Taylor, M. J. (2020, Jul 14). Resilience and Vulnerability: Neurodevelopment of Very Preterm Children at Four Years of Age. Front Hum Neurosci, 14, 219. https://doi.org/10.3389/fnhum.2020.00219

SUPPLEMENTAL RESULTS

As a control analysis, a multiple regression analysis was performed for each relative volume (computed by taking each volume as a percentage of the total intracranial volume) of all structures. Relative brain volumes were used as a control rather than outcome variable, because the volume of the cerebrospinal fluid has a large effect on this measure. Results are displayed in Table S1, Figure S1 and Figure S2.

*Table S1. Details of the multiple regression control analysis for the relative brain volumes*

Variable	As a % of		Covariate F/p	Group F/p	Interaction F/p
Total Brain Volume	ICV	1	9.1/0.003*	38.6/<0.001*	23.8/<0.001*
	ICV	2	5.0/0.027*	14.4/<0.001*	4.0/0.049*
Cerebrospinal Fluid	ICV	1	21.3/<0.001*	64.4/<0.001*	28.2/<0.001*
	ICV	2	3.5/0.066	7.8/0.006*	3.8/0.054*
Ventricles	ICV	1	18.2/<0.001*	21.7/<0.001*	0.7/0.400
	ICV	2	5.5/0.020*	33.0/<0.001*	0.4/0.530
Cortical Gray Matter	ICV	1	361.6/<0.001*	206.1/<0.001*	0.9/0.342
	ICV	2	64.4/<0.001*	27.2/<0.001*	0.7/0.416
Unmyelinated White Matter	ICV	1	80.1/<0.001*	129.0/<0.001*	14.1/<0.001*
	ICV	2	8.0/0.005*	6.3/0.013*	1.7/0.201
Myelinated White Matter	ICV	2	8.8/0.004*	13.6/<0.001*	3.0/0.085
Cerebellum	ICV	1	9.1/0.003*	9.4/0.003*	4.5/0.036*
	ICV	2	9.9/0.002*	0.2/0.639	6.9/0.010*
Deep Gray Matter	ICV	1	11.9/<0.001*	7.3/0.008*	6.0/0.015*
	ICV	2	0.0/0.988	0.0/0.952	3.8/0.053
Brainstem	ICV	1	2.6/0.112	12.3/<0.001*	4.9/0.028*
	ICV	2	0.8/0.366	3.2/0.075	0.0/0.875

*Significant effect of covariate, group or interaction between both. ICV = Intracranial volume. Covariate: postmenstrual age at the moment of scanning. Groups: extremely preterm born or typically developing infants. Interaction: shows the interaction between group and covariate.
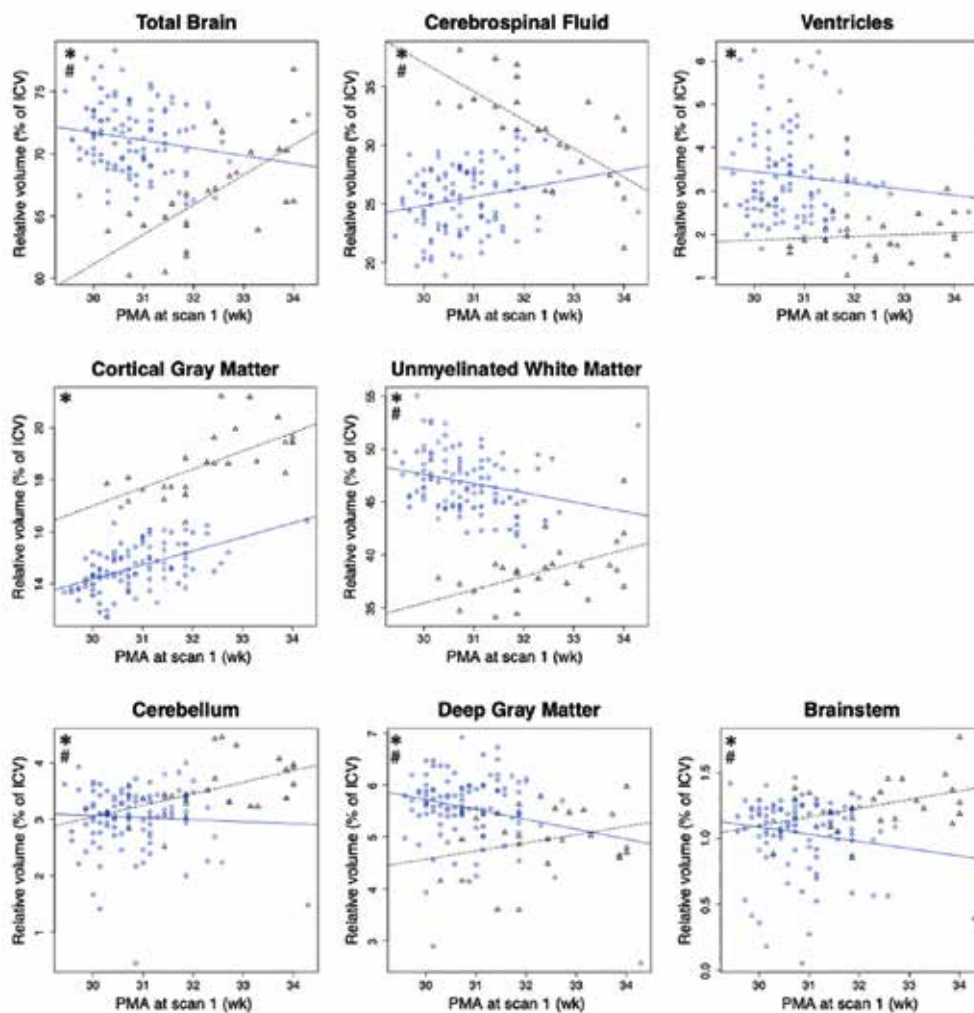
Figure S1. Relative volumes at MRI scan 1.

Figure shows brain and tissue volumes plotted against postmenstrual age (PMA) at scan 1 in the preterm (circles in blue) and typically developing (triangle in black) cohorts. *Significant difference in intercepts. #Significant difference in slope.
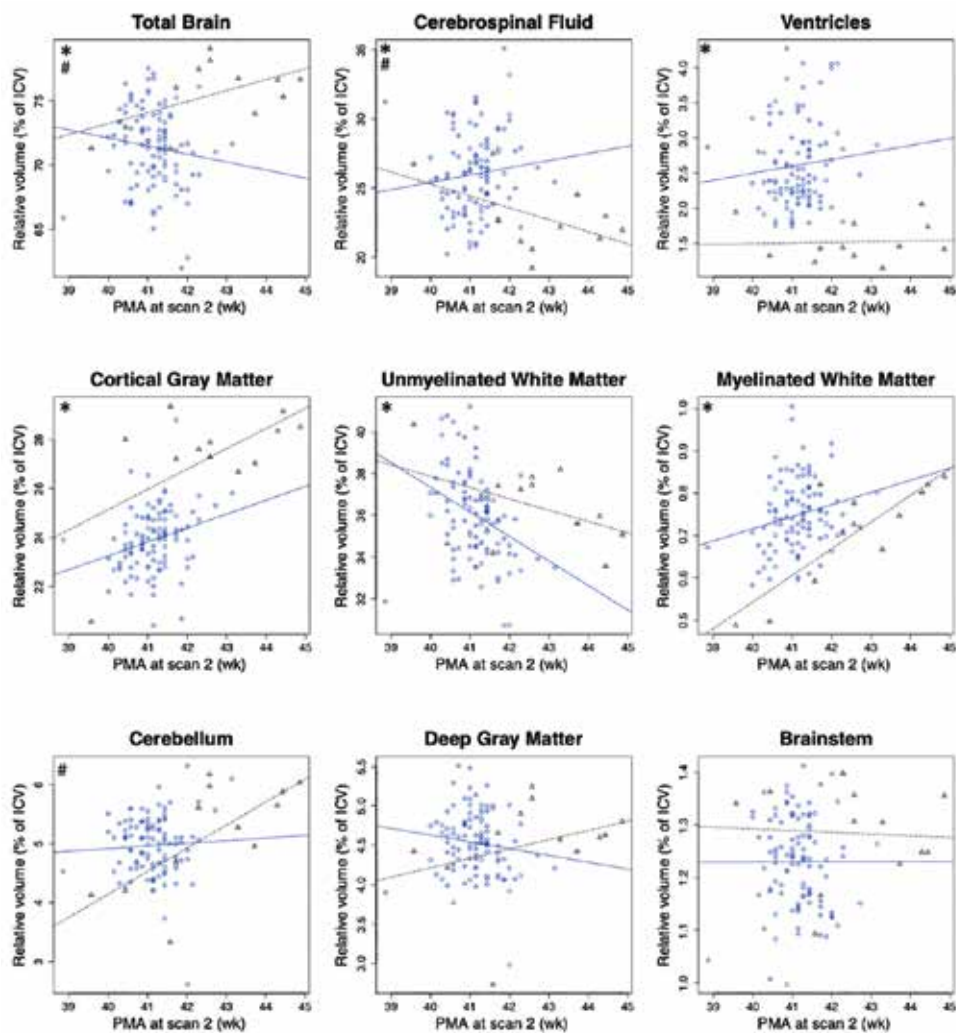
Figure S2. Relative volumes at scan 2.
Figure shows brain tissue and fluid volumes plotted against postmenstrual age (PMA) at scan 2 in the preterm (circles in blue) and typically developing (triangle in black) cohorts. *Significant difference in intercepts. #Significant difference in slope.
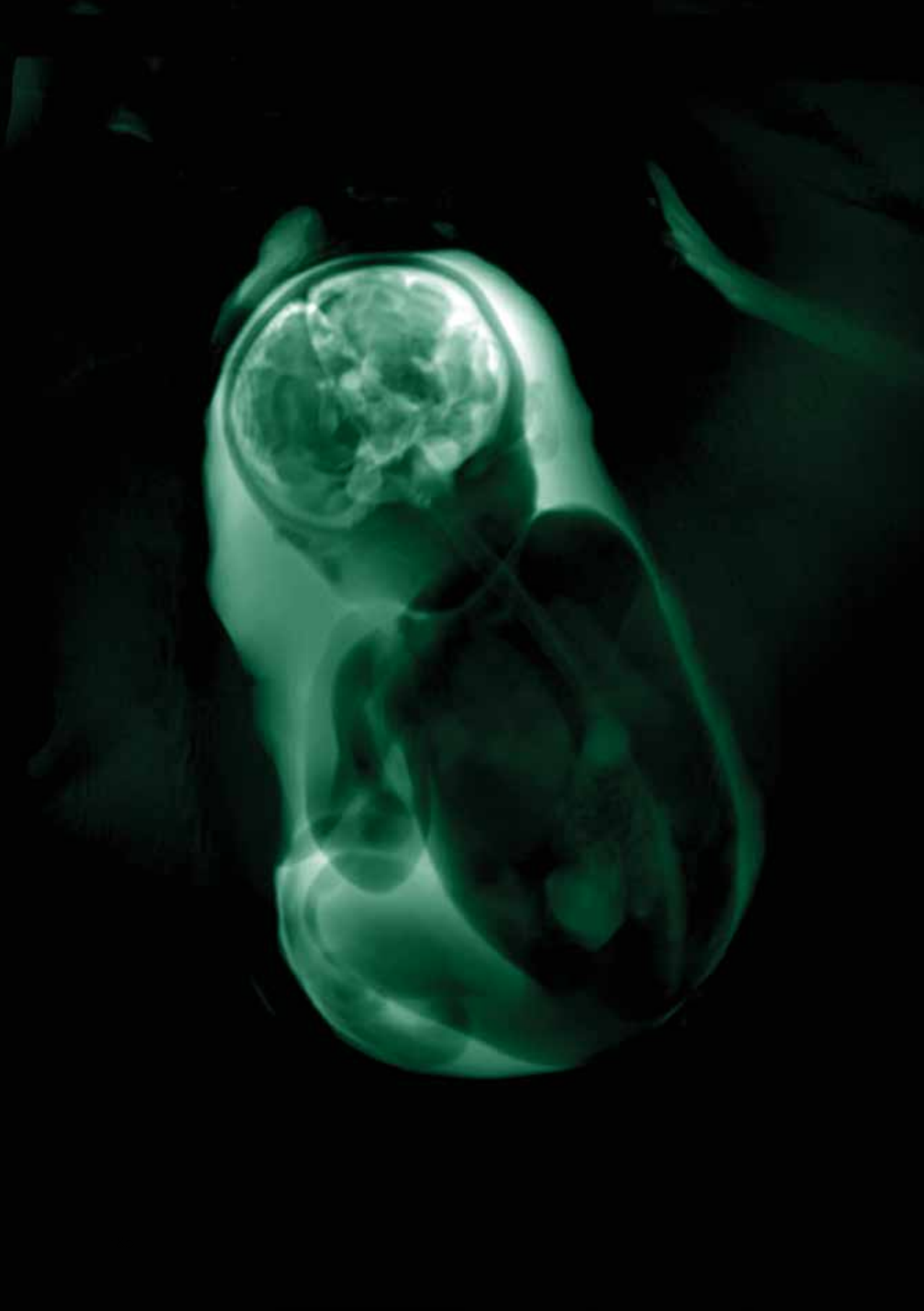
Chapter 8

Summarizing discussion and future directions
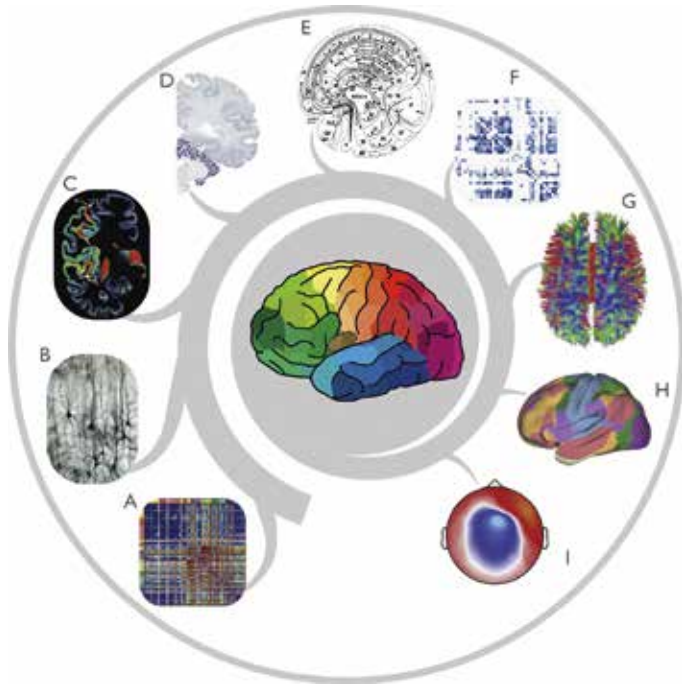
Figure 1. Multimodal approach to study the organization of the brain.
Brain organization can be studied on a wide range of scales, each providing a unique and complemen-
tary perspective on brain structure and function: (A) gene expression); (B) cell morphology;
(C) neurotransmitter receptor fingerprint (chemoarchitecture); (D) cortical laminar architecture;
(E) effective functional connectivity; (F) tract-tracing structural connectome; (G) diffusion-weighted
imaging; (H) resting-state functional magnetic resonance imaging networks; (I) and electroencephalo-
graphy (EEG). The figure and legend are reused from Scholtens et al. 2018, with permission from
Elsevier and authors (Scholtens & van den Heuvel, 2018).

The structural and functional foundation of the human brain develops in utero, making the fetal period essential for normal development and perturbations to these processes render the brain at risk for neurodevelopmental deficits. Mapping and understanding global fetal and neonatal brain growth *in vivo* are great challenges, data is sparse and multimodal approaches are needed to fill the gap in our knowledge on neuroimaging interpretation. The main aim of this thesis was twofold: 1) to map the tremendous structural transformation and maturation of the developing brain *in utero* and neonatal period, both in healthy individuals and preterm born infants; 2) to reveal its functional blueprint in the second half of pregnancy. In this chapter, I will summarize the main findings and integrate them with existing knowledge. Thereafter I will give my perspective on future progression in the field of perinatal MRI research and beyond.

STRUCTURAL BRAIN GROWTH

For centuries, researchers have been intrigued by the rapidly developing brain of the human fetus and infant (see for a historical overview of the last 150 years, Altman & Bayer, 2015). Structural brain growth observations are largely based on study of post-mortem materials (Altman & Bayer, 2015; Flechsig, 1920) and estimations from ultrasound imaging (Pistorius et al., 2008). Recent advances in neuroimaging techniques now enable longitudinal study of the fetal and neonatal brain making detailed measurements of brain growth possible, and enable to see what happens in the very early development of the healthy human brain *in vivo*. Following up on pioneering fetal and neonatal MRI studies, I aimed to map third trimester volumetric brain growth in multiple groups of healthy pregnant volunteers (and their neonates) and hospitalized preterm born infants (**chapter 7**) using our newest methods on brain segmentation (**chapter 6**).

Cerebral and cerebellar growth rates have been shown to change with gestational time, in **chapter 2** I show an absolute increase in global growth of the total brain, cortex, cerebellum, brainstem, extra cerebrospinal fluid (CSF) and ventricles around 29-34 weeks of gestation and neonatal period after birth. The results from our first healthy perinatal MRI cohort in the Netherlands, as presented in **chapter 7**, are in line with and complementary to recent MRI studies of healthy fetuses (fetuses without visual malformations and brain damage) (Andescavage et al., 2017; Clouchoux et al., 2012; Grossman et al., 2006). Regional fetal cortical growth patterns between 26 and 38 postconceptional weeks (pcw) as shown in **chapter 2** are consistent with global cortical growth patterns measured in preterm born neonates from other studies, starting at the primary motor and (somato) sensory cortices around 26 postconceptional weeks, followed by the visual cortex, which in turn matures earlier than the lateral parts of temporal and frontal lobe around term equivalent age (Garcia et al., 2018).

Genetic control and fetal cortical growth
Cortical growth during the last stage of pregnancy is likely under strong genetic control. Combining fetal weighted T1 MRI (Gholipour et al., 2017) and transcriptome profiles (BrainSpan, Atlas of the Developing Human Brain, brainspan.org), I show a spatiotemporal relationship of gene expression patterns and cortical growth in **chapter 2**. Specifically, expression patterns of genes related to biological pathways of neuronal systems, axon and synapse development and neural communication correspond to rapid cortical growth during 34 to 38 postconceptional weeks. Moreover, Dr. Wei and I correlate spatial gene expression with cortical growth, and reveal the top 100 correlating genes for three fetal age stages (24-30 pcw, 30-34 pcw, and 34-38 pcw). With this work I link molecular developmental mechanisms to macroscopic measures of cortical anatomy in early life, demonstrating the relationship between fetal gene expression and brain development

and highlight a future framework to demonstrate specific impact of early exposure to developmental risks.

MRI IN PRETERM BORN INFANTS

Being able to map perinatal brain development *in vivo* in healthy and patient groups brings the opportunity to compare them and thereby detect detailed alterations at an early stage. Comparing fetal brain volumes with extremely preterm born neonates (without moderate-to-large brain malformations and brain damage) around the beginning of the third trimester, I demonstrate in **chapter 7** that extremely preterm born infants have decreased size and growth of almost all (regional) brain volumes (total brain, cortical gray matter, unmyelinated white matter, deep gray matter, brainstem) around 30 weeks of gestation. These results are in line with former research (Andescavage et al., 2017; Clouchoux et al., 2012; Grossman et al., 2006), showing an increase in total brain, cerebrum, cerebellum, brainstem, extra and intra cerebrospinal fluid in healthy fetuses around 30 weeks of gestation.

Moreover, I show that the preterm brain is characterized by enlarged ventricles, presumably as a result of atrophy of other brain tissues due to brain damage common in preterm born infants. Variances in volumes of healthy and preterm born infants could be established by delays in brain growth, or other biological processes like disrupted apoptosis. Since up to 70% of neurons in the human cortex undergo apoptotic death in the last trimester (Rabinowicz et al., 1996), disruptions could exist due to preterm birth. Recent literature in mice models suggests this reduction might be caused by enhanced apoptosis and degeneration in the immature preterm neurons (Bhutta & Anand, 2001).

The timing and duration of adverse environmental experiences or clinical implications might affect the number of adverse effects in neonates admitted to the NICU (Bhutta & Anand, 2001). While various studies correct for gestational age at MRI, the reason for preterm birth or number of clinical complications had never been incorporated in MRI analyses. For example, differences between preterm birth with or without intrauterine growth restriction (IUGR) requires further exploration (Bruno et al., 2017). Monitoring these IUGR infants, prior to birth, could establish differences between in-utero disturbances and ex-utero influences. Longitudinal examinations of these perinatal patients and healthy controls will give us new insights over the course of development.

Acceleration in brain growth after preterm birth
In **chapter 7** I show that volumetric and growth alterations between healthy and preterm born neonates are only detectable for a couple of brain regions around term equivalent age. Our preterm cohort showed enlarged ventricles, smaller volumes of the cortical gray matter, and larger areas of myelinated white matter. The results suggest that brain

growth was delayed in neonates shortly after extremely preterm birth, but catch up by an acceleration of (regional) brain growth during the third trimester. However, healthy data acquisition for this sample is still in progress and conclusions from this study need to be taken with caution due to low participation numbers. It would be interesting to further explore the speed of volumetric brain growth in preterm infants around term birth in a larger population.

Cortical maturation features (such as surface area, gyrification index, sulcal depth and curvature) are biomarkers to explain how well the preterm infant is doing, while early maturation of the cortex may not be favorable if the developmental trajectory differs from a healthy trajectory (Kline et al., 2020). To scrutinize this notion further, future research should focus on microstructural development of the brain's connections (DTI) and its functionality (fMRI), comparing brains of healthy perinates and preterm infants. Microscale properties of the preterm infant brain (or from animal models) could be of additional value to tell the complete story of different growth trajectories, and thereby suggest if a higher maturation score (e.g., higher accelerated development) is favorable or not.

Neonatal brain growth after brain injury
Global differences on the developmental trajectory of preterm born infants and healthy fetuses are pointed out in **chapter 7**, but even larger differences between the two populations may be expected when there is MRI-detectable brain damage involved due to clinical complications. Cerebellar damage is a common (9%) neonatal complication in preterm born infants (Limperopoulos, Benson, et al., 2005; Zayek et al., 2012) and makes them vulnerable for a delay in cognition, motor, language, and/or behavioral development (Hortensius et al., 2018) or developing an autism spectrum disorder (Volpe, 2009; Wang et al., 2014). Even in the visual absence of cerebellar damage, mean cerebellar volume in premature infants is significantly smaller (Limperopoulos, Soul, et al., 2005), compared to healthy infants at term equivalent age (Andescavage et al., 2017). In our previous work, we aimed to estimate the influence of cerebellar injury on cortical growth during the neonatal period (Dijkshoorn et al.). Following up the study of Limperopoulos (2005), we believed that decreased innervation from the cerebellum, may alter early growth of structurally and functionally connected thalamic and cortical regions. Preterm born infants with or without cerebellar injury showed no global differences in cortical thickness or surface area, indicating that cerebellum injury did not affect the contralateral part of the cortex. Instead, we found a heterogeneous widespread pattern of bilateral thinning and thickening, which implicate complex cerebello-cerebral interactions to be present at term birth.

The relation between neurodevelopmental sequelae and cerebellar hemorrhages could be explained by 'diaschisis'. In 1910, Monakow beautifully postulated this concept

describing brain function as a balance between the brain's different components. Damage to one of the brain's components could affect other parts of the brain, which are seemingly unassociated with the site of injury (Finger et al.). Diaschisis could explain the relation between cerebellar hemorrhages and neurodevelopmental sequelae in extremely preterm infants when the cerebellum is part of dynamic brain networks that shape higher order brain function. Hypothetically, decreased innervation from the cerebellum, may alter growth of structurally and functionally connected thalamic and cortical regions.

BLUEPRINT OF THE FUNCTIONAL CONNECTOME

After having chartered structural development, I report on early brain function by studying the fetal functional connectome in **chapter 3** and **4**. My extensive fMRI research in fetuses from mid gestation to birth reveals that a robust fetal functional connectome of the cortex can be visualized and analyzed in the fetal brain for the very first time.

In **chapter 3**, I show that the fetal functional connectome displays a blueprint of the connectome that we observe in the adult brain. The collective set of fetal functional connections show an overlap of 62% with the adult brain. High associations between adult and fetal temporal, default mode, visual and motor networks were already observed, whereas frontomedial modules were less similar to the adult observed modules. Our research highlights the origin of proto-type resting-state networks, indicating that the ontogeny and important developmental stages of the connectome take place before the second trimester of pregnancy.

In **chapter 3** I show that the fetal functional connectome has a small world structure and a rich club architecture, which is comparable to the adult brain. In correspondence with neonatal hubs (Arichi et al., 2017; De Asis-Cruz et al., 2015; Fransson et al., 2010; Gao et al., 2009), fetal functional rich club nodes of chapter 4 and 5 are predominantly confined to temporal and midline cortical regions of the insular and frontal lobes, as well as the primary somatosensory regions. Taking the whole brain in consideration using ICA networks in **chapter 4**, we show that important fetal functional nodes (hubs) are also located in visual, motor and cerebellar regions as well as in association cortices close to fusiform facial and Wernicke regions. Taken together, my observations show that adult-like functional connectivity is established early in the womb, indicating that the prenatal period may be foundational for adult 'connectome health' (Krontira et al., 2020; Thomason, 2020).

Functional development of the fetal and preterm infant brain
Environmental perturbations such as preterm birth, may potentially bring the development of our functional networks at risk. Consulting some recent literature about fMRI research in preterm born infants (extrauterine) and healthy fetuses (intrauterine),

differences between functional developmental growth trajectories are not straightforward. Instead, many similarities can be found between intra- and extrauterine functional brain development. First, prototypes of resting state networks have been portrayed both in preterm and fetal brains (Damaraju et al., 2010; Doria et al., 2010; Gao et al., 2009; Schöpf et al., 2012; Smyser et al., 2010; Thomason et al., 2013; Thomason et al., 2015; van den Heuvel et al., 2015), whereby both primary and association brain regions demonstrate centrality in network organization (Thomason, 2018). Second, medial-to-lateral development of brain functional connectivity has been demonstrated in preterm infants (Smyser et al., 2010), and in fetuses (Thomason et al., 2013). Third, global efficiency and functional coupling have a similar developmental trajectory in the developing fetal and preterm brain (Cao et al., 2016; De Asis-Cruz et al., 2015; Fransson et al., 2010; Scheinost et al., 2016; van den Heuvel et al., 2015).

The role of regions described as functional hubs in the fetal and preterm infant brain is a topic of debate and could be different between populations. Rich club nodes in the adult brain enhance network efficiency and therefore global communication and information integration between brain systems (van den Heuvel et al., 2012). Presumably, hubs in the fetal brain facilitate early connectivity strengthening (Thomason, 2018), but they may also form potential points of vulnerability for network development as well (Di Martino et al., 2014). The location of fetal network hubs largely overlapped with hubs in preterm infants (Ball et al., 2014; Bouyssi-Kobar et al.; De Asis-Cruz et al.; Fransson et al., 2010; Gao et al., 2015; Limperopoulos, Soul, et al., 2005; van den Heuvel et al., 2015), and hubs in the fusiform gyrus are found in the fetal (**Chapter 4**; (van den Heuvel et al., 2018) as well as the preterm infant brain (van den Heuvel et al., 2015). Most cortical hubs in the brains of preterm infants are located in the auditory and visual areas (Damaraju et al., 2010; Doria et al., 2010; Fransson et al., 2007), while hubs in the visual cortex seem less well represented in the fetal brain.

The differences between hubs in the fetal and preterm infant brain may be caused by the differences of sensory input of the two populations. Since the visual and default mode network are based on and developed through visual experiences (Buckner et al., 2008), the observation of less well-developed sensory networks in utero (De Asis-Cruz et al.) may be due to absence of sensory experiences, while ex-utero preterm infants are exposed to various sensory stimuli in the NICU (Pineda et al., 2017). Asis-Cruz et al. (2020) indeed observed that sensory input and stress-related brain regions have stronger connectivity values in the preterm brain (without visible brain damage) compared to fetuses, suggesting that early extra-uterine environment exposure alters the development of select neural networks. However, any conclusions from this or related studies have to be drawn extra carefully, because differences in physiology might be originate from differences in the acquisition parameters. Future research has to explore how external stimuli influence network development, by directly comparing functional

connectomes between intra- and extrauterine brain development, before strong conclusions can be drawn.

**Microscale underpinnings of functional connectivity**
To broaden our knowledge on the underlying construct of functional connectivity patterns in the primate brain I reported on the relation between the chemoarchitecture at the microscale and effective region-to-region functional interactions, described in **chapter 5**. Cross-correlating regional receptor density levels and effective (strychnine induced) functional connectivity in the macaque cortex, I showed the strength of macroscale connectivity pathways to be related to the excitatory versus inhibitory neurotransmitter receptor architecture of cortical regions. Specifically, the chemoarchitecture and functional connectivity measures have shown regions with a larger proportion of excitatory versus inhibitory neurotransmitter receptor levels to have stronger induced functional connections in the macaque (**chapter 5**) and stronger resting-state fMRI connections in the adult human cortex (van den Heuvel et al., 2016). To conclude, functional connectivity patterns reflect macroscale functional signals by measuring correlations of intrinsic fluctuations in the blood oxygen level dependent signal orchestrated by the underlying chemoarchitecture, at least in the adult primate brain.

Macroscale connectivity patterns in the fetal and adult brain show much overlap and reflect common features (**chapter 3**). Still, fetal functional brain activity might be established from different microscale processes. The fetal transcriptome for example, differs a lot from the adult transcriptome (see for example (Hawrylycz et al., 2012; Miller et al., 2014). Many neurons are not fully mature or at their final location during fetal development, and perhaps neurons have a totally different excitatory or inhibitory function (Ben-Ari, 2002), additionally, axonal connections are not fully myelinated. A multimodal analysis combining fetal functional connectivity with structural connectivity derived from DTI could provide more insights into the structural-functional relationship of the fetal brain, especially in combination with gene expression data. Understanding the underlying construct of functional connectivity patterns could provide more insights in the development of spontaneous bursting activity into neural circuitry development and could perhaps extend our knowledge in understanding early alterations in the developing connectome.

TECHNICAL CHALLENGES

The technical challenges of fetal and neonatal MRI cannot be ignored in the discussion of this thesis. As any new field of research, challenges in fetal and neonatal neuroimaging are due to multiple facets of the research. First, finding 'healthy' or 'normal' pregnant and neonatal participants for a control group is challenging. Pregnant and healthy newborn volunteers of 'an average society' are hard to include in studies, due to: the

burden of lying still in a small tube while being highly pregnant, the difficulty to get and keep a newborn asleep while being in a noisy scanner, and the fear of safety of an MRI for a newborn or unborn child. As a consequence, some of my studies have low participation numbers (such as **chapter 7**, the inclusion of new participants is still in progress) and conclusions from these works should be drawn with some caution, and validated in the future using larger samples. Additionally, the background of the cohorts is homogeneous. Utrecht's YOUth cohort for example has a high number of highly educated women in their sample (for an overview of the rationale, design and open data repository see, Onland-Moret et al., 2020). These women are likely more motivated to participate in academic research and are presumably less scared for the MRI risks, due to their experience in the field of medicine and research. Wayne State University's cohort has a high rate of mothers with high stress, low education and low socioeconomic status. Fortunately, perinatal MRI databases and templates become publicly available through various sources (e.g., Serag et al., Boston's CRL database, Utrecht's YOUth cohort, London's dHCP, Detroit's fetal fMRIs), bringing a comprehensive analysis of fetuses and neonates with different backgrounds within reach.
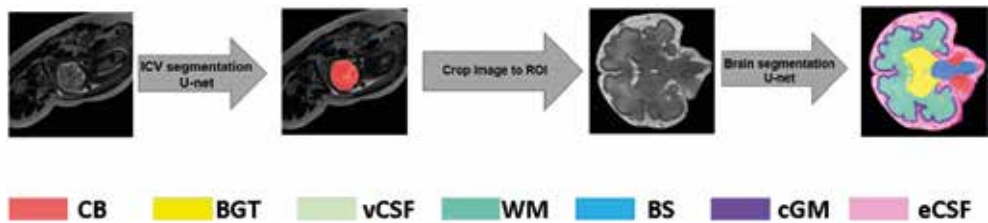
Figure 2. Automatic fetal MRI segmentation pipeline.
Displayed are the deep learning segmentation-processing steps including intracranial tissue segmentation, image extraction of the intracranial tissue, brain segmentation into different neural tissue classes: cerebellum (red), basal ganglia and thalami (yellow), ventricles (light green), white matter (turquoise), brainstem (blue), cortical gray matter (purple) and cerebrospinal fluid (pink). Figure is reused with permission from (N. Khalili, N. Lessmann, et al., 2019).

A second challenge of fetal MRI and neonatal MRI during natural sleep can be found in acquisition and processing difficulties. High motion during imaging, due to a freely moving fetus or neonate and maternal respiration, is a common problem of fetal and neonatal MRI. Consequently, acquisition time may be long to get high quality images, not all MRI scans can be useful for research and processing of the data can be time consuming. For example, due to movement (Ferrazzi et al., 2014), significant amounts of fMRI data have been discarded, varying from 41% (Wheelock et al., 2019) to 81.6% (Thomason et al., 2013). Apart from inefficient costly scanning time, it might bias the

results by reflecting a particular sleep state (Thomason et al., 2015). Thereby, even movement as small as 0.2mm shows to impact the functional connectome, by decreasing long-range and increasing short range connectivity (Power et al., 2012; Van Dijk et al., 2012). Ideally, improvements in acquisition and post-processing should be made. Comparisons between groups often include differences in MRI scanners, magnetic field strengths and image post-processing pipelines, including motion correction. Some new publicly available processing pipelines, such as our automatic segmentation algorithm to parcellate the intracranial volume (**chapter 6**), and our newest in house-developed pipelines for further fetal and neonatal neural tissue segmentation (see **Figure 2**, (Claessens et al., 2019; N. Khalili, N. Lessmann, et al., 2019; N. Khalili, E. Turk, et al., 2019; Nadieh Khalili et al., 2019), can help overcome this problem. Additionally, new freely available pipelines for the processing of the fetal and neonatal images may help to get brain volumes (e.g. Makropoulos et al., 2016; Makropoulos et al., 2018), fMRI processing and number and strength of connections (SPM's conn toolbox) as well as connectomic properties of the fetal and neonatal brain (Bastiani et al., 2019). Still, age-specific (per gestational week for example) development of especially functional (fMRI) and structural (DTI) connections are difficult to analyze due to macroscopic structural changes and the introduction of motion into the data. I choose to analyze the average fetal connectome, but with age specific templates (Gholipour et al., 2017; Khan et al., 2019) and higher quality (automized) motion correction, it will be possible to give a more detailed description of the functional and structural development of the connectome over time.

RELEVANCE FOR NEUROPSYCHIATRIC RISK IN FUTURE RESEARCH

Results presented in this thesis show that the fetal and neonatal period is important for the development of specialized functional domains in an economic and integrative network, suggesting that the prenatal period is important to point out vulnerable windows for developing later life brain function deficits. It however does not show a complete model yet. Many developmental neuropsychiatric disorders such as schizophrenia, autism spectrum disorder (ASD) and attention deficit hyperactivity disorder (ADHD) potentially have a prenatal origin. Still, the majority of research to these disorders are at the adult stage when a clinical diagnosis is more stable and MRI research is less complicated to conduct. Potential avenues for future research in fetal or neonatal MRI and connectomic research lie in the understanding of prenatal origins of developmental disorders and predicting future brain health, by studying the complex interplay of early altered volumetric growth, neural connectivity and the susceptibility for environmental risk factors and (epi)genetic programming.

Genetics and perinatal risk factors
Key to understanding developmental disorders is having knowledge on the underlying etiology. Although many genes and genetic mutations are linked to neurodevelopmental

disorders, the genetic etiology of these disorders is not clear (Misiak et al., 2018). Research on the spatio-(regional gene expression levels) temporal (over time) pattern of the transcriptome may illuminate the underlying biology of neurodevelopmental disorders (Tebbenkamp et al., 2014). For example, developmental transcriptome data is a key to interpreting disease-associated mutations and transcriptional changes. Novel approaches integrating the spatial and temporal dimensions of these data have increased our understanding of when and where pathology occurs. Examples can be found in the genetic predispositions of schizophrenia and ASD, which can be traced back to the second trimester of pregnancy (Gulsuner & McClellan, 2014; Willsey et al., 2013).

Environmental risk factors are other great candidates that can help understand or predict the outcome of altered neurocognition in the developing infant (Neville & Bavelier, 2000). Many infants develop normal, even with a genetic predisposition for schizo-phrenia and altered neural connectivity (Collin et al., 2014) or after exposure to environmental insults such as preterm birth showing the plasticity of the developing brain, and the complexity of the nature nurture interplay. Perhaps, many neurodevelopmental disorders are a result of environmental factors that trigger altered epigenetic mechanisms that play a significant role in fetal brain development. For example, in utero exposure to risky maternal lifestyle (e.g., stress, food intake, obesity, smoking and alcohol or drug intake) and maternal infections are linked to changes in the placental epigenome and subsequently associated with developmental disorders (see for review, Banik et al., 2017). Knowledge on how emerging neural networks adapt (or maladapt) to pathological perturbation is needed to understand the progression of brain disorders (Fornito et al., 2015) and how alterations may be prevented. In other words, maternal lifestyle, age and infections may influence placental and fetal epigenetic pathways that may lead to altered fetal and neonatal brain development that is common in developmental disorders. To understand this mechanism, more research into the fetal and neonatal brain is needed.

Developmental disconnectivity
Combining perinatal risk factors with the field of developmental connectomics would provide a perfect framework to study developmental disorders and disconnectivity in a new perspective. DTI and fMRI studies show that schizophrenia, ADHD and ASD can be characterized as 'disconnectivity' disorders (Craddock et al., 2013; Friston & Frith, 1995), showing altered network properties or distributed alterations of connectivity patterns between brain regions (de Lange et al., 2019; Griffa et al., 2013; Zalesky et al., 2011). Abnormal functional integration as a consequence of these connectomic alterations can be observed as well and possibly underlie different cognitive impairments related to the pathology (Friston, 2002; Friston & Frith, 1995).

Connectivity measurements during development could be a valuable biomarker to detect and follow connectivity alterations at an early stage (Di Martino et al., 2014; Thomason,

2020)., because prenatal processes may interfere with the developing connectome. For example, preterm birth may influence the functional architecture of thalamo-cortical networks (Ball et al., 2013). Maternal viral infections, extensive stress, food-intake, alcohol and medication use, among others, all have strong influence on later life functional connectivity of children (de Water et al., 2018; Grewen et al., 2015; Infante et al., 2017; Li et al., 2016; Rudolph et al., 2018; Salzwedel et al., 2016; Van den Bergh et al., 2020). Without the direct comparisons of fetal neural connectivity and prenatal risk factors these claims are hard to make. Carefully, first fetal fMRI studies comparing connectivity patterns of different (patient) cohorts are published. For example, differences in functional network development between preterm born infants and healthy fetuses can be detected around 30 weeks of gestation (De Asis-Cruz et al., 2015), and even prior to actual preterm birth (Thomason et al., 2017). Furthermore, fetal fMRI may prospect future brain function as increased connectivity between motor regions showed more mature motor functions later in life (Thomason et al., 2018), and this connectivity was stronger in females. The female brain could, therefore, be less susceptible to early environmental programming (Thomason et al., 2019).

Connectomic research between different patient and healthy cohorts during fetal and neonatal development could provide valuable new information on developmental disorders. A recent study of de Lange et al. (de Lange et al., 2019) shows that connections central to network integration and communication are potential hotspots for disruptions across multiple psychiatric and neurological disorders. Also, alterations of connectomic hubs are pointed out as hotspots in the psychiatric brain (Bullmore & Sporns, 2009). It would be interesting to follow the developmental trajectory of the central communication paths and hubs across early development to test whether these could serve as early biomarkers for common developmental disorders as well. Connectome-based predictive modelling (CPM) might be a valuable tool to investigate the relation of which connectome measures predict future outcome (see for example the CPM study on the maternal brainRutherford et al., 2020).

Longitudinal follow up
Large cohort studies are needed to prove causal relations between early neurodevelopmental alterations that are detectable on MRI, maternal and environmental risk factors and epigenetic changes. Following up these infants, potentially early perinatal perturbations can be linked to changes in behavior, cognition or well-being of the developing child.

Utrecht's YOUth cohort follows children from 20 weeks of pregnancy until late childhood and is a perfect example of such an extensive longitudinal study (YOUth study, Onland-Moret et al., 2020). It would be an opportunity to analyze the connectome at different time points in these children, and link early connectivity alterations to environmental

Figure 3. Mother-infant EEG setup.
Figure displays an EEG hyperscanning setup, connecting two EEG boxes of mother and infant to the same computer. In combination with video material, mother-infant EEG enables the simultaneous measurement of activity in two brains and behavioral synchronization.

perturbations such as prenatal maternal stress or anxiety for example. Following these children, we will probably see that connectivity patterns in most children normalize and in some not. Our job will be to understand why this is the case, by analyzing parenting behavior, child social and behavioral competence, genetics and other measurements from EEG or MRI.

Research into the influence of maternal prenatal and postnatal risk factors is done at Tilburg University. Hypothetically, prenatal maternal risk factors such as stress and anxiety may program the fetal brain in a vulnerable state. On top of that, maternal stress and anxiety might also interfere with the manner of caregiving of the mother when the baby is born (Atzil & Gendron, 2017). These perturbations, separated or accumulated, could potentially lead to altered connectome development. A way to get insights into this mechanism, is to monitor the mother and baby. Recently, an innovative paradigm shift from one-person-neuroscience to two-person-neuroscience enables the simultaneous measurement of neural activity in mother and infant and thereby provide a framework to

measure brain-to-brain synchrony during rest, behavioral or social tasks (see for reviews (Turk, Endevelt-Shapira, et al., 2022; Turk, Vroomen, et al., 2022). This mother-child EEG (e.g., EEG hyperscanning) set up could potentially bring even more insight on how parents and children are connected on a biological level.

With more and more open data of large fetal, neonatal and infant cohorts appearing online, new discoveries on the etiology of neurodevelopmental disorders are within reach in the near future, especially when multimodal information on the developing brain is combined. Eventually, mapping the fetal and neonatal brain will contribute to the early recognition and treatment of illnesses of the emerging mind.

CONCLUDING REMARKS

The human brain undergoes a fascinating transformation during the second half of pregnancy and around birth, making it a critical period for the developing brain. Acquiring knowledge on early brain maturation contributes to our understanding of the brain's functioning, and perhaps even more important, it can give us insights on the impacts of risk factors in the time course of development. Research into fetal and neonatal brain development is still in its infancy, but fortunately, windows of opportunities have been opened to study fetal and preterm neonatal brain development in vivo and, in more detail, using current progress in MRI techniques and new available (healthy) perinatal MRI data. In this thesis, MRI has been adopted to visualize and study altered and healthy brain development around birth, making a significant contribution towards our understanding of normal structural and functional maturation stages of the human brain. The future of perinatal MRI in combination with connectomics, knowledge on maternal and early developmental risk factors, follow up research and transcriptomics, will provide new unique opportunities to study individual differences in structural and functional brain growth during early development. By connecting multimodal information of the developing mind, the potential of perinatal MRI is to study neuropsychiatric risk and thereby find new targets for therapeutic strategies.

REFERENCES

Altman, J., & Bayer, A. (2015). Development of the Human Neocortex. A Review and Interpretation of the Histological Record. USA: The Laboratory of Developmental Neurobiology, Inc. https://neurondevelopment.org/wp-content/uploads/2015/11/human-neocortical-development-complete.pdf

Andescavage, N. N., du Plessis, A., McCarter, R., Serag, A., Evangelou, I., Vezina, G., Robertson, R., & Limperopoulos, C. (2017, Nov 1). Complex Trajectories of Brain Development in the Healthy Human Fetus. Cereb Cortex, 27(11), 5274-5283. https://doi.org/10.1093/cercor/bhw306

Arichi, T., Whitehead, K., Barone, G., Pressler, R., Padormo, F., Edwards, A. D., & Fabrizi, L. (2017, Sep 12). Localization of spontaneous bursting neuronal activity in the preterm human brain with simultaneous EEG-fMRI. Elife, 6, e27814. https://doi.org/10.7554/eLife.27814

Atzil, S., & Gendron, M. (2017, Oct). Bio-behavioral synchrony promotes the development of conceptualized emotions. Curr Opin Psychol, 17, 162-169. https://doi.org/10.1016/j.copsyc.2017.07.009

Ball, G., Aljabar, P., Zebari, S., Tusor, N., Arichi, T., Merchant, N., Robinson, E. C., Ogundipe, E., Rueckert, D., Edwards, A. D., & Counsell, S. J. (2014, May 20). Rich-club organization of the newborn human brain. Proc Natl Acad Sci U S A, 111(20), 7456-7461. https://doi.org/10.1073/pnas.1324118111

Ball, G., Boardman, J. P., Aljabar, P., Pandit, A., Arichi, T., Merchant, N., Rueckert, D., Edwards, A. D., & Counsell, S. J. (2013, Jun). The influence of preterm birth on the developing thalamocortical connectome. Cortex, 49(6), 1711-1721. https://doi.org/10.1016/j.cortex.2012.07.006

Banik, A., Kandilya, D., Ramya, S., Stunkel, W., Chong, Y. S., & Dheen, S. T. (2017, May 24). Maternal Factors that Induce Epigenetic Changes Contribute to Neurological Disorders in Offspring. Genes (Basel), 8(6), 150. https://doi.org/10.3390/genes8060150

Bastiani, M., Andersson, J. L. R., Cordero-Grande, L., Murgasova, M., Hutter, J., Price, A. N., Makropoulos, A., Fitzgibbon, S. P., Hughes, E., Rueckert, D., Victor, S., Rutherford, M., Edwards, A. D., Smith, S. M., Tournier, J. D., Hajnal, J. V., Jbabdi, S., & Sotiropoulos, S. N. (2019, Jan 15). Automated processing pipeline for neonatal diffusion MRI in the developing Human Connectome Project. NeuroImage, 185, 750-763. https://doi.org/10.1016/j.neuroimage.2018.05.064

Ben-Ari, Y. (2002, Sep). Excitatory actions of gaba during development: the nature of the nurture. Nat Rev Neurosci, 3(9), 728-739. https://doi.org/10.1038/nrn920

Bhutta, A. T., & Anand, K. J. (2001, Mar). Abnormal cognition and behavior in preterm neonates linked to smaller brain volumes. Trends Neurosci, 24(3), 129-130; discussion 131-122. https://doi.org/10.1016/s0166-2236(00)01747-1

Bouyssi-Kobar, M., du Plessis, A. J., McCarter, R., Brossard-Racine, M., Murnick, J., Tinkleman, L., Robertson, R. L., & Limperopoulos, C. (2016, Nov). Third Trimester Brain Growth in Preterm Infants Compared With In Utero Healthy Fetuses. Pediatrics, 138(5), e20161640. https://doi.org/10.1542/peds.2016-1640

Bruno, C. J., Bengani, S., Gomes, W. A., Brewer, M., Vega, M., Xie, X., Kim, M., & Fuloria, M. (2017). MRI Differences Associated with Intrauterine Growth Restriction in Preterm Infants. Neonatology, 111(4), 317-323. https://doi.org/10.1159/000453576

Buckner, R. L., Andrews-Hanna, J. R., & Schacter, D. L. (2008, Mar). The brain's default network: anatomy, function, and relevance to disease. Ann N Y Acad Sci, 1124, 1-38. https://doi.org/10.1196/annals.1440.011

Bullmore, E., & Sporns, O. (2009, Mar). Complex brain networks: graph theoretical analysis of structural and functional systems [10.1038/nrn2575]. Nat Rev Neurosci, 10(3), 186-198. https://doi.org/10.1038/nrn2575

Cao, M., He, Y., Dai, Z., Liao, X., Jeon, T., Ouyang, M., Chalak, L., Bi, Y., Rollins, N., & Dong, Q. (2016). Early development of functional network segregation revealed by connectomic analysis of the preterm human brain. Cerebral Cortex, 27(3), 1949-1963.

Claessens, N. H. P., Khalili, N., Isgum, I., Ter Heide, H., Steenhuis, T. J., Turk, E., Jansen, N. J. G., de Vries, L. S., Breur, J., de Heus, R., & Benders, M. (2019, May). Brain and CSF Volumes in Fetuses and Neonates with Antenatal Diagnosis of Critical Congenital Heart Disease: A Longitudinal MRI Study. AJNR Am J Neuroradiol, 40(5), 885-891. https://doi.org/10.3174/ajnr.A6021

Clouchoux, C., Kudelski, D., Gholipour, A., Warfield, S. K., Viseur, S., Bouyssi-Kobar, M., Mari, J. L., Evans, A. C., du Plessis, A. J., & Limperopoulos, C. (2012, Jan). Quantitative in vivo MRI measurement of cortical development in the fetus. Brain Struct Funct, 217(1), 127-139. https://doi.org/10.1007/s00429-011-0325-x

Collin, G., Kahn, R. S., de Reus, M. A., Cahn, W., & van den Heuvel, M. P. (2014, Mar). Impaired rich club connectivity in unaffected siblings of schizophrenia patients. Schizophr Bull, 40(2), 438-448. https://doi.org/10.1093/schbul/sbt162

Craddock, R. C., Jbabdi, S., Yan, C. G., Vogelstein, J. T., Castellanos, F. X., Di Martino, A., Kelly, C., Heberlein, K., Colcombe, S., & Milham, M. P. (2013, Jun). Imaging human connectomes at the macroscale. Nat Methods, 10(6), 524-539. https://doi.org/10.1038/nmeth.2482

Damaraju, E., Phillips, J. R., Lowe, J. R., Ohls, R., Calhoun, V. D., & Caprihan, A. (2010). Resting-state functional connectivity differences in premature children. Front Syst Neurosci, 4, 23. https://doi.org/10.3389/fnsys.2010.00023

De Asis-Cruz, J., Bouyssi-Kobar, M., Evangelou, I., Vezina, G., & Limperopoulos, C. (2015, Dec 7). Functional properties of resting state networks in healthy full-term newborns. Sci Rep, 5, 17755. https://doi.org/10.1038/srep17755

De Asis-Cruz, J., Kapse, K., Basu, S. K., Said, M., Scheinost, D., Murnick, J., Chang, T., du Plessis, A., & Limperopoulos, C. (2020, Oct 1). Functional brain connectivity in ex utero premature

infants compared to in utero fetuses. NeuroImage, 219, 117043. https://doi.org/10.1016/j.neuro-image.2020.117043

de Lange, S. C., Scholtens, L. H., Alzheimer's Disease Neuroimaging, I., van den Berg, L. H., Boks, M. P., Bozzali, M., Cahn, W., Dannlowski, U., Durston, S., Geuze, E., van Haren, N. E. M., Hillegers, M. H. J., Koch, K., Jurado, M. A., Mancini, M., Marques-Iturria, I., Meinert, S., Ophoff, R. A., Reess, T. J., Repple, J., Kahn, R. S., & van den Heuvel, M. P. (2019, Sep). Shared vulnerability for connectome alterations across psychiatric and neurological brain disorders. Nat Hum Behav, 3(9), 988-998. https://doi.org/10.1038/s41562-019-0659-6

de Water, E., Proal, E., Wang, V., Medina, S. M., Schnaas, L., Tellez-Rojo, M. M., Wright, R. O., Tang, C. Y., & Horton, M. K. (2018, Jan). Prenatal manganese exposure and intrinsic functional connectivity of emotional brain areas in children. NeuroToxicology, 64, 85-93. https://doi.org/10.1016/j.neuro.2017.06.006

Di Martino, A., Fair, D. A., Kelly, C., Satterthwaite, T. D., Castellanos, F. X., Thomason, M. E., Craddock, R. C., Luna, B., Leventhal, B. L., Zuo, X. N., & Milham, M. P. (2014, Sep 17). Unraveling the miswired connectome: a developmental perspective. Neuron, 83(6), 1335-1353. https://doi.org/10.1016/j.neuron.2014.08.050

Dijkshoorn, A. B. C., Turk, E., Hortensius, L. M., van der Aa, N. E., Hoebeek, F. E., Groenendaal, F., Benders, M., & Dudink, J. (2020, Mar 24). Preterm infants with isolated cerebellar hemorrhage show bilateral cortical alterations at term equivalent age. Sci Rep, 10(1), 5283. https://doi.org/10.1038/s41598-020-62078-9

Doria, V., Beckmann, C. F., Arichi, T., Merchant, N., Groppo, M., Turkheimer, F. E., Counsell, S. J., Murgasova, M., Aljabar, P., Nunes, R. G., Larkman, D. J., Rees, G., & Edwards, A. D. (2010, Nov 16). Emergence of resting state networks in the preterm human brain. Proc Natl Acad Sci U S A, 107(46), 20015-20020. https://doi.org/10.1073/pnas.1007921107

Ferrazzi, G., Kuklisova Murgasova, M., Arichi, T., Malamateniou, C., Fox, M. J., Makropoulos, A., Allsop, J., Rutherford, M., Malik, S., Aljabar, P., & Hajnal, J. V. (2014, Nov 1). Resting State fMRI in the moving fetus: a robust framework for motion, bias field and spin history correction. NeuroImage, 101, 555-568. https://doi.org/10.1016/j.neuroimage.2014.06.074

Finger, S., Koehler, P. J., & Jagella, C. (2004, Feb). The Monakow concept of diaschisis: origins and perspectives. Archives of Neurology, 61(2), 283-288. https://doi.org/10.1001/archneur.61.2.283

Flechsig, P. E. (1920). Anatomie des menschlichen Gehirns und Rückenmarks auf myelogenetischer Grundlage (Vol. 1). G. Thieme.

Fornito, A., Zalesky, A., & Breakspear, M. (2015, Mar). The connectomics of brain disorders. Nat Rev Neurosci, 16(3), 159-172. https://doi.org/10.1038/nrn3901

Fransson, P., Åden, U., Blennow, M., & Lagercrantz, H. (2010). The functional architecture of the infant brain as revealed by resting-state fMRI. Cerebral Cortex, 21(1), 145-154.

Fransson, P., Skiold, B., Horsch, S., Nordell, A., Blennow, M., Lagercrantz, H., & Aden, U. (2007, Sep 25). Resting-state networks in the infant brain. Proc Natl Acad Sci U S A, 104(39), 15531-15536. https://doi.org/10.1073/pnas.0704380104

Friston, K. J. (2002, Jun). Dysfunctional connectivity in schizophrenia. World psychiatry, 1(2), 66-71. https://www.ncbi.nlm.nih.gov/pubmed/16946855

Friston, K. J., & Frith, C. D. (1995). Schizophrenia: a disconnection syndrome? Clin Neurosci, 3(2), 89-97. https://www.ncbi.nlm.nih.gov/pubmed/7583624

Gao, W., Alcauter, S., Elton, A., Hernandez-Castillo, C. R., Smith, J. K., Ramirez, J., & Lin, W. (2015, Sep). Functional Network Development During the First Year: Relative Sequence and Socioeconomic Correlations. Cereb Cortex, 25(9), 2919-2928. https://doi.org/10.1093/cercor/bhu088

Gao, W., Zhu, H., Giovanello, K. S., Smith, J. K., Shen, D., Gilmore, J. H., & Lin, W. (2009, Apr 21). Evidence on the emergence of the brain's default network from 2-week-old to 2-year-old healthy pediatric subjects. Proc Natl Acad Sci U S A, 106(16), 6790-6795. https://doi.org/10.1073/pnas.0811221106

Garcia, K. E., Robinson, E. C., Alexopoulos, D., Dierker, D. L., Glasser, M. F., Coalson, T. S., Ortinau, C. M., Rueckert, D., Taber, L. A., Van Essen, D. C., Rogers, C. E., Smyser, C. D., & Bayly, P. V. (2018, Mar 20). Dynamic patterns of cortical expansion during folding of the preterm human brain. Proc Natl Acad Sci U S A, 115(12), 3156-3161. https://doi.org/10.1073/pnas.1715451115

Gholipour, A., Rollins, C. K., Velasco-Annis, C., Ouaalam, A., Akhondi-Asl, A., Afacan, O., Ortinau, C. M., Clancy, S., Limperopoulos, C., Yang, E., Estroff, J. A., & Warfield, S. K. (2017, Mar 28). A normative spatiotemporal MRI atlas of the fetal brain for automatic segmentation and analysis of early brain growth. Sci Rep, 7(1), 476. https://doi.org/10.1038/s41598-017-00525-w

Grewen, K., Salzwedel, A. P., & Gao, W. (2015). Functional Connectivity Disruption in Neonates with Prenatal Marijuana Exposure. Front Hum Neurosci, 9, 601. https://doi.org/10.3389/fnhum.2015.00601

Griffa, A., Baumann, P. S., Thiran, J. P., & Hagmann, P. (2013, Oct 15). Structural connectomics in brain diseases. NeuroImage, 80, 515-526. https://doi.org/10.1016/j.neuroimage.2013.04.056

Grossman, R., Hoffman, C., Mardor, Y., & Biegon, A. (2006, Nov 1). Quantitative MRI measurements

of human fetal brain development in utero. *NeuroImage, 33*(2), 463-470. https://doi.org/10.1016/j. neuroimage.2006.07.005

Gulsuner, S., & McClellan, J. M. (2014). De novo mutations in schizophrenia disrupt genes co-expressed in fetal prefrontal cortex. *Neuropsychopharmacology(39)*, 238-239. https://doi.org/10.1038/npp.2013.219

Hawrylycz, M. J., Lein, E. S., Guillozet-Bongaarts, A. L., Shen, E. H., Ng, L., Miller, J. A., van de Lagemaat, L. N., et al. (2012, Sep 20). An anatomically comprehensive atlas of the adult human brain transcriptome. *Nature, 489*(7416), 391-399. https://doi.org/10.1038/nature11405

Hortensius, L. M., Dijkshoorn, A. B. C., Ecury-Goossen, G. M., Steggerda, S. J., Hoebeek, F. E., Benders, M., & Dudink, J. (2018, Nov). Neurodevelopmental Consequences of Preterm Isolated Cerebellar Hemorrhage: A Systematic Review. *Pediatrics, 142*(5). https://doi.org/10.1542/peds.2018-0609

Infante, M. A., Moore, E. M., Bischoff-Grethe, A., Tapert, S. F., Mattson, S. N., & Riley, E. P. (2017, Nov). Altered functional connectivity during spatial working memory in children with heavy prenatal alcohol exposure. *Alcohol, 64*, 11-21. https://doi.org/10.1016/j.alcohol.2017.05.002

Khalili, N., Lessmann, N., Turk, E., Claessens, N., Heus, R., Kolk, T., Viergever, M. A., Benders, M., & Isgum, I. (2019, Dec). Automatic brain tissue segmentation in fetal MRI using convolutional neural networks. *Magn Reson Imaging, 64*, 77-89. https://doi.org/10.1016/j.mri.2019.05.020

Khalili, N., Turk, E., Benders, M., Moeskops, P., Claessens, N. H. P., de Heus, R., Franx, A., Wagenaar, N., Breur, J., Viergever, M. A., & Isgum, I. (2019). Automatic extraction of the intracranial volume in fetal and neonatal MR scans using convolutional neural networks. *Neuroimage Clin, 24*, 102061. https://doi.org/10.1016/j.nicl.2019.102061

Khalili, N., Turk, E., Zreik, M., Viergever, M. A., Benders, M. J., & Išgum, I. (2019). Generative adversarial network for segmentation of motion affected neonatal brain MRI. *International Conference on Medical Image Computing and Computer-Assisted Intervention,*

Khan, S., Vasung, L., Marami, B., Rollins, C. K., Afacan, O., Ortinau, C. M., Yang, E., Warfield, S. K., & Gholipour, A. (2019, Jan 15). Fetal brain growth portrayed by a spatiotemporal diffusion tensor MRI atlas computed from in utero images. *NeuroImage, 185*, 593-608. https://doi.org/10.1016/j.neuro-image.2018.08.030

Kline, J. E., Illapani, V. S. P., He, L., Altaye, M., Logan, J. W., & Parikh, N. A. (2020). Early cortical maturation predicts neurodevelopment in very preterm infants. *Archives of Disease in Childhood-Fetal and Neonatal Edition, 105*(5), 460-465.

Krontira, A. C., Cruceanu, C., & Binder, E. B. (2020). Glucocorticoids as mediators of adverse outcomes

of prenatal stress. Trends Neurosci, 43(6), 394-405.

Li, X., Andres, A., Shankar, K., Pivik, R. T., Glasier, C. M., Ramakrishnaiah, R. H., Zhang, Y., Badger, T. M., & Ou, X. (2016, Dec). Differences in brain functional connectivity at resting state in neonates born to healthy obese or normal-weight mothers. Int J Obes (Lond), 40(12), 1931-1934. https://doi. org/10.1038/ijo.2016.166

Limperopoulos, C., Benson, C. B., Bassan, H., Disalvo, D. N., Kinnamon, D. D., Moore, M., Ringer, S. A., Volpe, J. J., & du Plessis, A. J. (2005, Sep). Cerebellar hemorrhage in the preterm infant: ultrasono-graphic findings and risk factors. Pediatrics, 116(3), 717-724. https://doi.org/10.1542/peds.2005-0556

Limperopoulos, C., Soul, J. S., Gauvreau, K., Huppi, P. S., Warfield, S. K., Bassan, H., Robertson, R. L., Volpe, J. J., & du Plessis, A. J. (2005, Mar). Late gestation cerebellar growth is rapid and impeded by premature birth. Pediatrics, 115(3), 688-695. https://doi.org/10.1542/peds.2004-1169

Makropoulos, A., Aljabar, P., Wright, R., Huning, B., Merchant, N., Arichi, T., Tusor, N., Hajnal, J. V., Edwards, A. D., Counsell, S. J., & Rueckert, D. (2016, Jan 15). Regional growth and atlasing of the developing human brain. NeuroImage, 125, 456-478. https://doi.org/10.1016/j.neuroimage.2015.10.047

Makropoulos, A., Robinson, E. C., Schuh, A., Wright, R., Fitzgibbon, S., Bozek, J., Counsell, S. J., Steinweg, J., Vecchiato, K., Passerat-Palmbach, J., Lenz, G., Mortari, F., Tenev, T., Duff, E. P., Bastiani, M., Cordero-Grande, L., Hughes, E., Tusor, N., Tournier, J. D., Hutter, J., Price, A. N., Teixeira, R., Murgasova, M., Victor, S., Kelly, C., Rutherford, M. A., Smith, S. M., Edwards, A. D., Hajnal, J. V., Jenkinson, M., & Rueckert, D. (2018, Jun). The developing human connectome project: A minimal processing pipeline for neonatal cortical surface reconstruction. NeuroImage, 173, 88-112. https://doi.org/10.1016/j.neuroimage.2018.01.054

Miller, J. A., Ding, S. L., Sunkin, S. M., Smith, K. A., Ng, L., Szafer, A., Ebbert, A., Riley, Z. et al. (2014, Apr 10). Transcriptional landscape of the prenatal human brain. Nature, 508(7495), 199-206. https:// doi.org/10.1038/nature13185

Misiak, B., Stramecki, F., Gaweda, L., Prochwicz, K., Sasiadek, M. M., Moustafa, A. A., & Frydecka, D. (2018, Jun). Interactions Between Variation in Candidate Genes and Environmental Factors in the Etiology of Schizophrenia and Bipolar Disorder: a Systematic Review. Mol Neurobiol, 55(6), 5075-5100. https://doi.org/10.1007/s12035-017-0708-y

Neville, H. J., & Bavelier, D. (2000). Specificity and plasticity in neurocognitive development. In The new cognitive neurosciences (pp. 83-98). MIT Press Cambridge, MA.

Onland-Moret, N. C., Buizer-Voskamp, J. E., Albers, M. E. W. A., Brouwer, R. M., Buimer, E. E. L., Hessels, R. S., de Heus, R., Huijding, J., Junge, C. M. M., Mandl, R. C. W., Pas, P., Vink, M., van der

Wal, J. J. M., Hulshoff Pol, H. E., & Kemner, C. (2020, 2020/12/01/). The YOUth study: Rationale, design, and study procedures. Developmental cognitive neuroscience, 46, 100868. https://doi.org/https://doi.org/10.1016/j.dcn.2020.100868

Pineda, R., Guth, R., Herring, A., Reynolds, L., Oberle, S., & Smith, J. (2017, Apr). Enhancing sensory experiences for very preterm infants in the NICU: an integrative review. J Perinatol, 37(4), 323-332. https://doi.org/10.1038/jp.2016.179

Pistorius, L. R., Hellmann, P. M., Visser, G. H., Malinger, G., & Prayer, D. (2008, Nov). Fetal neuro-imaging: ultrasound, MRI, or both? Obstet Gynecol Surv, 63(11), 733-745. https://doi.org/10.1097/OGX.0b013e318186d3ea

Power, J. D., Barnes, K. A., Snyder, A. Z., Schlaggar, B. L., & Petersen, S. E. (2012, Feb 1). Spurious but systematic correlations in functional connectivity MRI networks arise from subject motion. NeuroImage, 59(3), 2142-2154. https://doi.org/10.1016/j.neuroimage.2011.10.018

Rabinowicz, T., de Courten-Myers, G. M., Petetot, J. M., Xi, G., & de los Reyes, E. (1996, Mar). Human cortex development: estimates of neuronal numbers indicate major loss late during gestation. J Neuro-pathol Exp Neurol, 55(3), 320-328. https://www.ncbi.nlm.nih.gov/pubmed/8786390

Rudolph, M. D., Graham, A. M., Feczko, E., Miranda-Dominguez, O., Rasmussen, J. M., Nardos, R., Entringer, S., Wadhwa, P. D., Buss, C., & Fair, D. A. (2018, May). Maternal IL-6 during pregnancy can be estimated from newborn brain connectivity and predicts future working memory in offspring. Nat Neurosci, 21(5), 765-772. https://doi.org/10.1038/s41593-018-0128-y

Rutherford, H. J., Potenza, M. N., Mayes, L. C., & Scheinost, D. (2020, Mar 14). The Application of Connectome-Based Predictive Modeling to the Maternal Brain: Implications for Mother–Infant Bonding. Cerebral Cortex, 30(3), 1538-1547. https://doi.org/10.1093/cercor/bhz185

Salzwedel, A. P., Grewen, K. M., Goldman, B. D., & Gao, W. (2016, Jul-Aug). Thalamocortical func-tional connectivity and behavioral disruptions in neonates with prenatal cocaine exposure. Neurotoxicol Teratol, 56, 16-25. https://doi.org/10.1016/j.ntt.2016.05.009

Scheinost, D., Kwon, S. H., Shen, X., Lacadie, C., Schneider, K. C., Dai, F., Ment, L. R., & Constable, R. T. (2016, Jul). Preterm birth alters neonatal, functional rich club organization. Brain Struct Funct, 221(6), 3211-3222. https://doi.org/10.1007/s00429-015-1096-6

Scholtens, L. H., & van den Heuvel, M. P. (2018, Sep). Multimodal connectomics in psychiatry: Bridging scales from micro to macro. Biological Psychiatry: Cognitive Neuroscience and Neuroimaging, 3(9), 767-776. https://doi.org/10.1016/j.bpsc.2018.03.017

Schöpf, V., Kasprian, G., Brugger, P., & Prayer, D. (2012). Watching the fetal brain at 'rest'. *International Journal of Developmental Neuroscience, 30(1)*, 11-17.

Smyser, C. D., Inder, T. E., Shimony, J. S., Hill, J. E., Degnan, A. J., Snyder, A. Z., & Neil, J. J. (2010, Dec). Longitudinal analysis of neural network development in preterm infants. *Cereb Cortex, 20(12)*, 2852-2862. https://doi.org/10.1093/cercor/bhq035

Tebbenkamp, A. T., Willsey, A. J., State, M. W., & Sestan, N. (2014, Apr). The developmental transcriptome of the human brain: implications for neurodevelopmental disorders. *Curr Opin Neurol, 27(2)*, 149-156. https://doi.org/10.1097/WCO.0000000000000069

Thomason, M. E. (2018, Jan). Structured Spontaneity: Building Circuits in the Human Prenatal Brain. *Trends Neurosci, 41(1)*, 1-3. https://doi.org/10.1016/j.tins.2017.11.004

Thomason, M. E. (2020, Jul 1). Development of Brain Networks In Utero: Relevance for Common Neural Disorders. *Biol Psychiatry, 88(1)*, 40-50. https://doi.org/10.1016/j.biopsych.2020.02.007

Thomason, M. E., Dassanayake, M. T., Shen, S., Katkuri, Y., Alexis, M., Anderson, A. L., Yeo, L., Mody, S., Hernandez-Andrade, E., Hassan, S. S., Studholme, C., Jeong, J. W., & Romero, R. (2013, Feb 20). Cross-hemispheric functional connectivity in the human fetal brain. *Sci Transl Med, 5(173)*, 173ra124. https://doi.org/10.1126/scitranslmed.3004978

Thomason, M. E., Grove, L. E., Lozon, T. A., Jr., Vila, A. M., Ye, Y., Nye, M. J., Manning, J. H., Pappas, A., Hernandez-Andrade, E., Yeo, L., Mody, S., Berman, S., Hassan, S. S., & Romero, R. (2015, Feb). Age-related increases in long-range connectivity in fetal functional neural connectivity networks in utero. *Dev Cogn Neurosci, 11*, 96-104. https://doi.org/10.1016/j.dcn.2014.09.001

Thomason, M. E., Hect, J., Waller, R., Manning, J. H., Stacks, A. M., Beeghly, M., Boeve, J. L., Wong, K., van den Heuvel, M. I., Hernandez-Andrade, E., Hassan, S. S., & Romero, R. (2018, Aug). Prenatal neural origins of infant motor development: Associations between fetal brain and infant motor development. *Dev Psychopathol, 30(3)*, 763-772. https://doi.org/10.1017/S095457941800072X

Thomason, M. E., Hect, J. L., Rauh, V. A., Trentacosta, C., Wheelock, M. D., Eggebrecht, A. T., Espinoza-Heredia, C., & Burt, S. A. (2019, May 1). Prenatal lead exposure impacts cross-hemispheric and long-range connectivity in the human fetal brain. *NeuroImage, 191*, 186-192. https://doi.org/10.1016/j.neuroimage.2019.02.017

Thomason, M. E., Scheinost, D., Manning, J. H., Grove, L. E., Hect, J., Marshall, N., Hernandez-Andrade, E., Berman, S., Pappas, A., Yeo, L., Hassan, S. S., Constable, R. T., Ment, L. R., & Romero, R. (2017, Jan 9). Weak functional connectivity in the human fetal brain prior to preterm birth. *Sci Rep, 7*, 39286. https://doi.org/10.1038/srep39286

Turk, E., Endevelt-Shapira, Y., Feldman, R., van den Heuvel, M. I., & Levy, J. (2022, 2022-April-27). Brains in Sync: Practical Guideline for Parent–Infant EEG During Natural Interaction [Review]. Frontiers in Psychology, 13. https://doi.org/10.3389/fpsyg.2022.833112

Turk, E., Vroomen, J., Fonken, Y., Levy, J., & Heuvel, M. I. (2022). In sync with your child: The potential of parent–child electroencephalography in developmental research. Developmental psychobiology, 64(3). https://doi.org/10.1002/dev.22221

Van den Bergh, B. R. H., van den Heuvel, M. I., Lahti, M., Braeken, M., de Rooij, S. R., Entringer, S., Hoyer, D., Roseboom, T., Raikkonen, K., King, S., & Schwab, M. (2020, Oct). Prenatal developmental origins of behavior and mental health: The influence of maternal stress in pregnancy. Neurosci Biobehav Rev, 117, 26-64. https://doi.org/10.1016/j.neubiorev.2017.07.003

van den Heuvel, M. I., Turk, E., Manning, J. H., Hect, J., Hernandez-Andrade, E., Hassan, S. S., Romero, R., van den Heuvel, M. P., & Thomason, M. E. (2018, Apr). Hubs in the human fetal brain network. Dev Cogn Neurosci, 30, 108-115. https://doi.org/10.1016/j.dcn.2018.02.001

van den Heuvel, M. P., Kahn, R. S., Goni, J., & Sporns, O. (2012, Jul 10). High-cost, high-capacity backbone for global brain communication. Proc Natl Acad Sci U S A, 109(28), 11372-11377. https://doi.org/10.1073/pnas.1203593109

van den Heuvel, M. P., Kersbergen, K. J., de Reus, M. A., Keunen, K., Kahn, R. S., Groenendaal, F., de Vries, L. S., & Benders, M. J. (2015, Sep). The Neonatal Connectome During Preterm Brain Development. Cereb Cortex, 25(9), 3000-3013. https://doi.org/10.1093/cercor/bhu095

van den Heuvel, M. P., Scholtens, L. H., Turk, E., Mantini, D., Vanduffel, W., & Feldman Barrett, L. (2016, Sep). Multimodal analysis of cortical chemoarchitecture and macroscale fMRI resting-state functional connectivity. Hum Brain Mapp, 37(9), 3103-3113. https://doi.org/10.1002/hbm.23229

Van Dijk, K. R., Sabuncu, M. R., & Buckner, R. L. (2012, Jan 2). The influence of head motion on intrinsic functional connectivity MRI. NeuroImage, 59(1), 431-438. https://doi.org/10.1016/j.neuroimage.2011.07.044

Volpe, J. J. (2009, Jan). Brain injury in premature infants: a complex amalgam of destructive and developmental disturbances. Lancet Neurol, 8(1), 110-124. https://doi.org/10.1016/S1474-4422(08)70294-1

Wang, S. S., Kloth, A. D., & Badura, A. (2014, Aug 6). The cerebellum, sensitive periods, and autism. Neuron, 83(3), 518-532. https://doi.org/10.1016/j.neuron.2014.07.016

Wheelock, M. D., Hect, J. L., Hernandez-Andrade, E., Hassan, S. S., Romero, R., Eggebrecht, A. T., & Thomason, M. E. (2019, Apr). Sex differences in functional connectivity during fetal brain development.

Dev Cogn Neurosci, 36, 100632. https://doi.org/10.1016/j.dcn.2019.100632

Willsey, A. J., Sanders, S. J., Li, M., Dong, S., Tebbenkamp, A. T., Muhle, R. A., Reilly, S. K., Lin, L., Fertuzinhos, S., Miller, J. A., Murtha, M. T., Bichsel, C., Niu, W., Cotney, J., Ercan-Sencicek, A. G., Gockley, J., Gupta, A. R., Han, W., He, X., Hoffman, E. J., Klei, L., Lei, J., Liu, W., Liu, L., Lu, C., Xu, X., Zhu, Y., Mane, S. M., Lein, E. S., Wei, L., Noonan, J. P., Roeder, K., Devlin, B., Sestan, N., & State, M. W. (2013, Nov 21). Coexpression networks implicate human midfetal deep cortical projection neurons in the pathogenesis of autism. Cell, 155(5), 997-1007. https://doi.org/10.1016/j.cell.2013.10.020

Zalesky, A., Fornito, A., Seal, M. L., Cocchi, L., Westin, C. F., Bullmore, E. T., Egan, G. F., & Pantelis, C. (2011, Jan 1). Disrupted axonal fiber connectivity in schizophrenia. Biol Psychiatry, 69(1), 80-89. https://doi.org/10.1016/j.biopsych.2010.08.022

Zayek, M. M., Benjamin, J. T., Maertens, P., Trimm, R. F., Lal, C. V., & Eyal, F. G. (2012, Sep). Cerebellar hemorrhage: a major morbidity in extremely preterm infants. J Perinatol, 32(9), 699-704. https://doi.org/10.1038/jp.2011.185

Nederlandse samenvatting (summary in Dutch)

EEN BLAUWDRUK VAN HET ONTWIKKELENDE BREIN

Het menselijk brein is een complex orgaan dat gedurende onze hele levenscyclus verandert. Alles wat wij ervaren, zien of consumeren kan leiden tot negatieve of positieve subtiele anatomische of functionele aanpassingen van de cellen, hersengebieden of de verbindingen tussen deze gebieden. Het is dan ook niet gek dat het merendeel van het hersenonderzoek zich focust op deze (foute) aanpassingen, zodat wij uiteindelijk de psyche en het brein van elk individu beter kunnen gaan begrijpen. Steeds meer onderzoeken laten zien dat met name vroege verstoringen zoals vroeggeboorte, zuurstofgebrek tijdens de geboorte en virale infecties (e.g. toxoplasmose en Zika) van de zwangere vrouw tot grote veranderingen van het babybrein leiden. Dit komt doordat de blauwdruk, het fundament van de hersenen, al grotendeels gevormd wordt tijdens de zwangerschap en in het eerste jaar na de geboorte. Door complexiteit en snelheid van opvolgende groeiprocessen in de eerste fase van het leven is het brein bijzonder kwetsbaar voor verstorende invloeden.

Het in beeld brengen en het begrijpen van de foetale (tijdens zwangerschap) en neonatale (in de eerste maand na de geboorte) hersenontwikkeling *in vivo* is een grote uitdaging, omdat beschikbare data schaars is. Daarnaast zijn beeldverwerkingstechnieken om voor deze unieke data metingen te kunnen verrichten vaak niet beschikbaar. Het in kaart brengen van de hersenontwikkeling tijdens de zwangerschap of net na de geboorte is complex, waardoor er veel vragen over hoe de hersenen zich precies ontwikkelen of over hoe deze processen verstoord worden, onbeantwoord blijven. De inzichten in de hersenontwikkeling in deze eerste fase van het leven vormen het fundament en de motivatie voor de onderzoeken in dit proefschrift, waarin ik onderzoek heb gedaan naar hersenontwikkeling tijdens en in de eerste maand na de zwangerschap met behulp van de nieuwste (Magnetic Resonance Imaging) MRI, MRI-beeldverwerkingstechnieken en data van hersenweefsel (genexpressie en receptorlevels).

Dit proefschrift heeft globaal gezien twee doelen: 1) het in kaart brengen van de enorme structurele transformatie en rijping van het ontwikkelende brein *in utero* en in de neonatale periode in gezonde en te vroeg geboren baby's; 2) om nieuwe inzichten te verkrijgen in functionele hersenontwikkeling in de tweede helft van de zwangerschap.
In dit hoofdstuk zal ik de belangrijkste bevindingen van dit proefschrift samenvatten in context van de bestaande literatuur.

STRUCTURELE HERSENONTWIKKELING

Tijdens de 40 weken zwangerschap ontwikkelen de hersenen van een foetus zich razendsnel tot een structuur dat al veel lijkt op het volwassen brein. In de eerste helft van de zwangerschap staat vooral het ontstaan, vermeerderen en migreren van neurale cellen

centraal. In de tweede helft van de zwangerschap, worden deze processen opgevolgd door een enorme toename in volume van het brein en de karakteristieke vorming van de hersenschors (cortex). Naast de toename in het aantal cellen (grijze stof), is de toename in hersenvolume ook te wijten aan de toename in aantal verbindingen tussen deze cellen (witte stof banen).

De structurele groei van het babybrein is de afgelopen 150 jaar voornamelijk in kaart gebracht door *post mortem* (Altman & Bayer, 2015) en echografische onderzoeken (Pistorius et al., 2008). Recentelijke ontwikkelingen van MRI en MRI-verwerkingstechnieken maken nu ook longitudinaal onderzoek van de foetale en neonatale hersenen mogelijk. Hierdoor is het mogelijk om betere groei metingen te verrichten en de hersenen in nog meer detail te visualiseren.

In navolging van eerdere baanbrekende foetale en neonatale MRI-onderzoeken, breng ik, met behulp van onze nieuwste methoden voor hersensegmentatie (**hoofdstuk 6**), de volumetrische hersengroei van de foetus in het derde trimester in kaart bij meerdere groepen gezonde zwangere vrijwilligers (en hun pasgeborenen) en premature baby's die opgenomen zijn in het Wilhelmina ziekenhuis (**hoofdstuk 7**). De gezonde zwangeren en hun baby's zijn deelnemer van het YOUth cohort (zie, youthonderzoek.nl; Onland-Moret et al., 2020). Onze YOUth studie is de eerste in Nederland waarin gezonde zwangeren en pasgeboren baby's een MRI ondergaan zonder medische noodzaak. In **hoofdstuk 2** laat ik een absolute toename zien van de globale groei van de hersenen in zijn geheel, maar ook specifiek de cortex, het cerebellum, de hersenstam, de extra cerebrospinale vloeistof (CSF) en de ventrikels rond 29-34 weken van de zwangerschap. De resultaten van ons eerste gezonde perinatale MRI-cohort in Nederland, zoals gepresenteerd in **hoofdstuk 7**, zijn in lijn met- en complementair aan recente MRI-onderzoeken van gezonde foetussen (foetussen zonder visuele misvormingen en hersenbeschadiging) (Andescavage et al., 2017; Clouchoux et al., 2012; Grossman et al., 2006). Regionale foetale corticale groeipatronen tussen 26 en 38 postconceptionele weken (voortaan: pcw, dit zijn de weken die geteld worden na de conceptie en komen overeen met het aantal weken na menstruatie min twee weken) zoals getoond in **hoofdstuk 2** komen overeen met globale corticale groeipatronen gemeten bij te vroeg geboren pasgeborenen uit andere onderzoeken. Zo begint de snelste groei bij de primaire motorische en (somato) sensorische cortex rond 26 pcw, dit wordt gevolgd door de visuele cortex, die op zijn beurt eerder rijpt dan de laterale delen van de temporeel- en frontaalkwab (Garcia et al., 2018).

Genetische controle en foetale corticale groei
Corticale groei tijdens de laatste fase van de zwangerschap staat waarschijnlijk onder sterke genetische controle. Door foetaal gewogen T1 MRI (Gholipour et al., 2017) en transcriptoomprofielen (BrainSpan, Atlas of the Developing Human Brain, brainspan.

org) te combineren, laat ik in **hoofdstuk 2** een spatiotemporele relatie zien tussen genexpressiepatronen en corticale groei. Genen met een functie die gerelateerd zijn aan neuronale systemen, axon- en synapsontwikkeling en neurale communicatie correleren met de snelle corticale groei gedurende 34 tot 38 pcw. Bovendien correleren Dr. Wei en ik ruimtelijke genexpressie met corticale groei, en onthullen de top 100 correlerende genen voor drie foetale leeftijdsfasen (24-30 pcw, 30-34 pcw en 34-38 pcw). Met dit werk koppel ik moleculaire ontwikkelingsmechanismen aan macroscopische metingen van corticale anatomie in de zwangerschap, waarbij ik de relatie tussen foetale genexpressie en hersenontwikkeling aantoon en een toekomstig raamwerk belicht om de specifieke impact van vroege blootstelling aan ontwikkelingsrisico's te meten.

MRI BIJ TE VROEG GEBOREN BABY'S

Het *in vivo* in kaart kunnen brengen van de perinatale hersenontwikkeling bij gezonde baby's en patiëntgroepen biedt de mogelijkheid om deze met elkaar te vergelijken en daardoor in een vroeg stadium gedetailleerde veranderingen op te sporen. Het vergelijken van MRI-data van deze verschillende groepen deelnemers kan een behoorlijke uitdaging zijn. Vergelijkingen tussen foetale en neonatale groepen omvatten vaak verschillen in MRI-scanners, magnetische veldsterktes en beeldverwerkingspijplijnen, inclusief bewegingscorrectie. Enkele nieuwe publiek beschikbare verwerkingspijplijnen, zoals ons automatische segmentatie-algoritme om het intracraniale volume te verdelen (**hoofdstuk 6**) en onze nieuwste in eigen huis ontwikkelde pijplijnen voor verdere foetale en neonatale segmentatie van neuraal weefsel (Claessens et al., 2019; N. Khalili et al., 2019; Khalili et al., 2017; Nadieh Khalili et al., 2019), kunnen dit probleem helpen oplossen en zijn gebruikt in dit proefschrift.

Door foetale hersenvolumes te vergelijken met extreem vroeggeboren pasgeborenen (zonder matige tot grote hersenmisvormingen en hersenbeschadiging) rond het begin van het derde trimester, laat ik in **hoofdstuk 7** zien dat extreem vroeggeboren baby's een verminderde grootte en groei hebben van bijna alle (regionale en globale) hersenvolumes (zoals totale hersenen, corticale grijze stof, niet-gemyeliniseerde witte stof, diepe grijze stof en de hersenstam) rond 30 weken zwangerschap. Deze resultaten zijn in lijn met eerder onderzoek (Andescavage et al., 2017; Clouchoux et al., 2012; Grossman et al., 2006), waaruit blijkt dat de totale hoeveelheid hersenen, cerebrum, cerebellum, hersenstam, extra en intracerebrospinale vloeistof meer volume heeft in gezonde foetussen. Bovendien laat ik zien dat de hersenen van prematuur geboren neonaten worden gekenmerkt door vergrote ventrikels, vermoedelijk als gevolg van atrofie en beschadiging van andere hersenweefsels dat veel voorkomt bij te vroeg geboren baby's.

Versnelling van de hersengroei na vroeggeboorte

In **hoofdstuk 7** laat ik zien dat volumetrische en groeiveranderingen tussen gezonde en te vroeg geboren pasgeborenen alleen nog maar detecteerbaar zijn voor een paar hersengebieden rond de voldragen zwangerschapsduur (aterme leeftijd). Ons cohort van prematuur geboren neonaten vertoonde vergrote ventrikels, kleinere volumes van de corticale grijze stof en grotere gebieden van gemyeliniseerde witte stof rond de aterme leeftijd. De resultaten suggereren dat de hersengroei bij pasgeborenen kort na extreem vroeggeboorte vertraagd was, maar een inhaalslag maakte door een versnelling van de (regionale) hersengroei tijdens de laatste drie maanden van de zwangerschap. Het verzamelen van gezonde deelnemers voor deze studie is echter nog steeds aan de gang en conclusies uit deze studie moeten met de nodige voorzichtigheid worden getrokken vanwege de lage deelname aantallen. Het zou interessant zijn om de snelheid van volumetrische hersengroei bij premature baby's rond de voldragen geboorte in een grotere populatie verder te onderzoeken.

Corticale rijpingskenmerken (zoals oppervlakte, gyrificatie-index, sulcale diepte en kromming) zijn kenmerken die verklaren hoe goed de premature baby het doet, terwijl vroege rijping van de cortex mogelijk niet gunstig is als het ontwikkelingstraject verschilt van een gezond traject (Kline et al., 2020). Om dit begrip verder te onderzoeken, zou toekomstig onderzoek zich moeten concentreren op de microstructurele ontwikkeling van de hersenverbindingen (DTI) en de functionaliteit ervan (fMRI), waarbij de hersenen van gezonde perinaten en te vroeg geboren baby's worden vergeleken. Eigenschappen op microschaal van de hersenen van premature baby's (of van diermodellen) kunnen van toegevoegde waarde zijn om het volledige verhaal van verschillende groeitrajecten te vertellen, en daarmee te kunnen suggereren of een hogere rijpingsscore (bijv. hogere versnelde ontwikkeling) gunstig is of niet.

ONTWIKKELING VAN HERSENNETWERKEN

Al vanaf het tweede trimester van de zwangerschap worden de eerste zenuwcellen (neuronen) actief. Aangenomen wordt dat de eerste activiteit van deze cellen spontaan ontstaat en dat het vuren van kleine elektrische signalen, de ontwikkeling en versterking van verbindingen tussen verschillende cellen stimuleert (Arichi et al., 2017; Thomason, 2018). Het is daarom aannemelijk dat de eerste verbindingen in de hersenen detecteerbaar zijn rond diezelfde periode.

De verbindingen tussen neuronen worden gevormd door hun uitlopers: de axonen en dendrieten. Deze minuscule verbindingen zijn inderdaad al detecteerbaar op een microscopisch niveau vanaf 10 weken na conceptie (Vasung et al., 2010). Onze huidige MRI-technieken, zoals diffusie gewogen opnames (*diffusion tensor imaging,* DTI), kunnen dit niveau niet in kaart brengen, maar zijn wel in staat om de geclusterde axon bundels

tussen hersengebieden te laten zien. DTI-onderzoek van het foetale brein laat zien dat projectiebanen, de witte stof verbindingen tussen bijvoorbeeld de thalamus en cortex en de commissurale banen tussen de twee hersenhelften (zoals het corpus callosum), ongeveer vanaf het tweede trimester (Wang et al., 2017) voor het eerst worden gevormd. De derde groep verbindingen, de associatiebanen tussen verschillende corticale gebieden binnen een hersenhelft, worden als laatste gevormd en verstevigd (Mitter et al., 2015).

Gedurende het tweede en derde trimester van de zwangerschap zijn de drie groepen verbinden nog steeds onderhevig aan grove veranderingen en DTI-onderzoek laat zien dat verbindingen zich over het algemeen centraal naar perifeer en van beneden naar boven ontwikkelen (Khan et al., 2019). Dit komt overeen met de mate van complexiteit waar de verschillende hersenfuncties aan toegeschreven worden -van instinctief en motorisch tot hogere cognitieve processen. Na 40 weken zwangerschap zijn de belangrijkste witte banen gevormd, maar zij zullen in de postnatale periode nog wel versterkt en gefinetuned worden, bijvoorbeeld wanneer er nieuwe sensorische input komt en wanneer er nieuwe vaardigheden opgedaan worden.

Blauwdruk van het functionele connectoom
Met behulp van DTI kunnen alle grootschalige verbindingen van de hersenen in kaart worden gebracht. Zo'n wegenkaart van de hersenen wordt ook wel het neurale connectoom genoemd (Sporns et al., 2005). Een wegenkaart kan ook gemaakt worden met behulp van functionele MRI. De definitie van een verbinding is daar net even anders: als twee hersengebieden dezelfde activiteit vertonen over de tijd, zijn zij met elkaar verbonden. Met zo'n wegenkaart zijn onderzoekers in staat om complexe interacties tussen gebieden te beschrijven en te interpreteren (Rubinov & Sporns, 2010). Specifieke hersenfuncties zijn namelijk niet het resultaat van een enkel actief hersengebied, maar vloeien voort uit een samenwerking van verschillende hersengebieden verspreid over de hersenen.

Nadat ik de structurele ontwikkeling in kaart heb gebracht, rapporteer ik over de vroege hersenfunctie door het foetale functionele connectoom te bestuderen in **hoofdstuk 3 en 4**. Voor deze studie heb ik functionele MRI-data geanalyseerd van een groep foetussen afkomstig van de onderzoeksgroep onder leiding van dr. Moriah Thomason, Wayne State University, Detroit, USA. Mijn uitgebreide fMRI-onderzoek bij foetussen vanaf 20 weken zwangerschap tot de geboorte toont als eerste aan dat een robuust foetaal functioneel connectoom van de cortex kan worden gevisualiseerd en geanalyseerd.

In **hoofdstuk 3** laat ik zien dat het foetale functionele connectoom een blauwdruk is van het connectoom dat we waarnemen in het volwassen brein. De collectieve set van foetale functionele verbindingen vertoont een overlap van 62% met het volwassen brein. Ik

toon hoge associaties aan tussen het volwassen en foetale default netwerk (netwerk dat vooral actief is in rust), het temporele, het visuele en het motorische netwerk, terwijl het frontomediale netwerk minder lijkt op het volwassen equivalent van het netwerk. Ons onderzoek benadrukt de oorsprong van proto-type rusttoestand-netwerken, wat aangeeft dat het ontstaan en belangrijke ontwikkelingsstadia van het connectoom plaatsvinden vóór het tweede trimester van de zwangerschap.

Ook laat ik in **hoofdstuk 3** zien dat het foetale functionele connectoom een zogenaamde 'small-world' structuur bezit en een 'rich-club' architectuur heeft, en daarom vergelijkbaar is met het volwassen brein. Dit betekent dat het foetale functionele connectoom al efficiënt lijkt te functioneren met belangrijke centrale hubs en lange afstand verbindingen. Dit komt overeen met onderzoek naar het structurele weggenkaart van te vroeggeboren neonaten (van den Heuvel et al., 2015). De foetale functionele centrale knooppunten die worden gepresenteerd in **hoofdstuk 3 en 4** zijn overwegend temporale en middellijn corticale gebieden van de insulair en frontaalkwab, evenals de primaire somatosensorische gebieden. Deze foetale bevindingen zijn in overeenstemming met neonatale hubs (Arichi et al., 2017; De Asis-Cruz et al., 2015; Fransson et al., 2010; Gao et al., 2009). Door het hele brein in overweging te nemen met behulp van ICA-netwerken in **hoofdstuk 4**, laten we zien dat belangrijke foetale functionele knooppunten zich ook in visuele, motorische en cerebellaire regio's bevinden, evenals in associatiegebieden dichtbij de Wernicke-regio's. Al met al laten mijn observaties zien dat volwassen-achtige functionele connectiviteit al vroeg in de baarmoeder tot stand komt, wat aangeeft dat de prenatale periode van fundamenteel belang kan zijn voor de 'gezondheid' van het volwassen connectoom volwassenen (Krontira et al., 2020; Thomason, 2020). Toekomstig onderzoek over de ontwikkelende hersennetwerken kan veel nieuwe inzichten gaan geven in de ontwikkeling van vroege verstoringen in het brein.

Onderbouwing van functionele connectiviteit op microschaal
Om onze kennis over het onderliggende construct van functionele connectiviteitspatronen in de hersenen van primaten te verbreden, rapporteer ik over de relatie cel kenmerken op microschaal (receptoren die zich bevinden op de cellen) en effectieve regionale functionele interacties in **hoofdstuk 6**. Met behulp van correlatieanalyses tussen regionale receptordichtheidsniveaus en effectieve (strychnine-geïnduceerde) functionele connectiviteit in de makaakcortex, toon ik aan dat de sterkte van connectiviteit op macroschaal gerelateerd is aan de cel-kenmerken van corticale regio's. Met deze relatie tussen de chemoarchitectuur en functionele connectiviteitsmetingen toon ik aan dat regio's met een groter aandeel excitatoire versus remmende neurotransmitterreceptorniveaus sterkere geïnduceerde functionele verbindingen hebben in de makaak cortex (**hoofdstuk 5**). Dit is in lijn met ons gerelateerde onderzoek in de mens; daar tonen wij aan dat sterkere fMRI-verbindingen in rusttoestand in de volwassen menselijke cortex zijn geassocieerd met een groter aandeel excitatoire versus remmende neurotransmit-

terreceptorniveaus (van den Heuvel et al., 2016). Hieruit kan geconcludeerd worden dat functionele connectiviteitspatronen op macroschaal een weerspiegeling zijn van functionele signalen op microschaal in het volwassen brein.

Connectiviteitspatronen op macroschaal in het foetale en volwassen brein vertonen veel overlap en weerspiegelen gemeenschappelijke kenmerken (**hoofdstuk 3**). Toch is het mogelijk dat foetale functionele hersenactiviteit tot stand komt door verschillende onderliggende processen op microschaal. Het foetale transcriptoom verschilt bijvoorbeeld sterk van het volwassen transcriptoom (zie bijvoorbeeld, Hawrylycz et al., 2012; Miller et al., 2014). Daarnaast zijn veel neuronen nog niet volledig volgroeid of op hun definitieve locatie tijdens de foetale ontwikkeling. Ook is het mogelijk dat de neuronen nog een totaal andere functie en werking hebben (Ben-Ari, 2002). En bovendien zijn axonale verbindingen in het foetale brein nog niet volledig gemyeliniseerd en dus nog niet geheel functioneel. Een multimodale analyse die foetale functionele connectiviteit combineert met structurele connectiviteit afgeleid van DTI zou meer inzicht kunnen verschaffen in de structureel-functionele relatie van het foetale brein, vooral in combinatie met gegevens over genexpressie. Het begrijpen van de onderliggende constructie van functionele connectiviteitspatronen zou meer inzicht kunnen geven in de ontwikkeling van activiteitspatronen en zou misschien onze kennis kunnen vergroten in het begrijpen van vroege veranderingen in het zich ontwikkelende connectoom.

REFERENCES

Altman, J., & Bayer, A. (2015). Development of the Human Neocortex. A Review and Interpretation of the Histological Record. USA: The Laboratory of Developmental Neurobiology, Inc. https://doi.org/ https://neurondevelopment.org/wp-content/uploads/2015/11/human-neocortical-development-complete.pdf

Andescavage, N. N., du Plessis, A., McCarter, R., Serag, A., Evangelou, I., Vezina, G., Robertson, R., & Limperopoulos, C. (2017, Nov 1). Complex Trajectories of Brain Development in the Healthy Human Fetus. Cereb Cortex, 27(11), 5274-5283. https://doi.org/10.1093/cercor/bhw306

Arichi, T., Whitehead, K., Barone, G., Pressler, R., Padormo, F., Edwards, A. D., & Fabrizi, L. (2017, Sep 12). Localization of spontaneous bursting neuronal activity in the preterm human brain with simultaneous EEG-fMRI. Elife, 6, e27814. https://doi.org/10.7554/eLife.27814

Ben-Ari, Y. (2002, Sep). Excitatory actions of gaba during development: the nature of the nurture. Nat Rev Neurosci, 3(9), 728-739. https://doi.org/10.1038/nrn920

Claessens, N., Khalili, N., Isgum, I., ter Heide, H., Steenhuis, T., Turk, E., Jansen, N., de Vries, L., Breur, J., & de Heus, R. (2019). Brain and CSF Volumes in Fetuses and Neonates with Antenatal Diagnosis of

Critical Congenital Heart Disease: A Longitudinal MRI Study. American Journal of Neuroradiology.

Clouchoux, C., Kudelski, D., Gholipour, A., Warfield, S. K., Viseur, S., Bouyssi-Kobar, M., Mari, J. L., Evans, A. C., du Plessis, A. J., & Limperopoulos, C. (2012, Jan). Quantitative in vivo MRI measurement of cortical development in the fetus. Brain Struct Funct, 217(1), 127-139. https://doi.org/10.1007/s00429-011-0325-x

De Asis-Cruz, J., Bouyssi-Kobar, M., Evangelou, I., Vezina, G., & Limperopoulos, C. (2015, Dec 7). Functional properties of resting state networks in healthy full-term newborns. Sci Rep, 5, 17755. https://doi.org/10.1038/srep17755

Fransson, P., Åden, U., Blennow, M., & Lagercrantz, H. (2010). The functional architecture of the infant brain as revealed by resting-state fMRI. Cerebral Cortex, 21(1), 145-154.

Gao, W., Zhu, H., Giovanello, K. S., Smith, J. K., Shen, D., Gilmore, J. H., & Lin, W. (2009, Apr 21). Evidence on the emergence of the brain's default network from 2-week-old to 2-year-old healthy pediatric subjects. Proc Natl Acad Sci U S A, 106(16), 6790-6795. https://doi.org/10.1073/pnas.0811221106

Garcia, K. E., Robinson, E. C., Alexopoulos, D., Dierker, D. L., Glasser, M. F., Coalson, T. S., Ortinau, C. M., Rueckert, D., Taber, L. A., Van Essen, D. C., Rogers, C. E., Smyser, C. D., & Bayly, P. V. (2018, Mar 20). Dynamic patterns of cortical expansion during folding of the preterm human brain. Proc Natl Acad Sci U S A, 115(12), 3156-3161. https://doi.org/10.1073/pnas.1715451115

Gholipour, A., Rollins, C. K., Velasco-Annis, C., Ouaalam, A., Akhondi-Asl, A., Afacan, O., Ortinau, C. M., Clancy, S., Limperopoulos, C., & Yang, E. (2017). A normative spatiotemporal MRI atlas of the fetal brain for automatic segmentation and analysis of early brain growth. Scientific reports, 7(1), 476. https://www.ncbi.nlm.nih.gov/pmc/articles/PMC5428658/pdf/41598_2017_Article_525.pdf

Grossman, R., Hoffman, C., Mardor, Y., & Biegon, A. (2006, Nov 1). Quantitative MRI measurements of human fetal brain development in utero. NeuroImage, 33(2), 463-470. https://doi.org/10.1016/j.neuroimage.2006.07.005

Hawrylycz, M. J., Lein, E. S., Guillozet-Bongaarts, A. L., Shen, E. H., Ng, L., Miller, J. A., van de Lagemaat, et al. (2012, Sep 20). An anatomically comprehensive atlas of the adult human brain transcriptome. Nature, 489(7416), 391-399. https://doi.org/10.1038/nature11405

Khalili, N., Lessmann, N., Turk, E., Claessens, N., Heus, R., Kolk, T., Viergever, M. A., Benders, M., & Isgum, I. (2019, Dec). Automatic brain tissue segmentation in fetal MRI using convolutional neural networks. Magn Reson Imaging, 64, 77-89. https://doi.org/10.1016/j.mri.2019.05.020

Khalili, N., Moeskops, P., Claessens, N. H., Scherpenzeel, S., Turk, E., de Heus, R., Benders, M. J., Vier-

gever, M. A., Pluim, J. P., & Išgum, I. (2017). Automatic segmentation of the intracranial volume in fetal

MR images. In Fetal, Infant and Ophthalmic Medical Image Analysis (pp. 42-51). Springer.
Khalili, N., Turk, E., Zreik, M., Viergever, M. A., Benders, M. J., & Išgum, I. (2019). Generative adversarial network for segmentation of motion affected neonatal brain MRI. International Conference on Medical Image Computing and Computer-Assisted Intervention,

Khan, S., Vasung, L., Marami, B., Rollins, C. K., Afacan, O., Ortinau, C. M., Yang, E., Warfield, S. K., & Gholipour, A. (2019, Jan 15). Fetal brain growth portrayed by a spatiotemporal diffusion tensor MRI atlas computed from in utero images. NeuroImage, 185, 593-608. https://doi.org/10.1016/j.neuroimage.2018.08.030

Kline, J. E., Illapani, V. S. P., He, L., Altaye, M., Logan, J. W., & Parikh, N. A. (2020). Early cortical maturation predicts neurodevelopment in very preterm infants. Archives of Disease in Childhood-Fetal and Neonatal Edition, 105(5), 460-465.

Krontira, A. C., Cruceanu, C., & Binder, E. B. (2020). Glucocorticoids as mediators of adverse outcomes of prenatal stress. Trends Neurosci, 43(6), 394-405.

Miller, J. A., Ding, S. L., Sunkin, S. M., Smith, K. A., Ng, L., Szafer, A., Ebbert, A., Riley, Z. et al. (2014, Apr 10). Transcriptional landscape of the prenatal human brain. Nature, 508(7495), 199-206. https://doi.org/10.1038/nature13185

Mitter, C., Prayer, D., Brugger, P. C., Weber, M., & Kasprian, G. (2015). In vivo tractography of fetal association fibers. PLoS One, 10(3), e0119536. https://doi.org/10.1371/journal.pone.0119536

Onland-Moret, N. C., Buizer-Voskamp, J. E., Albers, M. E. W. A., Brouwer, R. M., Buimer, E. E. L., Hessels, R. S., de Heus, R., Huijding, J., Junge, C. M. M., Mandl, R. C. W., Pas, P., Vink, M., van der Wal, J. J. M., Hulshoff Pol, H. E., & Kemner, C. (2020, 2020/12/01/). The YOUth study: Rationale, design, and study procedures. Developmental cognitive neuroscience, 46, 100868. https://doi.org/https://doi.org/10.1016/j.dcn.2020.100868

Pistorius, L. R., Hellmann, P. M., Visser, G. H., Malinger, G., & Prayer, D. (2008, Nov). Fetal neuroimaging: ultrasound, MRI, or both? Obstet Gynecol Surv, 63(11), 733-745. https://doi.org/10.1097/OGX.ob013e318186d3ea

Rubinov, M., & Sporns, O. (2010, Sep). Complex network measures of brain connectivity: uses and interpretations. NeuroImage, 52(3), 1059-1069. https://doi.org/10.1016/j.neuroimage.2009.10.003

Sporns, O., Tononi, G., & Kotter, R. (2005, Sep). The human connectome: A structural description of the human brain. PLoS Comput Biol, 1(4), e42. https://doi.org/10.1371/journal.pcbi.0010042

Thomason, M. E. (2018, Jan). Structured Spontaneity: Building Circuits in the Human Prenatal Brain. Trends Neurosci, 41(1), 1-3. https://doi.org/10.1016/j.tins.2017.11.004

Thomason, M. E. (2020, Jul 1). Development of Brain Networks In Utero: Relevance for Common Neural Disorders. Biol Psychiatry, 88(1), 40-50. https://doi.org/10.1016/j.biopsych.2020.02.007

van den Heuvel, M. P., Kersbergen, K. J., de Reus, M. A., Keunen, K., Kahn, R. S., Groenendaal, F., de Vries, L. S., & Benders, M. J. (2015, Sep). The Neonatal Connectome During Preterm Brain Development. Cereb Cortex, 25(9), 3000-3013. https://doi.org/10.1093/cercor/bhu095

van den Heuvel, M. P., Scholtens, L. H., Turk, E., Mantini, D., Vanduffel, W., & Feldman Barrett, L. (2016, Sep). Multimodal analysis of cortical chemoarchitecture and macroscale fMRI resting-state functional connectivity. Hum Brain Mapp, 37(9), 3103-3113. https://doi.org/10.1002/hbm.23229

Vasung, L., Huang, H., Jovanov-Milosevic, N., Pletikos, M., Mori, S., & Kostovic, I. (2010, Oct). Development of axonal pathways in the human fetal fronto-limbic brain: histochemical characterization and diffusion tensor imaging. J Anat, 217(4), 400-417. https://doi.org/10.1111/j.1469-7580.2010.01260.x

Wang, R., Wilkinson, M., Kane, T., & Takahashi, E. (2017). Convergence of Cortical, Thalamocortical, and Callosal Pathways during Human Fetal Development Revealed by Diffusion MRI Tractography. Front Neurosci, 11, 576. https://doi.org/10.3389/fnins.2017.00576

Chapter 10

List of co-authors
List of publications
Dankwoord (acknowledgements)
Curriculum vitae

LIST OF CO-AUTHORS

Manon J. Benders
Department of Neonatology, University Medical Center Utrecht, Utrecht University, Utrecht, the Netherlands
Nathalie Claessens
Department of Neonatology, University Medical Center Utrecht, Utrecht University, Utrecht, the Netherlands
Arie Franx
Department of Obstetrics, University Medical Center Utrecht, Utrecht University, the Netherlands
Sonia S. Hassan
Perinatology Research Branch, NICHD/NIH/DHHS, Bethesda, MD, and Detroit, MI, USA
Jasmine L. Hect
Merrill Palmer Skillman Institute for Child and Family Development, Wayne State University, Detroit, MI, USA
Edgar Hernandez-Andrade
Perinatology Research Branch, NICHD/NIH/DHHS, Bethesda, MD, and Detroit, MI, USA
Roel de Heus
Department of Obstetrics, University Medical Center Utrecht, Utrecht University, Utrecht, the Netherlands
Ivana Isgum
Image science institute, University medical Center Utrecht, Utrecht University, Utrecht, the Netherlands
René S. Kahn
Department of Psychiatry, Icahn School of Medicine at Mount Sinai, New York, USA
Nadieh Khalili
Image science institute, University medical Center Utrecht, Utrecht University, Utrecht, the Netherlands
Tessa Kolk
Department of Neonatology, University Medical Center Utrecht, Utrecht University, Utrecht, the Netherlands
Femke Lammertink
Department of Neonatology, University Medical Center Utrecht, Utrecht University, Utrecht, the Netherlands
Nikolas Lessmann
Image science institute, University medical Center Utrecht, Utrecht University, Utrecht, the Netherlands
Janessa H. Manning

Merrill Palmer Skillman Institute for Child and Family Development, Wayne State University, Detroit, MI, USA
Maaike Nijman
Department of Neonatology, University Medical Center Utrecht, Utrecht University, Utrecht, the Netherlands
Eva Overbeek
Department of Neonatology, University Medical Center Utrecht, Utrecht University, Utrecht, the Netherlands
Roberto Romero
Perinatology Research Branch, NICHD/NIH/DHHS, Bethesda, MD, and Detroit, MI, USA
Lianne H. Scholtens
Department of Psychiatry, University Medical Center Utrecht, Utrecht University, Utrecht, the Netherlands
Moriah E. Thomason
Department of Child and Adolescent Psychiatry, New York University Langone Health, New York, USA
Martijn P. van den Heuvel
Department of Complex Traits Genetics, Center for Neurogenomics and Cognitive Research, Amsterdam Neuroscience, VU Amsterdam
Marion I. van den Heuvel
Department of Cognitive Neuropsychology, Tilburg University, Tilburg, The Netherlands
Max A. Viergever
Image science institute, University medical Center Utrecht, Utrecht University, Utrecht, the Netherlands
Yongbin Wei
Department of Complex Traits Genetics, Center for Neurogenomics and Cognitive Research, Amsterdam Neuroscience, VU Amsterdam, the Netherlands

LIST OF PUBLICATIONS

Claessens, N., Khalili, N., Isgum, I., ter Heide, H., Steenhuis, T., **Turk, E.**, Jansen, N., de Vries, L., Breur, J., & de Heus, R. (2019). Brain and CSF Volumes in Fetuses and Neonates with Antenatal Diagnosis of Critical Congenital Heart Disease: A Longitudinal MRI Study. *American Journal of Neuroradiology*.

Collin, G.*, **Turk, E.** *, & van den Heuvel, M. P. (2016, May). Connectomics in Schizophrenia: From Early Pioneers to Recent Brain Network Findings. *Biol Psychiatry Cogn Neurosci Neuroimaging, 1*(3), 199-208. https://doi.org/10.1016/j.bpsc.2016.01.002

Dijkshoorn, A. B. C., **Turk, E.**, Hortensius, L. M., van der Aa, N. E., Hoebeek, F. E., Groenendaal, F., Benders, M., & Dudink, J. (2020, Mar 24). Preterm infants with isolated cerebellar hemorrhage show bilateral cortical alterations at term equivalent age. *Sci Rep, 10*(1), 5283. https://doi.org/10.1038/s41598-020-62078-9

Khalili, N., Lessmann, N., **Turk, E.**, Claessens, N., Heus, R., Kolk, T., Viergever, M. A., Benders, M., & Isgum, I. (2019, Dec). Automatic brain tissue segmentation in fetal MRI using convolutional neural networks. *Magn Reson Imaging, 64*, 77-89. https://doi.org/10.1016/j.mri.2019.05.020

Khalili, N., Moeskops, P., Claessens, N. H., Scherpenzeel, S., **Turk, E.**, de Heus, R., Benders, M. J., Viergever, M. A., Pluim, J. P., & Išgum, I. (2017). Automatic segmentation of the intracranial volume in fetal MR images. In *Fetal, Infant and Ophthalmic Medical Image Analysis* (pp. 42-51). Springer.

Khalili, N., **Turk, E.**, Benders, M., Moeskops, P., Claessens, N. H. P., de Heus, R., Franx, A., Wagenaar, N., Breur, J., Viergever, M. A., & Isgum, I. (2019). Automatic extraction of the intracranial volume in fetal and neonatal MR scans using convolutional neural networks. *Neuroimage Clin, 24*, 102061. https://doi.org/10.1016/j.nicl.2019.102061

Khalili, N., **Turk, E.**, Zreik, M., Viergever, M. A., Benders, M. J., & Išgum, I. (2019). Generative adversarial network for segmentation of motion affected neonatal brain MRI. International Conference on Medical Image Computing and Computer-Assisted Intervention,

Turk, E., Endevelt-Shapira, Y., Feldman, R., van den Heuvel, M. I., & Levy, J. (2022, 2022-April-27). Brains in Sync: Practical Guideline for Parent–Infant EEG During Natural Interaction [Review]. *Frontiers in Psychology, 13*. https://doi.org/10.3389/fpsyg.2022.833112

Turk, E. *, Scholtens, L. H. *, & van den Heuvel, M. P. (2016, May). Cortical chemoarchitecture shapes macroscale effective functional connectivity patterns in macaque cerebral

cortex. *Hum Brain Mapp, 37*(5), 1856-1865. https://doi.org/10.1002/hbm.23141

Turk, E., van den Heuvel, M. I., Benders, M. J., de Heus, R., Franx, A., Manning, J. H., Hect, J. L., Hernandez-Andrade, E., Hassan, S. S., Romero, R., Kahn, R. S., Thomason, M. E., & van den Heuvel, M. P. (2019, Dec 4). Functional Connectome of the Fetal Brain. *J Neurosci, 39*(49), 9716-9724. https://doi.org/10.1523/JNEUROSCI.2891-18.2019

Turk, E., Vroomen, J., Fonken, Y., Levy, J., & Heuvel, M. I. (2022). In sync with your child: The potential of parent–child electroencephalography in developmental research. *Developmental psychobiology, 64*(3). https://doi.org/10.1002/dev.22221

van den Heuvel, M. I., **Turk, E.**, Manning, J. H., Hect, J., Hernandez-Andrade, E., Hassan, S. S., Romero, R., van den Heuvel, M. P., & Thomason, M. E. (2018, Apr). Hubs in the human fetal brain network. *Dev Cogn Neurosci, 30*, 108-115. https://doi.org/10.1016/j.dcn.2018.02.001

van den Heuvel, M. P., Scholtens, L. H., **Turk, E.**, Mantini, D., Vanduffel, W., & Feldman Barrett, L. (2016, Sep). Multimodal analysis of cortical chemoarchitecture and macroscale fMRI resting-state functional connectivity. *Hum Brain Mapp, 37*(9), 3103-3113. https://doi.org/10.1002/hbm.23229

Wei, Y., Scholtens, L. H., **Turk, E.**, & van den Heuvel, M. P. (2019). Multiscale examination of cytoarchitectonic similarity and human brain connectivity. *Netw Neurosci, 3*(1), 124-137. https://doi.org/10.1162/netn_a_00057

LIST OF PREPRINTS

Turk, E., van den Heuvel, M.I., Sleurs, C., Billiet, T., Uyttebroeck, A., Sunaert, S., Mennes, M., Van den Bergh, B. (2022, preprint) Maternal anxiety during pregnancy is associated with weaker prefrontal functional connectivity in adult offspring, Research Square. https://doi.org/10.21203/rs.3.rs-1897872/v1

Turk, E. *, Wei, Y. *, Scholtens, L.H., Benders, M.J., de Heus, R., van den Heuvel, M.P. (submitted). Genetic foundation for fetal cortical growth.

Turk, E., Overbeek, E., R. de Heus, N. Khalili, N., Franx, A., van den Heuvel, M.P., Claessens., N., Lammertink, F., Nijman, M., Isgum, I., Benders, M.J. (manuscript in preparation). Third trimester brain growth in extremely preterm born neonates compared to intrauterine growth in a pilot study.

*Shared first co-author

ACKNOWLEDGEMENTS

Alle studenten, met in het bijzonder Eva, Aicha, Tessel, Nienke, Charlotte, Mariejean, Theresa, Robin en Demi. Bedankt voor al jullie inzet en hulp bij onze leuke projecten!

Alle MRI-laboranten en radiologen van divisie beeld. Bedankt voor de gezelligheid, deskundigheid en hulp tijdens de MRI-scans. In het bijzonder veel dank aan Johan en Niels voor de prettige samenwerking en al jullie ontwikkelingen van de foetale en neonatale MRIs.

Alle onderzoekers en medewerkers van YOUth onder leiding van Prof. dr. Chantal Kemner, Prof. dr. Hilleke Hulshoff Pol en daarvoor ook Prof. dr. René Kahn en dr. Charlotte Onland. Dank voor jullie ontzettende mooie studies naar het ontwikkelende brein en jullie vertrouwen in en ondersteuning van onze MRI sub-studie van de zwangeren en pasgeboren.

Mijn (oud) collega-onderzoekers van de psychiatrie UMC Utrecht en KT1: Jessica, Sonja, Martijn, Merel, Judith, Bart, Pascal, Elisabeth en Jelmer. Bedankt voor alle gezelligheid aan de begintijd van mijn PhD.

Lieve vrienden, oud-huisgenoten, Maurik's vrienden en gekozen 'hemelvaart'-familie, bedankt dat jullie in mijn leven zijn en voor jullie steun en interesse in mijn verschillende onderzoeken. Het was heel fijn en bijzonder om jullie waardering te ervaren vooral na de media-aandacht. Maar ik wil jullie vooral bedanken voor de afleiding van het soms toch wel zware werk. De borrels en feestjes, pizza-avonden, diners, het klussen aan ons huis, liefde voor katten die we delen, de humor en jullie vriendschap zijn zo waardevol voor mij!

Lieve Kim, bedankt dat je mijn lieve vriendin, collega en paranimf wil zijn. Bedankt voor de fijne tijd als collega's. Met jou samen kletsen, zitten op kantoor, koffie-drinken, werken aan onze onderzoeken waren de leukste momenten van mijn PhD!

Lieve schoonfamilie, Marjo, Jurriën, Dicky, Mart-Hein, Zoë, Rune, ik ben dankbaar dat ik dat ik deel uit mag maken van jullie gezin. Bedankt voor jullie interesse en aanmoediging van mijn werk!

Bedankt lieve families Koopman en Turk, bedankt oma Tina, opa Co in gedachten, Dick, Rob, Hilda, Bonnie, Bart en Christine, voor jullie waardering en liefde die jullie me altijd geven. Rob, een extra dikke bedankt voor jou, dat je me helpt om dit boekje af te maken.

Lieve Janou, mijn paranimf, beste zus ter wereld en liefste vriendin. Bedankt voor de geweldige persoon die je bent, voor alles wat we delen en de grootste steun die ik me kan bedenken. Mijn ouders, lieve John en Astrid. Ik had me geen fijner en warmer gezin

kunnen bedenken om in op te groeien. Jullie hebben mij gemaakt tot de persoon die ik ben. Bedankt voor alles wat jullie me geleerd hebben, jullie onvoorwaardelijke liefde en steun, en bedankt dat jullie altijd zo trots zijn.

En als laatste ben ik ontzettend dankbaar voor mijn eigen gezin. Mijn allerliefste Juliette en Laurent, mijn grootste trots en leukste studieobjecten. Het was heel bijzonder en inspirerend om zelf tweemaal moeder te worden tijdens het schrijven van dit proefschrift. Allerliefste Maurik, de vader van mijn twee dierbaarsten, bedankt dat je mijn leven zo mooi, zo perfect, maakt in alle opzichten die ik me maar kan voorstellen.

CURRICULUM VITAE

Elise Turk was born on January 6th, 1990 (35 gestational weeks) in Leiderdorp, the Netherlands. After graduating high school in 2009 (Gymnasium, Teylingen College Leeuwenhorst), she started the interdisciplinary study Bèta-Gamma at the University of Amsterdam (UvA). During this study, she discovered her passion for the interdisciplinary approach for studying the brain by bridging the gap in our knowledge between psychology and biology. And therefore, she switched to a Psychobiology (BSc, UvA) and Biomedical Sciences course with a major in Neurobiology (research MSc, UvA). She performed multiple research projects during her studies: on the prenatal origin and comorbidity of autism and schizophrenia under supervision of Dr. A. Ploeger at the UvA; a network perspective on personality disorders under supervision of dr. R. Goekoop and prof. dr. L. Eurelings-Bontekoe at Leiden University; Functional connectivity and Schizophrenia under supervision of prof. dr. M. van den Heuvel, prof. dr. R. Kahn and Dutch connectome lab, University Medical Center Utrecht (UMCU).

After obtaining her biomedical research master's degree, she was given the opportunity to start as a PhD candidate at the department of Neonatology and gynecology in the Wilhelmina Children's Hospital and Dutch Connectome Lab in the UMCU under supervision of prof. dr. Manon Benders, prof dr. Martijn van den Heuvel, prof. dr. Arie Franx and dr. Roel de Heus. She was the coordinator of the baby MRI YOUth cohort, as part of her PhD program. During her PhD, she studied perinatal brain development using fetal and neonatal MRI and processing techniques such as connectomics in various UMCU cohorts and in collaboration with dr. Moriah Thomason, Wayne State University, Detroit, USA.

Since October 2020, she was given the opportunity to expand her interests in perinatal brain development and the parental bond even further by starting as a (semi) postdoctoral researcher to study behavioral and neural synchrony (dual-EEG) between mother and infant. Supervised by dr. Marion van den Heuvel, Tilburg University and dr. Jonathan Levy, Aalto University, Finland and Interdisciplinary Center Herzliya, Israel.
Elise is currently living in Haarlem with her husband, Maurik and their children Juliette (2019) and Laurent (2022).

Brain development during pregnancy is characterized by tremendous brain growth and the construction of connections between communicating brain regions (brain networks). This makes the fetal period essential for normal development and perturbations to these processes render the brain at risk for neurodevelopmental deficits. Mapping and understanding global fetal and neonatal brain growth in vivo are great challenges, data is sparse and multimodal approaches are needed to fill the gap in our knowledge on neuroimaging interpretation. Recent advances in MRI now enable longitudinal study of the fetal and neonatal brain making detailed measurements of brain growth possible. For our studies, we used data from different resources including the first Dutch cohort of healthy pregnant participants that underwent MRI (YOUth study). The main aims of this thesis are: 1) to map the tremendous structural transformation and maturation of the developing brain in utero and neonatal period, both in healthy individuals and preterm born infants; 2) to reveal its functional blueprint in the second half of pregnancy. Different findings on fetal and neonatal MRI are discussed, with a focus on connectome (brain networks) development. Using fetal fMRI, this work shows a large overlap of fetal and adult functional networks, revealing that the blueprint of our brain is established before birth. Other findings on novel baby-brain MRI analyzing techniques, cortical chemoarchitecture and functional connectivity, cortical expansion and the association with gene expression patterns, will be discussed as well.

UMC Utrecht

Universiteit Utrecht